

Identification of germline loss-of-function mutations in *DOCK11* in a novel immune dysregulation disorder

Doctoral thesis at the Medical University of Vienna
for obtaining the academic degree

Doctor of Philosophy

Submitted by

Jana Block, MSc

Supervisor:

Kaan Boztug, MD

St. Anna Children's Cancer Research Institute (CCRI)
Zimmermannplatz 10, 1090 Vienna, Austria

CeMM Research Center for Molecular Medicine
of the Austrian Academy of Sciences

Medical University of Vienna
Department of Paediatrics and Adolescent Medicine

Vienna, 07/2023

DECLARATION

This doctoral thesis is written in a cumulative format. Chapter 2 includes a first author publication published in the New England Journal of Medicine on June 21, 2023. The publication is the result of a collaborative effort carried out in different laboratories. The majority of the published data was acquired by the author of the thesis. Individual contributions from co-authors are listed below. I performed specific experiments and was involved in the coordination as well as data analysis and interpretation of all experiments. I wrote the manuscript together with Irinka Castanon, Loïc Dupré, Kaan Boztug and with critical input from Christina Rashkova. I was involved in the assembly of all figures and tables. All other chapters of this thesis were written by me.

My individual contributions to the manuscript: Interpreting whole-exome and Sanger sequencing data (Figures 1A and S7A, S14B); collecting and interpreting clinical data (Figures 1B-G, S1A-C and Tables S1-S5); performing alignment analysis and preparing a 3D-model of Deducator of Cytokinesis 11 (DOCK11) protein structure (Figure S11); generating CRISPR/Cas9 (clustered regularly interspaced short palindromic repeats and associated Cas9 homing endonucleases)-edited cells (Figures S14B-D), preparing lysates and performing immunoblot analysis (Figures 2A, S9-S10, S14C, S21A) and enzyme-linked immunosorbent assay (ELISA) (Figure S21B-C) together with Christina Rashkova; performing quantitative polymerase chain reaction (PCR) analysis (Figures S15A and S15D); performing flow cytometry (Figures 3F, 4B-D, S2-S4, S19A-B, S22B-C, S25B-E) and microscopy (Figures 3A-C, 3I, S14A, S14D, S15B-C, S15E-F, S22A, S26A) experiments on human and zebrafish-derived cells; designing and interpreting data together with collaborators (Figures 2B, 3D-E, 3G-H, 3E-F, S5, S7B, S8, S12-S13, S16-S18, S20, S23, S24, S25A, S26B, S27).

Contributions of co-authors: Raul Jimenez Heredia, Karin R. Engelhardt, Sophie Hambleton, Kerstin Kutsche, Frederike L. Harms, Michael Schuster and Caspar I. van der Made analyzed WES data, identified *DOCK11* variants and performed Sanger sequencing validation experiments (Figures 1A, S6, S7A, Tables S6-S15); Frederike L. Harms performed *DOCK11* transcript analysis and X-chromosome inactivation analysis (Figures S7B and S8); Laurène Pfajfer helped with generating CRISPR/Cas9-edited *DOCK11*-knockout cells (Figure S21A); Rico C. Ardy generated plasmids (Figure S15D-F), Julien Viaud performed the CDC42 activation assay (Figures 2B and S12-13); Beatriz Chaves, Rouven Schoppmeyer performed and interpreted T-cell migration assays (Figure 3D and 3E); Bernhard Ransmayr performed in vitro B-cell proliferation and class-switch assays (Figure S5); René Platzer, Samaneh Zoghi and Anna-Katharina Mautner performed B-cell synapse experiments (Figure S23); Martin

Distel and Jeffrey A. Yoder generated the *lck:nlsmCherry;myl7:EGFP^{vi004}* transgenic zebrafish line with intellectual input from David Traver (Figure S18); Irinka Castanon generated zebrafish models and performed characterization of *dock11*-knockout, *dock11* and *cdc42* MO zebrafish by sequencing analysis, flow cytometry and microscopy with help from the author of this thesis and intellectual input from Martin Distel (Figures 4A-D, S16-S17 and S25-S26). Irinka Castanon performed and analyzed T-cell migration experiments in zebrafish embryos (Figure S18) Mitsuhiro Fujiwara, Ryohei Kondo and Akihiko Nishikimi performed characterization of *Dock11*-knockout mice, including flow cytometry, assessment of proliferation and cytokine production, NFATc1 translocation and JNK phosphorylation analysis (Figures 3G-H, S20 and S24); Jessica Platon and Thomas Boyer performed CD34⁺ erythroid differentiation experiments (Figures 4E-F and S27B-C); Michael Caldera provided imaging analysis pipeline for further modification by the first author of this thesis (Figure 3B and C); Anna Tinnacher and J. Thomas Hannich performed mass-spectrometry analysis (Figure S27A); Samin Alavi, Laia Alsina, Paula Sanchez Moreno, Caspar I. van der Made, Han G. Brunner, Judith E. Nooitgedagt-Frons, Estíbaliz Iglesias, Angela Deyà-Martinez, Marisol Camacho-Lovillo, Tobias Linden, Alexander Hoischen, Sabine Illsinger, Zahra Chavoshzadeh, Jordi Antón, Joan Calzada-Hernández and Olaf Neth took care of patients, collected patient samples and provided and interpreted clinical and immunological data (Figures 1, S1 and Tables S1-S5); Samaneh Zoghi coordinated sample collection from patient 1 and translated clinical documents (Table S3); Sevgi Kostel Bal helped to collect and interpret the patient clinical data (Tables S3-S4); Rainiero Ávila Polo and Rocío Cabrera-Pérez provided histopathologic evaluation of biopsies (Figures 1D and S1C); Loïc Dupré helped design and analyze microscopy-based experiments on patient-derived cells (Figures 3E, S15B, S15E-F, S22A and S23); Cecilia Domínguez Conde, Elisabeth Salzer, Sophie Hambleton, Jaap D. van Buul, Jörg Menche, Johannes B. Huppa, Winfried F. Pickl, Christoph Bock, Leo Kager, Sevgi Kostel Bal and Lydie Da Costa provided intellectual input. Loïc Dupré, together with the author of this thesis and Kaan Boztug coordinated part of the experimental work. Kaan Boztug conceived, designed, and coordinated the study.

TABLE OF CONTENTS

Declaration	ii
Table of Contents	iv
List of Figures	vi
Abstract	vii
Zusammenfassung	ix
Publications Arising From This Thesis	xi
Abbreviations	xii
Acknowledgments	xvii
1. Introduction	18
1.1 Hematopoietic system	18
1.1.1 Overview of blood cell types	18
1.1.2 Model systems to study development and function of hematopoietic cells.....	20
1.2 Immune system development and function	23
1.2.1 Innate immune system - Inflammasome assembly	23
1.2.2 Adaptive immune system – B- and T-cell development.....	24
1.2.3 T-cell activation and homeostasis.....	26
1.3 Structure and regulators of the actin cytoskeleton.....	30
1.3.1 Actin filament assembly - structure and regulators	30
1.3.2 Network of RHO GTPases, GEFs, GAPs and GDIs	33
1.3.3 Deducator of cytokinesis family proteins.....	35
1.4. Rare inherited disorders of the hematopoietic system and the actin cytoskeleton	38
1.4.1 Introduction to inborn errors of immunity.....	38
1.4.2 IELs with immune dysregulation	39
1.4.3 Actin-related inborn errors of immunity	42

1.5 Role of the actin cytoskeleton in hematopoietic cells uncovered through study of inborn errors of immunity.....	45
1.5.1 Overview of immune cell functions associated with actin-related IELs.....	45
1.5.2 Actin cytoskeleton remodeling in migrating immune cells	46
1.5.3 Actin dynamics during immune synapse formation and cell activation.....	48
1.5.4 <i>Role of actin-regulatory proteins in red blood cell formation and morphology</i>	50
1.6 Aims	53
2. Results	54
3. Discussion	161
3.1 General Discussion	161
3.1.1 <i>Study of IELs to dissect the role of actin regulators in immune cells</i>	161
3.1.2 <i>DOCK11 deficiency - similarities and differences to the clinical phenotypes observed in patients with mutations in CDC42, DOCK2 or DOCK8</i>	162
3.1.3 <i>DOCK proteins fine-tune lymphocyte morphology and migration - novel insights from DOCK11 deficiency</i>	164
3.1.4 <i>Distinct roles of CDC42 GEFs in T-cell cytokine production</i>	165
3.1.5 <i>DOCK11 as a novel negative regulator of TCR signaling</i>	166
3.1.6 <i>Dissecting the origin of anemia in DOCK11 deficiency</i>	169
3.2 Conclusion and Future Prospects	171
4. Materials and Methods.....	175
5. References	176
6. Curriculum Vitae.....	210

LIST OF FIGURES

Figure 1. Simplified scheme of hematopoiesis	19
Figure 2. Schematic representation of zebrafish hematopoiesis	22
Figure 3. T-cell receptor signaling scheme	29
Figure 4. Scheme of actin cytoskeleton regulators	31
Figure 5. RHO GTPase regulation	33
Figure 6. Scheme of DOCK family protein structure	36
Figure 7. DOCK family members - single cell RNA expression	37
Figure 8. Model of DOCK11-mediated regulation of cytokine production	168

ABSTRACT

Study of inborn errors of immunity (IEI) caused by defects in actin-regulatory proteins has enabled insight into non-redundant roles of actin regulators during basic cellular processes, critical for immune-cell function. Initially, IEI research focused on immune defects leading to increased susceptibility to infections. More recently, it has been recognized that a large proportion of manifestations in IEI patients is linked to an overt reaction of the immune system. Many actinopathies also present as complex diseases with autoinflammatory or immune dysregulation features, yet the underlying pathomechanisms are often poorly understood.

Dedicator of cytokinesis (DOCK) proteins act as guanine nucleotide exchange factors (GEFs) to activate the small RHO guanosine triphosphatases (GTPases) RAC1 and cell division cycle (CDC42), key regulators of actin dynamics. Defects in DOCK2 and DOCK8 cause distinct combined immunodeficiency disorders. DOCK11, which is predominantly expressed in hematopoietic cells and specifically activates CDC42 has been linked to B-cell development and function in mice, was suspected to play a role in the human immune system and for human disease, however this had not yet been reported.

In this work, we studied four male patients from four unrelated families presenting with recurrent infections, early-onset systemic inflammation and immune dysregulation, normocytic anemia of unknown origin and developmental delay. Using whole-exome sequencing, we identified four rare, X-linked germline mutations in *DOCK11* in these patients, leading to complete loss of DOCK11 protein expression in cells from two patients, while expression of mutant DOCK11 was retained in the other two patients. In line with the known role of DOCK11 as CDC42 GEF, we observed impaired CDC42 activation in B lymphoblastoid cells (BLCLs) from all four patients.

Using patient-derived material, CRISPR-Cas9 (clustered regularly interspaced short palindromic repeats and associated Cas9 homing endonucleases)-edited cell lines and a *Dock11*-knockout mouse model, we revealed perturbed filopodia formation, abnormal migration and aberrant T-cell proliferation and cytokine production in DOCK11-deficient T cells. We investigated the underlying molecular mechanism and uncovered increased nuclear translocation of nuclear factor of activated T cell 1 (NFATc1), a T-cell transcription factor, known to regulate various cytokines. In line with previous reports suggesting that c-Jun N-terminal kinase (JNK), a known CDC42 effector, negatively regulates NFATc1 translocation, we observed reduced JNK phosphorylation in T cells from *Dock11*-knockout mice.

A *dock11*-knockout zebrafish model, generated to uncover the cause of anemia in human DOCK11 deficiency, recapitulated both the anemia as well as the abnormal erythrocyte morphology. Expression of constitutively active CDC42 in *dock11*-knockout zebrafish larvae rescued the anemia phenotype, suggesting that DOCK11 regulates erythrocyte development in a CDC42-dependent manner. Short hairpin RNA (ShRNA)-mediated knockdown of *DOCK11* in human CD34⁺ cells resulted in impaired cell growth and altered expression of differentiation markers upon induction of erythropoiesis in liquid culture.

Conclusively, in a collaborative effort, we identified germline mutations in *DOCK11* as the underlying cause of a novel inborn error of immunity leading to aberrant T-cell signaling and cytokine production and disturbed erythroid development.

ZUSAMMENFASSUNG

Durch die Erforschung angeborener Immundefekte (IEIs), die durch Mutationen in Regulatoren des Aktin-Zytoskeletts verursacht werden, erlangen wir Erkenntnisse über nicht-redundante Aufgaben dieser Regulatoren während grundlegender zellulärer Prozesse, die für die Funktion von Immunzellen entscheidend sind. Ursprünglich konzentrierte sich die Forschung auf die Immundefizienz und die damit einhergehende erhöhten Anfälligkeit für Infektionen. Zuletzt hat man jedoch erkannt, dass ein großer Teil der Symptome von Patienten mit einem Immundefekt mit einer Überreaktion des Immunsystems zusammenhängt. Viele Defekte des Aktin-Zytoskeletts verursachen komplexe Krankheitsbilder mit Autoinflammation oder Immundysregulation, wobei die zugrundeliegenden Pathomechanismen oft nur unzureichend verstanden sind.

DOCK (Dedicator of cytokinesis) Proteine fungieren als Guanin-Nukleotid-Austauschfaktoren (GEF) und aktivieren die RHO Guanosintriphosphatasen (GTPasen) RAC1 und CDC42 (cell division cycle 42), die eine wichtige Rolle für die Dynamik des Aktin-Zytoskeletts spielen. Defekte in DOCK2 und DOCK8 sind Auslöser für die Entstehung von zwei verschiedenen kombinierten Immundefekten. DOCK11 wird vorwiegend in hämatopoetischen Zellen exprimiert und aktiviert spezifisch CDC42. In Mausversuchen konnte eine Rolle für DOCK11 bei der Entwicklung und Funktion von B-Zellen gezeigt werden. Daher wurde zwar vermutet, dass DOCK11 wichtig für das humane Immunsystem ist und eine potenzielle Rolle bei der Entstehung von Krankheiten spielen könnte, jedoch konnte dies bisher noch nicht gezeigt werden.

In dieser Arbeit haben wir vier männliche Patienten aus vier nicht verwandten Familien untersucht, die an rezidivierenden Infektionen, früh einsetzenden systemischen Entzündungen, Immundysregulation, normozytärer Anämie unbekannter Herkunft, sowie Entwicklungsverzögerungen litten. Mithilfe der Exom-Sequenzierung konnten wir vier seltene, X-chromosomale Keimbahnmutationen in *DOCK11* in diesen Patienten identifizieren. Zwei Mutationen führten zu einem vollständigen Verlust der Expression in Zellen, während die anderen zwei Mutationen keinen Einfluss auf die Proteinherstellung hatten. Übereinstimmend mit der bekannten Rolle von DOCK11 als CDC42 GEF konnten wir eine verminderte Aktivierung von CDC42 in B-Lymphoblastoiden Zelllinien (BLCLs) aller vier Patienten beobachten.

Mit Hilfe von Patientenmaterial, CRISPR/Cas9 (clustered regularly interspaced short palindromic repeats and associated Cas9 homing endonucleases)-editierten Zelllinien und

einem *Dock11*-Knockout Mausmodell konnten wir bei T-Zellen mit einer DOCK11-Defizienz eine gestörte Bildung von Filopodien, veränderte Zellfortbewegungseigenschaften sowie eine abnorme T-Zellproliferation und Zytokinproduktion nachweisen. Wir untersuchten den zugrundeliegenden molekularen Mechanismus und entdeckten eine erhöhte Translokation des T-Zell-Transkriptionsfaktors NFATc1 (nuclear factor of activated T cell 1) in den Zellkern. Es ist bekannt, dass NFATc1 die Produktion verschiedener Zytokine reguliert. In Übereinstimmung mit früheren Berichten, die darauf hindeuten, dass JNK (c-Jun N-terminal kinase), ein bekannter CDC42-Effektor, als negativer Regulator der NFATc1-Translokation fungiert, konnten wir eine reduzierte Phosphorylierung von JNK in T-Zellen von *Dock11*-Knockout Mäusen beobachten.

Ein *dock11*-Knockout Zebrafischmodell, das entwickelt wurde, um die Ursache der Anämie aufzudecken, rekapitulierte sowohl die Anämie als auch die abnorme Morphologie der Erythrozyten, die zuvor bei Patienten mit DOCK11-Defizienz beobachtet wurde. Die Expression von konstitutiv aktivem CDC42 in *dock11*-Knockout Zebrafischlarven führte zur Normalisierung der Anzahl der roten Blutkörperchen, was darauf hindeutet, dass DOCK11 die Produktion von Erythrozyten mittels CDC42 Aktivierung reguliert. Die verminderte Expression von DOCK11 mittels RNA-Interferenz durch eine short hairpin RNA (shRNA) in humanen CD34-positiven Zellen, führte ebenfalls zu einer Beeinträchtigung des Zellwachstums und einer veränderten Expression von Differenzierungsmarkern während der *in vitro* Erythropoese.

Zusammenfassend haben wir Keimbahnmutationen in *DOCK11* als Ursache für einen neuartigen angeborenen Immundefekt identifiziert, der zu einer veränderten T-Zell-Signalübertragung und Zytokinproduktion sowie einer gestörten Erythropoese führt.

PUBLICATIONS ARISING FROM THIS THESIS

Chapter 2 of this thesis contains content reproduced with permission from N Engl J Med. 2023 Jun 21. doi: 10.1056/NEJMoa2210054. Epub ahead of print. PMID: 37342957, Copyright © (2023) Massachusetts Medical Society.

Systemic Inflammation and Normocytic Anemia in DOCK11 Deficiency

Jana Block, M.Sc., Christina Rashkova, M.Sc., Irinka Castanon, Ph.D., Samaneh Zoghi, Ph.D., Jessica Platon, M.Sc., Rico C. Ardy, Ph.D., Mitsuhiro Fujiwara, Ph.D., Beatriz Chaves, M.Sc., Rouven Schoppmeyer, Ph.D., Caspar I. van der Made, M.D., Raul Jimenez Heredia, M.Sc., Frederike L. Harms, Ph.D., Samin Alavi, M.D., Laia Alsina, M.D., Ph.D., Paula Sanchez Moreno, M.D., Rainiero Ávila Polo, M.D., Ph.D., Rocío Cabrera-Pérez, M.D., Sevgi Kostel Bal, M.D., Ph.D., Laurène Pfajfer, Ph.D., Bernhard Ransmayr, M.D., Anna-Katharina Mautner, M.Sc., Ryohei Kondo, Ph.D., Anna Tinnacher, M.Sc., Michael Caldera, Ph.D., Michael Schuster, Ph.D., Cecilia Domínguez Conde, Ph.D., René Platzter, Ph.D., Elisabeth Salzer, M.D., Ph.D., Thomas Boyer, M.D., Ph.D., Han G. Brunner, M.D., Judith E. Nooitgedagt-Frons, M.D., Estíbaliz Iglesias, M.D., Ph.D., Angela Deyà-Martinez, M.D., Ph.D., Marisol Camacho-Lovillo, M.D., Jörg Menche, Ph.D., Christoph Bock, Ph.D., Johannes B. Huppa, Ph.D., Winfried F. Pickl, M.D., Martin Distel, Ph.D., Jeffrey A. Yoder, Ph.D., David Traver, Ph.D., Karin R. Engelhardt, Ph.D., Tobias Linden, M.D., Leo Kager, M.D., J. Thomas Hannich, Ph.D., Alexander Hoischen, Ph.D., Sophie Hambleton, M.D., Ph.D., Sabine Illsinger, M.D., Lydie Da Costa, M.D., Ph.D., Kerstin Kutsche, Ph.D., Zahra Chavoshzadeh, M.D., Jaap D. van Buul, Ph.D., Jordi Antón, M.D., Ph.D., Joan Calzada-Hernández, M.D., Olaf Neth, M.D., Julien Viaud, Ph.D., Akihiko Nishikimi, Ph.D., Loïc Dupré, Ph.D., and Kaan Boztug, M.D.

Ms. Rashkova and Dr. Castanon contributed equally to this article.

ABBREVIATIONS

µg	microgram
µl	microliter
µm	micrometer
µM	micromolar
3D	three dimensional
Ab	antibody
AGM	aorta-gonad-mesonephros
ALC	absolute lymphocyte count
ALPS	autoimmune lymphoproliferative syndrome
AMC	absolute monocyte count
ANA	nuclear antibodies
ANC	absolute neutrophil count
ANCA	antineutrophil cytoplasmic antibodies
ANOVA	analysis of variance
APCs	antigen-presenting cells
AR	androgen receptor
ARDS	acute respiratory distress syndrome
ASC	apoptosis-associated speck-like protein
ATC	absolute thrombocyte count
BCG	Bacille Calmette–Guérin
BCGitis	BCG vaccine–related lymphadenitis and skin ulcer at injection site
BCR	B-cell receptor
BLCLs	B lymphoblastoid cells
bp	base pair
CADD	combined annotation dependent depletion
CaM	calmodulin
CCL19	C-C motif chemokine ligand 19
CCR7	C-C chemokine receptor type 7
CD	cluster of differentiation
CDC42	cell division cycle
cDNA	complementary DNA
cDNA	complementary DNA
Chr	chromosome
CHT	caudal hematopoietic tissue
CM	central memory
CR	Congo Red
CRAC	Ca ²⁺ release-activated Ca ²⁺
CRISPR-Cas9	clustered regularly interspaced short palindromic repeats and associated Cas9 homing endonucleases
CRP	C-reactive protein
CTLA-4	cytotoxic T-lymphocyte antigen 4
D	diversity genes
DAG	diacyl glycerol
DAMPs	damage-associated molecular patterns
DAPI	nuclear marker 4',6-diam- idino-2-phenylindole
DHR	DOCK homology regions

DMSO	dimethyl sulfoxide
DN	double negative
DNA	deoxyribonucleic acid
DOCK	dedicator of cytokinesis
dpf	days post fertilization
dsDNA	double stranded DNA
dsRed	red fluorescent protein
EBV	Epstein Barr virus
ECs	endothelial cells
ELISA	enzyme-linked immunosorbent assay
EM	effector memory
EMA	endomysial antibodies
ENST	Ensembl transcript ID
EPO	erythropoietin
ESR	erythrocyte sedimentation rate
FACS	fluorescence-activated cell sorting
F-actin	filamentous actin
FCS	fetal calf serum
FMF	Familial Mediterranean fever
FOXP3	forkhead box P3
FSC	forward scatter
FTT	failure to thrive
G-actin	globular actin
GAD65	glutamic acid decarboxylase 65-kilodalton isoform
GAPs	GTPase activating proteins
GDI	guanine nucleotide dissociation inhibitors
gDNA	genomic dna
GDP	guanosine diphosphate
GEFs	guanine nucleotide exchange factors
GFP	green fluorescent protein
gnomadAD_AC	total allele counts in gnomad
gnomadAD_AF	minor allele frequency in gnomad
GST-PBD	GST-tagged Rac/Cdc42 (p21) binding domain
GTP	guanosine triphosphate
GTPases	guanosine triphosphatases
Hb	hemoglobin
HCT	hematocrit
HD	healthy donor
HE	hematoxylin and eosin
HGNC_ID	HUGO Gene Nomenclature Committee Identifier
HGVS	Human Genome Variation Society
HI index	haploinsufficiency score
HIDS	hyperimmunoglobulinemia D syndrome
HLH	hemophagocytic lymphohistiocytosis
HPCs	hematopoietic progenitor cells
hpf	hours post fertilization
HSCs	hematopoietic stem cells
HSP90	heat shock protein 90
HSPCs	hematopoietic stem/progenitor cells

HUVEC	human umbilical vein endothelial cells
IA2	tyrosine phosphatase-like protein insulinoma antigen 2
ICAM-1	intercellular cell adhesion molecule 1
ICM	intermediate cell mass
IEI	inborn errors of immunity
IFN- γ	interferon gamma
IHC	immunohistochemical
IL	interleukin
IP3	inositol 1,4,5-trisphosphate
IPEX	immune dysregulation, polyendocrinopathy, enteropathy, X-linked
IS	immune synapse
IV	intravenous
IVIg	intravenous immune globulin
J	joining genes
JNK	c-Jun N-terminal kinase
kDa	kilo Dalton
KI	knock-in
KO	knockout
LA/SSB	La/Sjögren syndrome B
LAMP-1/CD107a	lysosome-associated membrane protein 1
LC1	liver cytosol type 1
LCK	lymphocyte-specific protein tyrosine kinase
LDH	lactate dehydrogenase
LKM1	liver-kidney microsomal type 1
LOEUF	loss-of-function observed/expected upper bound fraction
LPS	lipopolysaccharide
MAF	minor allele frequency
MCH	mean corpuscular hemoglobin
MCV	mean corpuscular volume
MFI	mean fluorescence intensity
MHC	major histocompatibility complex
min	minute
mL	milliliter
MO	morpholino
MPO	myeloperoxidase
MPV	mean platelet volume
MRI	magnetic resonance imaging
mRNA	messenger RNA
MSC	mutation significance cutoff
MTOC	microtubule-organizing center
MVK	mevalonate kinase
n.a.	not available
NFATc1	nuclear factor of activated T cell 1
ng	nanogram
NK	natural killer
NLRP3	NACHT, LRR, and PYD domains-containing protein 3
NLRs	NOD-like receptors
NOCARH	neonatal-onset cytopenia with dyshematopoiesis, autoinflammation, rash, and hemophagocytic lymphohistiocytosis

P	patient
P/S	penicillin/streptomycin
Pam3CSK4	Pam3CysSerLys4
PAMPs	pathogen associated molecular patterns
PBI	posterior blood island
PBMCs	peripheral blood mononuclear cells
PCR	polymerase chain reaction
PH	pleckstrin homology
PH3	phospho-histone H3
PHA	phytohemagglutinin
PI	propidium iodide
PIDs	primary immunodeficiencies
PIP2	phosphatidylinositol 4,5-bisphosphate
PMA	phorbol 12-myristate 13-acetate
POS	position in the chromosome (b37 assembly)
PRRs	pattern recognition receptors
PxxP	proline-rich region
RBCs	red blood cells
RDW-CV	red cell distribution width - coefficient of variation
REF/ALT	reference and alternative allele
RNA	ribonucleic acid
RNP	ribonucleoproteins
Ro/SSA	Ro/Sjögren syndrome A
RP2	activator of ARL3 GTPase
RT	reverse transcription
RVIS	residual variation intolerance score
<i>S. epidermidis</i>	<i>Staphylococcus epidermidis</i>
<i>S. hominis</i>	<i>Staphylococcus hominis</i>
SC	subcutaneous
SCIg	subcutaneous immune globulin
SD	Standard Deviation
SDS	sodium dodecyl sulfate
SEM	standard error of the mean
sgRNA	single guide RNA
SH2/SH3	src homology 2/3
shRNA	short hairpin RNA
SIRS	systemic inflammatory response syndrome
SLA	soluble liver antigen
Sm	Smith
SNPs	single nucleotide polymorphisms
SNVs	single nucleotide variants
SOCE	store-operated Ca ²⁺ entry
SSC	side scatter
ssODN	single stranded oligodeoxynucleotide
TcdB	<i>Clostridium difficile</i> -derived cytotoxin
TCR	T-cell receptor
TEM	transendothelial migration
Texp	expanded T Cells
Th1	T helper 1

TIDE	tracking of indels by decomposition
TLRs	toll-like receptors
TMT	tandem mass tag
TNF- α	tumor necrosis factor α
Tregs	regulatory T cells
tTG	tissue transglutaminase
V	variable genes
WAS	Wiskott-Aldrich syndrome
WASP	Wiskott-Aldrich syndrome protein
WBCs	white blood cells
WES	whole exome sequencing
WIP	WAS protein-interacting protein
XCI	X-chromosome inactivation

ACKNOWLEDGMENTS

First, I would like to express my sincere gratitude to all the patients and their families who participated in the study that forms the basis of my PhD thesis. Their trust in scientific research to advance our understanding of basic biological processes, with the ultimate goal of developing novel therapeutic options for rare diseases, made this project possible. Furthermore, I would like to thank my PhD supervisor, Kaan Boztug, for providing me with the opportunity to join his lab, and for his scientific guidance and support.

I would like to thank all past and present members of my lab. The support I received from each of you was beyond measure, and I am incredibly grateful that you were part of my PhD journey. Thank you for all the scientific help, for cheering me up whenever needed, and for becoming close colleagues and friends. Chrise and Irinka, you both have been my "Dream Team," and I can't thank you enough for being there during all the important stages of this project. A special thanks goes to Loïc Dupré for his immense support, particularly during the initial stages of my PhD. Thank you for spending countless hours with me at the microscope and teaching me all the crucial imaging skills.

The publication resulting from this thesis is an incredible team effort, with clinicians and scientists from more than 9 countries making valuable contributions. I extend my heartfelt thanks to all the people at the institutes in Spain, France, Germany, Iran, the Netherlands, the United Kingdom, Japan, the United States, and, of course, Austria for their dedication and collaboration. It has been truly inspiring to work with each and every one of you.

I am grateful to the people at CCRI, LBI-RUD and CeMM for fostering an environment that promotes scientific exchange and facilitates the formation of friendships. Furthermore, I am thankful to the Austrian Academy of Sciences for awarding me the DOC fellowship, which provided financial support throughout 2 years of my PhD.

Lastly, my deepest gratitude goes to all my friends and family. To my parents and my sister, thank you for your wholehearted support throughout every decision I have made in life. And to Lennart, thank you for inspiring me every day to explore new activities and cherish every moment of life. You are the person I want to have by my side when embarking on new adventures.

1. INTRODUCTION

1.1 Hematopoietic system

1.1.1 Overview of blood cell types

In an adult human more than 500 billion blood cells are produced on a daily basis (Fliedner et al., 2002). Red blood cells (RBCs), also termed erythrocytes, which supply the body with oxygen and remove carbon dioxide (Rieger & Schroeder, 2012) are the most abundant cell type in the blood, followed by platelets (thrombocytes), which are shed from parental megakaryocytes and are involved in blood clotting. White blood cells (WBCs), also called leukocytes, are part of the immune system involved in protecting the body from infectious and toxic agents, and from malignant cells, in removing tissue debris and dying cells, and in wound healing (Cyster & Allen, 2019; Murray & Wynn, 2011; Raskov et al., 2021; Vivier et al., 2008). Blood cells in adults arise from hematopoietic stem cells (HSCs) present mainly in specialized, perivascular niches in the bone marrow or in the spleen (Morrison & Scadden, 2014). Self-renewing HSCs provide a lifelong reservoir for the formation of all blood cell types and lineages (Figure 1) (Rieger & Schroeder, 2012). The myeloid lineage consists of erythrocytes and platelets arising from a common megakaryocyte erythrocyte progenitor, as well as neutrophils, eosinophils, basophils, monocytes, and tissue-resident macrophages, which are derived from a common granulocyte macrophage progenitor (Figure 1) (Akashi et al., 2000). T, B and natural killer (NK) cells, belong to the lymphoid lineage (Kondo et al., 1997), whereas dendritic cells can arise from both lymphoid and myeloid progenitors (Ardavín, 2003; Helft et al., 2017; Manz et al., 2001; Orkin & Zon, 2008; Shortman & Liu, 2002; Traver et al., 2000). The formation of mature blood cells occurs in a hierarchical, lineage-restricting manner. With each differentiation step, cells become progressively committed to a specific lineage and cell type until highly specialized mature blood cells with distinct physiological functions emerge. In the so-called HSC niche, HSCs are surrounded by mesenchymal stem and progenitor cells as well as endothelial cells (ECs). These cells produce cytokines and chemokines that are critical for the survival and proliferation of hematopoietic progenitor cells as well as lineage determination during hematopoiesis (Metcalf, 1998; Miao et al., 2020; Rieger & Schroeder, 2009, 2012). While such extrinsic signals mediate lineage induction, cell-intrinsic lineage-specific genetic programs maintain lineage commitment and specification (Cantor & Orkin, 2002; Graf & Enver, 2009; Moignard et al., 2013; Orkin, 2000; Orkin & Zon, 2008; Pevny et al., 1991).

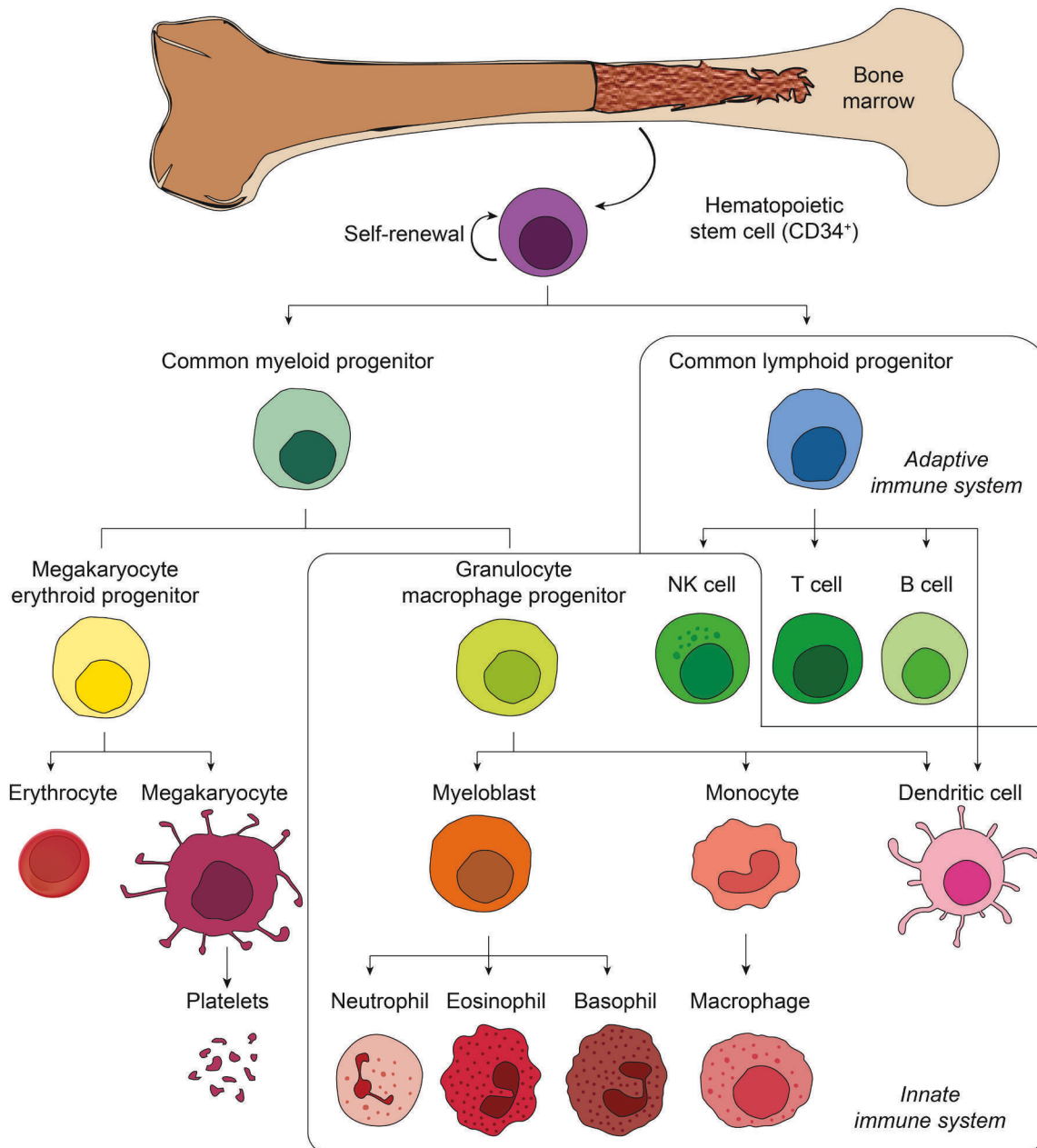


Figure 1. Simplified scheme of hematopoiesis

Hematopoietic stem cells harbor self-renewing potential and give rise to all blood cell lineages. CD34 is expressed on hematopoietic stem/progenitor cells (HSPCs) and commonly used to distinguish HSPCs from differentiated blood cells. Common myeloid progenitors develop into erythrocytes and platelets and replenish many cells of the innate immune system, including neutrophils, eosinophils, basophils, and monocytes. Common lymphoid progenitors give rise to T and B cells, critical for mounting an adaptive immune response, as well as NK cells. Dendritic cells arise from progenitors of both the myeloid and lymphoid lineage. Figure adapted from (Godin, 2016; Raza et al., 2021).

The classical hierarchical HSC differentiation model is a simplified model. As has been shown by cellular reprogramming through forced expression of specific transcription factors, lineage commitment is not unidirectional (Iwasaki & Akashi, 2007; Orkin & Zon, 2008). New

technologies, including the combination of single cell transcriptomics with lineage-tracing experiments have deepened our understanding of the complex biological system underlying cell fate determination during hematopoiesis (Loughran et al., 2020; Weinreb et al., 2020).

1.1.2 Model systems to study development and function of hematopoietic cells

For the study of hematopoiesis and particularly erythropoiesis, researchers have explored a variety of experimental methods, including the use of animal models, immortalized erythroleukemia and erythroid cell lines, as well as RBCs differentiated from murine and human embryonic stem cells or human CD34⁺ umbilical cord blood cells (Dias et al., 2011; Fujimi et al., 2008; Giarratana et al., 2005; Hirose et al., 2013; Huang et al., 2014; Kurita et al., 2013; Olivier et al., 2006; Parker & Peterson, 2018; Song et al., 2019; Trakarnsanga et al., 2017). While hematopoiesis had been historically primarily studied in mice, the identification of zebrafish (*Danio rerio*) mutants with hematopoietic defects through large-scale genetic screens (Driever et al., 1996; Ransom et al., 1996; Weinstein et al., 1996) led to the recognition of zebrafish as a suitable model system to study the hematopoietic system.

Zebrafish harbor several advantageous traits, including *ex vivo* fertilization/embryonic development, optical transparency, and high fecundity (Carradice & Lieschke, 2008; Sugiyama et al., 2022). In addition, zebrafish embryos can survive without red blood cells during early development (Avagyan & Zon, 2016). Both forward genetic screens, and reverse genetic techniques such as transient knockout, knockdown, or overexpression, as well as stable transgenesis, have been utilized to identify and study genes involved in zebrafish hematopoiesis (Lieschke & Currie, 2007).

While there are certain differences between zebrafish and mammal erythropoiesis, such as the lack of enucleation during the terminal steps of zebrafish RBC development, many genes involved in erythropoiesis are conserved across the two vertebrates (Thisse & Zon, 2002; Zon, 1995). Both mammalian (Figure 1) and zebrafish hematopoiesis (Figure 2) occur in sequential waves (primitive and definitive erythropoiesis), which take place at different anatomical sites. In mammals, the first primitive erythroblasts arise exclusively from blood islands in the yolk sac, whereas the definitive hematopoiesis occurs at several sites, including the yolk sac, the aorta-gonad-mesonephros (AGM), the placenta, fetal liver and eventually the bone marrow (Ivanovs et al., 2017; Ivanovs et al., 2011; Medvinsky & Dzierzak, 1996; Mikkola & Orkin, 2006; Orkin & Zon, 2008). By contrast, primitive erythroblasts in the zebrafish (reviewed in (Avagyan & Zon, 2016; Carradice & Lieschke, 2008; Davidson & Zon, 2004; Kulkeaw & Sugiyama, 2012; Zhang et al., 2021) derive from a structure called the intermediate cell mass

(ICM), conceptually analogous to the blood island of the yolk sac in mammals. Hemangioblasts in the ICM give rise to both HSCs, which further differentiate into erythrocytes, monocytes and macrophages, as well as vascular endothelial cells. Primitive macrophages also arise from a second region, the rostral blood island (RBI), which is located in the head. The first definitive erythroblasts and monocytes/macrophages arise from erythromyeloid progenitors in the posterior blood island (PBI). Later during embryonic development, HSCs and hematopoietic progenitor cells (HPCs) arise from the AGM-like region in the ventral wall of the dorsal aorta, migrate to the caudal hematopoietic tissue (CHT) and subsequently expand and differentiate into definitive erythrocytes, monocytes/macrophages, platelets and neutrophils. Expanded HSCs further migrate to the developing kidney (pronephros), the site of definitive erythropoiesis in the adult zebrafish (C. M. Bennett et al., 2001; Kulkeaw & Sugiyama, 2012).

While erythroid cells expressing Gata1a and few myeloid cells can be found as early as 12-24 hours post fertilization (hpf) in the developing zebrafish, the first lymphoid progenitor cells arise at 3-4 days post fertilization (dpf) (Davidson & Zon, 2004; Kulkeaw et al., 2018; Lyons et al., 2002; Trede et al., 2004). The first transient wave of HSC-independent T-cell lymphopoiesis originates from the AGM-like region and mostly gives rise to CD4 T_{αβ} cells (Tian et al., 2017). A second HSC-dependent wave produces various types of T cells. These HSCs arise in the AGM, migrate to the CHT, differentiate into T-lymphoid progenitor cells, which then home to the thymus, the site of T-cell maturation (Langenau et al., 2004). Many genes involved in T-cell development and function are conserved (Haire et al., 2000; Thisse & Zon, 2002). As in mammals, γδ and αβ T-cell lineages are formed and VDJ recombination contributes to T-cell receptor (TCR) specificity (Covacu et al., 2016; Meeker et al., 2010; Trede et al., 2004; Wan et al., 2016). Lck, a non-receptor tyrosine kinase, is expressed in both lymphoid progenitors and mature T cells (Langenau et al., 2004). Development of B lymphocytes takes place in the pronephros of zebrafish larvae and the kidney marrow of adult fish. Fully mature B cells can be found at 3-4 weeks post fertilization (Lam et al., 2004; Trede et al., 2004).

Given the high evolutionary conservation of hematopoietic-cell development and function between zebrafish and human and the possibility to use live imaging of an intact organism, provides huge potential to study the physiological consequences of genetic defects underlying human immunological diseases.

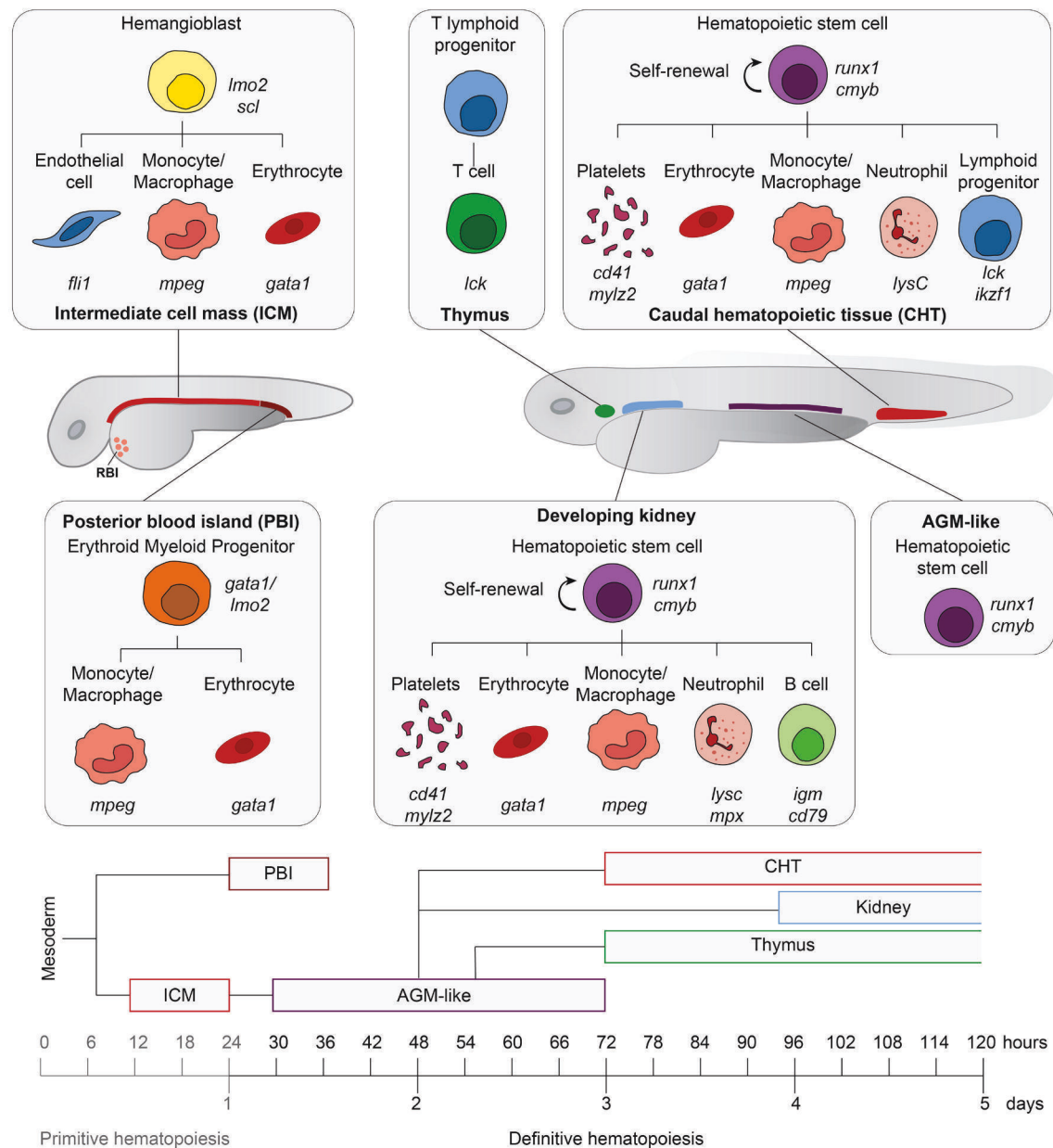


Figure 2. Schematic representation of zebrafish hematopoiesis

Primitive hematopoiesis in zebrafish occurs at the intermediate cell mass (ICM) and in the rostral blood island. Hemangioblasts differentiate into vascular endothelial cells, erythrocytes and monocytes/macrophages. Definitive erythropoiesis starts around 24 hours post fertilization. Erythromyeloid progenitors in the posterior blood island (PBI) give rise to the first definitive erythroblasts, monocytes and macrophages. Hematopoietic stem cells (HSC) and hematopoietic progenitor cells (HPC) that are produced in the aorta-gonad-mesonephros (AGM)-like region migrate to the caudal hematopoietic tissue (CHT) and subsequently expand and differentiate into definitive erythrocytes, monocytes/macrophages, platelets, neutrophils and lymphoid progenitors. The latter home to the thymus, the place of T-cell maturation. Expanded HSCs migrate from the CHT to the developing kidney (pronephros), the site of definitive erythropoiesis in the adult zebrafish. Marker genes for the distinct blood cell types are displayed in *Italic*. Figure adapted from (Chen & Zon, 2009; Jing & Zon, 2011; Paik & Zon, 2010).

1.2 Immune system development and function

1.2.1 Innate immune system - Inflammasome assembly

The immune system, which can be divided into the innate and the adaptive immune system, has evolved to protect the human body from potentially harmful foreign pathogens, toxins and allergens, while maintaining immune tolerance against self. The innate immune system, which is the first line of defense, mounts a quick but non-specific response. It consists of physical and physiological barriers, which include skin and mucosal tissue, sweat, saliva and gastric acid, as well as of specialized cells, that are derived from HSCs.

The innate immune response is based on the recognition of danger signals through germline-encoded pattern recognition receptors (PRRs). These receptors enable the recognition of specific structures present in a variety of invasive pathogens, so called pathogen associated molecular patterns (PAMPs), or the sensing of tissue damage via damage-associated molecular patterns (DAMPs). PRRs can be divided into four different classes, namely Toll-like receptors (TLRs), NOD-like receptors (NLRs), C-type lectin receptors and Retinoic acid-inducible gene 1-like receptors. Upon engagement of these receptors through the recognition of DAMPs or PAMPs, intracellular signaling cascades trigger microbe phagocytosis and lead to the production of antimicrobial proteins, chemokines and proinflammatory cytokines (reviewed in (Fitzgerald & Kagan, 2020; Iwasaki & Medzhitov, 2010).

Interleukin (IL)-1 β and IL-18 are two inflammatory cytokines, which are produced as inactive precursors. The generation of their bioactive forms are mediated through cleavage by multimeric protein complexes, termed inflammasomes (reviewed in (Schroder & Tschopp, 2010; Zheng et al., 2020). They consist of an innate sensor protein, such as pyrin (encoded by *MEFV*), AIM2, NLRP3 or NLRC4, which gives the inflammasome its specific name, an apoptosis-associated speck-like protein (ASC) adaptor protein, and a procaspase-1 enzyme. Upon inflammasome assembly, pro-caspase-1 is cleaved into its active form, which subsequently cleaves pro-IL-1 β and IL-18, as well as gasdermin D. The latter forms pores in the plasma membrane, mediating the release of active IL-1 β and IL-18 and inducing a specific form of cell death, called pyroptosis. The assembly of inflammasome complexes is triggered by various exogenous or endogenous stimuli. For instance, canonical activation of the NLRP3 inflammasome requires a first priming step, which triggers the NF κ B-dependent transcriptional upregulation of NLRP3 and pro-IL1 β , as well as post-transcriptional changes. Priming can be triggered through Toll-like receptors, such as lipopolysaccharide-induced TLR-4 activation, or through IL-1 β and tumor necrosis factor α (TNF- α) signaling. In a second activation step,

pathogen virulence factors, as well as intracellular danger signals, including ion flux, mitochondrial injury and release of reactive oxygen species, lead to the assembly of the NLRP3 inflammasome (Franchi et al., 2009; Swanson et al., 2019; Zheng et al., 2020).

The pyrin inflammasome can be activated in response to pathogen-induced modification of RHO guanosine triphosphatase (GTPase) activation. For instance, *Clostridium difficile*-derived cytotoxin (TcdB) glycosylates RHOA, resulting in its inactivation and decreased activity of its downstream effectors PKN-1/2. The serine/threonine protein kinases PKN-1/2 phosphorylate pyrin on serine residues S208 and S242, enabling binding of the chaperone protein 14-3-3, which sequesters pyrin thereby preventing inflammasome assembly. Consequently, modulation of RHOA or PKN-1/2 activity by bacterial toxins or effectors, such as TcdB, or YopE and YopT from *Yersinia*, lead to pyrin inflammasome activation (Jamilloux et al., 2018; Malik & Bliska, 2020; Xu et al., 2014).

Recognition of microbial PAMPs by innate immune cells initiates a direct antimicrobial response, but it also controls the amplitude and type of adaptive immune response thereby ensuring an effective immune response against foreign pathogens while maintaining tolerance against self (Iwasaki & Medzhitov, 2010; Palm & Medzhitov, 2009).

1.2.2 Adaptive immune system – B- and T-cell development

The adaptive immune system is the second line of defense and acts in conjunction with the innate immune response to fight and destroy foreign pathogens. In contrast to the innate immune system, cells of the adaptive immune system, which also originate from HSCs, can recognize specific antigen and therefore mediate a slower but more targeted immune response. In addition, the adaptive immune system has the capability to generate immunologic memory and therefore respond in a faster and stronger manner upon repeated encounter of the same pathogen. To mount an antigen-specific immune response to the vast number of potential pathogens humans encounter throughout their lifetime, cells of the adaptive immune system need to achieve a tremendous receptor diversity. Mammalian T- and B-cell receptor (TCR and BCR) diversity is generated through similar mechanisms including the existence of multiple variable (V), diversity (D), and joining (J) genes and genetic recombination of these, as well as generation of junctional diversity through insertion or deletion of nucleotides at the junction sites of the VDJ genes. Isotype class-switching through the usage of different constant region genes (α , δ , ϵ , γ , μ), and somatic hypermutation, which alters the antigen affinity of the BCR through enhanced accumulation of point mutations in the V region genes, further

increases the diversity of the B-cell receptor repertoire (reviewed in (Chi et al., 2020; Nikolich-Zugich et al., 2004)).

Human B and T cells arise from a common lymphoid progenitor (Figure 1), but while T cells mature in the thymus, B-cell differentiation and maturation continues in the bone marrow. Through sequential rearrangements, pro-B cells develop into pre-B cells and eventually immature B cells, which after successful VDJ recombination of the immunoglobulin heavy and light-chain loci, express a complete immunoglobulin (Ig) M (IgM) molecule on their surface (LeBien & Tedder, 2008). Central tolerance in the bone marrow selects immature B cells for self-tolerance through induction of apoptosis or receptor editing (Nemazee, 2017). Transitional B cells leave the bone marrow and home to secondary lymphoid organs, like spleen and lymph nodes to develop into mature, naïve B cells that express both IgM and IgD (LeBien & Tedder, 2008). Upon antigen encounter naïve B cells are activated and proliferate. Co-stimulation with CD40L and cytokines from T follicular helper cells induces class-switch recombination resulting in the isotype switching of activated B cells (Crotty, 2014; Qi, 2016). The specific cytokines determine whether B cells start producing IgA, IgG or IgM antibodies (Moens & Tangye, 2014). This T-cell dependent B-cell activation in secondary lymphoid tissues leads to the formation of germinal centers, transient microstructures from which long-lived plasma cells and memory B cells emerge, which can mediate a humoral immune response (Mesin et al., 2016).

By contrast, for the generation of mature T cells, progenitor cells leave the bone marrow and seed the thymus. Double negative T cells, which lack the expression of both the CD4 and CD8 co-receptor, mature through several developmental stages and start expressing CD4 and CD8. During a process called positive selection, double positive T cells encounter self-antigen presented by major histocompatibility complex (MHC) class I or class II molecules, with three potential outcomes: 1) If the TCR of a T cell is incapable of binding to either MHC molecule, the cell will undergo apoptotic cell death; 2) if the TCR of a T cell binds to MHC class II, the cell receives a survival signal, downregulates CD8 expression and becomes a CD4⁺ single positive cell; and 3) if the TCR of a T cell binds less strongly to MHC class II and binds to MHC class I, it matures into a CD8⁺ single-positive cell (Germain, 2002; Klein et al., 2014). While positive selection ensures that mature T cells recognize MHC-peptide complexes to fight infection, a process called negative selection is critical to avoid recognition and destruction of self. Hence, if T cells bind too strongly to self-antigen-MHC complexes and are prone for self-reactivity, they are either eliminated through induction of apoptosis, or if they have a medium affinity selected for differentiation into regulatory T cells (Tregs) (Klein et al., 2014; Xing & Hogquist, 2012). This mechanism of central tolerance is critical to avoid the development of

autoimmune disorders. Tregs are critical for maintaining peripheral tolerance by suppressing autoreactive T cells that escaped the negative selection process in the thymus (Sakaguchi et al., 2008; Xing & Hogquist, 2012).

Mature T cells can be subdivided into two major classes, CD8⁺ cytotoxic and CD4⁺ helper T cells. CD8⁺ cells recognize antigen-MHC class I complexes, which are expressed by all nucleated cells (Shah et al., 2021). Upon recognition of a foreign antigen, naïve CD8⁺ T cells expand and differentiate into effector T cells, which can mount specific effector responses, for instance the release of lytic granules like perforin and granzyme B, which mediate target cell killing. Further effector T cell responses include secretion of cytokines, such as TNF- α and IFN- γ , leading to the activation and recruitment of macrophages, as well as inhibition of viral replication (Barry & Bleackley, 2002). Following clearance of the pathogen, most CD8⁺ effector cells undergo apoptosis, however some differentiate into memory cells (Harty & Badovinac, 2008). Memory cells are critical to mount rapid effector responses upon encounter of the same pathogen. Naïve CD4⁺ helper T cells are also activated upon antigen encounter, however they recognize specifically antigen-MHC class II complexes, which are only presented by antigen-presenting cells (APCs), such as dendritic cells, macrophages and B cells (Shah et al., 2021). As their name suggests, CD4⁺ T cells provide help to other lymphocytes to mount effective immune responses. Upon activation, naïve CD4⁺ T cells expand and differentiate into distinct T helper cell subsets. T follicular helper cells are one of such specialized subsets. Located in secondary lymphoid organs, T follicular helper cells provide co-stimulatory signals to B cells critical for affinity maturation and antibody production (Crotty, 2014; Qi, 2016). T helper 1 (Th1), Th2 and Th17 CD4⁺ subsets are characterized by the expression of subset specific transcription factors (Th1 - Tbet; Th2 - Gata3, and Th17 - ROR γ t) and produce IFN- γ , IL-4 and IL17 cytokines, respectively (Fang & Zhu, 2017; Tuzlak et al., 2021).

1.2.3 T-cell activation and homeostasis

T-cell activation (reviewed in (Gaud et al., 2018; Shah et al., 2021; Smith-Garvin et al., 2009)) is mediated through the TCR complex, consisting of a TCR α /TCR β or TCR γ /TCR δ heterodimer and six CD3 chains, which form CD3 ϵ /CD3 δ and CD3 γ /CD3 ϵ heterodimers and a CD3 ζ /CD3 ζ homodimer (Figure 3). The majority of cells are $\alpha\beta$ T cells, as they express the TCR α /TCR β heterodimer and only 0.5-5% of T cells express the TCR γ and TCR δ isoforms. The TCR/CD3 complex further associates with CD4 or CD8 co-receptors, and intracellular molecules to form a functional signaling hub. Upon peptide-MHC recognition by the TCR, Src family kinase LCK phosphorylates tyrosines in the ITAM motif of the CD3 chains, leading to the recruitment of ZAP70 kinase, which is activated through phosphorylation by LCK.

Subsequently, ZAP70 phosphorylates the adaptor protein LAT, which in turn recruits the adaptor protein Gads and its constitutive binding partner SLP-76. Together LAT, Gads and SLP76 create a platform for the binding of additional effector molecules, such as PLC γ 1. Protein interaction is often mediated through Src homology 2/3 (SH2/SH3) protein domains. SH2 domains bind to phosphotyrosine-containing sequences, while SH3 domains bind to sequences containing proline and hydrophobic amino acids. For instance, the interaction of PLC γ 1 with LAT and SLP-76 is mediated through its SH2 and SH3 domains, respectively. PLC γ 1 activation following TCR ligation leads to the initiation of several downstream signaling pathways. PLC γ 1 is an enzyme that cleaves phosphatidylinositol 4,5-bisphosphate (PIP₂) into diacyl glycerol (DAG) and inositol 1,4,5-trisphosphate (IP₃), each of them serving as second messengers for signal transduction.

DAG initiates the Ras-Raf-MEK-ERK signaling cascade, which affects the transcriptional activity of several transcription factors, including Elk-1, STAT3 and AP-1 complex (Zhang & Liu, 2002). Recruitment of PKC θ to the plasma membrane and its subsequent activation is also mediated by DAG. PKC θ regulates NF κ B signaling by controlling the assembly of the CBM complex (CARMA1, BCL10, and MALT1), which is critical for activating the I κ B kinase (IKK) complex (Thome et al., 2010). The IKK complex phosphorylates I κ B, leading to its ubiquitination and degradation, thereby releasing NF κ B from its inhibition and enabling NF κ B translocation into the nucleus (Shah et al., 2021).

Moreover, PLC γ 1-generated IP₃ induces Ca²⁺-mediated signaling through stimulation of IP₃R on surface of the endoplasmic reticulum (ER) leading to the release of Ca²⁺ ions stored in the ER (Streb et al., 1983). Consequently, through a mechanism known as store-operated Ca²⁺ entry (SOCE), influx of extracellular Ca²⁺ through Ca²⁺ release-activated Ca²⁺ (CRAC) channels is triggered (Putney, 2011). SOCE is initiated by the transmembrane protein STIM1, which can sense Ca²⁺ concentrations in the ER and upon ER-Ca²⁺ store depletion interacts with the pore-forming, plasma membrane protein ORAI1 to form CRAC channels (Prakriya et al., 2006; Vaeth et al., 2017). Increase in intracellular Ca²⁺ levels following TCR stimulation leads to the activation of Ca²⁺-dependent proteins, such as the calcium and calmodulin-dependent serine/threonine phosphatase calcineurin (Klee et al., 1998). Ca²⁺ binds to calcineurin and calmodulin, required for the phosphatase activity of calcineurin. Removal of phosphates from the N terminus of nuclear factor of activated T-cells (NFAT) transcription factor proteins leads to the exposure of the nuclear localization signal, allowing translocation of NFAT proteins into the nucleus (Macian, 2005; Vaeth & Feske, 2018). Of the five NFAT family proteins, NFATc2 (NFAT1), NFATc1 (NFAT2) and NFATc3 (NFAT4) are expressed in T cells. Despite redundant functions, differences in subset expression, upstream

regulation and interactions with co-activators exist, suggesting distinct roles of NFAT proteins for T-cell functions. For instance, while calcineurin-induced NFATc2 translocation is inhibited by activated p38 mitogen-activated protein (MAP) kinase, but not c-Jun N-terminal kinase (JNK), NFATc1 is phosphorylated and inhibited by JNK (Chow et al., 2000; Gómez del Arco et al., 2000). JNK and p38 signaling are also induced upon TCR stimulation, and involvement of small RHO GTPases in regulation of these two pathways has been suggested (Saoudi et al., 2014; Tybulewicz & Henderson, 2009).

For optimal T-cell activation, T cells engage co-stimulatory molecules (reviewed in (Chen & Flies, 2013)). For instance, binding of CD28 to its ligands B7-1 (CD80) and B7-2 (CD86), which are expressed on APCs, leads to enhanced IL-2 secretion and T-cell survival. While T cells must be rapidly activated and secrete high amounts of proinflammatory cytokines upon infection, a large network of negative regulators exists to avoid chronic immune activation and inflammation. Cytotoxic T-lymphocyte antigen 4 (CTLA-4) binds to B7-1 and B7-2 with greater affinity, but in contrast to CD28, it functions as an immune checkpoint receptor by dampening IL-2 production, cell cycle progression and inhibition of critical T-cell transcription factors, such as NF- κ B, NFAT, and AP1 (Fraser et al., 1999; Krummel & Allison, 1996). CTLA-4 is constantly expressed on regulatory T cells, while in effector T cells it is upregulated upon TCR stimulation. T-cell homeostasis is further regulated by intracellular signaling molecules, for instance SHP-1 (also known as PTPN6), PTPN12 and PTPN22 phosphatases, which dephosphorylate key TCR signaling molecules, including LCK and ZAP70 (Stanford et al., 2012).

Overall, the interplay of activatory and inhibitory receptors and signaling molecules modulates the threshold for T-cell activation. Defects in these proteins can alter the threshold, thereby affecting responses to self-antigen or induction of anergy (Guram et al., 2019; Seidel et al., 2018).

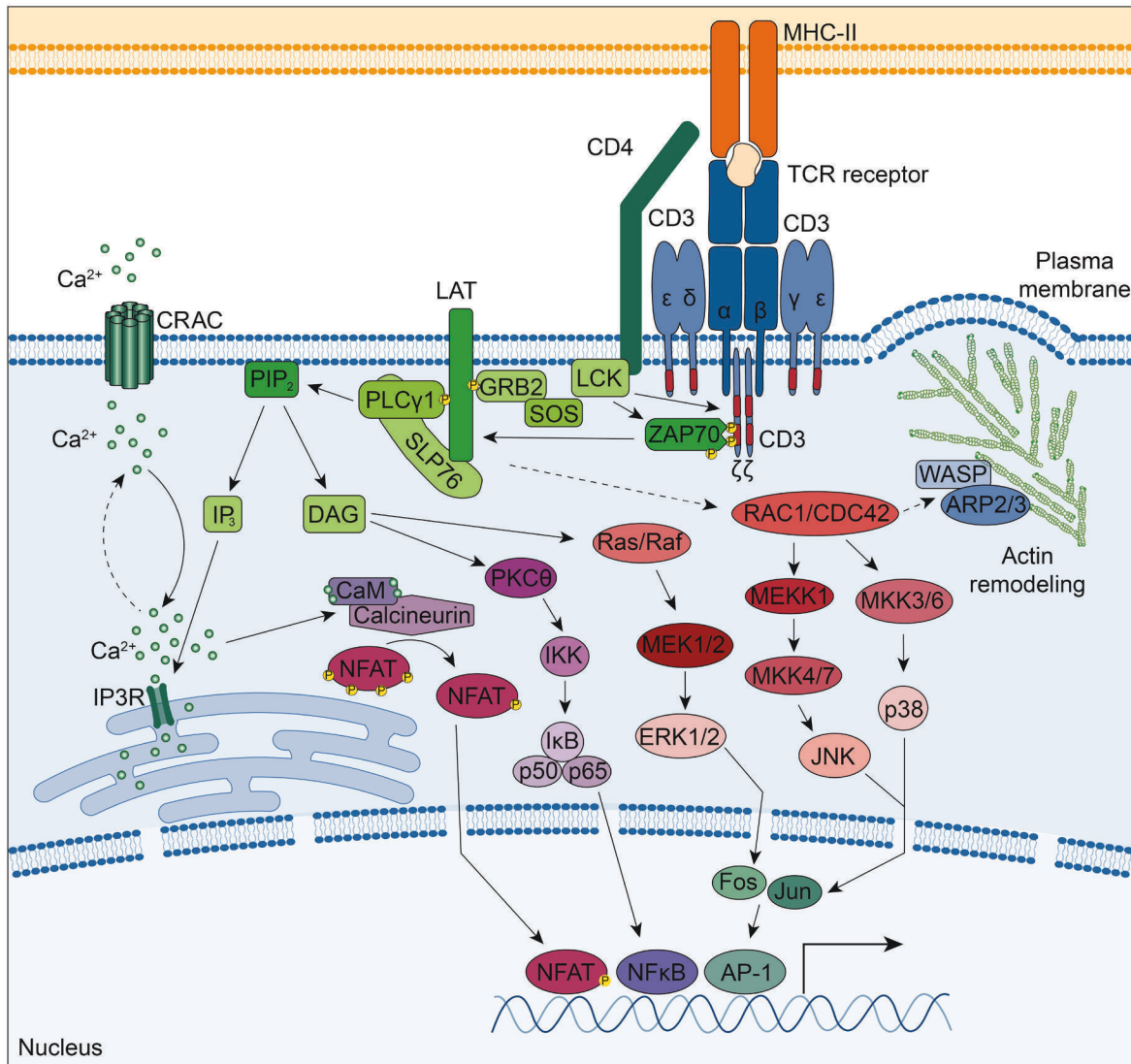


Figure 3. T-cell receptor signaling scheme

Upon peptide-MHC recognition by the TCR, Src family kinase LCK phosphorylates tyrosines in the ITAM motif of the CD3 chains, leading to the recruitment of ZAP70 kinase, which is activated through phosphorylation by LCK. Subsequently, ZAP70 phosphorylates the adaptor protein LAT, which in turn recruits the adaptor protein Gads and its constitutive binding partner SLP-76. Together LAT, Gads and SLP76 create a platform for the binding of additional effector molecules, such as PLCγ1. PLCγ1-generated diacyl glycerol (DAG) initiates the Ras-Raf-MEK-ERK and the PKCθ-IKK-NFκB signaling cascades. PLCγ1-generated IP₃ induces Ca²⁺-mediated signaling, and subsequently Calmodulin (CaM)/Calcineurin-mediated NFAT nuclear translocation. RAC1 and CDC42 small RHO GTPases are activated following TCR ligation leading to actin remodeling and the activation of JNK and p38 effector proteins. Signaling pathways induced by the TCR and co-stimulatory receptors converge in the nucleus and results in the transcriptional activity of key transcription factors, including NFAT, NFκB and AP-1 (Fos/Jun). Figure adapted from (Bhattacharyya & Feng, 2020; Gaud et al., 2018).

1.3 Structure and regulators of the actin cytoskeleton

1.3.1 Actin filament assembly - structure and regulators

There are three basic types of cytoskeletal filaments in eukaryotic cells, actin filaments, microtubules and intermediate filaments. These filaments provide stability against exogenous forces, but at the same time enable rapid changes of cell shape and movement through dynamic remodeling (Pollard & Borisy, 2003; Pollard & Cooper, 2009). With cellular concentrations above 100 μ M, actin is the most abundant protein in most eukaryotic cells. Globular actin (G-actin) polymerizes in a head-to-tail manner to form polar, double-stranded helical actin filaments (F-actin) (reviewed in (Pollard, 2016)). During the transition from the monomeric to the filamentous state, the ATPase activity of F-actin is activated. ATP hydrolysis occurs in two sequential steps, rapid cleavage of ATP followed by slower P_i dissociation. Actin filaments constantly assemble and disassemble in a polarized fashion, as one end, termed barbed end, grows much faster than the other end, the pointed end. This phenomenon, known as treadmilling is essential for actin turnover during cell motility (Pollard & Borisy, 2003).

A large number of actin-binding proteins regulate actin elongation, capping, severing and cross-linking (reviewed in (Pollard, 2016)) (Figure 4). Profilin, a small protein, which preferably binds ATP-bound actin monomers, prevents spontaneous nucleation, promotes filament assembly specifically at barbed ends and catalyzes the ATP/ADP exchange thereby increasing the rate of polymerization (Krishnan & Moens, 2009). Severing of actin filaments is regulated by proteins belonging to the cofilin/ADF and gelsolin family, as well as formins (Andrianantoandro & Pollard, 2006; Goode & Eck, 2007; Nag et al., 2013; Paul & Pollard, 2009). Cofilin, a small essential protein in many organisms, can sever actin filaments to create free barbed and pointed ends. Gelsolin can associate with both monomeric and filamentous actin and regulates actin turnover through its severing and capping functions. The activity of actin-severing proteins is regulated by calcium and ATP levels, intracellular pH, interaction with phospholipids, phosphorylation, proteolytic cleavage and competition with other actin-binding proteins. Cofilin activity for instance is regulated by LIM kinases and phosphatases, such as Slingshot and chronophin (Mizuno, 2013). Several small RHO GTPases through ROCK, PAK and other signaling mediators, influence the activity of these kinases and phosphatases in response to inflammatory, chemotactic, or other stressors (Edwards et al., 1999; Maekawa et al., 1999).

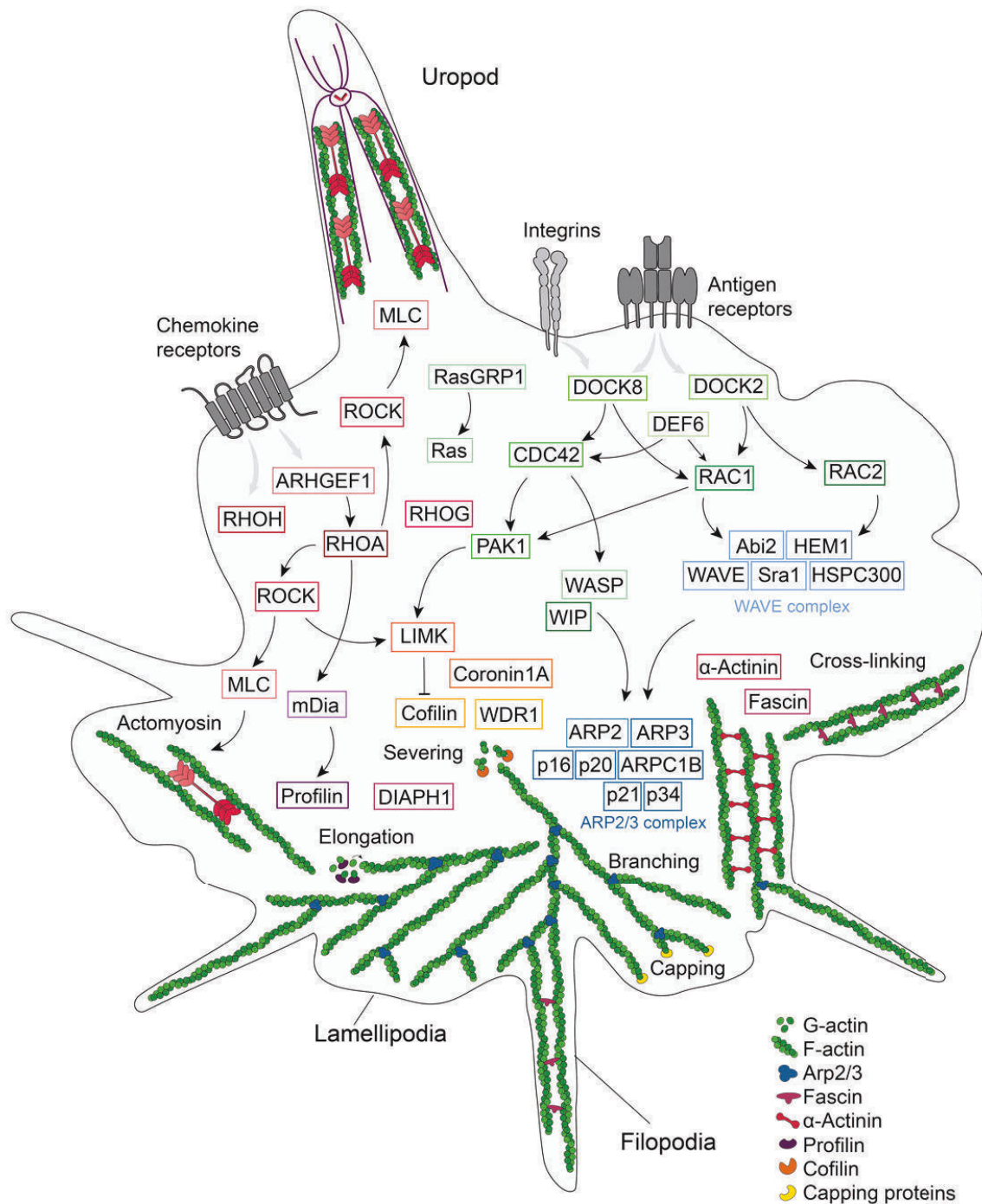


Figure 4. Scheme of actin cytoskeleton regulators

In response to extrinsic signals, antigen receptors, chemokine receptors and integrins initiate signaling cascades that lead to remodeling of the actin cytoskeleton. Upstream signal transducers include RHO GTPases (RHOA, RHOH, RHOG, RAC1, RAC2 and CDC42) and their regulators, such as the guanine nucleotide exchange factors DOCK2 and DOCK8. The RHO GTPases directly bind and activate actin-binding proteins or signal through downstream effectors, including kinases of the PAK, ROCK and LIMK families. Actin-binding proteins regulate actin dynamics by initiating actin nucleation, elongation and branching (profilin, ARP2/3, WASP, formins), actin severing (cofilin), actin cross-linking (fascin, α -actinin), actin capping and actomyosin contraction. Figure adapted from (Dupré et al., 2021).

Actin filament polymerization is initiated by three classes of actin-nucleating proteins. The ARP2/3 complex is critical for actin filament branching (Rouiller et al., 2008), formins stabilize actin polymerization intermediates thereby promoting the elongation of unbranched filaments (Goode & Eck, 2007), and proteins containing tandem repeats of WASP homology 2 domains align several actin monomers to initiate nucleation (Chereau et al., 2005). Small RHO GTPases also play a role in the regulation of actin-nucleating proteins, as they release ARP2/3-activating proteins, such as Wiskott-Aldrich Syndrome protein (WASP) and neural-WASP from their autoinhibitory state (Kim et al., 2000; Spiering & Hodgson, 2011; Takenawa & Miki, 2001).

Capping proteins regulate the access to free ends of actin filaments, critical for instance during actin polymerization at the leading edge of a migrating cells or for endosomal transport (Wang et al., 2021). Capping protein binds to barbed ends, while tropomodulin exclusively interacts with pointed ends (Edwards et al., 2014; Rao et al., 2014). Moreover, other actin-binding proteins such as gelsolin and the ARP2/3 complex also cap barbed or pointed ends, respectively, in addition to their actin severing and nucleating functions (Mullins et al., 1998; Nag et al., 2013).

Assembly of actin filaments into bundles or networks is mediated by actin cross-linking proteins (Matsudaira, 1994). The close proximity of actin-binding domains in α -actinin and fascin promotes the formation of actin bundles, whereas dystrophin connects the F-actin network to the plasma membrane via the dystroglycan complex (Borrego-Diaz et al., 2006; Broderick & Winder, 2005; Fealey et al., 2018; Vignjevic et al., 2006). Actin-binding proteins act in concert to form cell protrusions such as filopodia and lamellipodia. Lamellipodia are thin (0.1-0.2 μm) fan-like protrusions formed through the assembly of branched F-actin networks, which are critical for cell migration (Krause & Gautreau, 2014; Mattila & Lappalainen, 2008). Filopodia are thin protrusions consisting of densely packed bundles of parallel actin filaments. (Ahmed et al., 2010; Chhabra & Higgs, 2007; Mattila & Lappalainen, 2008; Mellor, 2010; Ridley, 2011). They have been suggested to play essential roles in several key immune-cell processes, including directed cell migration (Meyen et al., 2015), leukocyte extravasation (Song et al., 2014) and target capture during phagocytosis (Kress et al., 2007; Vonna et al., 2007).

1.3.2 Network of RHO GTPases, GEFs, GAPs and GDIs

The family of small RHO GTPases consists of around 20 family members, which are key regulators of actin cytoskeleton dynamics. RHO GTPases are a subfamily of the Ras superfamily of small GTPases, which function as binary molecular switches that cycle between an inactive guanosine diphosphate (GDP)-bound state and an active guanosine triphosphate (GTP)-bound state (Gray et al., 2020).

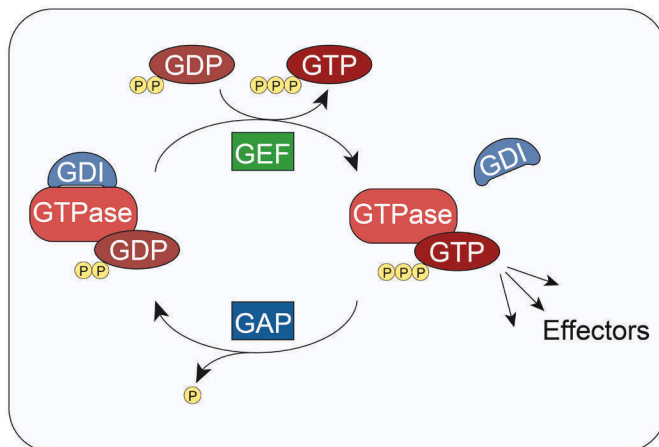


Figure 5. RHO GTPase regulation

RHO GTPases cycle between an inactive guanosine diphosphate (GDP)-bound state and an active guanosine triphosphate (GTP)-bound state. Upon activation, small RHO GTPases can bind to effector proteins and regulate downstream signaling pathways. Guanine nucleotide exchange factors (GEFs) catalyze the GDP/GTP exchange of GTPases, leading to their activation, while GTPase activating proteins (GAPs) facilitate GTP hydrolysis, thereby inactivating the GTPase. Guanine nucleotide dissociation inhibitors (GDI) bind GDP-bound RHO GTPases, block nucleotide dissociation and inhibit GTPase activation. Additionally, binding of GDIs to GTP-bound GTPases can block GTP hydrolysis and GDIs can facilitate the release of RHO GTPases from cellular membranes. Adapted from (Gray et al., 2020).

Upon activation, small RHO GTPases can bind to effector proteins and regulate downstream signaling pathways. The activation/deactivation cycle is regulated by a large number of guanine nucleotide exchange factors (GEFs), GTPase activating proteins (GAPs) and guanine nucleotide dissociation inhibitors (GDIs) (Figure 5). GEF proteins catalyze the GDP/GTP exchange of GTPases, resulting in their activation. Two structurally distinct GEF families, the DBL-homology domain family, consisting of over 70 proteins, and the dedicator of cytokinesis (DOCK) homology region domain family, regulate the activation of small RHO GTPases (Rossman et al., 2005; Thompson et al., 2021). In contrast, GAP proteins facilitate GTP hydrolysis, leading to the inactivation of the GTPase (Bos et al., 2007; Cherfils & Zeghouf,

2013). GDI proteins have three distinct functions (Cherfils & Zeghouf, 2013; DerMardirossian & Bokoch, 2005; Garcia-Mata et al., 2011). They can bind GDP-bound RHO GTPases and block nucleotide dissociation, thereby inhibiting GTPase activation. Moreover, binding of GDIs to GTP-bound GTPases can block GTP hydrolysis and GDIs can facilitate the release of RHO GTPases from cellular membrane. The complex interplay of GEFs, GAPs and GDIs enables spatiotemporally restricted activation of small RHO GTPases.

Effector proteins of small RHO GTPases, such as the serine/threonine protein kinase families ROCK, PAK and LIMK, as well as WASP, N-WASP and WAVE complex family members, subsequently transmit the signal to actin-binding proteins, including ARP2/3 and cofilin, which control the nucleation, severing and capping of actin fibers (Figure 4) (Spiering & Hodgson, 2011). Hence, distinct sets of upstream regulators and downstream effector proteins, determine the specific functions of individual RHO GTPases, critical for various immune cell functions, including the formation of cell protrusions, cell contractility, adhesion and immune synapse (IS) formation (Etienne-Manneville & Hall, 2002; Heasman & Ridley, 2008; Ridley, 2011; Tybulewicz & Henderson, 2009). For instance, RHOA contributes to the formation of stress fibers and focal adhesions ensuring contractility of the cell by activating mDia, ROCK and further downstream effectors (Burrige & Guilluy, 2016; Chrzanowska-Wodnicka & Burrige, 1996). In contrast, cell division cycle 42 (CDC42) induces the formation of filopodia through several effector proteins, including mDia, IRSp53, WASP and PAK (Ahmed et al., 2010; Mellor, 2010). Further, interaction of RAC family members with the WAVE Regulatory Complex has been shown to be essential for lamellipodia formation (Mehidi et al., 2019; Ridley et al., 1992). While there is clear evidence for a role of RHOA in stress fiber, RAC1 in lamellipodia and CDC42 in filopodia formation, crosstalk between these atypical RHO GTPases during the formation of cell protrusions has been described. While CDC42 cannot initiate lamellipodia formation in cells lacking RAC expression, it can clearly promote RAC-dependent lamellipodia, demonstrating the cross-regulatory role of RHO GTPases (Schaks et al., 2021). Further, CDC42-mediated formation of lateral filopodia has been suggested to be initiated through a DOCK4 - RAC1 signaling axis (Abraham et al., 2015).

The importance of this finely tuned network of RHO GTPases, GEFs, GAPs, GDIs and effector proteins is further demonstrated by the fact that defects in several of these proteins underly distinct inborn errors of immunity (IEIs) (Aydin et al., 2015; Burns et al., 2017; Dobbs et al., 2015; Dupré et al., 2021; Dupré & Prunier, 2023; El Masri & Delon, 2021; Engelhardt et al., 2015; Hsu et al., 2019; Janssen & Geha, 2019; Kalinichenko et al., 2021; Lam et al., 2019; Lougaris et al., 2019; Martinelli et al., 2018; Papa et al., 2020; Salzer et al., 2016; Salzer et al., 2020; Sharapova et al., 2019; Sprenkeler et al., 2021; Su, 2010; Su & Orange, 2020;

Takenouchi et al., 2015). Hence, despite certain overlapping functions, for instance GEF activity towards CDC42, as has been described for numerous GEFs (Harada et al., 2012; Hayakawa et al., 2005; Mavrakis et al., 2004; Meller et al., 2004; Miyamoto et al., 2007; Nishikimi et al., 2005), each protein seems to have a distinct regulatory role that cannot be compensated for. This specificity is likely a consequence of tissue-specific expression, subcellular localization and interaction with distinct binding partners (Fritz & Pertz, 2016; Hodge & Ridley, 2016; Nakamura et al., 2017; Pertz, 2010; Tybulewicz & Henderson, 2009).

1.3.3 Dedicator of cytokinesis family proteins

In mammalian cells, the DOCK family consists of 11 members, which act as guanine nucleotide exchange factors to activate small RHO GTPases. Based on sequence similarity, the DOCK proteins can be grouped into four subfamilies, DOCK-A to DOCK-D (Figure 6). All DOCK proteins contain two evolutionary conserved DOCK homology regions (DHR). The DHR1 domain is critical for recruitment of DOCK proteins to specific intracellular membranes through binding of phosphatidylinositol (3,4,5)-trisphosphate (Côté et al., 2005; Kobayashi et al., 2001; Premkumar et al., 2010). Whereas the DHR2 domain is pivotal for binding and activation of the respective small RHO GTPase by catalyzing the GDP-GTP exchange reaction (Brugnera et al., 2002; Côté & Vuori, 2002; Yang et al., 2009). In addition to the common DHR1 and DHR2 domains, there are structural differences between the subfamilies. DOCK-A and -B subfamilies contain an additional SH3 domain and a proline-rich region (PxxP), while DOCK-D family members harbor an additional pleckstrin homology (PH) domain (Harlan et al., 1994; Lemmon, 2007). For DOCK11 it has also been shown that residues 66-126 within the N-terminus of the protein are required to provide a positive feedback loop for CDC42 activation (Lin et al., 2006).

Moreover, DOCK family members preferentially activate specific RHO GTPases. For instance, DOCK-A and DOCK-B show a substrate specificity for RAC1, while DOCK-D (also called zizimin in mice) family members have been shown to activate CDC42. DOCK-C family members show undefined or dual substrate specificities (Kulkarni et al., 2011; Meller et al., 2005; Shi, 2013). In addition to difference in structure and substrate specificity, DOCK proteins also show distinct cellular expression (Figure 7). While many DOCK family members are more ubiquitously expressed, DOCK2, DOCK8, DOCK10 and DOCK11 are expressed predominantly in cells of the hematopoietic system.

Defects in DOCK2 and DOCK8 cause distinct inborn errors of immunity, demonstrating the role of DOCK family members for immune cell function (Alizadeh et al., 2018; Aydin et al.,

2015; Dobbs et al., 2015; Engelhardt et al., 2015; Moens et al., 2019; Su, 2010). Studies of patients presenting with these inherited immune disorders as well as murine models have uncovered a variety of immune-cell functions regulated by DOCK2 and DOCK8 (Biggs et al., 2017; Kearney et al., 2017; Kunimura et al., 2020; Nishikimi et al., 2013).

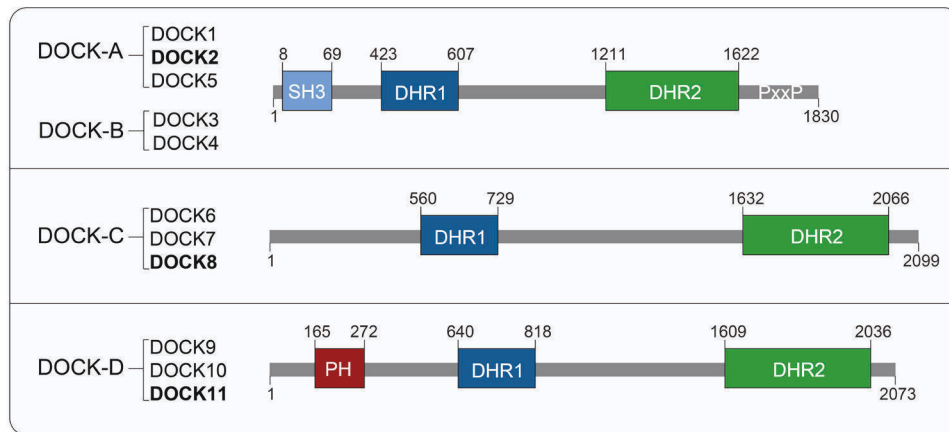


Figure 6. Scheme of DOCK family protein structure

The 11 DOCK proteins are grouped into four subfamilies, DOCK-A to DOCK-D, based on sequence similarity. Members of each subfamily are listed and the DOCK proteins on which the schematic structures are based are highlighted in **bold**. DOCK homology regions 1 (DHR1) and DHR2 are found in all DOCK proteins. The DHR1 domain mediates binding to phospholipids and the DHR2 domain catalyzes the GDP-GTP exchange reaction to activate the respective RHO GTPase. Additionally, DOCK-A and -B subfamilies contain a Src-homology 3 (SH3) domain and a proline-rich region (PxxP), while DOCK-D family members harbor a pleckstrin homology (PH) domain. Figure adapted from (Shi, 2013).

For instance, DOCK8 has been shown to be critical for CD4 T helper cell subset formation (Tangye et al., 2017), T-cell proliferation and effector functions (Janssen et al., 2017; Randall et al., 2011; Zhang et al., 2009), the development and survival of NKT cells (Crawford et al., 2013), immune synapse formation (Ham et al., 2013; Janssen et al., 2017; Mizesko et al., 2013; Randall et al., 2009), NK-cell cytotoxicity (Ham et al., 2013; Mizesko et al., 2013), migration of T cells, dendritic cells and macrophages (Harada et al., 2012; Krishnaswamy et al., 2015; Shiraishi et al., 2017; Zhang et al., 2014), B-cell development, peripheral B-cell tolerance and antibody production (Aydin et al., 2015; Engelhardt et al., 2015; Jabara et al., 2012; Janssen et al., 2014; Randall et al., 2009).

DOCK2 has also been associated with critical roles in T- and B-cell development (Fukui et al., 2001; Tanaka et al., 2007), T-cell proliferation and immune synapse formation (Sanui et al., 2003), NK-cell cytotoxicity (Dobbs et al., 2015; Moens et al., 2019; Sakai et al., 2013),

chemotaxis and migration of lymphocytes, neutrophils as well as dendritic cells (Dobbs et al., 2015; Fukui et al., 2001; Gotoh et al., 2008; Kunisaki et al., 2006; Moens et al., 2019; Nishikimi et al., 2009; Nombela-Arrieta et al., 2004), as well as cytokine production (Dobbs et al., 2015; Gotoh et al., 2010).

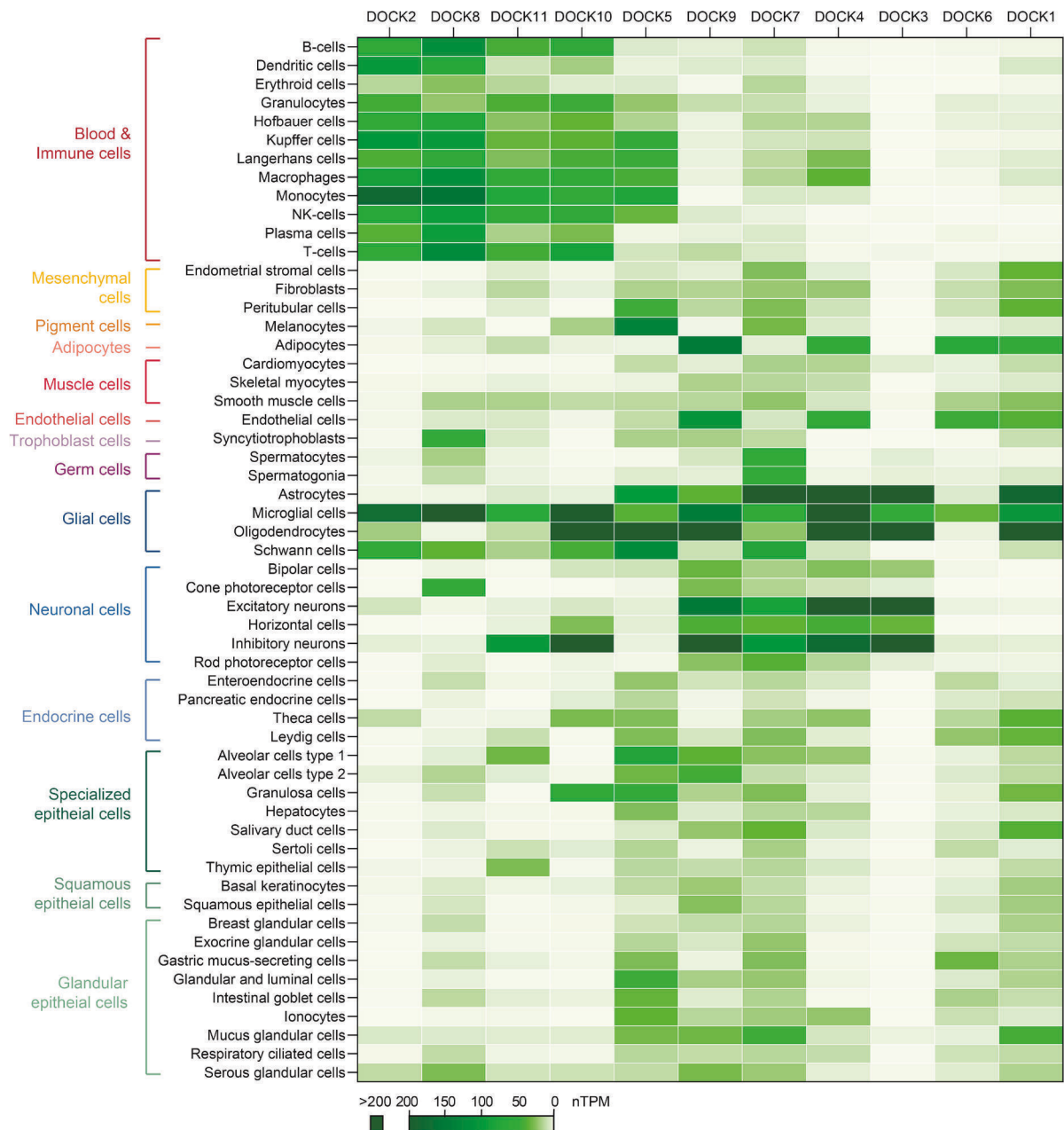


Figure 7. DOCK family members - single cell RNA expression

Heatmap depicts transcript expression levels of DOCK family members in selected cell types. Normalized expression ("nTPM"), summarized per gene from 30 datasets (rna_single_cell_type.tsv.zip), was retrieved from the Human Protein Atlas version 22.0 (<https://v22.proteinatlas.org/download>) (Karlsson et al., 2021).

Given their tissue expression (Figure 7), other DOCK proteins, such as DOCK10 or DOCK11, may also play a role in hematopoietic cells. Indeed, DOCK10 has been suggested to play a role in B-cell maturation and function, as *Dock10*-knockout mice showed lower marginal zone and follicular helper B cells in spleen and peripheral blood (García-Serna et al., 2016), increased CD23 expression on follicular B cells (García-Serna et al., 2016), and reduced proliferation capacity upon anti-CD40 and IL-4 stimulation (Gerasimčik et al., 2017).

Similarly, the study of *Dock11*-knockout mice, has revealed a role for DOCK11 in early bone marrow development and marginal zone B-cell formation, and in B-cell intrinsic signaling critical for the expansion of antigen-specific germinal center B cells following immunization (Matsuda et al., 2015; Sakamoto & Maruyama, 2020). Moreover, reduction of DOCK11 expression was associated with immunosenescence along with aging in mice (Sakabe et al., 2012; Sakamoto et al., 2017). DOCK11 has been shown to activate the small RHO GTPase CDC42 and thereby promote the formation of filopodia.

Despite these findings suggesting a role for DOCK10 and DOCK11 in murine B-cell development and function, the function of these two DOCK proteins in other hematopoietic cells, including T lymphocytes, or their implication in human immunological disease is unknown.

1.4. Rare inherited disorders of the hematopoietic system and the actin cytoskeleton

1.4.1 Introduction to inborn errors of immunity

To date more than 485 distinct IELs or primary immunodeficiencies (PIDs) are known (Bousfiha et al., 2022; Tangye et al., 2022). The advancement in next-generation sequencing and the increasing accessibility and affordability of this technique have accelerated the discovery of novel IELs (Bamshad et al., 2011; Meyts et al., 2016; Tangye et al., 2022). Historically, PIDs were defined mainly by increased susceptibility to infections. However, in the past few years it has become apparent that overt activation of the immune system also contributes to a plethora of manifestations in patients with IELs (Flinn & Gennery, 2022; Goudouris, 2021; Notarangelo et al., 2019; Ren et al., 2021; Tangye et al., 2022).

The identification of pathogenic variants underlying inborn errors of immunity is critical for patient care. In addition, through in-depth research aiming to dissect the central molecular

mechanisms of these novel diseases, researchers have frequently uncovered basic principles of immune-cell function.

1.4.2 IEIs with immune dysregulation

Defects leading to overt immune-cell activation or impairment of regulatory mechanisms critical for preventing immune reactions against self can lead to the development of autoinflammatory or immune dysregulation disorders.

The IUIS classification from 2022 categorizes 52 diseases as IEI with immune dysregulation and 56 as autoinflammatory disorders (Bousfiha et al., 2022; Tangye et al., 2022). The immune dysregulation disorders are further divided into subclasses, such as familial or primary hemophagocytic lymphohistiocytosis (HLH), regulatory T-cell defects, immune dysregulation with colitis, and autoimmune lymphoproliferative syndrome (ALPS, Canale-Smith syndrome) (Bousfiha et al., 2022; Tangye et al., 2022). Autoinflammatory disorders include type 1 interferonopathies, as well as inflammasome-dependent and independent disorders. Patients with these disorders often suffer from a combination of immunodeficiency with additional manifestations, including systemic inflammation, autoimmunity, lymphoproliferation and in some cases an increased risk of cancer (Costagliola et al., 2022; López-Nevado et al., 2021). In recent years many distinct pathomechanisms have been identified which underly disorders of immune dysregulation or autoinflammation (Alroqi et al., 2017; Lin & Goldbach-Mansky, 2022; Masters et al., 2009; Papa et al., 2020; Ren et al., 2021). For instance, defects in perforin or other proteins involved in cytotoxic granule formation and release, which result in severely impaired lymphocyte cytotoxicity, have been associated with hemophagocytic lymphohistiocytosis (Bode et al., 2012; Filipovich, 2009; Janka, 2007; Janka & Lehmborg, 2013; Morimoto et al., 2016; Stepp et al., 1999; Voskoboinik & Trapani, 2013). In case of familial HLH, cytotoxic defects result in accumulation of infected antigen-presenting cells, which in turn causes chronic stimulation of cytotoxic T and NK cells. These cells respond to the constant stimulation with production of inflammatory cytokines and infiltration of various tissues, including bone marrow, liver and central nervous system. The cytokine storm caused by hyperactivation and uncontrolled proliferation of T cells, results in hyperactivation of macrophages. In such conditions, hemophagocytosis, and predominantly phagocytosis of erythrocytes, is often observed in the bone marrow, spleen or lymph nodes. In addition, affected patients show other clinical manifestations commonly seen in immune dysregulation syndromes, such as persistent fever, hepatosplenomegaly and multiorgan failure.

The prototypic immune dysregulation disorder related to impaired function of regulatory T cells is the immune dysregulation, polyendocrinopathy, enteropathy, X-linked (IPEX) syndrome (C. L. Bennett et al., 2001; Park et al., 2020; Wildin et al., 2001; Wildin et al., 2002). IPEX is a rare genetic disorder caused by mutations in the X-linked gene Forkhead box P3 (*FOXP3*). Common clinical symptoms include autoimmune enteropathy, rash, thyroid disease and diabetes. The transcription factor *FOXP3* is critical for determining the lineage specification and function of CD4⁺CD25⁺ Tregs (Fontenot et al., 2003; Hori et al., 2003; Khattry et al., 2003). *FOXP3* induces the expression of several of the key Treg surface markers, including the inhibitory receptor CTLA-4 and the IL-2 receptor (CD25), which competes with activated effector T cells for endogenous IL-2 (Gavin et al., 2007; Lin et al., 2007; Ohkura et al., 2013; Pandiyan et al., 2007). Moreover, *FOXP3* is critical for the expression of the inhibitory cytokine IL-35, and also dampens the expression of pro-inflammatory cytokines through inhibition of other T-cell transcription factors, such as NFAT and NF- κ B (Bettelli et al., 2005; Collison et al., 2007; Olson et al., 2013). Pathogenic mutations in *FOXP3* lead to impaired Treg function and consequently lack of immune suppression, resulting in an overactivated immune response. Treg cells are specifically crucial to maintain the immune tolerance against self-antigens, through suppression of autoreactive CD4⁺ T cells, which have “escaped” the negative selection process in the thymus (Josefowicz et al., 2012; Rocamora-Reverte et al., 2020). Consequently, patients with *FOXP3* mutations commonly present with autoimmune manifestations. Germline mutations in *FOXP3* target genes, such as *CTLA-4* and *IL2RA* have also been described to cause immune dysregulation disorders with predominant autoimmune manifestations (Caudy et al., 2007; Gambineri et al., 2018; Kuehn et al., 2014; Schubert et al., 2014; Schwab et al., 2018; Sharfe et al., 1997; Teft et al., 2006; Walker & Sansom, 2011).

Patients with mutations in *LRBA* and *DEF6*, which affect trafficking of CTLA-4, showed similar clinical manifestations (Alkhairy et al., 2016; Habibi et al., 2019; Lo et al., 2015; Serwas et al., 2019). While CTLA-4 is constitutively expressed on regulatory T cells, other CD4⁺ and CD8⁺ subsets upregulate CTLA-4 surface expression following T-cell activation. In line with a role of CTLA-4 in negatively regulating T-cell activation, murine studies have linked CTLA-4 deficiency to lymphoproliferation, increased levels of T-cell activation markers and cytokine production (McCoy et al., 1999; Tivol et al., 1995; Walunas et al., 1994; Waterhouse et al., 1995).

In addition to reduced number of function of Tregs, shifts in CD4⁺ Th1, Th2 and Th17 cell subsets have also been linked to various autoimmune and immune dysregulation disorders including inflammatory bowel diseases, systemic lupus erythematosus and rheumatoid

arthritis (Chemin et al., 2019; Imam et al., 2018; Romagnani, 1997; Suárez-Fueyo et al., 2016; Talaat et al., 2015).

Autoinflammatory disorders have frequently been associated with increased activation of the inflammasome. In 1997, inherited mutations in *MEFV*, encoding for pyrin, were suggested to cause Familial Mediterranean fever (FMF), the most common monogenic autoinflammatory disease, characterized by recurrent episodes of fever and polyserositis ("A candidate gene for familial Mediterranean fever," 1997; Consortium, 1997; The French FMF Consortium et al., 1997; The International FMF Consortium, 1997). Since then several gain-of-function mutations in inflammasome sensors, including *NLRP3*, *NLRC4* and *NLRP1*, have been identified as the underlying cause of systemic inflammation with increased levels of pro-inflammatory cytokines, such as IL-1 β and IL-18 (Aganna et al., 2002; Aksentijevich et al., 2002; Aksentijevich et al., 2007; Canna et al., 2014; Dowds et al., 2004; Grandemange et al., 2017; Hoffman et al., 2001; Romberg et al., 2014).

In addition, several defects in other genes that induce inflammasome activation have been identified. These include hypermorphic *PLCG2* mutations, suggested to increase intracellular calcium levels and thereby trigger assembly of the NLRP3 inflammasome (Chae et al., 2015; G. S. Lee et al., 2012; Zhou et al., 2012). Moreover, biallelic hypomorphic mutations in Mevalonate Kinase (*MVK*) underlying hyperimmunoglobulinemia D syndrome (HIDS) have been linked to increased IL-1 β secretion and inflammasome activation (Akula et al., 2016; Dorfleutner & Stehlik, 2016; Drenth et al., 1999; Houten et al., 1999; Kuijk et al., 2008; Mandey et al., 2006; Normand et al., 2009; Park et al., 2016). *MVK* is a key enzyme in the mevalonate pathway, critical for cholesterol/isoprenoid biosynthesis (Miziorko, 2011). Defective *MVK* leads to depletion of intracellular geranylgeranyl pyrophosphate, thereby affecting the activity of small RHO GTPases, which depend on isoprenylation. For instance, isoprenoid depletion diminishes the activity of RHOA, a small RHO GTPase known to activate the serine-threonine kinases PNK1 and PNK2. These kinases have been shown to phosphorylate pyrin, initiating 14-3-3 binding and pyrin inhibition (Gao et al., 2016; Park et al., 2016). Hence, *MVK* deficiency is suggested to induce pyrin activation through reduced RHOA activity (Park et al., 2016). Moreover, diminished isoprenylation has also been linked to RAC1/PI3K/PKB-mediated caspase-1 activation and increased IL-1 β secretion (Kuijk et al., 2008). Eventually, defects in *MVK* have also been linked to NLRP3 inflammasome activation, although the exact underlying pathomechanisms is not fully understood (Skinner et al., 2019).

Taken together, these studies have identified potential molecular links between HIDS, FMF and other inflammasome-related diseases, thereby opening novel avenues for patient

treatment. Nevertheless, dissecting the impact of each of the suggested pathomechanisms to the clinical presentation of patients with mevalonate kinase deficiency will be an interesting field for future research.

More recently, mutations in actin-related genes, such as *WAS*, *WDR1* and *CDC42*, have also been associated with inflammasome activation. The Wiskott-Aldrich Syndrome (*WAS*) was initially described as an X-linked inherited disease characterized by recurrent infections, thrombocytopenia and eczema (Aldrich, 1954; Ochs et al., 1980; Wiskott, 1937). Over the past decades, the identification of additional patients with *WAS* deficiency revealed a broad clinical spectrum, including predominant autoimmune and autoinflammatory features. Molecularly, *WAS* mutations have been linked to enhanced NLRP3 inflammasome activation and increased IL1- β and IL-18 cytokine levels (Lee et al., 2017; Rivers et al., 2021). In contrast, mutations in *WDR1* have been linked to pyrin inflammasome activation, likely triggered through the formation of mutant *WDR1* aggregates (Kim et al., 2015; Standing et al., 2017). The concept that protein aggregates might trigger inflammasome assembly is further supported through reports of *CDC42* C-terminal variants, which lead to aberrant palmitoylation and localization in the Golgi, thereby promoting pyrin activation (Bekhouche et al., 2020; Lam et al., 2019; Nishitani-Isa et al., 2022). Although inflammasome components have been shown to co-localize with actin-rich cellular compartments (Waite et al., 2009), it is unclear whether defects in proteins that regulate actin dynamics, such as *WASP* or *WDR1*, control inflammasome activation in an actin-dependent or -independent manner.

1.4.3 Actin-related inborn errors of immunity

An increasing number of inborn errors of immunity is caused by defects in actin-regulatory proteins. Besides the above discussed role in inflammasome formation and hyperinflammation, study of these clinically distinct actin-related IELs has unraveled key roles of actin regulators in numerous immune cell functions (Aydin et al., 2015; Burns et al., 2017; Dobbs et al., 2015; Dupré et al., 2021; Dupré & Prunier, 2023; El Masri & Delon, 2021; Engelhardt et al., 2015; Hsu et al., 2019; Janssen & Geha, 2019; Kalinichenko et al., 2021; Lam et al., 2019; Lougaris et al., 2019; Martinelli et al., 2018; Papa et al., 2020; Salzer et al., 2016; Salzer et al., 2020; Sharapova et al., 2019; Sprenkeler et al., 2021; Su, 2010; Su & Orange, 2020; Takenouchi et al., 2015). For example, the Wiskott-Aldrich Syndrome, first described clinically in 1937 (Aldrich, 1954; Wiskott, 1937) and later linked to mutations in the *WAS* gene (Derry et al., 1994), has been subject of extensive research over the past decades and revealed critical roles for actin remodeling in both the adaptive and the innate immune system, as well as in other hematopoietic cells. *WAS* deficiency has been linked to alterations

in T-cell activation, Th subset differentiation, function of regulatory T cells, B-cell homeostasis and autoantibody formation, as well as inflammasome assembly (discussed in chapter 1.5.2.) (Bouma et al., 2014; Calvez et al., 2011; Castiello et al., 2014; Kolhatkar et al., 2015; Lee et al., 2017; Maillard et al., 2007; Morales-Tirado et al., 2004; Recher et al., 2012; Simon et al., 2014; Trifari et al., 2006). In line with its role in actin nucleation, WASP has been shown to be critical for cell morphology, such as podosome formation (Linder et al., 1999), as well as migration of several hematopoietic cells, such as dendritic cells, neutrophils, macrophages and lymphocytes (de Noronha et al., 2005; Snapper et al., 2005; Zicha et al., 1998). These cellular and molecular changes have been linked to a plethora of clinical manifestations in WAS, the most common being microthrombocytopenia and susceptibility to infections, and varying frequency of eczema, autoimmunity and autoinflammation, as well as malignancy (Albert et al., 2011; Candotti, 2018). Moreover, patients with homozygous mutations in Wiskott-Aldrich syndrome (WAS) protein-interacting protein (*WIP*) have been identified. *WIP* deficiency leads to premature degradation of WASP, explaining the WAS-like clinical resemblance with recurrent infections, bloody diarrhea, and thrombocytopenia (Lanzi et al., 2012; Pfajfer et al., 2017; Schwinger et al., 2018).

To date, roughly 20 inborn errors of immunity caused by defects in actin-related proteins have been described. Some of the affected proteins, such as WASP, *WIP*, but also *PSTPIP1*, *ARPC1B*, *HEM1*, *WDR1* and *CARMIL2* are directly involved in several steps of actin remodeling, including actin filament branching, cross-linking, actin elongation and severing, as well as actin capping (Figure 4) (reviewed in (Dupré & Prunier, 2023; Pollard, 2016)).

Other actin-related disorders are caused by mutations in upstream regulators of actin dynamics, namely small RHO GTPases, such as *RAC2*, *CDC42*, *RHOG* and *RHOH*, and their regulators, including *DOCK2*, *DOCK8* and *ARHGEF1* (Alizadeh et al., 2018; Bouafia et al., 2019; Crequer et al., 2012; Dobbs et al., 2015; Engelhardt et al., 2015; Hsu et al., 2019; Kalinichenko et al., 2021; Lam et al., 2019; Lougaris et al., 2019; Martinelli et al., 2018; Sharapova et al., 2019; Su, 2010; Su & Orange, 2020; Takenouchi et al., 2015; Zhang et al., 2009). For instance, defects in the dedicator of cytokinesis family members, *DOCK2* and *DOCK8*, guanine nucleotide exchange factors that activate the small RHO GTPases *RAC1* and *CDC42*, cause distinct combined immunodeficiencies (Alizadeh et al., 2018; Dobbs et al., 2015; Engelhardt et al., 2015; Moens et al., 2019; Su, 2010; Zhang et al., 2009). Specific clinical and cellular features, including bacterial and viral recurrent infections, T-cell lymphopenia, impaired lymphocyte migration and impaired NK-cell degranulation have been reported for both *DOCK2* and *DOCK8* deficiency (Alizadeh et al., 2018; Dobbs et al., 2015; Engelhardt et al., 2015; Moens et al., 2019; Su, 2010; Zhang et al., 2009). Other

manifestations, for instance severe food allergy, atopic dermatitis, as well as increased susceptibility to malignancy and autoimmunity are more commonly observed in *DOCK8*-deficient patients (Engelhardt et al., 2015; Su, 2010; Zhang et al., 2009), while *DOCK2* deficiency seems to have generally a more severe disease progression with early-onset life-threatening invasive bacterial and viral infections (Dobbs et al., 2015; Moens et al., 2019). Studies using *Dock2*- and *Dock8*-knockout mice have further suggested a role for these *DOCK* proteins in regulating CD8⁺ T-cell synapse assembly and cytotoxicity (Randall et al., 2011; Sakai et al., 2013; Sanui et al., 2003).

The clinical spectrum of patients with de novo heterozygous missense mutations in *CDC42* is unusually broad and clinically challenging (Su & Orange, 2020). In 2015, the first patients with *CDC42* mutations at p.Tyr64Cys were described (Takenouchi et al., 2015). The characteristic clinical features of this new disease, called Takenouchi-Kosaki syndrome, included facial dysmorphism, neurodevelopmental delay and macrothrombocytopenia (Takenouchi et al., 2015). Since the initial description, additional *CDC42* mutations associated with Takenouchi-Kosaki syndrome have been identified. The identified mutations have been demonstrated to have variable impact on *CDC42* activity, localization and interaction with downstream effectors (Martinelli et al., 2018). Clinical disease manifestations include neurodevelopmental delay with variable degrees of intellectual disability, facial dysmorphism, as well as certain cardiovascular, genitourinary, hematological, and immunological defects. Milder forms of the disease are reminiscent of Noonan syndrome, caused by mutations affecting RAS signaling (Martinelli et al., 2018; Roberts et al., 2013; Tartaglia & Gelb, 2010). More recently, C-terminal *CDC42* mutations at p.R186C have been identified as the cause of a distinct disease termed NOCARH (neonatal-onset cytopenia with dyshematopoiesis, autoinflammation, rash, and hemophagocytic lymphohistiocytosis) (Lam et al., 2019). Patients with NOCARH show impaired NK-cell cytotoxicity, a classical feature of HLH, as well as diminished NK-cell migration and conjugate formation. Moreover, increased production of proinflammatory cytokines was observed and several patients responded to treatment with IL-1 or IFN- γ antagonists (Lam et al., 2019). Further, C-terminal *CDC42* variants have been associated with predominant autoinflammatory and hematological disease manifestations (Bekhouche et al., 2020; Gernez et al., 2019; Nishitani-Isa et al., 2022). These initial indications of genotype-phenotype correlations have been challenged through the discovery of a patient carrying the p.Tyr64Cys mutation, previously associated exclusively with Takenouchi-Kosaki syndrome, that also presented with systemic inflammation and life-threatening recurrent infections (Buccioli et al., 2020; Verboon et al., 2020). The ongoing identification of patients with *CDC42* mutations that present with new disease features, including elevated serum IgE and malignancy, illustrates the broad clinical spectrum of *CDC42*

deficiency (Buccioli et al., 2020; He et al., 2020; Szczawinska-Poplonyk et al., 2020; Verboon et al., 2020). Due to the distinct clinical and cellular phenotypes, diagnosis and treatment of these patients remains challenging, further highlighted by the variable outcomes of hematopoietic stem cell transplantation in patients with *CDC42* mutations (Bekhouche et al., 2020; Su & Orange, 2020; Verboon et al., 2020).

Identification of additional actin-related genes underlying novel IELs with distinct clinical and cellular features will help to further uncover the role of specific actin regulators during basic cellular processes, critical for immune-cell function during homeostasis or upon encounter of an infection or malignant cells. Besides their prominent role in regulating actin dynamics, other functions of these proteins may depend on actin-independent activities.

For instance, in addition to its ARP2/3-mediated role in actin nucleation and consequently cell-shape remodeling, WASP has been connected to transcriptional regulation via interaction with chromatin remodeling proteins, for instance in Th1 T cells (Adriani et al., 2007; Taylor et al., 2010; Thrasher & Burns, 2010; Verboon et al., 2015). Moreover, DOCK8, which on one hand regulates actomyosin dynamics in a *CDC42* GEF-dependent manner, has been shown to regulate IL-31 production by helper T cells independent from its GEF function through interaction with MST1 (Kunimura et al., 2020; Yamamura et al., 2017).

In addition to the prominent immune-driven manifestations, many patients with actin-related disorders present with systemic features affecting various cell types and organs. Hence, the study of IELs with a broad clinical spectrum may uncover functions of actin-regulatory proteins beyond the immune system. Eventually, disentangling the pathomechanisms driving these diseases can foster the development of personalized treatment options to further improve patient care.

1.5 Role of the actin cytoskeleton in hematopoietic cells uncovered through study of inborn errors of immunity

1.5.1 Overview of immune cell functions associated with actin-related IELs

In general, study of actin-related IELs has enabled the discovery of many basic principles of actin remodeling and dynamics and uncovered crucial roles of the actin cytoskeleton during various immune cell functions.

The human body is constantly facing challenges, such as the encounter of different kinds of pathogens, mechanical injuries or malignantly transformed cells, which require a rapid and coordinated response from the immune system. Migration to sites of infection, interaction with antigen-presenting cells and engulfment of pathogens or cell debris require constant changes of cell shape, which is mediated by the actin cytoskeleton. Consequently, deleterious mutations in genes encoding for actin binding proteins and actin regulators have been associated to impaired immune cell functions, including defects in cell adhesion, cell migration, phagocytic cup formation, cell-cell interactions, such as immune synapse formation, intracellular signaling and cell activation (Burns et al., 2017; Dupré et al., 2021; Dupré & Prunier, 2023; Moulding et al., 2013; Sprenkeler et al., 2021; Vicente-Manzanares & Sánchez-Madrid, 2004). Many of the involved molecular signaling pathways have been unraveled through study of actin-related IELs. In addition to studies on primary patient material, modeling of these genetic defects in animal models has further advanced our understanding of the distinct roles of actin-regulatory proteins in immune cell function.

1.5.2 Actin cytoskeleton remodeling in migrating immune cells

Immune cell migration is a process that heavily relies on actin remodeling. Leukocytes for instance need to adapt their cellular shape to the surrounding environment during their development in the bone marrow and thymus, when entering or exiting the blood stream during migration in secondary lymphoid organs as well as in the peripheral tissue. For instance, when leukocytes leave the blood circulation to reach a site of infection or tissue damage, a process called transendothelial migration (TEM), they must undergo sequential changes in their cell morphology. The dynamics changes in cell shape are achieved through remodeling of the cytoskeleton and formation of various types of cell protrusions, including lamellipodia, filopodia and podosomes (Ridley, 2011; Vicente-Manzanares & Sánchez-Madrid, 2004).

As a first step of the leukocyte adhesion cascade, proinflammatory stimuli, produced in response to exogenous or endogenous triggers, lead to the upregulation of selectins and intercellular cell adhesion molecule 1 (ICAM-1) on endothelial cells, which mediate the tethering and rolling of leukocytes (van Buul & Hordijk, 2004). A study on WASP deficiency revealed that neutrophils lacking the actin-regulatory protein WASP show impaired clustering of beta2 integrins, which mediate adhesion to ICAM-1 (Fagerholm et al., 2019; Zhang et al., 2006). As a consequence, WASP-deficient neutrophils showed impaired adhesion to endothelial cells and reduced TEM under shear flow conditions (Zhang et al., 2006). In addition to actin-related IELs which influence beta2-integrin clustering and signal transduction, inherited genetic defects in the beta2-integrin-chain itself or in the focal adhesion protein kindlin-3,

which mediates beta2 integrin activation, have been shown to cause leukocyte adhesion deficiency type I and type III, further highlighting the crucial role of beta2 integrins in leukocyte trafficking (Fagerholm et al., 2019).

Following more firm adhesion, intraluminal crawling allows leukocytes to reach the site of transmigration (also called diapedesis). During the migration on the apical endothelial surface, leukocytes form lamellipodia and “invasive podosomes” to sense the endothelial topography and scan the surface to determine the sites permissive for TEM (Carman et al., 2007; Song et al., 2014). Defects in WASP and WASP interacting protein (WIP) have been linked to impaired podosome formation and defective transmigration and the study of these actin regulators underlying IEIs has revealed the crucial role in ARP2/3-driven actin polymerization in the formation of these podosomes (Chou et al., 2006; Linder et al., 1999). Neutrophils of patients with defects in ARPC1B, which is part of the ARP2/3 complex, also showed defective TEM, further underlying the importance of ARP2/3-induced actin remodeling in this process.

Filopodia, thin actin-rich protrusions, which are known for their role in pathfinding and exploration in the environment, have also been linked to TEM (Heasman & Ridley, 2010; Jacquemet et al., 2015; Shulman et al., 2009; Song et al., 2014). It was shown that shear stress can increase the number of filopodia underneath crawling leukocytes and that cells extend these thin protrusions below the layer of endothelial cells before and during transmigration (Shulman et al., 2009). The RHO GTPases RHOA and CDC42 have been implicated in filopodia formation during these processes (Heasman & Ridley, 2010; Shulman et al., 2009; Ward, 2009), however a deeper mechanistic understanding of the involved signaling pathways is still missing. DOCK8, which activates the small RHO GTPases RAC1 and CDC42, has also been shown to play a role during TEM.

In addition to actin cytoskeleton remodeling in leukocytes, actin dynamics in the interacting endothelial cells also influence the leukocyte extravasation (Schnoor, 2015). For instance, the transendothelial migration process can occur transcellularly or paracellularly and changes in cortical actin in ECs can shift the preference between the different routes (Martinelli et al., 2014). In addition, ECs form lamellipodia to close gaps generated by transmigrating leukocytes (Mooren et al., 2014).

Beyond the role of actin-regulatory proteins during TEM, study of actin-related IEI has advanced our understanding of basic molecular processes during many types of immune cell migration. For instance, DOCK8-deficient lymphocytes that migrate in collagen-dense tissues, as can be found in the skin dermis, display an aberrantly elongated phenotype and upon

prolonged migration cell shattering occurs, a new form of cell death that was termed cytothripsis (Zhang et al., 2014). Moreover, several defects in actin regulators have been linked to impaired egress of T cells from the thymus, including deficiencies in DOCK8, CORO1A, DIAPH1 and STK4/MST1 (Föger et al., 2006; Katagiri et al., 2009; Sakata et al., 2007).

1.5.3 Actin dynamics during immune synapse formation and cell activation

In addition to defects in cell migration, leukocytes from patients with actin-related IELs, including WASP, WIP, WDR1, DIAPH1, DOCK2, DOCK8 and HEM1 deficiencies, often show impaired immune synapse (IS) formation and activation (Cook et al., 2020; Dupré et al., 2002; Dupré et al., 2021; Le Floc'h et al., 2013; Orange et al., 2002; Pfajfer et al., 2018; Pfajfer et al., 2017; Randall et al., 2011; Salzer et al., 2020; Sanui et al., 2003; Sasahara et al., 2002). Upon encounter of antigen-presenting cells, migrating leukocytes need to undergo morphological changes, driven by dynamic actin remodeling, to form an immune synapse and induce intracellular signaling (reviewed in (Dupré et al., 2021; Dustin & Cooper, 2000). There are several steps during IS formation, which involve actin dynamics. As a first step, immune cells need to transition from an elongated “migratory” shape to a round shape during contact initiation. Inhibition of the migratory phenotype is mediated for instance through phosphorylation of myosin IIA downstream of TCR-induced signaling (Jacobelli et al., 2004). After the initial contact, T cells form protrusions to scan the APC surface for specific antigen-MHC complexes (Blumenthal & Burkhardt, 2020; Sage et al., 2012). If no specific antigen is found, T cells can detach and move towards the next APC (Bouso, 2008; Martín-Cófreces et al., 2018). The strength of antigen stimulation further determines the stability of an immune synapse. It has been proposed that strong antigen stimulation leads to a Ca²⁺ and ARP2/3-dependent arrest of the T cell leading to a stable immune synapse, whereas weaker antigen stimulation results in a motile synapse, also called kinapse (Dustin, 2008; Moreau et al., 2015). T cells deficient in WASP, known to regulate ARP2/3-dependent actin polymerization, show a tendency to form kinapses, instead of stable synapses, further supporting this concept (Calvez et al., 2011).

Actin dynamics do not only control changes in the overall cellular morphology, but they also promote the assembly of surface receptors into distinct spatial clusters. Retrograde actin flow enables distribution of the TCRs and associated signaling molecules in a supramolecular activation cluster (cSMAC) at the center of the synapse, which is surrounded by the peripheral SMAC (pSMAC) adhesion ring containing the integrin LFA-1 (Dustin, 2009; Dustin & Cooper, 2000; Freiberg et al., 2002). LFA-1 interaction with ICAM-1 is critical for close adhesion of the

T cell to the APC (Dustin, 2007; Springer, 1990). Impaired LFA-1 recruitment, activation and spatial organization of LFA-1 at the IS has been reported for several defects affecting actin regulators, such as WASP and DOCK8, highlighting the role of these proteins in this particular step (Houmadi et al., 2018; Lafouresse et al., 2012; Randall et al., 2011). At the center of the IS, F-actin density is reduced and allows the polarization of the microtubule-organizing center (MTOC) to the immune synapse. In cytotoxic T cells, MTOC polarization is critical for polarized delivery of lytic granules towards the target cell (Stinchcombe et al., 2006). Lytic granules of cytotoxic T cells contain cytotoxic proteins such as perforin or granzyme B and mediate target cell death (Barry & Bleackley, 2002; Voskoboinik et al., 2006). A defect in MTOC or lytic granule polarization has also been described for several actin-related IEIs, including DIAPH1 and WASP deficiencies (De Meester et al., 2010; Kaustio et al., 2021; Orange et al., 2002).

Overall, actin regulators control various steps of IS formation and are closely connected to TCR-induced signaling. On one hand, interaction of the TCR with the peptide-MHC complex present on the surface of APCs initiates a signaling cascade leading to the activation of actin regulators that mediate the above-named changes of the cytoskeletal network (Kumari et al., 2014). The actin filament network, on the other hand, has been implicated in the formation of TCR microclusters, serving as a platform to bring signaling molecules in closer proximity, as well as in modulating Ca^{2+} signaling, thereby regulating T-cell activation (Beemiller & Krummel, 2013; Campi et al., 2005; Valitutti et al., 1995). Concordantly, some defects in actin-regulatory proteins, such as WASP, VAV and DIAPH/mDia family proteins have been linked to diminished expression of specific T-cell cytokines, as well surface molecules, such as CD25 (IL-2R) or CD69 (Calvez et al., 2011; Fischer et al., 1998; Holsinger et al., 1998; Maillard et al., 2007; Thumkeo et al., 2020; Trifari et al., 2006; Wülfing et al., 2000; Zhang et al., 1999). In contrast, one study suggested an inhibitory role of actin remodeling for T-cell activation and cytokine production through modulation of plasma membrane calcium ATPase surface expression (Rivas et al., 2004).

Many links between actin and T-cell activation and signaling have been made based on studies of actin-regulatory proteins. Some studies have investigated whether the observed defects in T-cell activation and cytotoxicity are directly linked to impaired actin remodeling or whether actin-independent roles of the assessed proteins mediate these T cell functions (Butler & Cooper, 2009; Cotta-de-Almeida et al., 2015; Gorman et al., 2012). However, in most cases this remains to be determined. Overall, there seems to be a complex interplay between actin dynamics and TCR-induced signaling pathways and the integration of these multiple signals at the transcription factor level, all of which influence the duration and level of T-cell activation.

As in T cells, actin remodeling also plays a role in NK- and B-cell immune synapse formation and study of actin-related IELs has also helped to uncover many key players of IS formation in these cell types (Cook et al., 2020; Kritikou et al., 2016; Mizesko et al., 2013; Orange et al., 2002; Salzer et al., 2020). While certain actin-mediated pathways may play similar roles across different leukocyte subsets, other actin-dependent functions may be more cell-type specific. For instance, synapses formed between NK cells and activating target cells show increased F-actin densities compared to those formed with inhibitory target cells (Banerjee & Orange, 2010). Actin cytoskeleton dynamics at the NK-cell immune synapse have been proposed to regulate receptor clustering, sequester signaling molecules, such as the inhibitory protein tyrosine phosphatase SHP1, and to mediate the secretion of cytokines and lytic granules (Ben-Shmuel et al., 2021; Matalon et al., 2018). Similarly, actin remodeling has been shown to be critical for B-cell activation by governing the spreading and contraction at the contact zone between B cell and antigen-presenting cell (Fleire et al., 2006), and by modulating BCR mobility and microcluster formation (Treanor et al., 2011; Treanor et al., 2010; Wang et al., 2017). A recent study from the Boztug group showed that the actin regulator HEM1, which is part of the WAVE complex, is critical for cell spreading and B cell immune synapse formation through its role in lamellipodia formation (Salzer et al., 2020). As a consequence of aberrant B-cell synapse formation, disturbed BCR signaling may occur and affect B-cell development and B-cell fate choices, eventually contributing to loss of tolerance and the development of autoimmunity (Salzer et al., 2020).

1.5.4 Role of actin-regulatory proteins in red blood cell formation and morphology

Some inborn errors of immunity that are caused by defects in actin-regulatory proteins also show defects in red blood cell numbers, morphologies and functions (Aydin et al., 2015; Castro et al., 2020; Coppola et al., 2022; Nunes-Santos et al., 2023). While such defects are often attributed to autoimmune-driven destruction of red blood cells, animal studies or pharmacological targeting of actin regulators have suggested RBC intrinsic roles for some of these proteins (Chan et al., 2013; Park et al., 2008; Ubukawa et al., 2020; Wang et al., 2006; Yang et al., 2007).

Red blood cells supply the human body with oxygen, while clearing it from carbon dioxide. To perform this function, RBCs need to have the mechanical properties to withstand the fluid shear stress in larger blood vessels and at the same time be deformable in order to move through capillaries smaller than their diameter. Therefore, RBCs have a unique cortical membrane skeleton, consisting of a network of spectrin, actin, ankyrin, protein 4.1, as well as

several actin-binding proteins, and an overlying lipid bilayer (reviewed in (Gokhin & Fowler, 2016; Lux, 2016)). Band 3 molecules within the plasma membrane form multi-protein complexes, which are unbound or connected to the underlying ankyrin-bound or actin-bound spectrin networks (Lux, 2016). In contrast to other hematopoietic cells, whose actin filaments can extend up to several μm in length, RBCs contain short double-helical actin filaments that lie parallel to the plasma membrane. Roughly 30,000-40,000 of such filaments, which are each about 37 nm in size, exist in one cell (Fowler, 2013; Lux, 2016). The actin filaments are connected by spectrin tetramers forming a quasi-hexagonal network (An et al., 2005; Li & Bennett, 1996; Lux, 2016). Actin dynamics in RBCs are regulated by several actin-binding proteins. These include tropomyosin, suggested to stabilize actin filaments and spectrin-actin-4.1R junctional complexes (An et al., 2007; Cooper, 2002), the actin-capping protein tropomodulin and protein 4.1R, critical for spectrin-actin interactions and attachment of this network to the plasma membrane (Rao et al., 2014; Salomao et al., 2008; Yamashiro et al., 2012). Furthermore, RBCs contain adducin, a barbed-end capping protein, which recruits spectrin and promotes spectrin-actin interactions and dermatin, which also assists in actin-spectrin network assembly and through binding to the glucose transporter attaches actin to the plasma membrane (Khan et al., 2008; Koshino et al., 2012; Kuhlman et al., 1996; Li et al., 1998).

Less is known about the upstream regulators of actin remodeling during erythropoiesis and in mature red blood cells (Mulloy et al., 2010). Patients with defects in the RHO GTPase CDC42 frequently present with anemia, as well as further cytopenias including thrombocytopenia and neutropenia (Coppola et al., 2022; Lam et al., 2019; Takenouchi et al., 2015; Verboon et al., 2020). For patients carrying *CDC42* missense mutations that affect CDC42 prenylation (p.C188Y and p.*192Cext*24) it has been speculated that the anemia observed in these patients is caused by hyperinflammation. While these patients responded to the anti-inflammatory drug anakinra, an interleukin-1 receptor antagonist, anakinra seemed to have no effect on anemia reported in patients with p.R186C variants (Coppola et al., 2022). Instead, it was proposed that the p.R186C variant may affect hematopoietic progenitor cells (Coppola et al., 2022). In line with a role of CDC42 in early RBC development, genetic deletion of *CDC42GAP* in mice, resulting in increased CDC42 activity, caused impaired erythroid differentiation and subsequently severe anemia (Wang et al., 2006). Moreover, in a second study *CDC42*-deficient mice displayed anemia, probably due to a decreased number of erythroid progenitors, while they showed myeloid hyperproliferation and neutrophilia. This disbalance of myelopoiesis and erythropoiesis was suggested to be caused by an altered transcriptional program (Yang et al., 2007). While in humans the role of CDC42 in RBC

development has not been fully investigated, these studies in mice predict that a fine-tune regulation of CDC42 is critical for erythropoiesis.

Erythropoiesis in mammals ends with the enucleation of orthochromatic erythroblasts generating reticulocytes, which leave the bone marrow and mature to erythrocytes in the blood stream. F-actin assembly into an actin-myosin contractile ring is critical for nuclear expulsion and pharmacological inhibition of CDC42 with CASIN blocked the proliferation and enucleation of colony forming units-erythroid cells (Ubukawa et al., 2020). Defects in RAC1, RAC2 and their downstream effector mDia2 have also been shown to cause anemia associated with impaired enucleation, defective cytokinesis during early stages of erythropoiesis, as well as altered cellular deformability (Ji et al., 2008; Kalfa et al., 2006; Watanabe et al., 2013). Moreover, a murine study uncovered the WAVE complex member HEM1 as a critical regulator of erythrocyte skeleton integrity and membrane stability (Chan et al., 2013; Park et al., 2008). Anemia was also reported in two patients with HEM1 deficiency (Castro et al., 2020). The same study also showed that knockdown of *nckap1*, encoding for Hem1, causes anemia in zebrafish, further underling the role of HEM1 for erythrocyte homeostasis (Castro et al., 2020). Defects in actin regulators that affect erythrocyte stability, deformability and enucleation have often been linked to aberrant F-actin structures, suggesting that dynamic remodeling of the actin cytoskeleton is critical for erythrocyte function (Kalfa et al., 2006; Mulloy et al., 2010; Ubukawa et al., 2020). Whether impaired intracellular signaling and transcriptional regulation is also a consequence of disturbed actin remodeling or whether actin regulators affect RBC development in an actin-independent manner often remains to be determined.

1.6 Aims

The aims of this thesis were (1) to identify the genetic defect underlying a novel immune dysregulation syndrome in four patients from four unrelated families (2) uncover novel functions of the identified gene in hematopoietic cells, with specific focus on T lymphocytes and erythroid cells (3) dissect the pathomechanisms in order to identify signaling molecules with potential roles for a larger group of inflammatory and immune dysregulation disorders.

To achieve these aims, we performed whole-exome sequencing on genomic DNA (gDNA) isolated from blood samples of patients. We confirmed and segregated the identified variants through Sanger sequencing using gDNA derived from patients and healthy family members. Using patient-derived material, CRISPR/Cas9 (clustered regularly interspaced short palindromic repeats and associated Cas9 homing endonucleases)-edited cell lines, as well as mouse and zebrafish models we performed a variety of functional and biochemical assays to explore novel functions of the gene of interest. Lastly, identification of the pathomechanisms underlying this novel disease may contribute to the discovery of potential drug targets, thereby fostering the development of personalized treatment options.

2. RESULTS

Chapter 2 of this thesis contains content reproduced with permission from N Engl J Med. 2023 Jun 21. doi: 10.1056/NEJMoa2210054. Epub ahead of print. PMID: 37342957, Copyright © (2023) Massachusetts Medical Society. Reprinted with permission.

The article resulted from work done during the period of this doctoral thesis and was published on June 21, 2023 at <https://www.nejm.org/doi/full/10.1056/NEJMoa2210054>. The author of this thesis acquired the majority of the published data and was involved in the coordination of all experiments, as well as in the assembly of all figures and writing of the manuscript. Individual contributions from all co-authors are specified under **Declaration** on page ii-iii.

ORIGINAL ARTICLE

Systemic Inflammation and Normocytic Anemia in DOCK11 Deficiency

J. Block, C. Rashkova, I. Castanon, S. Zoghi, J. Platon, R.C. Ardy, M. Fujiwara, B. Chaves, R. Schoppmeyer, C.I. van der Made, R. Jimenez Heredia, F.L. Harms, S. Alavi, L. Alsina, P. Sanchez Moreno, R. Ávila Polo, R. Cabrera-Pérez, S. Kostel Bal, L. Pfajfer, B. Ransmayr, A.-K. Mautner, R. Kondo, A. Tinnacher, M. Caldera, M. Schuster, C. Domínguez Conde, R. Platzner, E. Salzer, T. Boyer, H.G. Brunner, J.E. Nooitgedagt-Frons, E. Iglesias, A. Deyà-Martinez, M. Camacho-Lovillo, J. Menche, C. Bock, J.B. Huppa, W.F. Pickl, M. Distel, J.A. Yoder, D. Traver, K.R. Engelhardt, T. Linden, L. Kager, J.T. Hannich, A. Hoischen, S. Hambleton, S. Illsinger, L. Da Costa, K. Kutsche, Z. Chavoshzadeh, J.D. van Buul, J. Antón, J. Calzada-Hernández, O. Neth, J. Viaud, A. Nishikimi, L. Dupré, and K. Boztug

ABSTRACT

BACKGROUND

Increasing evidence links genetic defects affecting actin-regulatory proteins to diseases with severe autoimmunity and autoinflammation, yet the underlying molecular mechanisms are poorly understood. Deducator of cytokinesis 11 (DOCK11) activates the small Rho guanosine triphosphatase (GTPase) cell division cycle 42 (CDC42), a central regulator of actin cytoskeleton dynamics. The role of DOCK11 in human immune-cell function and disease remains unknown.

METHODS

We conducted genetic, immunologic, and molecular assays in four patients from four unrelated families who presented with infections, early-onset severe immune dysregulation, normocytic anemia of variable severity associated with anisopoikilocytosis, and developmental delay. Functional assays were performed in patient-derived cells, as well as in mouse and zebrafish models.

RESULTS

We identified rare, X-linked germline mutations in *DOCK11* in the patients, leading to a loss of protein expression in two patients and impaired CDC42 activation in all four patients. Patient-derived T cells did not form filopodia and showed abnormal migration. In addition, the patient-derived T cells, as well as the T cells from *Dock11*-knockout mice, showed overt activation and production of proinflammatory cytokines that were associated with an increased degree of nuclear translocation of nuclear factor of activated T cell 1 (NFATc1). Anemia and aberrant erythrocyte morphologic features were recapitulated in a newly generated *dock11*-knockout zebrafish model, and anemia was amenable to rescue on ectopic expression of constitutively active CDC42.

CONCLUSIONS

Germline hemizygous loss-of-function mutations affecting the actin regulator DOCK11 were shown to cause a previously unknown inborn error of hematopoiesis and immunity characterized by severe immune dysregulation and systemic inflammation, recurrent infections, and anemia. (Funded by the European Research Council and others.)

The authors' full names, academic degrees, and affiliations are listed in the Appendix. Dr. Boztug can be contacted at kaan.boztug@ccri.at or at St. Anna Children's Cancer Research Institute (CCRI), Zimmermannplatz 10, 1090 Vienna, Austria.

Ms. Rashkova and Dr. Castanon contributed equally to this article.

This article was published on June 21, 2023, at NEJM.org.

This is the *New England Journal of Medicine* version of record, which includes all *Journal* editing and enhancements. The Author Accepted Manuscript, which is the authors' version after external peer review and before publication in the *Journal*, is available at PubMed Central.

DOI: 10.1056/NEJMoa2210054

Copyright © 2023 Massachusetts Medical Society.

A PLETHORA OF HUMAN NEUROLOGIC, vascular, and immune diseases and cancer are associated with aberrant homeostasis of the actin cytoskeleton.^{1,2} Actin remodeling is pivotal for numerous cellular processes, including morphologic changes, migration, cell-cell interaction, and signal transduction, all of which are critical for immune-cell development and function.¹

Dedicator of cytokinesis (DOCK) family members participate in actin cytoskeleton dynamics through their guanine nucleotide exchange factor (GEF) activity, resulting in activation of the small Rho guanosine triphosphatases (GTPases) RAC and cell division cycle 42 (CDC42).³ Their importance for human immunity has been exemplified by germline mutations in *DOCK2* and *DOCK8* underlying combined immunodeficiencies with severe and recurrent infections, as well as autoimmune manifestations including thrombocytopenia, hemolytic anemia, and vasculitis.⁴⁻⁶ As is the case with *DOCK2* and *DOCK8*, *DOCK11* is predominantly expressed in hematopoietic cells, and in mice it has a role in early B-cell development and function.⁷ However, its role in human immune-cell biology and disease remains unknown. Here, we implicate *DOCK11* deficiency in an immune dysregulation disorder in patients with susceptibility to infection, systemic inflammation, and normocytic anemia.

METHODS

STUDY OVERSIGHT

Written informed consent was provided by the legal representatives of the patients at the respective institutions. All experiments in animals were performed with the approval of the institutional review board at the National Center for Geriatrics and Gerontology in Obu, Japan.

GENETIC, BIOCHEMICAL, AND FUNCTIONAL ANALYSES

Details of genetic analyses and the generation of CRISPR-Cas9 (clustered regularly interspaced short palindromic repeats and associated Cas9 homing endonucleases)-edited cells and zebrafish lines are provided in the Supplementary Appendix, available with the full text of this article at NEJM.org. Biochemical and immunochemical assays in which various hematopoietic cell types were used and statistical analysis of the performed

experiments are also described in the Supplementary Appendix.

RESULTS

CLINICAL HISTORIES

We studied four male patients who presented with early-onset immune dysregulation and hematopoietic defects of unknown origin; the patients were from four unrelated families with healthy parents (Fig. 1A, Table 1, and Tables S1 through S4 in the Supplementary Appendix). The patients showed transient (Patients 2 and 4) or chronic (Patients 1 and 3) normocytic (rarely microcytic) anemia of unknown origin (Table 1, and Fig. S1A and S1B). In Patient 1, who received regular erythrocyte transfusions, a bone marrow smear showed moderate erythroid hypoplasia (Fig. 1B). Coombs' tests that were performed in Patient 1 were negative. A morphologic study of erythrocytes showed anisocytosis and poikilocytosis, suggesting a defect in red-cell shape integrity. Known erythrocyte membranopathies involve altered osmotic fragility, hemolysis, and increased levels of bilirubin and lactate dehydrogenase,⁸ but these measures were normal or only slightly increased in tested patients (Patients 1 through 3). In addition, Patient 1 had thrombocytopenia (platelet count, 15,000 to 56,000 per cubic millimeter); Patient 3 had thrombocytosis (platelet count, 500,000 to 800,000 per cubic millimeter), which was most likely caused by hyperinflammation; and Patients 2 and 4 had mostly normal platelet counts.

The patients showed a range of early-onset systemic or organ-specific inflammatory manifestations, including recurrent fever and leukocytosis (Patients 1 and 3), skin inflammation and amyloid A amyloidosis (Patient 3), splenomegaly (Patients 1 and 3), systemic inflammatory response syndrome (Patients 2 and 3), and early-onset Crohn's disease (Patient 4) (Fig. 1C through 1F, Table 1, and Fig. S1C). Patients had recurrent respiratory tract infections, bacille Calmette-Guérin vaccine-related lymphadenitis and skin ulcer at injection site (BCGitis) (Patient 1), and one episode of sepsis (Patient 3) (Table 1). Patient 2 had pectus excavatum (Fig. 1G), and pyloric stenosis and recurrent vomiting had developed. Inguinal hernias were present in Patients 1 and 2. Failure to thrive was observed in Patients 1 through 3. Neurologic symptoms, in-

cluding muscular hypotonia and delayed developmental milestones, were observed in Patient 2. The patients received immunosuppressive agents, including glucocorticoids (Patients 1 through 4), tocilizumab and anakinra (Patient 3), and azathioprine (Patient 4). In addition, Patients 1 through 3 received antibiotic prophylaxis and underwent immunoglobulin substitution. No autoantibodies were detected in any of the patients who were evaluated (Table 1; clinical histories are provided in the Supplementary Appendix).

Immunophenotyping revealed normal numbers and subset distributions of T cells, natural killer cells, and monocytes (Figs. S2 and S3 and Table S5). Given the immune dysregulation in the patients, we specifically investigated regulatory T cells, the numbers of which were also within the normal range in all the patients who were evaluated (Patients 1, 3, and 4). Patient 4 had an increase in the absolute number of natural killer T cells and double-negative T cells at one time point. B-cell abnormalities included reduced proportions of marginal zone–like and switched-memory B cells (Patient 1) and intermittently increased proportions of CD21^{low}CD38^{low} B cells (Patients 1 through 4) (Fig. S4). Assessment of B-cell differentiation and proliferation in vitro in Patients 1 and 4 showed intact immunoglobulin class-switch recombination in response to both T-cell–dependent and independent stimuli (Fig. S5), a finding that suggests that the reduction of switched-memory B cells in Patient 1 may be due to a B-cell extrinsic defect, possibly resulting from aberrant interactions between T and B cells.

GERMLINE DOCK11 LOSS-OF-FUNCTION MUTATIONS

We identified, through exome sequencing, four hemizygous variants in *DOCK11* that cosegregated with disease in an X-linked inheritance pattern (Fig. 1A, and Fig. S6 and Tables S6 through S15). These four variants (Fig. S7A) — an early stop-gain mutation in Patient 1 (c.75dup [p.Glu26Ter]), a splice-site variant in Patient 2 (c.1718+5G→A [p.Pro533_Lys573del]) leading to skipping of exon 15 (Fig. S7B), and two missense mutations in Patients 3 and 4 (c.5120G→C [p.Trp1707Ser] and c.323A→G [p.Tyr108Cys]) — are predicted to be damaging according to the associated Combined Annotation-Dependent Depletion scores.⁹ Each of the four healthy male relatives from the maternal side of the families who were tested did not carry the relevant *DOCK11* variants, so

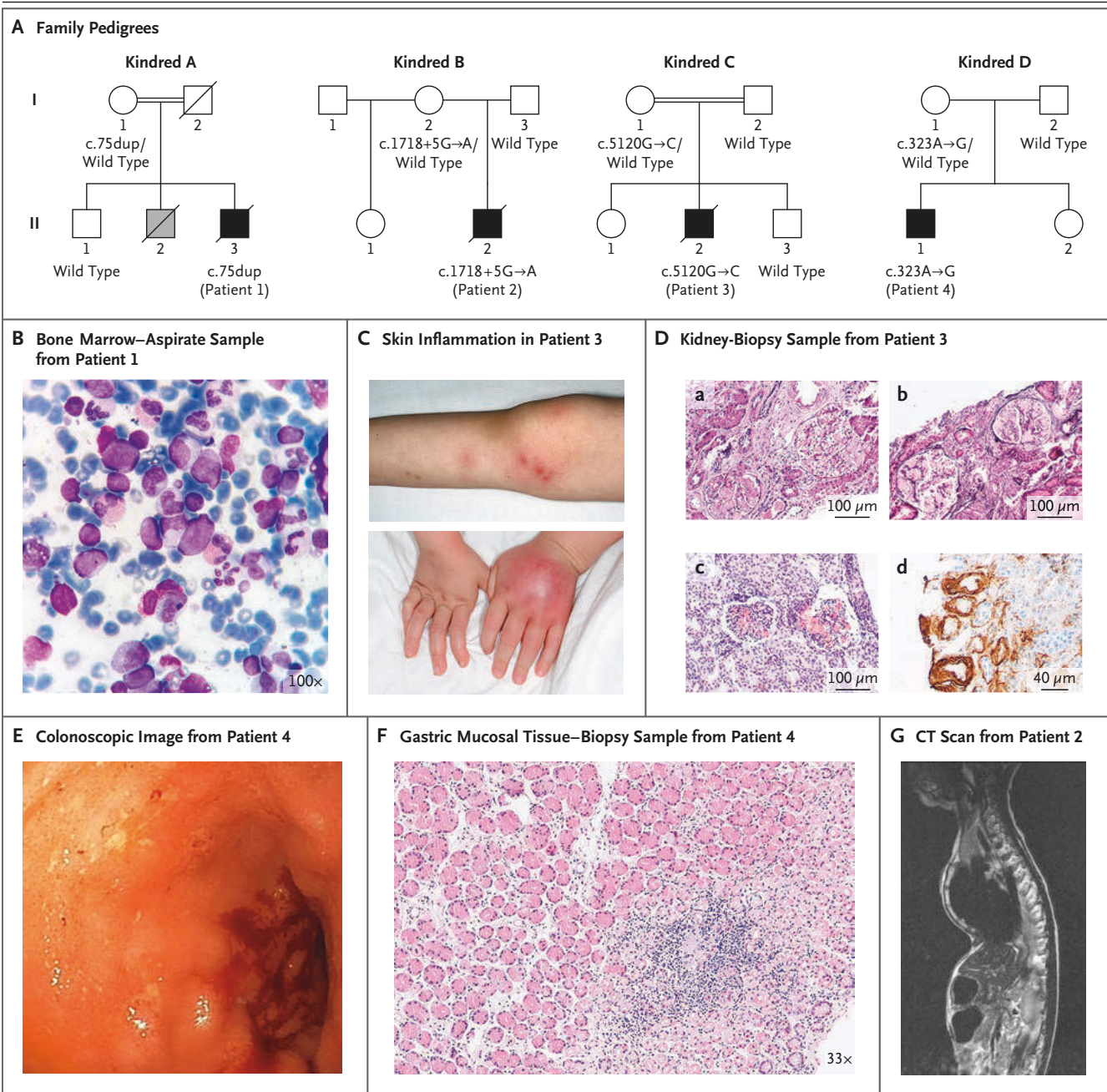
there is support for complete penetrance. We did not find evidence of skewed X-chromosome inactivation in the mothers of the patients (Fig. S8).

Immunoblotting revealed absent *DOCK11* expression in lymphocytes from Patients 1 and 2 and retained expression of *DOCK11*^{W1707S} and *DOCK11*^{Y108C} in cells from Patients 3 and 4, respectively (Fig. 2A, and Figs. S9 and S10). The *DOCK11*^{W1707S} substitution was in the *DOCK* homology region 2 (DHR-2) domain harboring the GEF activity, and the *DOCK11*^{Y108C} variant amino acid was in the N-terminal CDC42-binding region (Fig. S11)¹⁰; these findings support our hypothesis that the variants impair *DOCK11*-dependent activation of CDC42. C-C motif chemokine ligand 19 (CCL19)-dependent CDC42 activation was nearly abrogated in B-lymphoblastoid cells from all four patients (Fig. 2B, and Figs. S12 and S13).

LEUKOCYTE MORPHOLOGIC FEATURES, MIGRATION, AND CYTOKINE PRODUCTION

We next tested whether the *DOCK11* mutations might alter CDC42-dependent cell polarization and filopodia formation in lymphocytes.¹¹ Whereas the majority of control T cells were elongated in a polarized manner and formed actin-rich filopodia on interaction with fibronectin-coated surfaces, the patient-derived T cells were devoid of such protrusions and were more circular (Fig. 3A and 3B, and Fig. S14A). The morphologic defects were phenocopied by knocking in the implicated pathogenic variants into healthy donor T cells or knocking down *DOCK11* in Jurkat T cells (Fig. 3C, Fig. S14B through S14D, and Fig. S15A through S15C), a result consistent with the previous demonstration of induction of filopodia through *DOCK11* overexpression in murine bone marrow–derived dendritic cells.¹² Expression of wild-type *DOCK11*, but not mutant *DOCK11*^{W1707S}, partially restored the number of filopodia per cell, corresponding to the transgene expression level (Fig. S15D through S15F). Taken together, these results show that the implicated *DOCK11* variants lead to deficits in actin remodeling and morphologic features in the patient-derived T cells.

We then investigated whether such defects might affect T-cell migration. Although the patient-derived T cells showed reduced migration across a monolayer of activated endothelial cells under physiological flow conditions (Fig. 3D), their migration speed was enhanced in a confined in



vitro environment (Fig. 3E). Aberrant T-cell migration was confirmed in vivo in a newly generated F0 *dock11*-knockout zebrafish model (Figs. S16 through S18 and Videos S1 and S2 [links to the videos are provided in the Supplementary Appendix]).¹³ Collectively, these data indicate that *DOCK11*-mediated actin remodeling may differentially govern T-cell motility depending on the environmental context.

CDC42 and some of its effectors, such as Wiskott–Aldrich syndrome protein (WASP), are critical to T-cell activation.^{5,14–18} Given the hyper-

inflammatory phenotype of our patients, we hypothesized that *DOCK11* regulates T-cell activation and cytokine production. We observed an increase in the proinflammatory cytokines interleukin-2, interferon- γ , and tumor necrosis factor α (TNF- α) in CD8+ T cells from Patient 1 (Fig. 3F), although cytokine levels were normal in CD8+ T cells from Patients 2 and 3 (Fig. S19A). Slightly increased levels of interferon- γ and slightly reduced levels of interleukin-4 were observed in CD4+ T cells from Patients 1 and 3 (Fig. S19B).

Figure 1 (facing page). Identification of Germline DOCK11 Loss-of-Function Variants.

Panel A shows the pedigrees of four unrelated families. Double lines indicate consanguinity, black solid symbols affected persons with a hemizygous dedicator of cytokinesis 11 (*DOCK11*) variant, and gray solid symbols affected persons with an unknown genotype. Genotypes are indicated below the symbols. Squares indicate male family members, and circles female members. A slash indicates that the person had died. Roman numerals indicate generations, and Arabic numbers persons within a generation. Panel B shows erythroid hypoplasia and hypersegmented neutrophils in a bone marrow–aspirate sample (Wright–Giemsa stain) obtained from Patient 1. Panel C shows erythematous, painful, swollen lesions on the right knee (upper picture) and left hand (lower picture) of Patients 3; the lesions were diagnosed as cellulitis. Panel D shows nodular glomerulosclerosis with extension to interstitial vessels caused by amyloid A deposits in a kidney-biopsy sample obtained from Patient 3. Renal amyloid A amyloidosis was confirmed by a weak periodic acid–Schiff reaction (a), negative methenamine silver staining (b), intense staining of both glomerular and tubular basal membranes for Congo red (c), and immunohistochemical staining of the renal interstitial vessel walls for amyloid A (d). No marked tubular atrophy, interstitial fibrosis, or relevant interstitial inflammation was observed. Panel E shows mucosal erythema with small ulcerations in a macroscopic colonoscopy image in Patient 4. Panel F shows focal, chronic inflammation in a hematoxylin and eosin–stained section of a gastric mucosal tissue–biopsy sample obtained from Patient 4. Panel G shows pronounced pectus excavatum in a computed tomographic (CT) scan in Patient 2.

To overcome the limited availability of primary patient material and the potential effect of drug treatment on cellular functions, we further explored the role of DOCK11 in T cells from a *Dock11*-knockout mouse model⁷ and observed no overt abnormalities in T-cell development (Fig. S20A through S20C). However, *Dock11*-knockout mice showed increased rates of proliferation of CD4+ and CD8+ T cells (Fig. S20D and S20E). Lack of DOCK11 in mouse CD8+ T cells led to increased levels of interleukin-2, interferon- γ , and TNF- α (Fig. 3G), findings that were similar to our observations in T cells from Patient 1. Moreover, levels of interleukin-2 were increased in CD4+ T cells, whereas TNF- α and interleukin-4 levels were decreased (Fig. 3H), which was also consistent with DOCK11 regulating cytokine production in T cells. Such regulation is probably cell type–dependent; we observed no changes in cytokine production in a monocyte-

like cell line that had been rendered deficient in *DOCK11* (Fig. S21).

Aberrant cytokine production has been linked to defective immune synapse formation in several actin-related defects with immune dysregulation.^{16,18,19} However, CD8+ T cells from patients with DOCK11 deficiency showed no overt changes in immune synapse formation, polarization of the microtubule organization center, degranulation, or perforin levels in either T or natural killer cells (Fig. S22). B-cell synapse formation was normal in the primary B cells of Patient 4 and in the B-lymphoblastoid cells of all four patients (Fig. S23); these findings suggest that DOCK11 regulates cytokine production independent of synapse formation.

To explore alternative regulatory mechanisms, we investigated T-cell–receptor signaling and transcriptional regulation, which were previously associated with small Rho GTPase–mediated regulation of cytokine production.^{14,15,20–22} T cells from the patients and the *Dock11*-knockout mice showed higher nuclear translocation of the protein nuclear factor of activated T cell 1 (NFATc1), which regulates the transcription of messenger RNAs encoding interleukin-2, interferon- γ , and interleukin-4 (Fig. 3I, and Fig. S24A and S24B).²³ Translocation of NFATc1 to the nucleus is negatively regulated by phosphorylated c-Jun N-terminal kinase (JNK), a CDC42 effector.²⁴ We observed that JNK phosphorylation was reduced in T cells from *Dock11*-knockout mice (Fig. S24C), a finding that suggests that DOCK11 controls T-cell cytokine levels through the CDC42–JNK–NFATc1 axis.

ANEMIA AND ABERRANT MORPHOLOGIC FEATURES OF RED CELLS

Given the characterized bias in lymphocyte activation, we reasoned that red-cell abnormalities observed in patients with DOCK11 deficiency might be autoimmune-driven. However, the finding of an absence of erythrocyte-directed antibodies supported an erythrocyte-intrinsic role of DOCK11 in erythroid homeostasis.

Zebrafish have been used to model vertebrate hematopoiesis — in particular, erythropoiesis.²⁵ It is notable that *dock11*-knockout transgenic *fli1:GFP;gata1a:dsRed* embryos showed a striking defect in blood circulation that was characterized by the accumulation of blood cells in the posterior part of the body (Fig. 4A, Fig. S25A, and Videos S3 through S6). The *dock11*-knockout

Table 1. Clinical and Genetic Characteristics of Patients with DOCK11 Deficiency.*

Characteristic	Patient 1†	Patient 2†	Patient 3†	Patient 4
DOCK11 genomic change (HGVS, NC_000023.10)	g.117630009dup	g.117718825G→A	g.117805029G→C	g.117677487A→G
DOCK11 cDNA change (HGVS, NM_144658.3)	c.75dup	c.1718+5G→A	c.5120G→C	c.323A→G
DOCK11 protein change (HGVS, NP_653259.3)	p.Glu26Ter	p.Pro533_Lys573del	p.Trp1707Ser	p.Tyr108Cys
ClinVar accession number	SCV003841184	SCV003841185	SCV003841186	SCV003841187
Age at onset	40 days	Birth	4 mo	2 yr
Red-cell manifestations	Transfusion-dependent anemia Anisocytosis	Transient anemia Anisocytosis Fragmentocytes	Anemia Anisocytosis	Anisocytosis
Inflammatory manifestations	Leukocytosis Hepatosplenomegaly ARDS	SIRS	Leukocytosis SIRS Amyloid A amyloidosis Hepatosplenomegaly	Early-onset Crohn's disease
Infections	Otitis media Mastoiditis BCGitis	Pneumonia Bronchitis Gastroenteritis	Pneumonia Gastroenteritis Sepsis	Gastroenteritis (rotavirus)
Immunoglobulin levels	Low-normal IgG Normal IgM and IgE	Normal IgG, IgA, and IgM	Low IgG, IgA, and IgM Normal IgE	Normal IgG, IgA, and IgM Increased IgE
Gastrointestinal manifestations	None	Pyloric stenosis Recurrent vomiting	None	Constipation Diarrhea Rectal bleeding Colitis Antrum gastritis
Skin manifestations	Skin ulcer	Wrinkled skin	Cellulitis Myositis Arthritis	None
Neurologic manifestations	Facial-nerve palsy	Delayed developmental milestones Floppy infant Muscular hypotonia	None	None
Miscellaneous	FTT BCG vaccine-related lymphadenitis Inguinal hernia	FTT Pectus excavatum Inguinal hernia	FTT Nephrotic syndrome Hypothyroidism	None
Therapy	Blood transfusions IVIg Prednisolone	Antibiotic prophylaxis IVIg Gastric-tube feeding Budesonide	Steroids Cyclosporine Colchicine Anakinra Tocilizumab, IV or SC Sirolimus Secukinumab Antibiotic prophylaxis IVIg or SCIg	5-aminosalicylic acid mesalamine Budesonide Azathioprine

* ARDS denotes acute respiratory distress syndrome, BCG bacille Calmette–Guérin, BCGitis BCG vaccine–related lymphadenitis and skin ulcer at injection site, cDNA complementary DNA, FTT failure to thrive, HGVS Human Genome Variation Society, IV intravenous, IVIg intravenous immune globulin, SC subcutaneous, SCIg subcutaneous immune globulin, and SIRS systemic inflammatory response syndrome.

† Patient 1 died at 6 years of age after undergoing splenectomy. Patient 2 died at 2 years 10 months of age and Patient 3 at 6 years 1 month of age, both due to multiorgan failure related to sepsis or SIRS.

embryos were anemic; they harbored a lower percentage of erythroid cells (*Gata1a*⁺) than did controls. In contrast, the percentage of endothelial cells (*Fli1*⁺) was similar in the *dock11*-knock-

out embryos and controls (Fig. 4B, and Fig. S25B and S25C). Moreover, *dock11* knockdown recapitulated the anemia observed in *dock11*-knock-

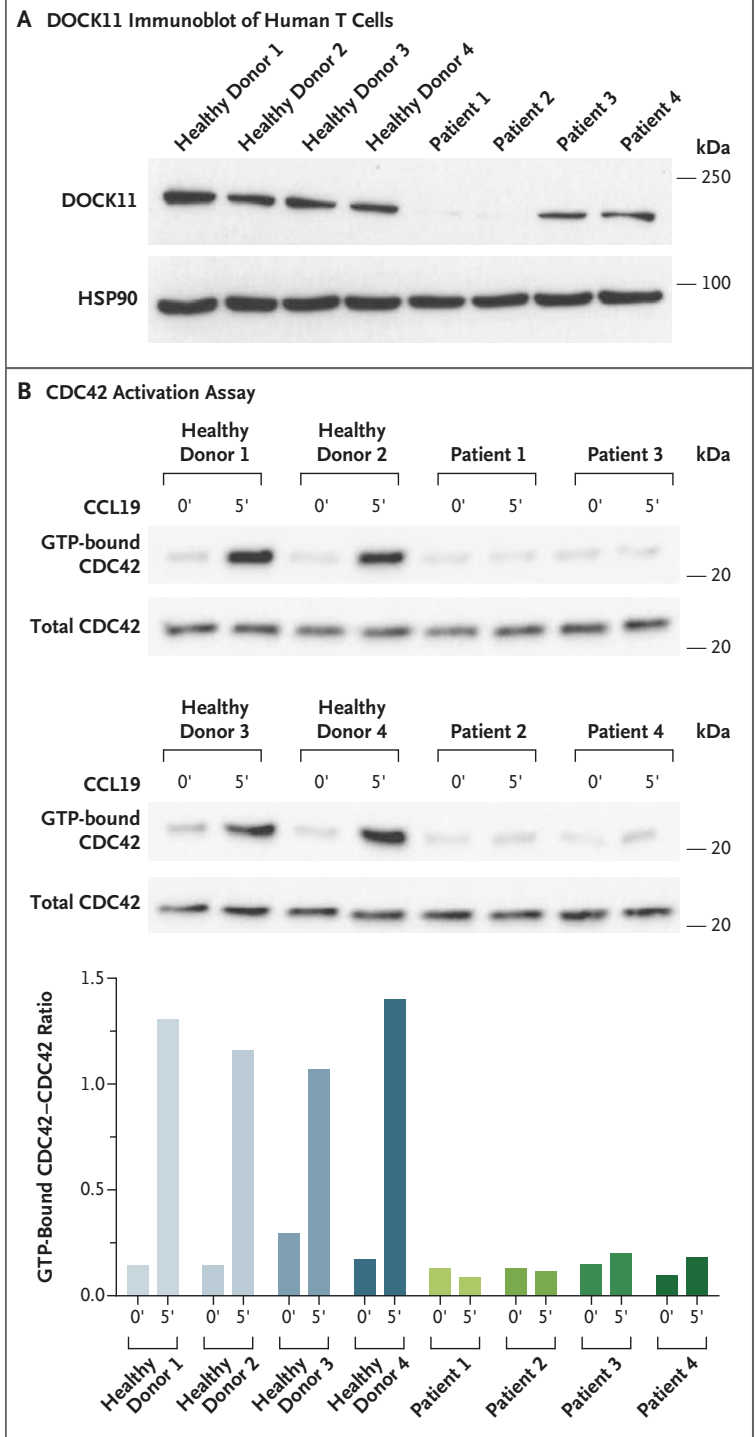
Figure 2. DOCK11 Protein Expression and CDC42 Activation in Lymphocytes.

Panel A shows absent DOCK11 expression in T cells from Patients 1 and 2 and retained DOCK11 expression in T cells from Patients 3 and 4 in representative immunoblots. Antibodies against heat shock protein 90 (HSP90) were used as a loading control. Panel B shows representative immunoblots and quantification of guanosine triphosphate (GTP)-bound (active) cell division cycle 42 (CDC42) and total CDC42. CDC42 activation on C-C motif chemokine ligand 19 (CCL19) stimulation was lower in B-lymphoblastoid cells from the patients than in the cells from healthy donors. The graph shows the ratio of GTP-bound CDC42 to total CDC42. Biologic replicates and quantification of the immunoblots displayed in Panels A and B are shown in Figures S9B and S12, respectively, in the Supplementary Appendix.

for murine erythropoiesis,^{26,27} we speculated that a reduction in Gata1a⁺ cells in *dock11*-knockout zebrafish embryos results from defective Cdc42 activity. The *cdc42*-knockdown embryos showed a reduction in the number of erythrocytes that was similar to the reduction in the *dock11*-knockout embryos (Fig. 4C).

To test our hypothesis that impaired activation of Cdc42 by Dock11 causes the anemia phenotype, we expressed a constitutively active form of human CDC42 (CDC42^{Q61L}) in *dock11*-knockout zebrafish embryos. Expression of CDC42^{Q61L} led to restoration of the numbers of Gata1a⁺ cells (Fig. 4D). The percentages of apoptotic and mitotic red cells in *dock11*-knockout embryos were unaltered (Fig. S25D and S25E), although the morphologic features of the red cells were abnormal (Fig. S26). Moreover, the altered nuclear-cytoplasmic ratio, a measure for terminal differentiation, suggested hampered erythroid maturation.

To explore whether DOCK11 plays a similar role in human erythropoiesis, we investigated its role in CD34⁺ cord blood cells. DOCK11 was expressed at different stages during erythroid differentiation of CD34⁺ cells (Fig. S27A). On *DOCK11* knockdown, cell expansion during differentiation was reduced, concomitant with increased cell death, but no difference in the percentage of apoptotic cells was detected (Fig. 4E and Fig. S27B). A relative paucity of CD117⁺CD36⁺ and CD71⁺CD235⁺ erythroid cells was identified, a finding that is consistent with early developmental delay (Fig. 4F and Fig. S27C). Collectively, these experiments highlight the pivotal



function of the DOCK11-CDC42 axis in regulating erythropoiesis across species.

DISCUSSION

We identified rare hemizygous loss-of-function mutations in *DOCK11* that led to impaired CDC42 activation as the cause of a novel immune dys-

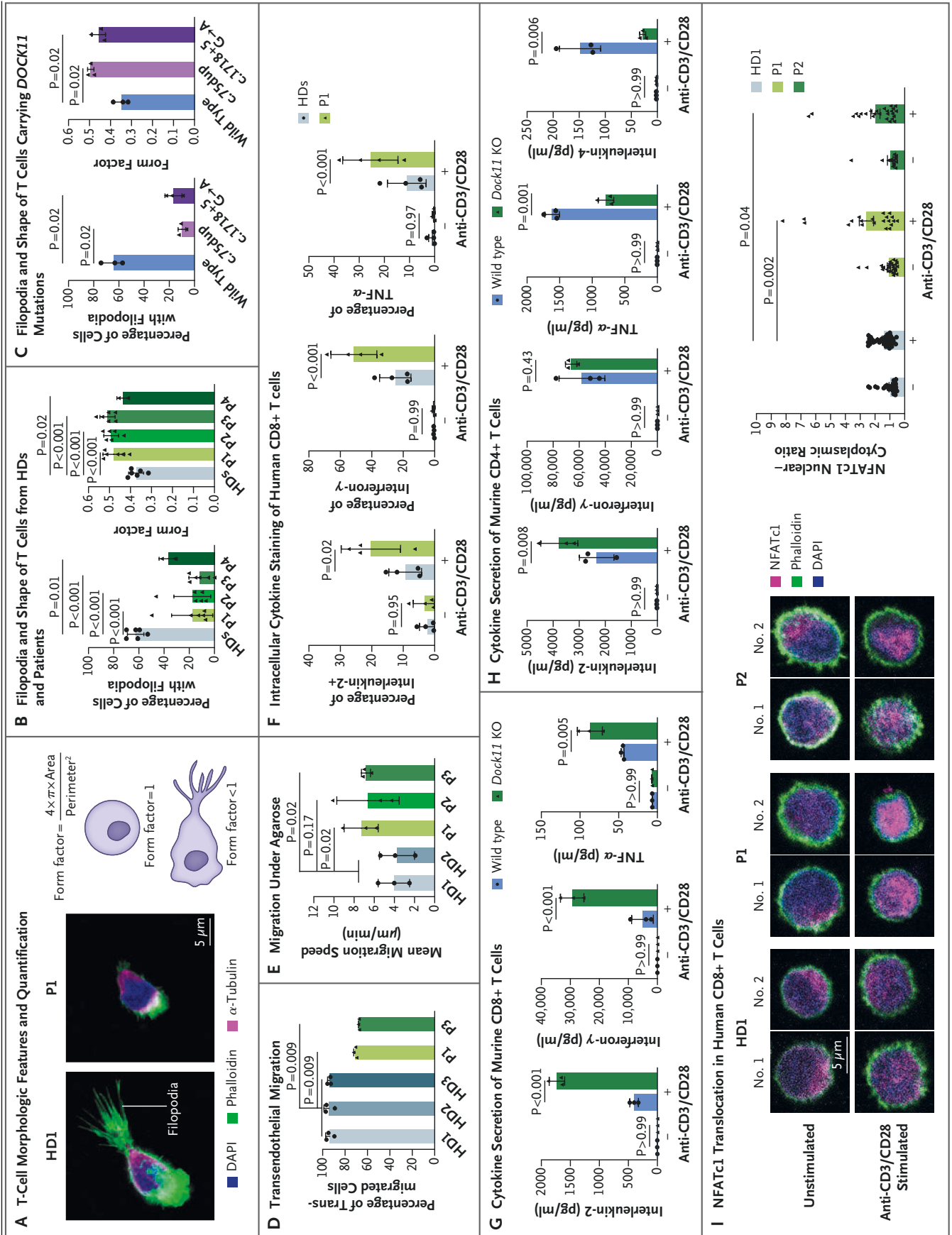


Figure 3 (facing page). DOCK11 Deficiency and Morphologic and Functional Defects in Lymphocytes.

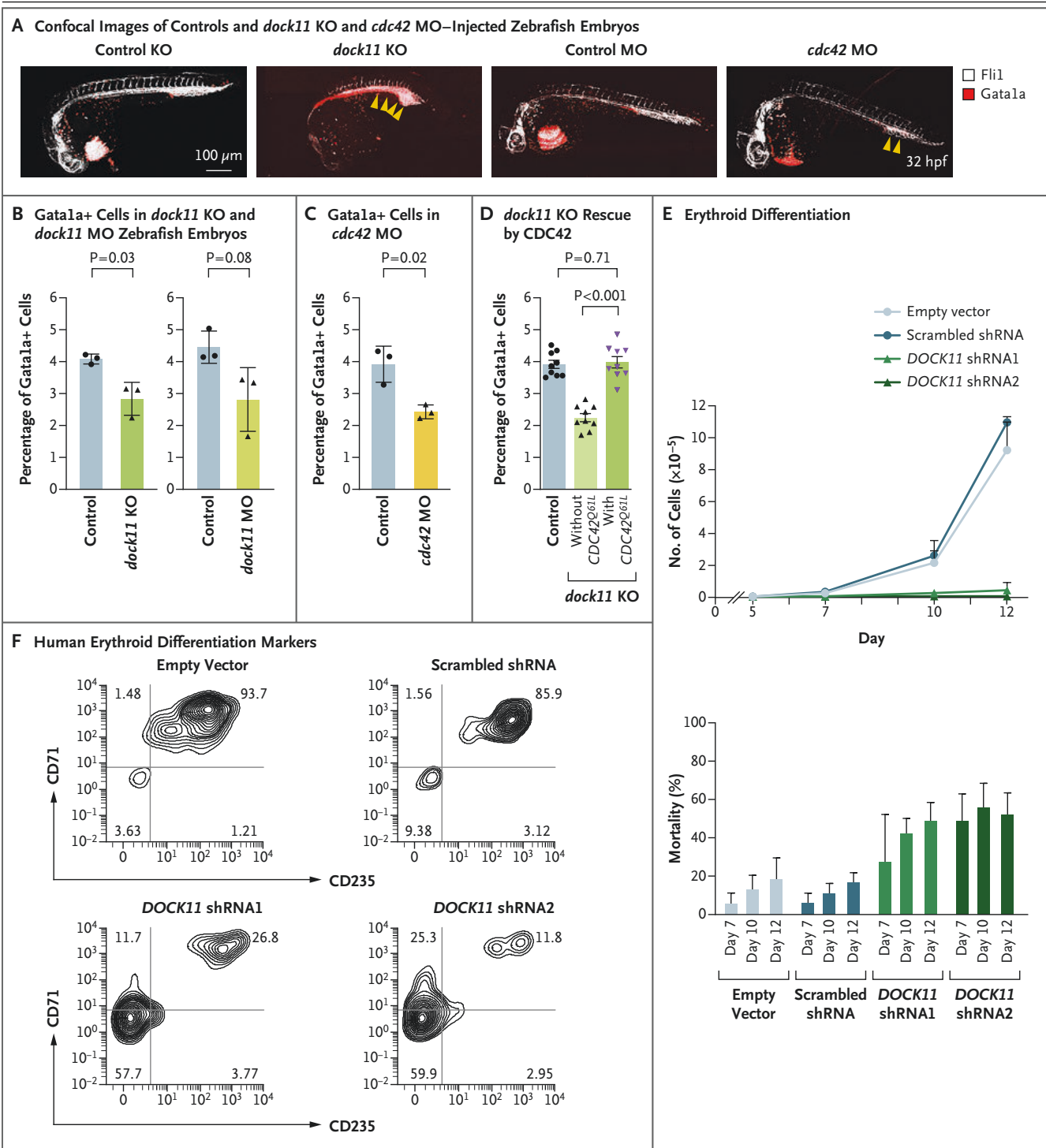
Panel A shows representative images of T-cell morphologic changes on interaction with fibronectin (left side of panel) in Healthy Donor (HD) 1 and Patient (P) 1 and the quantification scheme used (right side of panel). Magnified images correlate with those in Figure S14A. The form factor equals 1 when the object is perfectly circular. DAPI denotes nuclear marker 4',6-diamidino-2-phenylindole. Panel B shows that the percentage of T cells with filopodia was lower in the patients than in the HDs. Cell circularity was higher in the T cells from the patients than in those from the HDs. Panel C shows the quantification of confocal images. The number of cells with filopodia was lower and cell circularity (form factor) was greater in *DOCK11* knock-in T cells (*DOCK11* c.75dup and c.1718+5G→A) than in wild-type cells. Panel D shows that the transmigration capacity of T cells was lower in the patients than in the HDs. Panel E shows that the mean migration speed of the CD8+ T cells under agarose was higher in the patients than in the HDs. Panel F shows that the intracellular cytokine levels on anti-CD3 and anti-CD28 (anti-CD3/CD28) stimulation (plus sign), as assessed by flow cytometry, was higher in the T cells from P1 than in those from the HDs. The minus sign denotes no stimulation and TNF- α tumor necrosis factor α . Panels G and H show that the cytokine levels in CD8+ (Panel G) and CD4+ (Panel H) T cells from *Dock11*-knockout (KO) mice were altered on anti-CD3/CD28 stimulation, as compared with wild-type cells. Panel I shows two representative images per condition (No. 1 and No. 2, left side of panel) and quantification of nuclear factor of activated T cell 1 (NFATc1) nuclear–cytoplasmic ratio from one representative experiment (right side of panel). The degree of nuclear translocation on anti-CD3/CD28 stimulation was higher in the T cells from the patients than in those from the HDs. In Panels B and C and E through H, the results are given as mean values, with standard deviations (I bars), derived from multiple measurements. In Panel D, the results are given as mean values, with the standard deviations (I bars), derived from five imaging fields in each of three measurements. In Panel I, the results are given as mean values of multiple measurements, with standard errors (I bars). Solid triangles indicate T cells from the patients (Panels B, D through F, and I), *DOCK11* knock-in T cells (*DOCK11* c.75dup and c.1718+5G→A) (Panel C), or T cells from *Dock11*-knockout mice (Panels G and H). Solid circles indicate the respective controls including HDs (Panels B, D through F, and I), unedited HD-derived wild-type T cells (Panel C), and wild-type mice (Panels G and H). In Panels B through E, statistical analysis was performed with the use of a Mann–Whitney test; in Panels F through H, with the use of a two-way analysis of variance with a Šidák correction test for multiple comparison; and in Panel I, with the use of an unpaired Student's t-test. Details are provided in the Supplementary Appendix.

regulation disorder. Clinically, *DOCK11* deficiency includes phenotypes associated with *CDC42* mutations, such as recurrent infections, immune dysregulation, anemia, platelet anomalies, and neurodevelopmental abnormalities. Unlike patients carrying *CDC42* mutations,²⁸⁻³¹ patients with *DOCK11* deficiency had no detectable facial abnormalities, neutropenia, monocytopenia, or hemophagocytic lymphohistiocytosis.

Despite the systemic inflammatory phenotype in *DOCK11* deficiency, we did not detect autoantibodies, alterations in regulatory T-cell numbers, or overt defects in immune synapse assembly, features that are seen in other genetic disorders involving aberrant actin assembly.^{17,19,32,33} It is notable that patients with *DOCK11* deficiency showed increased frequencies of CD21^{low} B cells and double-negative T cells, which indicate a propensity toward immune dysregulation.³⁴ Identification of additional patients with *DOCK11* mutations would permit delineation of a broader phenotypic spectrum of the disease.

DOCK11-deficient T cells showed reduced transendothelial migration in vitro, yet also increased migration speed under confinement in vitro and in vivo, which suggests that *DOCK11* is involved in leukocyte diapedesis and interstitial migration. Together with the impaired capacity to form filopodia, this may translate into aberrant target recognition and tissue positioning. Such homing and migration alterations in T-cell subsets could contribute to infection susceptibility and severity.

Autoinflammation, which has been observed in several actin-related deficiencies, has been linked to increased inflammasome-mediated secretion of interleukin-1 β and interleukin-18.^{28,31,35-37} However, we did not find evidence of this mechanism in *DOCK11*-deficient monocytes. Instead, we observed altered levels of proinflammatory cytokines and an increased degree of nuclear translocation of NFATc1 in T cells from two patients. Similarly, T cells from the *Dock11*-knockout mice showed aberrant JNK phosphorylation, nuclear translocation of NFATc1, and altered cytokine production. These data, in combination with data from studies involving mice showing that *CDC42* negatively regulates effector and memory T-cell activation,^{14,15} implicate the *DOCK11*–*CDC42* axis in T-cell proliferation, activation, and cytokine production.



Defects in DOCK8, another CDC42-activating GEF, cause type 2 cytokine skewing and reduced proliferation.^{5,16} Given the developmental stage-specific role of CDC42 in regulating T-cell activation¹⁵ and the link between specific spatiotemporal patterns of CDC42 with T-cell functions,³⁸ we speculate that GEFs, including DOCK8 and

DOCK11, regulate CDC42-dependent processes in a manner dependent on cell type, localization, and stimulus. The distinct clinical presentation of patients with DOCK11 deficiency as opposed to DOCK2 and DOCK8 deficiencies further supports the notion that DOCK family proteins promote nonredundant Rho GTPase activation.^{4,5}

Figure 4 (facing page). DOCK11 Deficiency and Anemia and Aberrant Red-Cell Morphologic Forms across Species.

Panel A shows representative confocal images of the accumulation of intravascular blood (yellow arrows) in *dock11*-KO and *cdc42* morpholino (MO)-mediated knockdown *fli1:GFP;gata1a:dsRed* transgenic zebrafish embryos as compared with their respective controls. Single color images are shown in Figure S25A. The abbreviation hpf denotes hours postfertilization. Panels B and C show that the Gata1a⁺ erythroid cell number, assessed by flow cytometry, is lower in *dock11* KO and *dock11* MO-mediated (Panel B) or *cdc42* MO-mediated (Panel C) knockdown zebrafish embryos than in their respective controls. Panel D shows rescue of Gata1a⁺ erythroid cell numbers in *dock11* KO embryos injected with *CDC42^{Q61L}* messenger RNA for expression of constitutively active CDC42. Panels E and F show human CD34⁺ cells during erythroid differentiation, which are transduced with empty, scramble, or *DOCK11* short hairpin RNA (shRNA)-containing pLKO.1-CMV-tGFP vectors at day 2 and sorted for green fluorescent protein (GFP)-positive cells at day 5. Panel E shows that the cell counts were lower (upper graph) and mortality was higher (lower graph) at different stages of differentiation (days 5 through 12) in *DOCK11*-silenced cells than in control cells. Panel F shows a delay in erythroid differentiation in *DOCK11*-silenced cells in representative flow-cytometry plots of GFP-positive cells stained with CD71 and CD235 (glycophorin A) after 10 days in erythroid culture. In Panels B, C, and E, the results are given as the mean values of multiple measurements, with standard deviations (I bars or T bars [lower graph in Panel E]). In Panel D, the results are given as the mean values of multiple measurements, with standard errors (I bars). Solid triangles indicate Gata1a⁺ cells from *dock11*-knockout, *dock11*-knockdown or *cdc42*-knockdown zebrafish embryos (Panels B through D), or *DOCK11*-silenced CD34⁺ cells (Panels E and F). Solid circles indicate the respective control zebrafish embryos (Panels B through D) and control CD34⁺ cells (Panels E and F). In Panels B and C, statistical analysis was performed with the use of a paired Student's t-test, and in Panel D, with the use of a Mann-Whitney test. Details are provided in the Supplementary Appendix.

Data from the patients and the zebrafish model indicate that the anemia was not autoimmune-related. The erythroid hypoplasia in Patient 1 is consistent with a bone marrow defect and the observed erythroid-differentiation defect in *DOCK11*-knockdown CD34⁺ cord blood cells. The erythrocyte morphologic features in the zebrafish model were reminiscent of the anisopoikilocytosis that was observed in the patients with *DOCK11* deficiency. The contribution of aberrant assembly of the red-cell membrane skeleton

(in which actin is a component) to the anemia is probably less important; we did not observe increased red-cell hemolysis, which is characteristic of erythrocyte membranopathies.⁸

Clinical management of complex immune dysregulation disorders remains challenging because of the need for immunosuppressive agents, the use of which further increases the risk of severe and life-threatening infections. The high mortality among the patients with *DOCK11* deficiency that we observed in this study (Patients 1, 2, and 3 had died during the evaluation [Table 1]) underlines the importance of developing more specific treatment strategies. In a finding that was consistent with the unaltered levels of interleukin-1 β in a *DOCK11*-knockout monocyte-like cell line, the interleukin-1-receptor antagonist anakinra, used in other autoinflammatory conditions,²⁸ had no sustained effect in Patient 3. It was intriguing that targeting interferon- γ by emapalumab was successful in one patient with a missense variant in *CDC42*.²⁸ Emapalumab or other drugs targeting specific cytokines with increased levels in *DOCK11*-deficient T cells may be thus beneficial, yet finding the right balance between efficiency and potential side effects is challenging. Allogenic hematopoietic stem-cell transplantation had been considered for the three patients who died during the evaluation. The clinical condition of the remaining patient is currently stable, but in case of deterioration, the risk-benefit for hematopoietic stem-cell transplantation will be reassessed. Future studies may also assess whether gene therapy may offer an alternative curative treatment strategy.

Supported by the European Research Council under the European Union's Horizon 2020 Research and Innovation Program (820074, to Dr. Boztug), the Vienna Science and Technology Fund (WWTF-LS16-060, to Drs. Boztug, Dupré, and Menche; WWTF-LS14-031, to Drs. Platzer and Hupp), the Deutsche Forschungsgemeinschaft (KU 1240/13-1, to Dr. Kutsche), the Doctoral Fellowship Program of the Austrian Academy of Sciences (25590, to Ms. Block; 24486, to Dr. Ardy), grants from the Centre National de la Recherche Scientifique (International Research Project program, SysTact project, to Dr. Dupré) and Programa Institucional de Internacionalização da Coordenação de Aperfeiçoamento de Pessoal de Nível Superior (CAPES-PrInt) (to Ms. Chaves), the Wellcome Trust (207556/Z/17/Z, to Dr. Hambleton), the Netherlands Organization for Health Research and Development and the Dutch Research Council (ZonMW NWO Vici grant 91819632, to Drs. van Buul and Schoppmeyer), the Austrian Research Promotion Agency (project 7940628, Danio-4Can, to Dr. Distel), a German Academic Exchange Service postdoctoral fellowship and a European Molecular Biology Organization fellowship (to Dr. Distel), and the Research Funding for Longevity Sciences from the National Center for Geriatrics and

Gerontology (21-27-2, to Dr. Nishikimi). This study makes use of data shared through the PhenomeCentral repository, funded by Genome Canada and the Canadian Institute of Health Research.

Disclosure forms provided by the authors are available with the full text of this article at NEJM.org.

We thank the clinical cooperation partners and the patients and their families; Jasmin Dmytrus, Özlem Yüce Petronczki, Inka Jantke, Dennis Zorndt, Junko Hirokawa, Megumi Banno, Benjamin Natha, Jane Rehberg, Karim El-Gedawi, Melanie Feichter, and Tatjana Hirschmugl for technical support; Maryam Kazemi Aghdam, Iris D. Nagtegaal, Melanie Hanser, Margreet Wessels, Willemijn Hobo, Carolina Estepa, and Patricia Ramírez for providing histologic stains, primary material, or data from patients

and family members; Alexandra Frohne, Galuh Astuti, and the personnel at the Biomedical Sequencing Facility, CeMM Research Center for Molecular Medicine of the Austrian Academy of Sciences (Vienna), the multidisciplinary immuno-exome sign-out meeting (MDO), and the Radboud Genomics Technology Center (Nijmegen) for exome sequencing and data analysis; Nara Marella for proteomic data analysis; Marion Gröger, Sabine Rauscher, Christoph Friedl, Sophie Allart, Simon Lachambre, and Fatima L'Faqihi-Olive for support with the imaging and cytometry platforms (Medical University of Vienna, Vienna, and Toulouse Institute for Infectious and Inflammatory Diseases, Toulouse); Mitsuo Maruyama for providing *Dock11*-knockout mice; and Ronen Alon, Stefanie Wissmann, and Jens Stein for their ideas.

APPENDIX

The authors' full names and academic degrees are as follows: Jana Block, M.Sc., Christina Rashkova, M.Sc., Irinka Castanon, Ph.D., Samaneh Zoghi, Ph.D., Jessica Platon, M.Sc., Rico C. Ardy, Ph.D., Mitsuhiro Fujiwara, Ph.D., Beatriz Chaves, M.Sc., Rouven Schoppmeyer, Ph.D., Caspar I. van der Made, M.D., Raul Jimenez Heredia, M.Sc., Frederike L. Harms, Ph.D., Samin Alavi, M.D., Laia Alsina, M.D., Ph.D., Paula Sanchez Moreno, M.D., Rainiero Ávila Polo, M.D., Ph.D., Rocío Cabrera-Pérez, M.D., Sevgi Kostel Bal, M.D., Ph.D., Laurène Pfajfer, Ph.D., Bernhard Ransmayr, M.D., Anna-Katharina Mautner, M.Sc., Ryohei Kondo, Ph.D., Anna Tinnacher, M.Sc., Michael Caldera, Ph.D., Michael Schuster, Ph.D., Cecilia Domínguez Conde, Ph.D., René Platzer, Ph.D., Elisabeth Salzer, M.D., Ph.D., Thomas Boyer, M.D., Ph.D., Han G. Brunner, M.D., Judith E. Nooitgedagt-Frons, M.D., Estíbaliz Iglesias, M.D., Ph.D., Angela Deyà-Martinez, M.D., Ph.D., Marisol Camacho-Lovillo, M.D., Jörg Menche, Ph.D., Christoph Bock, Ph.D., Johannes B. Huppa, Ph.D., Winfried F. Pickl, M.D., Martin Distel, Ph.D., Jeffrey A. Yoder, Ph.D., David Traver, Ph.D., Karin R. Engelhardt, Ph.D., Tobias Linden, M.D., Leo Kager, M.D., J. Thomas Hannich, Ph.D., Alexander Hoischen, Ph.D., Sophie Hambleton, M.D., Ph.D., Sabine Illsinger, M.D., Lydie Da Costa, M.D., Ph.D., Kerstin Kutsche, Ph.D., Zahra Chavoshzadeh, M.D., Jaap D. van Buul, Ph.D., Jordi Antón, M.D., Ph.D., Joan Calzada-Hernández, M.D., Olaf Neth, M.D., Julien Viaud, Ph.D., Akihiko Nishikimi, Ph.D., Loïc Dupré, Ph.D., and Kaan Boztug, M.D.

The authors' affiliations are as follows: St. Anna Children's Cancer Research Institute (CCRI) (J.B., C.R., I.C., S.Z., R.C.A., R.J.H., S.K.B., B.R., E.S., M.D., L.K., K.B.), the Ludwig Boltzmann Institute for Rare and Undiagnosed Diseases (J.B., C.R., I.C., S.Z., R.C.A., R.J.H., S.K.B., L.P., B.R., A.-K.M., C.D.C., E.S., C.B., L.D., K.B.), CeMM Research Center for Molecular Medicine of the Austrian Academy of Sciences (J.B., C.R., S.Z., R.C.A., R.J.H., S.K.B., B.R., A.T., M.C., M.S., C.D.C., E.S., J.M., C.B., J.T.H., K.B.), and the Departments of Pediatrics and Adolescent Medicine (C.R., R.J.H., E.S., L.K., K.B.) and Dermatology (A.-K.M., L.D.), the Institute for Hygiene and Applied Immunology (R.P., J.B.H.) and the Institute of Immunology (W.F.P.), Center for Pathophysiology, Infectiology, and Immunology, and the Institute of Artificial Intelligence, Center for Medical Data Science (C.B.), Medical University of Vienna, the St. Anna Children's Hospital (E.S., L.K., K.B.), the Department of Structural and Computational Biology, Max Perutz Labs, and the Faculty of Mathematics, University of Vienna (J.M.), Vienna, and the Karl Landsteiner University of Health Sciences, Krems (W.F.P.) — all in Austria; Hématopoièse et Immunologie (HEMATIM) Unité de Recherche 4666, Université de Picardie Jules Verne (J.P., T.B., L.D.C.), and Service d'Hématologie Biologique (Hematology Diagnostic Lab), Centre Hospitalier Universitaire d'Amiens (T.B.), Amiens, Toulouse Institute for Infectious and Inflammatory Diseases, INSERM and Paul Sabatier University (Unité Mixte de Recherche 1291), and Centre National de la Recherche Scientifique (Unité Mixte de Recherche 5051) (B.C., L.P., L.D.), and the Institute of Cardiovascular and Metabolic Diseases (I2MC), INSERM and Paul Sabatier University (Unité Mixte de Recherche 1297) (J.V.), Toulouse, and Service d'Hématologie Biologique (Hematology Diagnostic Lab), Assistance Publique-Hôpitaux de Paris, Hôpital Robert Debré, the University of Paris, and the Laboratory of Excellence for Red Cells, Laboratory of Excellence GR-Ex, Paris (L.D.C.) — all in France; the Biosafety Division, Research Institute, National Center for Geriatrics and Gerontology, Obu, Japan (M.F., R.K., A.N.); the National Institute of Science and Technology on Neuroimmunomodulation, Oswaldo Cruz Institute, Oswaldo Cruz Foundation (Fiocruz), Rio de Janeiro, and the Computational Modeling Group, Oswaldo Cruz Foundation (Fiocruz), Eusébio — both in Brazil (B.C.); the Molecular Cell Biology Lab, Department of Molecular Hematology, Sanquin Research, the Vascular Cell Biology Lab, Department of Medical Biochemistry, Amsterdam University Medical Centers, University of Amsterdam, and the Leeuwenhoek Center for Advanced Microscopy, Section of Molecular Cytology, Swammerdam Institute for Life Sciences, University of Amsterdam, Amsterdam (R.S., J.D.B.), the Department of Human Genetics (C.I.M., H.G.B., A.H.) and the Radboud University Medical Center for Infectious Diseases, Department of Internal Medicine, Radboud University Medical Center, Nijmegen (C.I.M., A.H.), the Department of Clinical Genetics, Maastricht University Medical Center, and GROW School for Oncology and Reproduction, Maastricht University, Maastricht (H.G.B.), and the Department of Pediatrics, Slingeland Hospital, Doetinchem (J.E.N.-F.) — all in the Netherlands; the Institute of Human Genetics, University Medical Center Hamburg-Eppendorf, Hamburg (F.L.H., K.K.), University Children's Hospital Oldenburg, Department of Neuropediatrics, Oldenburg (T.L., S.I.), and the Center for Pediatrics and Adolescent Medicine, Department of Pediatric Kidney, Liver, and Metabolic Diseases and Neuropediatrics, Hannover Medical School, Hannover (S.I.) — all in Germany; the Pediatric Congenital Hematologic Disorders Research Center, Research Institute for Children's Health (S.A.), and the Allergy and Clinical Immunology Department, Mofid Children's Hospital (Z.C.), Shahid Beheshti University of Medical Sciences, Tehran, Iran; the Clinical Immunology and Primary Immunodeficiencies Unit, Allergy and Clinical Immunology Department (L.A., A.D.-M.), and the Pediatric Rheumatology Department (E.I., J.A., J.C.-H.), Hospital Sant Joan de Déu, the Study Group for Immune Dysfunction Diseases in Children, Institut de Recerca Sant Joan de Déu (L.A., E.I., A.D.-M., J.A., J.C.-H.), and the Department of Surgery and Surgical Specializations, Facultat de Medicina i Ciències de la Salut, Universitat de Barcelona (L.A., J.A.), Barcelona, and the Pediatric Infectious Diseases, Rheumatology, and Immunology Unit (P.S.M., M.C.-L., O.N.) and the Department of Pathology (R.Á.P., R.C.-P.), Hospital Universitario Virgen del Rocío, Institute of Biomedicine of Seville, Seville — all in Spain; the Department of Molecular Biomedical Sciences, North Carolina State University, Raleigh (J.A.Y.); the Department of Cellular and Molecular Medicine and the Section of Cell and Developmental Biology, University of California, San Diego, La Jolla (D.T.); and the Primary Immunodeficiency Group, Newcastle University Translational and Clinical Research Institute, Newcastle upon Tyne, United Kingdom (K.R.E., S.H.).

REFERENCES

1. Janssen E, Geha RS. Primary immunodeficiencies caused by mutations in actin regulatory proteins. *Immunol Rev* 2019; 287:121-34.
2. Ramaekers FCS, Bosman FT. The cytoskeleton and disease. *J Pathol* 2004;204: 351-4.
3. Nishikimi A, Kukimoto-Niino M, Yokoyama S, Fukui Y. Immune regulatory functions of DOCK family proteins in health and disease. *Exp Cell Res* 2013; 319:2343-9.
4. Dobbs K, Domínguez Conde C, Zhang S-Y, et al. Inherited DOCK2 deficiency in patients with early-onset invasive infections. *N Engl J Med* 2015;372:2409-22.
5. Zhang Q, Davis JC, Lamborn IT, et al. Combined immunodeficiency associated with *DOCK8* mutations. *N Engl J Med* 2009; 361:2046-55.
6. Aydin SE, Kilic SS, Aytekin C, et al. DOCK8 deficiency: clinical and immunological phenotype and treatment options — a review of 136 patients. *J Clin Immunol* 2015;35:189-98.
7. Matsuda T, Yanase S, Takaoka A, Maruyama M. The immunosenescence-related gene *Zizimin2* is associated with early bone marrow B cell development and marginal zone B cell formation. *Immun Ageing* 2015;12:1.
8. Da Costa L, Galimand J, Fenneteau O, Mohandas N. Hereditary spherocytosis, elliptocytosis, and other red cell membrane disorders. *Blood Rev* 2013;27:167-78.
9. Kircher M, Witten DM, Jain P, O’Roak BJ, Cooper GM, Shendure J. A general framework for estimating the relative pathogenicity of human genetic variants. *Nat Genet* 2014;46:310-5.
10. Lin Q, Yang W, Baird D, Feng Q, Cerione RA. Identification of a DOCK180-related guanine nucleotide exchange factor that is capable of mediating a positive feedback activation of Cdc42. *J Biol Chem* 2006;281:35253-62.
11. Etienne-Manneville S. Cdc42 — the centre of polarity. *J Cell Sci* 2004;117: 1291-300.
12. Sakabe I, Asai A, Iijima J, Maruyama M. Age-related guanine nucleotide exchange factor, mouse *Zizimin2*, induces filopodia in bone marrow-derived dendritic cells. *Immun Ageing* 2012;9:2.
13. Kroll F, Powell GT, Ghosh M, et al. A simple and effective F0 knockout method for rapid screening of behaviour and other complex phenotypes. *Elife* 2021;10:e59683.
14. Guo F, Hildeman D, Tripathi P, Velu CS, Grimes HL, Zheng Y. Coordination of IL-7 receptor and T-cell receptor signaling by cell-division cycle 42 in T-cell homeostasis. *Proc Natl Acad Sci U S A* 2010;107: 18505-10.
15. Guo F, Zhang S, Tripathi P, et al. Distinct roles of Cdc42 in thymopoiesis and effector and memory T cell differentiation. *PLoS One* 2011;6(3):e18002.
16. Tangye SG, Pillay B, Randall KL, et al. Dedicator of cytokinesis 8-deficient CD4⁺ T cells are biased to a T_H2 effector fate at the expense of T_H1 and T_H17 cells. *J Allergy Clin Immunol* 2017;139:933-49.
17. Dupré L, Aiuti A, Trifari S, et al. Wiskott-Aldrich syndrome protein regulates lipid raft dynamics during immunological synapse formation. *Immunity* 2002; 17:157-66.
18. Trifari S, Sitia G, Aiuti A, et al. Defective Th1 cytokine gene transcription in CD4⁺ and CD8⁺ T cells from Wiskott-Aldrich syndrome patients. *J Immunol* 2006;177:7451-61.
19. Calvez R, Lafouresse F, De Meester J, Galy A, Valitutti S, Dupré L. The Wiskott-Aldrich syndrome protein permits assembly of a focused immunological synapse enabling sustained T-cell receptor signaling. *Haematologica* 2011;96:1415-23.
20. Ahmad Mokhtar AM, Salikin NH, Haron AS, et al. RhoG’s role in T cell activation and function. *Front Immunol* 2022; 13:845064.
21. Kaminuma O, Deckert M, Elly C, Liu YC, Altman A. Vav-Rac1-mediated activation of the c-Jun N-terminal kinase/c-Jun/AP-1 pathway plays a major role in stimulation of the distal NFAT site in the interleukin-2 gene promoter. *Mol Cell Biol* 2001;21:3126-36.
22. Tamehiro N, Nishida K, Sugita Y, et al. Ras homolog gene family H (RhoH) deficiency induces psoriasis-like chronic dermatitis by promoting T_H17 cell polarization. *J Allergy Clin Immunol* 2019;143: 1878-91.
23. Vaeth M, Feske S. NFAT control of immune function: New Frontiers for an Abiding Trooper. *F1000Res* 2018;7:260.
24. Coso OA, Chiariello M, Yu JC, et al. The small GTP-binding proteins Rac1 and Cdc42 regulate the activity of the JNK/SAPK signaling pathway. *Cell* 1995;81: 1137-46.
25. Zhang Y, Chen M, Chen C. Using the zebrafish as a genetic model to study erythropoiesis. *Int J Mol Sci* 2021;22: 10475.
26. Wang L, Yang L, Filippi M-D, Williams DA, Zheng Y. Genetic deletion of Cdc42GAP reveals a role of Cdc42 in erythropoiesis and hematopoietic stem/progenitor cell survival, adhesion, and engraftment. *Blood* 2006;107:98-105.
27. Yang L, Wang L, Kalfa TA, et al. Cdc42 critically regulates the balance between myelopoiesis and erythropoiesis. *Blood* 2007;110:3853-61.
28. Lam MT, Coppola S, Krumbach OHF, et al. A novel disorder involving dysmyelopoiesis, inflammation, and HLH due to aberrant CDC42 function. *J Exp Med* 2019;216:2778-99.
29. Martinelli S, Krumbach OHF, Pantaleari F, et al. Functional dysregulation of CDC42 causes diverse developmental phenotypes. *Am J Hum Genet* 2018;102:309-20.
30. Takenouchi T, Kosaki R, Niizuma T, Hata K, Kosaki K. Macrothrombocytopenia and developmental delay with a de novo CDC42 mutation: yet another locus for thrombocytopenia and developmental delay. *Am J Med Genet A* 2015;167A:2822-5.
31. Gernez Y, de Jesus AA, Alsaleem H, et al. Severe autoinflammation in 4 patients with C-terminal variants in cell division control protein 42 homolog (CDC42) successfully treated with IL-1 β inhibition. *J Allergy Clin Immunol* 2019;144(4):1122-1125.e6.
32. Salzer E, Zoghi S, Kiss MG, et al. The cytoskeletal regulator HEM1 governs B cell development and prevents autoimmunity. *Sci Immunol* 2020;5:eabc3979.
33. Davidson A, Diamond B. Autoimmune diseases. *N Engl J Med* 2001;345: 340-50.
34. Freudenhammer M, Voll RE, Binder SC, Keller B, Warnatz K. Naive- and memory-like CD21^{low} B cell subsets share core phenotypic and signaling characteristics in systemic autoimmune disorders. *J Immunol* 2020;205:2016-25.
35. Kim ML, Chae JJ, Park YH, et al. Aberrant actin depolymerization triggers the pyrin inflammasome and autoinflammatory disease that is dependent on IL-18, not IL-1 β . *J Exp Med* 2015;212:927-38.
36. Lee PP, Lobato-Márquez D, Pramanik N, et al. Wiskott-Aldrich syndrome protein regulates autophagy and inflammasome activity in innate immune cells. *Nat Commun* 2017;8:1576.
37. Nishitani-Isa M, Mukai K, Honda Y, et al. Trapping of CDC42 C-terminal variants in the Golgi drives pyrin inflammasome hyperactivation. *J Exp Med* 2022; 219(6):e20211889.
38. Tskvitaría-Fuller I, Seth A, Mistry N, Gu H, Rosen MK, Wülfing C. Specific patterns of Cdc42 activity are related to distinct elements of T cell polarization. *J Immunol* 2006;177:1708-20.

Copyright © 2023 Massachusetts Medical Society.

Supplementary Appendix

Supplement to: Block J, Rashkova C, Castanon I, et al. Systemic inflammation and normocytic anemia in DOCK11 deficiency. *N Engl J Med*. DOI: 10.1056/NEJMoa2210054

This appendix has been provided by the authors to give readers additional information about the work.

TABLE OF CONTENTS

Author Contributions	8
Supplementary Patient Clinical Histories	9
Supplementary Material and Methods	14
Supplementary Figures, Tables and Legends	39
Figure S1. Longitudinal Hemoglobin Values and Stainings of Biopsy-----	
Samples from Patients-----	39
Figure S2. Flow Cytometry Analysis Gating of Human Immune-Cell Subsets	40
Figure S3. Immunophenotyping Analysis of Human T-Cell, NK-Cell and	
Monocyte Subsets	41
Figure S4. Immunophenotyping Analysis of Human B-cell Subsets	42
Figure S5. Evaluation of B-Cell Class-Switch and Proliferation	43
Figure S6. WES Filtering Strategy for Identification of Novel Rare Variants-----	44
Figure S7. Evaluation of Identified <i>DOCK11</i> Germline Mutations	45
Figure S8. Assessment of X-chromosome Inactivation in Female Carriers	46
Figure S9. <i>DOCK11</i> Expression in Different Cell Types	47
Figure S10. <i>DOCK11</i> Expression in T Cells - Uncropped Immunoblot	48
Figure S11. <i>DOCK11</i> Protein Scheme with Identified Variants	49
Figure S12. Assessment of <i>CDC42</i> Activation in B Lymphoblastoid Cells	50
Figure S13. <i>CDC42</i> Activation in B Lymphoblastoid Cells - Uncropped	
Immunoblot	51
Figure S14. T-Cell Morphology in <i>DOCK11</i> Deficiency	52
Figure S15. <i>DOCK11</i> -Knockdown in Jurkat T Cells Mimics Cell Shape	
Abnormalities of <i>DOCK11</i> -Deficient Patient Cells	53
Figure S16. Generation of <i>dock11</i> -Knockout Zebrafish	54
Figure S17. Evaluation of <i>dock11</i> -Knockout Zebrafish	55
Figure S18. T-Cell Migration in <i>dock11</i> -Knockout Zebrafish	56
Figure S19. Cytokine Production in Human CD4+ and CD8+ T Cells	57
Figure S20. T-Cell Development and Proliferation in <i>Dock11</i> -Knockout Mice	58
Figure S21. Normal Production of Cytokines by Human <i>DOCK11</i> -Deficient	
Monocyte-like Cells-----	59
Figure S22. Human T-Cell Synapse Formation and Cytotoxicity	60
Figure S23. Human B-Cell Synapse Morphologic Features	61
Figure S24. NFATc1 Nuclear Translocation in Murine CD4+ and CD8+ T Cells	62
Figure S25. Evaluation of Gata1a-Positive Cells in <i>dock11</i> -Knockout Zebrafish	63

Figure S26. Morphologic features of Gata1a-Positive Cells in <i>dock11</i> -Knockout Zebrafish	64
Figure S27. Evaluation of <i>dock11</i> -Knockout Zebrafish and <i>DOCK11</i> -Silenced Erythroid Cells	65
Table S1. Extended Laboratory Parameters of Female Carriers of Pathogenic <i>DOCK11</i> Variants	66
Table S2. Immunological Characteristics of Female Carriers	68
Table S3. Extended Laboratory Parameters of Patients 1 and 2 with <i>DOCK11</i> Deficiency	69
Table S4. Extended Laboratory Parameters of Patients 3 and 4 with <i>DOCK11</i> Deficiency	73
Table S5. Immunological Characteristics of Patients with <i>DOCK11</i> Mutations	77
Table S6. Hemizygous/Homozygous Variants in Known IUIS Genes Identified by Trio Whole-Exome Sequencing in Patient 1	79
Table S7. Heterozygous Variants in Known IUIS Genes Identified by Trio Whole-Exome Sequencing in Patient 1	80
Table S8. Hemizygous/Homozygous Variants in Known IUIS Genes Identified by Trio Whole-Exome Sequencing in Patient 3	81
Table S9. Heterozygous Variants in Known IUIS Genes Identified by Trio Whole-Exome Sequencing in Patient 3	82
Table S10. Heterozygous Variants in Known IUIS Genes Identified by Trio Whole-Exome Sequencing in Patient 4	83
Table S11. Hemizygous and Homozygous Variants Identified by Trio Whole-Exome Sequencing in Patient 1	84
Table S12. Hemizygous and Homozygous Variants Identified by Trio Whole-Exome Sequencing in Patient 2	85
Table S13. Hemizygous and Homozygous Variants Identified by Whole-Exome Sequencing in Patient 3	86
Table S14. Hemizygous and Homozygous Variants Identified by Whole-Exome Sequencing in Patient 4	87
Table S15. Evaluation of the Detected Variants in <i>DOCK11</i>	88
Supplementary Videos	89
Video S1. T cell Migration in a 5 dpf Control Zebrafish Embryo	89
Video S2. T-cell Migration in a 5 dpf <i>dock11</i> -Knockout Zebrafish Embryo	89
Video S3. Blood Circulation in a 48 hpf Control Zebrafish Embryo	89
Video S4. Blood Circulation in a 48 hpf <i>dock11</i> -Knockout Zebrafish Embryo	89

Video S5. Dynamics of the Blood Circulation in 54 hpf -----
Control Zebrafish Embryos ----- 90
Video S6. Dynamics of the Blood Circulation in 54 hpf -----
dock11-Knockout Zebrafish Embryos ----- 90
Supplementary References ----- 91

Author List

Jana Block^{1,2,3}, M.Sc., Christina Rashkova^{1,2,3,4,*}, M.Sc., Irinka Castanon^{1,2,*}, Ph.D., Samaneh Zoghi^{1,2,3}, Ph.D., Jessica Platon⁵, M.Sc., Rico C. Ardy^{1,2,3}, Ph.D., Mitsuhiro Fujiwara⁶, Ph.D., Beatriz Chaves^{7,8,9}, M.Sc., Rouven Schoppmeyer^{10,11,12}, Ph.D., Caspar I. van der Made^{13,14}, M.D., Raul Jimenez Heredia^{1,2,3,4}, M.Sc., Frederike L. Harms¹⁵, Ph.D., Samin Alavi¹⁶, M.D., Laia Alsina^{17,18,19} M.D., Ph.D., Paula Sanchez Moreno²⁰, M.D., Rainiero Ávila Polo²¹, M.D., Ph.D., Rocío Cabrera-Pérez²¹, M.D., Sevgi Kostel Bal^{1,2,3}, M.D., Ph.D., Laurène Pfajfer^{2,7}, Ph.D., Bernhard Ransmayr^{1,2,3} M.D., Anna-Katharina Mautner^{2,22}, M.Sc., Ryohei Kondo⁶, Ph.D., Anna Tinnacher³, M.Sc., Michael Caldera³, Ph.D., Michael Schuster³, Ph.D., Cecilia Domínguez Conde^{2,3}, Ph.D., René Platzer²³, Ph.D., Elisabeth Salzer^{1,2,3,4,24}, M.D., Ph.D., Thomas Boyer^{5,25}, M.D., Ph.D., Han G. Brunner^{13,26}, M.D., Judith E. Nooitgedagt-Frons²⁷, M.D., Estíbaliz Iglesias^{18,28}, M.D., Ph.D., Angela Deyà-Martinez^{17,18}, M.D., Ph.D., Marisol Camacho-Lovillo²⁰, M.D., Jörg Menche^{3,29,30}, Ph.D., Christoph Bock^{2,3,31}, Ph.D., Johannes B. Huppa²³, Ph.D., Winfried F. Pickl^{32,33}, M.D., Martin Distel¹, Ph.D., Jeffrey A. Yoder³⁴, Ph.D., David Traver³⁵, Ph.D., Karin R. Engelhardt³⁶, Ph.D., Tobias Linden³⁷, M.D., Leo Kager^{1,4,24}, M.D., J. Thomas Hannich³, Ph.D., Alexander Hoischen^{13,14}, Ph.D., Sophie Hambleton³⁶, M.D., Ph.D., Sabine Illsinger^{37,38}, M.D., Lydie Da Costa^{5,39,40,41}, M.D., Ph.D., Kerstin Kutsche¹⁵, Ph.D., Zahra Chavoshzadeh⁴², M.D., Jaap D. van Buul^{10,11,12}, Ph.D., Jordi Antón^{18,19,28}, M.D., Ph.D., Joan Calzada-Hernández^{18,28}, M.D., Olaf Neth²⁰, M.D., Julien Viaud⁴³, Ph.D., Akihiko Nishikimi⁶, Ph.D., Loïc Dupré^{2,7,22}, Ph.D., Kaan Boztug^{1,2,3,4,24}, M.D.

*, contributed equally to this work

¹St. Anna Children's Cancer Research Institute (CCRI), Vienna, Austria

²Ludwig Boltzmann Institute for Rare and Undiagnosed Diseases, Vienna, Austria

³CeMM Research Center for Molecular Medicine of the Austrian Academy of Sciences, Vienna, Austria

⁴Medical University of Vienna, Department of Pediatrics and Adolescent Medicine, Vienna, Austria

⁵Hématopoïèse et Immunologie (HEMATIM) Unité de Recherche (UR) 4666, Université de Picardie Jules Verne, Amiens, France

⁶Biosafety Division, Research Institute, National Center for Geriatrics and Gerontology, Obu, Aichi, Japan

⁷Toulouse Institute for Infectious and Inflammatory Diseases (INFINITY), INSERM and Paul Sabatier University (Unité Mixte de Recherche 1291) and Centre National de la Recherche Scientifique (CNRS) (Unité Mixte de Recherche 5051), Toulouse, France

- ⁸National Institute of Science and Technology on Neuroimmunomodulation (INCT-NIM), Oswaldo Cruz Institute, Oswaldo Cruz Foundation (Fiocruz), Rio de Janeiro, Brazil
- ⁹Computational Modeling Group, Oswaldo Cruz Foundation (Fiocruz), Eusébio, Brazil
- ¹⁰Molecular Cell Biology Lab, Department of Molecular Hematology, Sanquin Research, Amsterdam, the Netherlands
- ¹¹Vascular Cell Biology Lab, Department of Medical Biochemistry, Amsterdam University Medical Centers (UMC), University of Amsterdam, Amsterdam, the Netherlands
- ¹²Leeuwenhoek Center for Advanced Microscopy (LCAM), Section of Molecular Cytology, Swammerdam Institute for Life Sciences (SILS), University of Amsterdam, Amsterdam, the Netherlands
- ¹³Department of Human Genetics, Department of Internal Medicine, Radboud University Medical Center, Nijmegen, the Netherlands
- ¹⁴Radboud University Medical Center for Infectious Diseases (RCI), Department of Internal Medicine, Radboud University Medical Center, Nijmegen, the Netherlands
- ¹⁵Institute of Human Genetics, University Medical Center Hamburg-Eppendorf, Hamburg, Germany
- ¹⁶Pediatric Congenital Hematologic Disorders Research Center, Research Institute for Children's Health, Shahid Beheshti University of Medical Sciences, Tehran, Iran
- ¹⁷Clinical Immunology and Primary Immunodeficiencies Unit, Allergy and Clinical Immunology Department, Hospital Sant Joan de Déu, Barcelona, Spain
- ¹⁸Study Group for Immune Dysfunction Diseases in Children (GEMDIP), Institut de Recerca Sant Joan de Déu, Barcelona, Spain
- ¹⁹Department of Surgery and Surgical Specializations, Facultat de Medicina i Ciències de la Salut, Universitat de Barcelona, Barcelona, Spain
- ²⁰Pediatric Infectious Diseases, Rheumatology and Immunology Unit, Hospital Universitario Virgen del Rocío, Institute of Biomedicine of Seville (IBIS)/ Universidad de Sevilla/CSIC, Red de Investigación Traslacional en Infectología Pediátrica RITIP, Seville, Spain
- ²¹Department of Pathology, Hospital Universitario Virgen del Rocío, Seville, Spain
- ²²Medical University of Vienna, Department of Dermatology, Vienna, Austria
- ²³Medical University of Vienna, Institute for Hygiene and Applied Immunology, Center for Pathophysiology, Infectiology and Immunology, Vienna, Austria
- ²⁴St. Anna Children's Hospital, Vienna, Austria
- ²⁵Service d'Hématologie Biologique (Hematology Diagnostic Lab), CHU d'Amiens, Amiens, France
- ²⁶Department of Clinical Genetics, Maastricht University Medical Center, and GROW School for Oncology and Reproduction, Maastricht University, Maastricht, the Netherlands
- ²⁷Department of Pediatrics, Slingeland Hospital, Doetinchem, the Netherlands
- ²⁸Pediatric Rheumatology Department. Hospital Sant Joan de Déu Barcelona, Esplugues de Llobregat, Barcelona, Spain
- ²⁹Department of Structural and Computational Biology, Max Perutz Labs, University of Vienna, Vienna, Austria
- ³⁰Faculty of Mathematics, University of Vienna, Vienna, Austria
- ³¹Medical University of Vienna, Institute of Artificial Intelligence, Center for Medical Data Science, Vienna, Austria

³²Medical University of Vienna, Institute of Immunology, Center for Pathophysiology, Infectiology and Immunology, Vienna, Austria

³³Karl Landsteiner University of Health Sciences, Krems, Austria

³⁴Department of Molecular Biomedical Sciences, North Carolina State University, Raleigh, NC 27607, USA

³⁵Department of Cellular and Molecular Medicine and Section of Cell and Developmental Biology, University of California, San Diego, La Jolla, CA, USA

³⁶Primary Immunodeficiency Group, Newcastle University Translational and Clinical Research Institute, Newcastle upon Tyne, United Kingdom

³⁷University Children's Hospital Oldenburg, Department of Neuropediatrics, Oldenburg, Germany

³⁸Center for Pediatrics and Adolescent Medicine, Department of Pediatric Kidney, Liver and Metabolic Diseases and Neuropediatrics, Hannover Medical School, Hannover Germany

³⁹Service d'Hématologie Biologique (Hematology Diagnostic Lab), AP-HP, Hôpital Robert Debré, Paris, France

⁴⁰University of Paris, Paris, France

⁴¹Laboratory of Excellence for Red Cells, Laboratory of Excellence (LABEX) GR-Ex, Paris, France

⁴²Allergy and Clinical Immunology Department, Mofid Children's Hospital, Shahid Beheshti University of Medical Sciences, Teheran, Iran

⁴³Institute of Cardiovascular and Metabolic Diseases (I2MC), INSERM and Paul Sabatier University (Unité Mixte de Recherche 1297), Toulouse, France

Current affiliation for L.P.: Department of Clinical Microbiology, Institute of Clinical Medicine, University of Eastern Finland, Kuopio, Finland; for R.C.A.: Program for Computational and Systems Biology, Sloan Kettering Institute, Memorial Sloan Kettering Cancer Center, New York, NY 10065, USA; for M.C.: Proxygen GmbH, Vienna, Austria; for C.D.C.: Human Technopole, Milan, Italy; for E.S.: Department of Pediatrics, Laboratory for Pediatric Immunology, Willem-Alexander Children's Hospital, Leiden University Medical Center, Leiden, The Netherlands; for M.F.: Department of Physical Therapy, School of Health Science, Toyohashi Sozo University, Toyohashi, Aichi, Japan.

Correspondence:

Kaan Boztug, M.D., St. Anna Children's Cancer Research Institute (CCRI), Zimmermannplatz 10, 1090 Vienna, Austria. E-mail : kaan.boztug@ccri.at

Authorship Contributions

J.B., R.J.H., K.R.E., S.H., K.K., F.L.H., M.S. and C.I.M. analyzed WES data, identified *DOCK11* variants and performed Sanger sequencing validation experiments; F.L.H. performed *DOCK11* transcript analysis and X-chromosome inactivation analysis; J.B. and C.R. performed flow cytometry, immunoblotting, ELISA and confocal microscopy experiments; J.B., C.R. and L.P. generated CRISPR-edited *DOCK11*-knockout cells; R.C.A. generated plasmids; J.V. performed the CDC42 activation assay; B.C. and R.S. performed and interpreted T-cell migration assays; B.R. performed in vitro B-cell proliferation and class-switch assays; R.P., S.Z. and A.-K.M performed B-cell synapse experiments; M.D. and J.A.Y. generated the *lck:nlsmCherry;myl7:EGFP^{vi004}* transgenic zebrafish line with intellectual input from D.T.; I.C. generated zebrafish models and together with J.B. and C.R. characterized *dock11*-knockout, *dock11* and *cdc42* MO zebrafish embryos by sequencing analysis, flow cytometry and microscopy with intellectual input from M.D.; I.C. performed and analyzed T-cell migration experiments in zebrafish embryos; M.F., R.K. and A.N. performed characterization of *Dock11*-knockout mice including flow cytometry, assessment of proliferation and cytokine production, NFATc1 translocation and JNK phosphorylation analysis; J.P. and T.B. performed CD34⁺ erythroid differentiation experiments; J.B. generated DOCK11 protein models; M.C. provided imaging analysis pipeline for further modification by J.B.; A.T. and J.T.H. performed mass-spectrometry analysis; Z.C. and S.A. took care of patient 1; T.L. and S.I. took care of patient 2; P.S.M., M.C.-L., O.N., L.A., E.I., A.D.-M., J.A. and J.C.-H. took care of patient 3; C.I.M., J.E.N.-F., H.G.B. and A.H. took care of patient 4, collected patient samples and provided and interpreted clinical and immunological data; S.Z. coordinated sample collection from patient 1 and translated clinical documents; S.K.B. analyzed the patient clinical data; R.Á.P. and R.C.-P. provided histopathologic evaluation of biopsies; J.B. performed statistical analysis; C.D.C., E.S., S.H., J.D.B., J.M., J.B.H., W.F.P., C.B., L.K., S.K.B. and L.D.C. provided intellectual input; L.D. designed and analyzed microscopy-based experiments on patient-derived cells; J.B. and L.D coordinated part of the experimental work together with K.B.; K.B. conceived, designed, and coordinated the study; J.B., I.C., L.D. and K.B. wrote the manuscript with critical input from C.R.; All authors vouch for the data and the analysis; All authors approved the final version of the manuscript and agreed to publish the paper.

Supplementary Patient Clinical Histories

The patient cohort consists of four individuals from four unrelated families. Matchmaking through PhenomeCentral¹ facilitated patient enrollment in this rare genetic disease study.

Patient 1 (P1), the third male child of consanguineous parents from Iran, presented at 7 weeks of age with lymphocytosis, thrombocytopenia, splenomegaly, and severe anemia with anisocytosis requiring frequent erythrocyte suspension transfusions (Fig. S1A and Table 1 and Table S3). Despite severe thrombocytopenia, the patient did not exhibit any bleeding symptoms. Direct and indirect Coombs tests for detection of antiglobulin autoantibodies were negative (Table S3) and osmotic fragility test showed normal erythrocyte fragility. Complete blood count of the parents and hemoglobin (Hb) electrophoresis for the patient and his parents were normal. Bone marrow examination showed erythroid hypoplasia together with hypersegmented neutrophils (Figure 1B) without any ring sideroblasts. Neutrophil and red cell precursors were detected in the peripheral blood. The patient presented with pallor appearance and failure to thrive. Extensive diagnostics ruled out juvenile myelomonocytic leukemia, Noonan syndrome and monosomy 7 through karyotyping and genetic assessment of *KRAS*, *NRAS*, and *PTPN11*. Moreover, bone survey and skull-x-ray showed no signs of osteopetrosis, and brain computerized tomography scan was normal. Dihydrorhodamine flow cytometry analysis to test for chronic granulomatous disease was also normal. He suffered from several infections including suppurative otitis media and mastoiditis with facial paralysis, leading to mastoidectomy. At 4 months of age, the patient developed Bacillus Calmette-Guérin (BCG) lymphadenitis. At the age of 1 year, the patient further developed mild hypogammaglobulinemia prompting immunoglobulin replacement therapy (Table S3). From 3 years onward, the patient exhibited inflammatory lesions in the genital area, first responding to steroid treatment but later progressing to lymphangioma, which was treated with cryotherapy. Due to a life-threatening acute respiratory distress syndrome (ARDS) at the age of 5 years, the patient was admitted to the pediatric intensive care unit. He responded to antibiotics and steroid treatment, but severe anemia, hepatomegaly, and splenomegaly (span = 130 mm) persisted following the discharge. Severe enlargement of the spleen resulted in impaired walking ability and eventually splenectomy was performed. The patient died two days after removal of the spleen. Pathologic evaluation of splenic tissue after splenectomy revealed diffuse splenic extramedullary hematopoiesis and many hemosiderin-laden macrophages (Fig. S1B).

The brother of Patient 1 (see Figure 1A; Kindred A, II-2), who died at the age of 2 years, also presented with anemia, splenomegaly, and thrombocytopenia. He also developed a skin ulcer at the BCG injection site, ascites, and had an inguinal hernia. No genetic material from this patient was available.

Patient 2 (P2) was a male born to non-consanguineous parents from Turkish and Philippine origin. Prenatally, prenatal and neck edema, pleural effusions, and ventriculomegaly in the central nervous system were detected, and the nuchal fold was thickened. Prenatal chromosome analysis revealed a normal karyotype. After birth, he developed tachydyspnea and displayed features of a floppy infant with muscular hypotonia, further accompanied by delayed development of milestones. Strabismus and severe ametropia as well as hearing loss associated with bilateral tympanic effusion were present. Nerve conduction studies showed no evidence for peripheral neuropathy. Brain magnetic resonance imaging (MRI) showed age-appropriate myelination and no signs of cerebral seizures. The patient further developed gastrointestinal problems with pyloric stenosis and paralytic and adhesive ileus requiring several surgical interventions. Gastric tube feeding became necessary due to recurrent vomiting and failure to thrive. Furthermore, he developed pectus excavatum (Figure 1G) and an aspect of “wrinkled skin”. The patient had gastroenteritis and recurrent respiratory infections, including pneumonia and bronchitis, which often required oxygen supplementation. Besides detection of Influenza A and RSV during two distinct inflammatory episodes with pulmonary involvement, no bacterial or viral agents were found. Through extensive differential diagnostics, mitochondrial, energy and sterol metabolism disorders, aminoacidopathies, glycosylation disorders, peroxisomal diseases, certain lysosomal diseases, and neurogenetic diseases were excluded. Routine genetic testing did not reveal pathogenic variants in genes related to RASopathies or myopathies. Antinuclear antibodies and antineutrophil cytoplasmic antibodies (ANCA) tests for detection of autoantibodies were negative (Table S3). At the age of two years, the patient developed a severe life-threatening autoinflammatory condition with high fever of unknown origin requiring admission to the pediatric intensive care unit, developing into systemic inflammatory response syndrome (SIRS)-like illness. Transient anemia, erythrocyte and thrombocyte anisocytosis aggravated his condition (Table S3). His clinical condition benefited significantly from intravenous immunoglobulin (IVIg) administration as well as antibiotic prophylaxis with cotrimoxazole and cefaclor. Following this SIRS-like illness,

recurrent episodes of fever occurred. The patient died before the age of 3 years from a recurring SIRS-like episode.

Patient 3 (P3), a male born to consanguineous parents of Moroccan origin, presented from 4 months of age onwards with recurrent fever, hepatosplenomegaly, highly elevated acute phase reactants and septal and lobular neutrophilic panniculitis without discernible trigger. In some of these flares, skin lesions progressed to sterile cellulitis (Figure 1C), sometimes locally complicated with myositis and arthritis of the underlying structures. No infectious cause was found, and episodes were unresponsive to antibiotic treatment. The patient exhibited progressive cachexia, severe muscular atrophy and failure to thrive (weight: within 2nd percentile; height: below 1st percentile). He received enteral hypercaloric-hyperproteic supplements, initially administered by nasogastric tube and later by gastrostomy. Except for some intermittent diarrheic depositions, the patient did not present with any other gastrointestinal symptoms. Fecal calprotectin was normal. Fecal occult blood test was also negative. At the age of 3 years, he developed a nephrotic syndrome, which remained unresponsive to treatment with steroids and cyclosporine A, and secondary hypogammaglobulinemia prompting immunoglobulin and albumin replacement. Secondary amyloid A amyloidosis was assumed to underlie the nephrotic syndrome, illustrated by amyloid A deposits in kidney, liver, duodenum, rectum and retina, accompanied by elevated serum amyloid A (Figure 1D, Fig. S1C and Table S4). The patient had two episodes of catheter-related sepsis with isolation of *S. epidermidis* and *S. hominis* and an adenovirus-related gastroenteritis that resolved without antiviral treatment. Further, he presented with two life-threatening episodes of SIRS with bilateral pulmonary infiltrates and ARDS, requiring admission to the pediatric intensive care unit. No infectious etiology was found except for *Candida albicans* isolated from bronchoalveolar lavage. No atypical or invasive infectious agents were isolated over the disease course. However, some degree of immunodeficiency could not be ruled out, given that the patient had been receiving antibiotic prophylaxis with trimethoprim/sulfamethoxazole, itraconazole, and subcutaneous immunoglobulin substitution. Moreover, multidisciplinary assessment also led to diagnosing hypothyroidism of unknown origin. Autoantibody screening, including antinuclear, anti-neutrophil cytoplasmic, anti-smooth muscle, anti-thyroid, and anti-transglutaminase IgA antibodies, was negative (Table S4). Treatment with interleukin-1-(IL-1)-receptor antagonist anakinra allowed for a dose reduction of concomitant prednisolone. Nevertheless, inflammatory symptoms were only partially controlled. Colchicine also failed to resolve the clinical symptoms. Sirolimus treatment

did not show a clear benefit. Subsequent treatment with the anti-interleukin-6 receptor antibody tocilizumab led to partial clinical improvement with amelioration of fever episodes and lower acute phase reactants, but no discernible effect on lymphocytosis. He also received treatment with secukinumab (anti-interleukin-17A antibody) with some initial improvement but no sustained positive effect. T-cell receptor excision circles and K-deleting recombination excision circles were normal (39.0 copies/punch and 39.4 copies/punch, respectively). At the age of 6 years, the patient suffered from pneumonia followed by a severe sepsis, eventually leading to a progressive systemic failure resulting in the death of the patient.

Patient 4 (P4), a 6-year-old male born to non-consanguineous parents of Dutch descent, presented from 2 years of age onwards with symptoms of diarrhea and rectal bleeding, but normal growth development. Initial laboratory investigations during this period of sustained rectal bleeding revealed microcytic anemia, thrombocytosis, hypoalbuminemia, and elevated calprotectin levels, as well as increased levels of IgE (Table S4). Examination of the serum and stool of the patient failed to identify an infectious trigger. Subsequently, endoscopy of the stomach and gut was performed to evaluate the nature of the clinical enteropathy. At the macroscopic level, mucosal erythema with small ulcerations was observed from the descending colon to the rectum, increasing in severity from proximal to distal (Figure 1E). Histological analysis of the colon biopsies demonstrated focal, chronic inflammation with crypt destruction and infiltration of neutrophils and plasma cells without granuloma formation or eosinophilia. In addition, biopsies obtained from the gastric antrum displayed chronic inflammation (Figure 1F) with mild ulceration of the antrum of the stomach. The left-sided colitis and antrum gastritis were considered most adequately explained as features of early-onset Crohn's disease. Consequently, the patient was treated with the 5-aminosalicylic acid mesalazine, which was rapidly complemented with budesonide due to lack of a sustained therapeutic effect. Several months later, the patient presented with a flare-up of the inflammatory bowel disease, after which the therapeutic regimen was switched to azathioprine. Intercurrently, the patient had a severe rotavirus infection for which he was hospitalized and treated supportively with intravenous fluids and enteral feeding. Autoantibody screening, including antinuclear, anti-neutrophil cytoplasmic, anti-transglutaminase IgA and anti-deamidated gliadin antibodies, as well as anti-*Saccharomyces cerevisiae* antibodies were negative (Table S4). To date, the colitis has remained in remission under azathioprine monotherapy with only mild complaints

of abdominal pain and normal growth development (length +0.4SD, weight -1SD) and no other systemic symptoms are present.

Supplementary Material and Methods

Study Oversight

The studies including immunologic diagnostic procedures and genetic analyses were performed in accordance with guidelines of good clinical practice, the current version of the Declaration of Helsinki, with written informed consent from the legal representatives of the patients, and with approval from the appropriate Institutional Review Board of the Medical University of Vienna, the Newcastle and North Tyneside Research Ethics Committee, the Ethics Committee of the Hamburg Medical Chamber (PV3802) and the Medical Ethics Review Committee of East Netherland (medisch-ethische toetsingscommissie Oost15 Nederland). Routine clinical data were obtained by retrospective chart review.

Patient and Human Cell Lines

Peripheral blood mononuclear cells (PBMCs) from the patients (P) and healthy donors (HD) were isolated by Ficoll gradient. An Epstein-Barr virus-transformed B lymphoblastoid cell line (BLCL) was generated by EBV virus infection of PBMCs obtained from patients and subsequent culture in RPMI 1640 containing 10% fetal calf serum (FCS). T cells were expanded by stimulation of PBMCs with irradiated feeder cells (PBMCs from HDs), phytohemagglutinin (PHA) (1 µg/ml) and interleukin-2 (100 U/mL) in complete T-cell medium (RPMI 1640 containing 5% human serum (IBJB – Inst. Biotechnologies J.BOY, 201021334), supplemented with 1 mM sodium pyruvate (Thermo Scientific, 11360039) and MEM Non-essential Amino Acid Solution (Sigma Aldrich, M7145). Fibroblasts were isolated from skin biopsies from the patients and cultured in RPMI 1640 medium containing 10% FCS. THP-1 cells (ASC-GFP Reporter cells, InvivoGen) were cultured in RPMI 1640 medium containing 10% FCS. Human umbilical vein endothelial cells (HUVEC) (Lonza, 1052) were grown in EGM-2 medium (PromoCell, C-22011) containing the endothelial cell growth supplement. Jurkat T cells (clone E6.1, ATCC) were cultured in RPMI 1640 medium containing 10% FCS. If not otherwise specified, culture media were supplemented with 50 U/mL penicillin, 50 mg/mL streptomycin and 10 mM Hepes and cells were cultured at 37°C in a humidified atmosphere with 5% CO₂.

Mice and Zebrafish Strains

All mice were maintained on a C57BL/6 background under specific pathogen-free conditions. *Dock11*-knockout (KO) mice were a gift from Mitsuo Maruyama.² Genotypes were determined by polymerase chain reaction (PCR). All animal experiments were performed using 2- to 5-month-old *Dock11* *y*⁻ male and *Dock11* *-/-* female mice with the approval of the institutional review board (IRB) at the National Center for Geriatrics and Gerontology, Obu, Aichi, Japan.

All zebrafish (*Danio rerio*) strains were maintained and staged as described previously.³ The *lck:nls-mCherry;myl7:EGFP^{vi004}* transgenic line was established by amplifying a 7.4 kb fragment of the *lck* promoter from the BAC, CH211-135B6 (GenBank AL772189) by PCR, and cloning it into the pDONR4-P1R vector by a Gateway BP reaction (Addgene #58891). The *lck* promoter fragment was recombined with nuclear localization signal (nls)-mCherry and a polyA signal in the backbone vector pDESTTol2CG2 (CB395) (a kind gift of the Chien lab) by a Gateway reaction. The transgenesis vector was injected together with Tol2 messenger RNA (mRNA) into fertilized zebrafish eggs. Offspring of injected fish were screened for successful integration of the transgene and a transgenic strain was established. Wild type of the AB genetic background, *fli1:GFP;gata1a:dsRed* double transgenic line^{4,5} and *lck:nls-mCherry;myl7:EGFP^{vi004}* transgenic line were used for the generation of F0 *dock11* knockout, and/or all the Morpholino oligonucleotide (MO)-mediated knockdown experiments and rescue.

Whole-Exome Sequencing

Genomic DNA from Patient 1 and his mother was submitted to whole-exome sequencing (WES) using the Twist Human Core Exome EF Multiplex Complete Kit (Twist Biosciences) for exome capture and preparation of a library for paired-end sequencing on the Illumina NovaSeq 6000 system. Sequencing reads were assessed for quality using the FastQC and MultiQC tools.^{6,7} Reads were aligned with BWA-MEM to GRCh37/hg19 and variant calling was performed according to GATK best practices.⁸ Genotyping was performed using a combination of the HaplotypeCaller from GATK in gVCF mode and JointCalling program leveraging a catalogue of exome samples from other primary immunodeficiency (PID) patients. To avoid false positive calls, VQSR was performed on the raw variant callsets for indels and single nucleotide polymorphisms (SNPs). Downstream analysis was carried out using the online platform SeqR

(<https://github.com/macarthur-lab/seqr>) and standard filtering was done with an in-house developed software.

Trio WES was performed on genomic DNA extracted from leukocytes of Patient 2 and his parents by CeGaT GmbH (Tuebingen, Germany). Enrichment was carried out using the SureSelect Human All Exon V6 kit (Agilent). Each captured library was then loaded and sequenced on the HiSeq platform (Illumina). Variant analysis was performed as previously described.^{9,10} Briefly, the workflow of the Genome Analysis Toolkit (GATK) recommended by the developers was applied and sequencing reads were aligned to the GRCh37/hg19 reference genome.¹¹ Afterwards, variants were functionally annotated and compared to those documented in publicly accessible genetic variant databases (dbSNP138, 1,000 Genomes, and ExAC) using AnnoVar (v2015-03-22).¹² Only exonic and intronic variants that were *de novo* (absent from public databases) or rare (with a minor allele frequency [MAF] <0.1% and no homo- and hemizygotes in public databases) and located at exon-intron boundaries ranging from -8 to +8 were retained. Variants with poor depth (allele depth < 10) and in low quality regions (checked in IGV) were discarded.

For WES of Patient 3, a TrueSeq Rapid Exome kit as well as the Illumina HiSeq3000 system and the cBot cluster generation instruments were used as previously described,^{13,14} with minor changes. Briefly, reads were aligned to the human genome version 19 by means of the Burrows-Wheeler Aligner. Variant Effect Predictor was used for annotating single nucleotide variants and insertions/deletions lists. The obtained list was then filtered according to the presence of variants with a minor allele frequency >0.01 in 1000 Genomes, gnomAD, and dbSNP build 149.^{15,16} After further filtering steps for nonsense, missense, and splice-site variants using an in-house developed software, an internal database was used to filter for recurrent variants.

WES of Patient 4 and both parents was performed as described previously with minor modifications.¹⁷ In brief, genomic DNA samples isolated from whole blood were processed at the Beijing Genomics Institute (BGI) Europe (BGI Europe, Copenhagen, Denmark). All samples were enriched for exonic DNA using the Agilent SureSelect Human All Exon V5 kit (Agilent Technologies, Santa Clara, CA, United States). DNA samples were sequenced with the Illumina HiSeq4000 system. Sequencing was performed with 2x150 base pair paired-end sequencing reads.

Downstream processing was performed by an automated data analysis pipeline, including mapping of sequencing reads to the GRCh37/hg19 reference genome with the Burrows-Wheeler Aligner algorithm and Genome Analysis Toolkit variant calling and additional custom-made annotation.^{11,18} The DeNovoCheck tool is part of the custom-made annotation and was used to align variants called in each member of the patient-parent trios, providing an indication whether variants were inherited or de novo.¹⁷ Variants were filtered to retain rare (<0.1% allele frequency) in our in-house database containing the whole-exome sequencing data of >20,000 individuals run at the diagnostic laboratory of the Radboud University Medical Center and the population databases from Exome Aggregation Consortium (ExAC), Genome Aggregation Database (GnomAD) and dbSNP as well as <0.5% in the Genome of the Netherlands (GoNL) database),^{15,16} coding, non-synonymous possible de novo variants. Quality control steps excluded variants with <5 variation reads, <20% variant allele frequency or low coverage variants. Subsequently, synonymous single nucleotide variants (SNVs) and small indels were excluded from the analysis.

The remaining variants from all four patients were prioritized and systematically evaluated using nucleotide conservation, combined annotation dependent depletion (CADD v1.3) pathogenicity prediction score¹⁹, functional information and possible involvement in the immune system based on mouse KO models, pathway-based annotation (Gene Ontology terms), and literature studies.

Sanger Sequencing

Sanger sequencing was used to validate the *DOCK11* variants identified through WES in the affected patients and their family members. This was done by designing specific primers for each of the four identified variants.

Exon/Intron # (Patient #)	Variant	Forward Primer Sequence (5'-3')	Reverse Primer Sequence (5'-3')
Exon 1 (Patient 1)	NM_144658.3: c.75dup	AATTCACCAAACGGCTCAGC	TGCGAAAACCTTACTGGAGCG
Intron 15 (Patient 2)	NM_144658.3: c.1718+5G→A	ATACTCAAGGCTCTCTTGATCTGG	TGAATGCACTGGTTACCCTCTATC
Exon 46 (Patient 3)	NM_144658.3: c.5120G→C	CCTTTTGTGCATCTCATTGAA	TCTTCAGAGGACACAAGTCGAA
Exon 4 (Patient 4)	NM_144658.3: c.323A→G	CTGTCGGCATAGTACCAGAGTT	TTTACCACGTGCCAATCTGTG

Rna Isolation, cDNA Synthesis, and *DOCK11* Transcript Analysis

Total RNA was extracted from cultured primary fibroblasts of Patient 2 and a healthy donor (Monarch Total RNA Miniprep kit, New England BioLabs). RNA concentration and purity of the samples were assessed using the Microplate Spectrophotometer Epoch (BioTek). 1 µg total RNA was reverse transcribed (LunaScript RT Super Mix kit, New England BioLabs), and 1 µl of the reverse transcription reaction was used to amplify a *DOCK11* cDNA fragment encompassing exons 14 to 17.

The following PCR primers were used:

Gene	Forward Primer Sequence (5'-3')	Reverse Primer Sequence (5'-3')
<i>DOCK11</i>	GAAGGTGCACAGGACAGCTAAAC	CTTCAAGGGCACATATGA AGAAG

The PCR product was Sanger sequenced using the following primers:

Gene	Forward Primer Sequence (5'-3')	Reverse Primer Sequence (5'-3')
<i>DOCK11</i>	CCTTTTGTGCATCTCATTGAA	TCTTCAGAGGACACAAGTCGAA

X-Chromosome Inactivation Analysis

Examination of the methylation pattern at the *AR* locus was performed as previously described.²⁰ Examination of the methylation pattern at the *RP2* locus was performed analogous to the *AR* locus using the following fluorochrome-coupled primers for PCR after *HpaII* digestion published by Machado et al.²¹ The following primers were used:

Forward Primer Sequence (5'-3')	Reverse Primer Sequence (5'-3')
[6FAM] AGTGACATAGCRAGACCCTGTG	GTTTCTGGTGGGTTCTCTAGCTGGT

CRISPR/Cas9 Editing and ShRNA Knockdown of Human Cells

Knock-in of the implicated pathogenic variants (identified in patients) in healthy donor T cells was done by CRISPR/Cas9 editing. In brief, PBMCs were isolated from a healthy donor by Ficoll gradient and T cells were isolated from PBMCs by negative selection using the MagniSort™ Human T cell kit (Thermo Fisher Scientific, 8804-6810-74). T cells were seeded at 200,000 cells/well in 100 µl complete T-cell medium, supplemented with interleukin-2 (100 U/mL), onto 96-well flat bottom high binding plates (Corning, 3361) coated overnight at 4°C with 10 µg/ml

anti-CD3 (clone OKT3, eBiosciences) and 5 µg/ml anti-CD28 (Clone T44, CD28.2, eBiosciences) antibodies. After 66 hours, T cells were collected and resuspended in Opti-MEM (Thermo Fisher Scientific, 31985062). For electroporation, 10⁶ cells were used. 125 pmol of Cas9 protein (IDT, Alt-R® S.p. Cas9 Nuclease V3) and 150 pmol single gRNA (sgRNA) were mixed and incubated for 15 min at room temperature (RT). 600 pmol single-stranded oligodeoxynucleotide (ssODN) template were added and gently mixed with the T-cell suspension. Electroporation was performed using NEPA21 electroporator (NepaGene) with the following conditions: Poring pulse: V 275, length 1 ms pulse length, total two pulses with 50 ms interval between the pulses, 10% decay rate with + polarity; Transfer pulse: 20 V, 50 ms pulse length, total 5 pulses with 50 ms interval between the pulses, 40% decay rate with +/-polarity. After recovery in complete T-cell medium supplemented with interleukin-2 (100 U/mL) for 5-7 days, single cell clones were generated by serial dilution. The following sgRNAs and ssODNs were used:

Exon/ Intron #	sgRNA sequence	ssODN
Exon 1	CGGCCTCAGA CACGCTCTGC	TGCCCCGTCCCCGGCCACTCACCAGCACCACGGAGCCCCGCACGGCCTCAAG ACACGCTCTGCCGAAGCTCAGCCGCCGTGCCAGGCTTGCTGAGCCGTT
Intron 15	GAATATAAGA AGTAAGTGTT	AGCTTTCAAGTGAAGACATTCTCAAGTTGCTCTCAGAATATAAGAAGTAAATGT TTGATGTTTCTGCAATAAGTAAATATAATAGATGAATCCTCAGTTTT
Exon 46	TTGCTAGAAC AATGTGTGGA	AATGCAGGAGGTCTTGCTGGAGTTGCTAGAACAAATGCGTTGATGGCTTATCGA AGGCAGAACGTTATGAAATAATTTCTGAGATTTCCAAGTTGATCGTTC

The introduction of the desired mutation was verified by capillary sequencing and tracking of indels by decomposition (TIDE) analysis.²² The following primers were used:

Exon/Intron #	Forward Primer Sequence (5'-3')	Reverse Primer Sequence (5'-3')
Exon 1	CGAAGTGCGCAAATTCACCA	GTCGCTCTGCTTCCTCTGTT
Intron 15	CTTCTGTTGCTGTTTTAGACCCA	TGCCACGTAAACCTCAAGAAAAA
Exon 46	TCAGACATCCTCAATTTGGAACA	GCATTTTTAGGAATTGCACTTTGA

For knockout of *DOCK11* in THP-1 cells, CRISPR/Cas9 sgRNA targeting exon 7 of *DOCK11* was cloned into a lentiCRISPRv2 vector. The following sgRNA targeting sequence was used: TACTTGACCCAACCTTCCTGA. Lentivirus production in Lenti-X™ 293T HEK cells (Takara Bio) and spinfection of THP-1 cells were performed according to standard procedures. In brief,

lentiCRISPRv2, pMD2.g and psPAX2 plasmids were transfected into Lenti-X™ 293T HEK cells by calcium phosphate transfection, lentiviral supernatant was harvested after 48 hours and spinfection (2100 rpm, 45 min, 34°C) of THP-1 cells was carried out in complete RPMI supplemented with 8 µg/ml Polybrene. Transduced cells were selected with 2 µg/ml Puromycin (Sigma), starting 2 days post-transduction. Editing at genomic position was confirmed using capillary sequencing and subsequent analysis with TIDE.²² Four clonal cell lines generated by limiting dilution were used for further studies. Knockout efficiency was assessed by immunoblotting as described below. The following primers were used for PCR amplification and capillary sequencing:

Forward Primer Sequence (5'-3')	Reverse Primer Sequence (5'-3')
CAAATGTATCATTGCTGGG	CCCTGTTAGAAAAAGAGAAGG

For knockdown of *DOCK11* in Jurkat T cells, short hairpin RNAs (shRNAs) were ordered from Sigma-Aldrich as MISSION® shRNA bacterial glycerol stocks. The following shRNAs were used: shRNA1 (NM_144658/TRCN0000369611) target sequence: ACTAAATGAGCGGCTAATTAA; shRNA2 (NM_144658/TRCN0000376430) target sequence: TGATGGCCATAACCCATTAAT. Lentivirus production in Lenti-X™ 293T HEK cells and spinfection of Jurkat cells were performed according to standard procedures. Two days after transduction, puromycin selection (1 µg/ml) was initiated. Knockdown efficiency was assessed by quantitative reverse transcriptase PCR as described below.

For lentivirus production for erythroid culture assay, the above mentioned shRNAs were cloned into pKLO.1-CMV-tGFP vectors and used for transfection of HEK 293T cells with the appropriate viral packaging and genomic vectors (p-VSV-G and pCMV) using lipofectamine transfection reagent according to the manufacturer's protocol (Polyplus-transfection Inc., New York, NY, USA). After 24 hours and two ultracentrifugations at 5,000g and then 20,000g for 1 hour at 4°C, concentrated virus pellets were collected. Viral particle titers were determined by quantifying the number of GFP positive cells by flow cytometry following infection of HEK293T cell lines. Virus stocks were kept frozen at -80°C. For lentiviral transduction, CD34+ cell infection was performed with a multiplicity of infection of 10.

For reconstitution experiments, N-terminally HA-tagged wild-type DOCK11-IRES-GFP was cloned into a lentiviral vector (HIV 1Ψ-RRE-cPPT/CTS-EF1a-Strep-HA-DOCK11-IRES-EGFP) using NEBuilder® HiFi DNA Assembly Cloning Kit. The c.G5120C/p.W1707S mutation (present in patient 1) was introduced by site-directed mutagenesis. Viral particles, produced in Lenti-X™ 293T HEK cells, were concentrated using PEG-it Virus Precipitation Solution (LV825A-1, SBI) and spinfection of Jurkat *DOCK11*-knockdown and control shRNA Jurkat T cells were performed according to standard procedures. Transduced cells positive for GFP were sorted on FACS Aria™ Fusion cell sorter and used for further analysis. Reconstitution of *DOCK11* expression was analyzed by quantitative reverse-transcriptase PCR and cell morphology and filopodia formation, as a functional readout, was assessed as described below.

CRISPR/Cas9 Editing, Morpholino, and mRNA Injections in Zebrafish

F0 *dock11*-knockout zebrafish embryos were generated using multi-locus targeting CRISPR/Cas9 genome editing technology as described in ref.²³, where the *dock11* gene was disrupted at three target sites, two in exon 1 and one in exon 4. For this, three predesigned crRNAs (Integrated DNA Technologies (IDT)) were used. The crRNA sequences are listed below with the PAM sequence underlined.

Exon #	Name	Sequence
Exon 1	Dr.Cas9.DOCK11.1.AA	CTTCGTGAATTTTCGTA <u>CTTCGG</u>
Exon 1	Dr.Cas9.DOCK11.1.AB	AATGGACGTCCTCACCGC <u>CTCGG</u>
Exon 4	Dr.Cas9.DOCK11.1.AC	AAGCCTATTCGGGAGATT <u>TCCGG</u>

1 μl of each crRNAs (200 μM) was mixed with 1 μl of tracrRNA (200 μM) (IDT; Cat. #1072532) and 1 μl of Duplex buffer (IDT; Cat. #11-01-03-01) and annealed at 95°C for 5 min. To assemble the ribonucleoproteins (RNPs), each of the resulting sgRNAs were mixed with 1 μl of 57 μM Cas9 protein (IDT, 1081059) incubated at 37°C for 5 min and pooled together afterwards. 1 nl of the RNPs (3x *dock11* sgRNA+Cas9) was microinjected in one-cell stage wild-type or transgenic embryos. Mutants were identified at 24 hours post injection by isolation of genomic DNA and subsequent Sanger sequencing of exon 1 and exon 4, using the following primers:

Exon #	Foward Primer Sequence (5'-3')	Reverse Primer Sequence (5'-3')
Exon 1	TTATGCCTCAGCAGTCTGGC	AAGTGGCTGCAAATGAGACC
Exon 4	TTGATCGTCACAGGAGAACCA	AGGCTCAGTTTCCACCATCA

The editing efficiency was analyzed by TIDE.²² A Morpholino oligonucleotide (MO) against the coding sequence of *dock11* (ATG MO, 5'- CGTGAATTTTCGTA CTTCGGACATG-3', Gene Tools Inc.) was used to knockdown *dock11* in zebrafish embryos. To interfere with Cdc42, MO against *cdc42* was used (5'-CAACGACGCACTTGATCGTCTGCAT-3', Gene Tools Inc.).²⁴ Either 4 ng of the ATG *dock11* MO, 2 ng of the *cdc42* MO or the corresponding amount of standard control MO (CCTCTTACCTCAGTTACAATTTATA; Gene Tools Inc.) was injected in one-cell stage wild-type or transgenic embryos.

For the rescue experiments, the constitutively active form of the human CDC42 was cloned from the pECFP-Cdc42^{Q61L} Addgene vector (105294), a gift from Kenneth Yamada, into the pCS2+ vector, as an *XhoI-EcoRI* fragment. For capped mRNA synthesis, the construct was linearized by *NotI* restriction digestion and transcribed with SP6 polymerase using the mMACHINE mMACHINE Kit (Ambion). 2.5 pg mRNA of a constitutively active form of the human *CDC42* (*CDC42*^{Q61L}) were injected into one-cell stage embryos, additionally injected with either 3x *dock11* sgRNA without Cas9 (control embryos) or with Cas9. These embryos were further analyzed at 32 hours post fertilization (hpf) for their content in Gata1a (dsRed)-positive cells by flow cytometry as described below.

Culturing of Human CD34+ Primary Cells and Infection

CD34+ cells were isolated from human cord blood by immunomagnetic technique by autoMACS Pro Separator (Miltenyi). Purified CD34+ cells were cultured in Stemspan-SFEM (Stemcell technologies), with 200 µg/ml Holo-Transferrin (Sigma Aldrich), 10 ng/ml stem cell factor (SCF) (Miltenyi), 1 ng/ml interleukin-3 (Stemcell Technologies), 3 IU/ml erythropoietin (EPO) and 1% penicillin/streptomycin from day 0 to 6. This media was deprived of interleukin-3 from day 7 to 10 and both interleukin-3 and SCF from day 11 to day 14. From day 11 to 14, EPO was reduced from 3 IU/ml to 0.1 IU/ml. Lentiviral *DOCK11* shRNA CD34+ cells were cultured in IMDM supplemented with glutamax (Gibco), containing 3% AB serum (Sigma Aldrich), 2% human peripheral blood plasma (Stem Cell Technologies), 10 µg/ml insulin (Sigma Aldrich), 3 IU/ml

heparin (Sigma Aldrich), 200 µg/ml holo-transferrin (Sigma Aldrich), 10 ng/ml stem cell factor (Miltenyi biotech), 1 ng/ml interleukin-3 (Stemcell Technologies), 3 IU/ml EPO and 1% P/S from day 0 to 6. Isolated CD34⁺ cells were transduced with *DOCK11* shRNA, scramble or empty vectors at day 2 of erythroid differentiation. At day 5, transduced (GFP⁺) cells were sorted on the FACSAria flow cytometer. Erythroid cell counts were obtained from 5000 cells during the time course day 5 to day 12. Viable (trypan blue negative) cells were counted in triplicate with a Biorad cell counter. The mortality rate is defined by trypan blue positive cells divided by all cells counted. Remaining cells were used for flow cytometry analysis (see below).

Flow Cytometry

For immunophenotyping of human blood cells, PBMCs were isolated from patients or healthy donors by Ficoll gradient and used either fresh or after cryo-preservation in liquid nitrogen. For assessment of intracellular cytokines in T cells 3x10⁵ cells were used, for all other stainings 1.5x10⁵ cells were used. Blocking was performed in RPMI containing 10% FCS, followed by staining of surface antigens for 1 hour at 4°C. Immunophenotyping using flow cytometry analysis was performed on a BD LSR Fortessa. All data were analyzed using FlowJo X (Treestar). The following antibodies were used: from Beckman Coulter: CD16-FITC (clone 3G8), CD4-PECy7 (SFC112T4D11); from eBioscience, Affymetrix: CD19-PerCPCy5.5 (HIB19); from BD Biosciences: CD14-PECy5 (61D3) CD16-PECy7 (3G8), CD197 (CCR7) PE-CF594 (150503), CD21-PE (B-ly4), CD25-BV605 (2A3), CD27-V450 (M-T271), CD3-APC-H7 (SK7), CD38-PECy7 (HIT2), CD4-BV605 (RPA-T4), CD45RA-AF700 (HI100), CD56-V450 (B159), CD8-V450 (RPA-T8), CD8-V500 (RPA-T8) IgD-FITC (IA6-2), IgM-APC (G20-127), TCRαβ-FITC (WT31), TCRγδ-PE (11F2); from ThermoFisher Scientific: CD127-FITC (eBioRDR5). Gating strategy was as follows: naïve (CD45RA⁺CCR7⁺), central memory (CD45RA⁺CCR7⁺), effector memory (CD45RA⁺CCR7⁻) and exhausted effector memory (CD45RA⁺CCR7⁻) cells among CD8⁺ and CD4⁺ T cells, CD4⁺CD25^{high}CD127⁻ Treg cells among CD4⁺ T cells. TCRαβ⁺ and TCRγδ⁺ cells among CD3⁺ T cells; naïve (CD27-IgD⁺), marginal zone-like (CD27-IgD⁺), switched memory (CD27-IgD⁻), double negative (DN) memory (CD27-IgD⁻), CD21^{low}CD38^{low} cells and plasmablasts (IgM-CD38^{high}; CD27^{high}CD38^{high}) among CD3⁺CD19⁺ B cells; classical (CD14⁺⁺CD16⁻), intermediate (CD14⁺⁺CD16⁺) and non-classical (CD14⁻CD16⁺⁺) monocytes; CD16⁺CD56⁻, CD16⁺CD56⁺ and CD16⁻CD56^{bright} NK cells among CD3⁻ cells.

For B-cell class-switch and proliferation assays, isolated PBMCs were stimulated with CpG (75 nM, ODN 2006/ ODN 7909, InvivoGen), or CD40 ligand (200 ng/ml, Peprotech), in combination with recombinant human interleukin-4 (100 ng/ml Peprotech). To assess proliferation, PBMCs were loaded with 1 μ M of Violet Proliferation Dye 450 (VPD450, BD Horizon) for 15 min at 37°C. Following 7 days of stimulation, PBMCs were stained with anti-CD3-FITC (SK7, BD Biosciences), anti-CD19- BV510 (SJ25C1, BD Biosciences), anti-IgG-PE (IS11-3B2.2.3, Miltenyi Biotec) and anti-IgA-APC (IS11-8E10, Miltenyi Biotec) antibodies and flow cytometry analysis was performed on a BD LSR Fortessa. All data were analyzed using FlowJo X (Treestar).

For immunophenotyping of murine cells, spleen and lymph nodes were collected in RPMI 1640 medium. Single-cell suspensions were generated by mincing the spleen and lymph nodes using a flat syringe plunger. The cell suspension was passed through a 48 μ m nylon mesh and for T-cell subset analysis incubated in red blood cell (RBC) lysis buffer (17 mM Tris-HCl, 0.75% NH₄Cl, pH 7.65) for 2 min. Afterwards, the cells were washed and resuspended in fluorescence-activated cell sorting (FACS) buffer (PBS, 2% FCS, 0.1% NaN₃). After blocking with TruStain FcX (BioLegend 156603) buffer for 15 min on ice, cells were stained with fluorescent-conjugated antibodies in FACS buffer for 30 min on ice, washed and assessed by flow cytometry using a BD Bioscience FACS Canto II flow cytometer. All data were analyzed using FlowJo X (Treestar). The following antibodies were used: from Biolegend: CD62L-FITC (104405), CD44-PE (103008), Thy1.2-PE (BioLegend 105307), B220-FITC (103205), CD4-APC-Cy7 (100525) and CD8-Pacific Blue Blue-anti-CD8 (100728) for T-cell subsets. Gating strategy was as follows: naïve (CD62L+CD44-), central memory (CD62L+CD44+) and effector memory (CD62L-CD44+) cells among CD4+ and CD8+ T cells.

For flow cytometry analysis of Gata1⁺ erythroid and Fli1⁺ zebrafish cells, 32 hpf *fli1:GFP;gata1:dsRed*; transgenic zebrafish embryos injected with either 3x *dock11* sgRNA alone, 3x *dock11* sgRNA+Cas9, 3x *dock11* sgRNA+Cas9+*CDC42^{Q61L}* mRNA, control MO, *dock11* MO, or *cdc42* MO were dechorionated. Around 100 embryos per condition distributed in 10 samples with 10 embryos per sample were then lysed by adding 750 μ l of protease buffer (0.25% phenol-free trypsin (ThermoFisher Scientific, 15090046), 2.5 mg/ml Collagenase Type I (ThermoFisher Scientific, 17018029), 1 mM EDTA and 2 mM CaCl₂ in PBS). Embryos were then

mixed and homogenized by vigorously pipetting, followed by a 12-min incubation period at 37°C, where samples were shaking at 600 rpm during the first two minutes. The trypsin/collagenase reaction was stopped by adding 100 µl FCS and, after washing with FACS buffer (PBS, 2% FCS), cells were resuspended in FACS buffer and fluorescent markers were assessed by flow cytometry on a BD LSR Fortessa.

For apoptosis assessment, cells from 3 dpf *gata1:dsRed* transgenic zebrafish embryos were washed with PBS and stained with Annexin V-FITC (BD Biosciences, 556420) and propidium iodide solution (BioLegend, 421301) for 5 min on ice before direct assessment by flow cytometry. For staining of Phospho-Histone H3, cells from 30 hpf, 3 and 5 dpf *gata1:dsRed;flil:GFP* transgenic zebrafish embryos were fixed with prewarmed BD Cytifix (BD Biosciences, 554655) for 15 min at 37°C, washed with BD Stain Buffer (BD Pharmingen, 554656), permeabilized by slowly adding ice-cold BD Phosphoflow Perm Buffer III (BD Biosciences, 554656) while shaking and subsequent incubation for 30 min on ice. Cells were washed and stained with Histone H3 (Ser10) Alexa Fluor® 647 (Biozym Scientific, 650806) and anti-RFP (recognizes dsRed, rabbit, Biomedica GmbH, MB-PM005, 1:500) coupled to AF594 for 1 hour on ice²⁵ before washing and flow cytometry analysis. All data were analyzed using FlowJo X (Treestar).

For human erythroid differentiation and apoptosis, human cultured erythroid cells were immunophenotyped from day 5 (D5) to day 12 (D12) using several antibodies: CD123- PE/Cy7 (Interleukin-3R), CD117-APC, CD36- Vioblue, CD71-PE, and CD235-APC for erythroid differentiation (all from Miltenyi), and Annexin V-APC and PE/Cy7-7AAD (Sigma-Aldrich) to assess apoptosis. FACS analysis was conducted on a flow cytometer from Miltenyi. Data were analyzed using Flowjo (Treestar).

Immunoblot

Human cells were lysed in RIPA buffer (50 mM HEPES, 150 mM NaCl, 10% Glycerol, 2 mM EDTA, 1% sodium deoxycholate), supplemented with 1 mM PMSF, 20 mM NaF, 1 mM sodium orthovanadate and Roche cOmplete™ Protease Inhibitor Cocktail, for 5 min on ice, then centrifuged at 4°C at full speed for 5 min. The supernatant was then boiled with SDS loading dye for 5 min at 95°C. The indicated samples were treated with PNGase F (P0704S, New England BioLabs) according to the manufacturer's instructions. The samples were run on a 10%

Acrylamide/Bis solution (Bio-Rad, #1610158) gel, followed by wet transfer for 55-65 min at 100 V onto a ROTI®PVDF 0.45 membrane (Carl Roth). DOCK11 was detected with two rabbit polyclonal anti-DOCK11 antibodies (1:1,000 dilution; Bethyl, #A301_638A or 1:1,000 dilution; Bethyl, #A301_639A). Loading control HSP 90 α/β (F8) was detected with a mouse monoclonal antibody (1:10,000 dilution; Santa Cruz; sc-13119). Immunodetection was performed using secondary horseradish peroxidase-coupled goat anti-mouse (554002, BD Biosciences) or goat anti-rabbit (172-1019, BioRad) secondary antibodies with ECL solution, either homemade or Prime or ECL Select (Amersham).

For assessment of JNK and ERK phosphorylation in murine T cells, CD4⁺ T cells were purified from spleen and peripheral lymph nodes using Dynabeads™ DETACHaBEAD™ mouse CD4 Kit (12406D, Invitrogen) and CD8a⁺ T Cell Isolation Kit, mouse (Miltenyi 130-104-075). The cells were resuspended in RPMI 1640 medium containing 10% FCS, 100 U/ml penicillin, 100 μ g/ml streptomycin and 100 μ M 2-mercaptoethanol. Isolated T cells were cultured in anti-CD3/CD28 antibody-coated 24-well plates (1 x 10⁶ cells/well). On day 2, cells were washed twice with PBS at 1,200 rpm for 5 min. Cell pellets were resuspended in 500 μ l of RPMI 1640 medium containing 10 μ g/ml anti-CD3 ϵ antibody (145-2C11, BioLegend 100340) and incubated on ice for 20 min. Cells were then washed with 5 ml of RPMI 1640 medium three times, resuspended in RPMI 1640 (3~5 x 10⁷ cells/ml), and aliquoted into 1.5-ml tubes (30 μ l/tube). After incubation at 37 °C for 10 min, anti-hamster IgG (final 10 μ g/ml, Jackson ImmunoResearch 127-005-009) was added to the cell suspension and incubated for the indicated time. The reaction was stopped by adding an equal volume of 2x lysis buffer (40 mM Tris-HCl (pH 7.5), 300 mM NaCl, 2 mM EDTA, 2 mM EGTA, 2% Triton X-100, 5 mM sodium pyrophosphate, 2 mM beta-glycerophosphate, 2 mM Na₃VO₄, 2 mM PMSF, 2 μ g/ml aprotinin). After incubation for 15 min on ice, cells were centrifuged at 13,200 rpm for 5 min at 4°C. The supernatant was mixed with 4x loading buffer and heated at 95°C for 5 min. The following antibodies were used for immunoblot analysis: Phospho-SAPK/JNK (Thr183/Tyr185) (81E11) antibody (Cell Signaling Technologies #4668), SAPK/JNK antibody (Cell Signaling Technologies #9252), Phospho-p44/42 MAPK (Erk1/2) (Thr202/Tyr204) antibody (Cell Signaling Technologies #4370) and p44/42 MAPK (Erk1/2) antibody (Cell Signaling Technologies #4695).

Protein Modelling

3D structural model of wild-type DOCK11 was predicted using Alphafold.^{26,27} Structure representations of wild-type DOCK11 and DOCK11^{Y108C} and DOCK11^{W1707S} were generated with PyMOL (Molecular Graphics System, version 2.0 Schrödinger, LLC).

Quantitative Reverse Transcriptase PCR

For *DOCK11* mRNA level quantification, RNA was isolated from Jurkat T cells using the RNeasy Mini Kit (74106, Qiagen), treated with RQ1 (RNA-Qualified) Rnase-Free Dnase (M6101, Promega) and subsequently reverse transcribed into cDNA using M-MLV Reverse Transcriptase (M1701, Promega) and both oligo-dT and random hexamer primers. Gene expression was analyzed in technical duplicates by quantitative PCR using KAPA SYBR® FAST ABI PRISM® MasterMix (KK4605, Kappa Biosystems) on Roche LightCycler® 480 according to the manufacturers' instructions. For each gene standard curves were generated by serial dilution of Jurkat wild-type cDNA and used to determine the target mRNA quantity in each sample, which was expressed in arbitrary units. These values were normalized to *HPRT* gene expression and used for statistical analysis. *DOCK11* gene expression was plotted as fold change to respective control. The following primers were used:

Gene	Forward primer (5'-3')	Reverse primer (5'-3')
DOCK11	TTCAGAGGCTGCGATGTGTT	ACGCTGAACATCCGTTAGGA
HPRT	CCCTGGCGTCGTGATTAGTG	TCGAGCAAGACGTTTCAGTCC

CDC42 Activity Assay

Following overnight serum starvation, patient-derived BLCLs were stimulated for 0 min (0') or 5 min (5') with 100 ng/mL CCL19 (Preprotech). The amounts of GTP-bound active CDC42 were measured by pull-down with beads coated with GST-PDB (PAK1 binding domain) as described previously.²⁸

Immunohistochemistry

Staining of bone marrow aspirate with Wright-Giemsa stain (Arvin Shimi Delta Chemical Lab (IR)) was performed according to the manufacturer's instruction and images were taken with a Nikon E400 microscope.

For immunohistochemistry of zebrafish blood cells, zebrafish embryos at 48 hpf were anesthetized in calcium-free and magnesium-free PBS (pH 7.4) containing 0.02% tricaine (Sigma) and 1% bovine serum albumin (BSA). Circulating blood cells were collected in sampling buffer (PBS, 4% FCS, 5 mM EDTA, 0.1% BSA, 10 mM glucose) by cutting tails and, using a Shandon Cytospin2, deposited onto SuperFrostPlus microscopy slides by centrifugation at 500 rpm for 8 min. Slides were air-dried and stored protected from light until staining with May-Grünwald's eosin methylene blue staining solution (Sigma-Aldrich) and subsequent staining with Giemsa's azur eosin methylene blue solution (Merck) according to the manufacturer's protocol. Images were captured using Zeiss Axiovert 40C inverted phase contrast microscope connected to a PixeLINK Megapixel FireWire Camera (PL-A662) at 32-fold magnification. Cell area (in pixels), cell circularity and nuclear area of at least 60 randomly selected erythrocytes were measured by using Fiji software.²⁹

Microscopy Analysis of Human T-Cell Morphology

To assess human primary T-cell spreading on fibronectin, expanded T cells were resuspended in RPMI with 10% FCS and transferred to slides, which had been coated with 2 µg/mL fibronectin at 4°C overnight. After 25 min of incubation at 37°C, cells were fixed with BD Cytofix containing 4.2 % formaldehyde at 37°C for 10 min, permeabilized with 1x BD Perm/Wash buffer for 15 min at RT and stained with Phalloidin-AF488 (A12379, ThermoScientific), anti- α -Tubulin antibody (T9026, Sigma Aldrich) and 4',6-diamidino-2-phenylindole (DAPI). Goat anti-Rabbit-AF555 Ab (A-21429, ThermoScientific) was used to reveal the primary antibody staining. Slides were imaged with a Zeiss LSM700 or LSM980 confocal microscope and a 63x oil-immersion objective. Unsupervised analysis of cell morphology parameters was performed with the CellProfilerTM software.³⁰ Analysis of filopodia was performed using Fiji software.²⁹

Microscopy Analysis of Human T-Cell Synapse Formation

For T-cell immunological synapse formation, P815 cells were coated with 10 µg/mL anti-CD3 antibody (OKT3, eBioscience) for an hour, subsequently incubated with cytotoxic T cells at a 2:1 ratio for 20 min and then seeded on poly-L-lysine (P4832, Sigma) coated slides. Cells were then fixed with BD Cytofix at 37°C for 10 min, permeabilized with 1x BD Perm/Wash buffer for 15 min at RT and stained with Phalloidin-AF488 (A12379, ThermoScientific), anti- α -Tubulin antibody

(T9026, Sigma Aldrich) and DAPI. A goat anti-Rabbit AF555-coupled antibody (A21244, ThermoScientific) was used to reveal the α -Tubulin staining. Slides were examined with LSM700 or LSM780 confocal microscopes and a 63x oil-immersion objective.

Microscopy Analysis of Human B Lymphoblastoid Cells

For assessment of synapse assembly by BLCLs, a View-Plate-384 tissue culture treated plate (Perkin Elmer, 6007460) was coated with either 2 $\mu\text{g}/\text{ml}$ recombinant human ICAM-1-Fc chimera (R&D Systems, 720-IC), 10 $\mu\text{g}/\text{ml}$ goat anti-human IgM antibody (Southern Biotech, #2020-01) or a combination of both and incubated at 4°C overnight. BLCLs were seeded at 8,000 cells per well and incubated for 20 min at 37 °C. Cells were fixed with 4 % formaldehyde solution (Thermo Scientific, 28906) and stained with Phalloidin AF-488 (Thermo Fisher Scientific, A12379) and AF 647 mouse anti-phosphorylated BTK antibody (BD, 564846) in permeabilization buffer (Thermo Fisher Scientific, 00-8333-56). Nuclei were stained with DAPI (Thermo Fisher Scientific, D1306). Each condition was replicated in 3 wells. Images were acquired on an automated spinning disk confocal HCS device (Opera Phenix, PerkinElmer) with a 40x 1.1 NA Plan Apochromat water immersion objective. Image datasets were analyzed using the Harmony software (Perkin Elmer) to extract cell area and phosphorylated BTK intensity.

Microscopy Analysis of Human Primary B-Cell Synapse Formation

The formation and structure of B-cell synapses was assessed as described previously³¹ with the following amendments: Human B cells were isolated from PBMCs using the human B Cell Isolation Kit II (Miltenyi Biotec, 130-091-151) according to the manufacturer's instructions. B cells were washed with imaging buffer (HBSS (Life technologies) supplemented with 0.4 mg ml⁻¹ Ovalbumin (Merck), 2 mM CaCl₂ and 2 mM MgCl₂ (Merck)) and seeded on planar supported lipid bilayers (PLBs) functionalized with histidine-tagged (His₁₂) human ICAM-1 (~100 molecules per μm^2) and histidine-tagged (3xHis₆) monovalent streptavidin (mSav) conjugated to the IgM-reactive and biotinylated monoclonal antibody MHM88-STAR635P (129 \pm 4 or 468 \pm 4 molecules per μm^2).

To visualize B-cell synapses *in situ*, we operated an Eclipse Ti-E (Nikon) inverted microscope system that was equipped with a 100x objective (Nikon SR APO TIRF 100x, NA=1.49) and a 20x objective (Nikon S Fluor, NA=0.75). Videos of B-cell synapse formation were recorded with the

20x objective (Nikon S Fluor, NA=0.75) in epi fluorescence mode using 635/18 nm (Cy5) lamp illumination to visualize MHM88-biotin-STAR635P. We recorded an image stack (white light, Cy5 illumination) every 15 sec for 30 minutes. We extracted the area and integrated density of the monoclonal antibody MHM88-biotin-STAR635P enriched within a B-cell synapse and plotted the normalized intensity data over time. Microscopy images were processed and analyzed with Imaris software (Oxford Instruments). In addition to videos, we visualized the structure of mature B-cell synapses in total internal reflection fluorescence (TIRF) mode using the 100x TIRF objective (Nikon SR APO TIRF 100x, NA=1.49) 30 min after synapse formation. To this end, we recorded a red image (640 nm laser excitation, ZT405/488/532/640rpc beam splitter ET700/75 emission filter, 10 ms exposure time) to visualize recruited mSav:MHM88-biotin-STAR635P under the B-cell synapse, followed by an interference reflection microscopy (IRM) image (lamp ET554/23 excitation, ET Dualb. “Sedat” CFP/YFP sbxm + HC510/20 beamsplitter, ET 535/30 emission filter, 5 ms exposure time) to verify complete adherence of the cell, and a white light image (HC Quadband beam splitter, 500 ms exposure time). We used a 640 nm laser power density of 0.01-0.02 kWcm⁻² to excite the enriched STAR635P.

Immunofluorescence Analysis of NFATc1 Translocation

For assessment of NFATc1 (NFAT2) translocation in human CD8⁺ T cells, expanded T cells were seeded at 100,000/25 μ l RPMI 1640 supplemented with 0.1% human serum (IBJB – Inst. Biotechnologies J.BOY, 201021334) in a 96-well U-bottom plate and starved for 2 hours. Following incubation for another 2 hours with anti-CD3 (0.5 μ g/ml) and anti-CD28 (0.5 μ g/ml) antibodies in a total of 50 μ l starvation medium, cells were transferred to poly-L-lysine (P4832, Sigma) coated slides and allowed to settle for 10 min at 37°C. Cells were fixed with BD Cytofix for 10 min at 37°C and permeabilized with BD 1x Perm/Wash buffer for 15 min at room temperature. Cells were stained with anti-NFATc1 antibody (Cell Signaling Technology, 8032S, clone D15F1, 1:100 in 1x Perm/Wash) overnight, washed, stained with Phalloidin-AF488 (ThermoFisher Scientific, A12379, 1:40 in 1x Perm/Wash) and secondary goat anti-mouse AF555 antibody for 2 hours at room temperature, labeled with DAPI and viewed with Zeiss LSM 700 or LSM 890 inverted confocal microscope.

For assessment of NFATc1 translocation in murine T cells, CD4⁺ and CD8⁺ T cells were purified from spleen and peripheral lymph nodes using Dynabeads™ DETACHaBEAD™ mouse CD4 Kit

(12406D, Invitrogen) and CD8a+ T Cell Isolation Kit, mouse (Miltenyi 130-104-075). The cells were resuspended in RPMI 1640 medium containing 10% FCS, 100 U/ml penicillin, 100 µg/ml streptomycin and 100 µM 2-mercaptoethanol. The purified CD4+ and CD8+ T cells were seeded on 48-well plates coated with anti-CD3e (clone 145-2C11, BioLegend) and anti-CD28 (clone 37.51, BioLegend) antibodies and incubated at 37°C, 5% CO₂ for 24 hours and 6 hours, respectively. Following stimulation, the cells were washed and deposited on poly-L-lysine coated cover slides. The cells were allowed to adhere for 10 min and then fixed with 4% paraformaldehyde for 15 min at room temperature. Subsequent to permeabilization with 1x BD Perm/Wash buffer, the cells were stained overnight with anti-NFATc1 antibody (Cell Signaling Technology, 8032S, clone D15F1, 1:100 in 1x Perm/Wash). After washing with PBS, the cells were stained with anti-rabbit-IgG-Rhodamine (Jackson, 711-025-152, 1:300) and Phalloidin-FITC (Sigma P5282.1MG, 1:300) in Perm/Wash at room temperature for 2 hours. The cells were labeled with DAPI and after mounting of cover slides using antifade mounting media, images were taken using a deconvolution microscopy system (Keyence) equipped with a 40x objective lens. The nuclear/cytoplasmic ratio was calculated by dividing the average intensity of the nucleus by that of the cytoplasm for each cell. Unsupervised analysis was performed with the CellProfilerTM software and manual analysis using Fiji software.^{29,30}

Immunofluorescence and Microscopy of Zebrafish

For whole-mount antibody staining of zebrafish embryos, 48hpf *gata1a:dsRed* transgenic zebrafish embryos were fixed in 4% formaldehyde in PBS for 12 h at 4°C. Then embryos were transferred to 100% methanol and stored at -20°C. Embryos were incubated for 5 min with cold acetone and then transferred back to 100% methanol. After rehydration by successive incubations with 75%, 50% and 25% methanol, embryos were transferred to PBX (PBS containing 0.1% Triton X-100). They were rinsed 3x with 0.3% Triton X-100 and incubated 1 h with 0.1% Triton X-100. Embryos were blocked in antibody blocking buffer (PBX, 10% goat serum, 0.5% BSA, 1% dimethyl sulfoxide (DMSO)) overnight at 4°C. Embryos were incubated with anti- α -Tubulin antibody (mouse, Sigma Aldrich T9026-.2ML, 1:200) and anti-RFP (recognizes dsRed, rabbit, Biomedica GmbH, MB-PM005, 1:500) in antibody blocking buffer overnight at 4°C with rocking agitation. After washing with PBX and subsequent blocking in antibody blocking buffer for 2 h at room temperature (RT), secondary antibodies (goat-anti-rabbit AF555 and goat-anti-mouse AF647

diluted in antibody blocking buffer) and Phalloidin AF488 (1:100 in antibody blocking buffer) were added and embryos were incubated with rocking agitation for 3 h at RT. Embryos were washed with PBX and then mounted in 1% low-melting point agarose in E3 fish medium. Whole-mount embryos were then imaged using a Zeiss LSM 890 inverted confocal microscope.

32 hpf live *fli1:GFP;gata1a:dsRed* transgenic zebrafish embryos injected with either control, 3X *dock11* sgRNAs without Cas9, 3X *dock11* sgRNAs+Cas9, control MO or *cdc42* MO were anesthetized as mentioned above. Automated scanning tile imaging of whole mount zebrafish embryos was performed at room temperature using an inverted Zeiss LSM 980 confocal microscope with a 20X objective. Images were acquired of defined z-stacks with a step size of 20 μm .

To visualize the blood circulation of control and *dock11* KO zebrafish embryos, the double transgenic *fli1:GFP;gata1a:dsRed* reporter was used. 48 hpf, alive, control and *dock11* KO embryos were anesthetized as described above and mounted in 3% methylcellulose in the center of a depression of a glass depression slide. Complete zebrafish embryos were then imaged in both GFP and dsRed fluorescence contrast using Zeiss Axio Zoom. V16 stereo microscope.

To visualize in detail the defects in blood circulation of *dock11*-knockout zebrafish, time-lapse images of 54 hpf zebrafish larvae were taken using inverted Zeiss LSM 980 confocal microscope with a 40X objective.

Live zebrafish embryos injected with either 3X *dock11* sgRNAs without Cas9 or with 3X *dock11* sgRNAs+Cas9 were imaged at 24 hpf using the LEICA MC170 stereomicroscope to screen embryos for morphological abnormalities. Mutant phenotypes were classified according to the severity of defects in ventral-dorsal patterning with a particular focus in the posterior region (tail) of the body.

Microscopy Analysis of Zebrafish T-Cell Progenitor Migration

Live *lck:nlsmCherry;myl7:EGFP^{vi004}* transgenic embryos injected with either control, 3X *dock11* sgRNAs without Cas9 or with 3X *dock11* sgRNAs+Cas9 were anesthetized at 5 days post fertilization (dpf) in calcium-free and magnesium-free PBS (pH 7.4) containing 0.02% tricaine (Sigma) and mounted in 1% low-melting-point agarose in E3 fish medium. Time-lapse recording was then performed to monitor the migration of Lck (mCherry)-positive T-cell progenitors in the proximity of the thymus. Embryos were imaged at room temperature using an inverted Zeiss LSM

980 confocal microscope with a 20X objective. Images of defined z-stacks with a step size of 20 μm were acquired for at least 50 time points with no time interval between them. Tracking of the migration of T-cell progenitors was done manually using TrackMe plugin from Fiji.²⁹

Live Cell Imaging of Human T-Cell Migration

Live cell imaging of T-cell transendothelial migration (TEM) across HUVEC cells stimulated with tumor necrosis factor α (TNF- α) under flow was done as previously described.³² In brief, HUVEC were grown as continuous culture on fibronectin (Sanquin Reagents) coated plastic culture dishes (TPP). HUVEC were stimulated with TNF- α (10 ng/mL) in EGM-2 for 20 hours. Patient-derived CD8+ T cells used for transmigration assay were recovered in RPMI containing 10% FCS. Flow channels were prepared by coating μ -channels VI 0.4 (80606, Ibidi) with 30 μL fibronectin (Sanquin Reagents) for 1 hour at room temperature followed by a washing step with PBS. Afterwards, trypsinized HUVEC resuspended in EGM-2 (1×10^6 cells/mL) were added at 30,000 cells per channel (30 μL medium) and allowed to adhere for 20 to 30 min assured by visual inspection under a microscope. The chambers were then filled up with EGM-2 medium (120 μL) which was exchanged twice a day by aspirating and replacing with 120 μL fresh, pre-warmed EGM-2. For stimulation 120 μL of 10 ng/mL TNF- α was added to each channel and fresh medium was added when the stimulation time point was reached, and the experiments were started.

TNF- α treated HUVEC were washed with HEPES buffer (20 mM HEPES, 132 mM NaCl, 6 mM KCL, 1 mM CaCl₂, 1 mM MgSO₄, 1.2 mM K₂HPO₄, 1 g/L D-glucose, and 0.5 % (w/v) human serum albumin). HEPES flow buffer was prepared fresh for every experiment, filtered, warmed to 37 °C and used on the same day. A flow rate of 0.5 mL/min, corresponding to ~ 0.8 dyne/cm², was set on a table-top pump (Prosense) with a BD 60 mL Syringe Luer-Lok tip (Becton, Dickinson and Company). Endothelial cells were exposed to flow for 10 min prior to injection of 1 mL containing CD8+ T cells at 1×10^6 /mL in RPMI 10% FCS 1% Pen/Strep. Imaging of live cells was performed using a Zeiss Axiovert 200 Widefield microscope with a HXP lighting unit and incubation (37° C and 5% CO₂). For each channel multiple random positions were recorded and analyzed.

Recorded image series were analyzed using Fiji software.²⁹ For analysis of transmigration efficiency all adherent T cells were counted, as well as all transmigration events. TEM efficiency is given as percentage of adherent cells that transmigrate. For distant TEM all transmigrating CD8+ T cells in a series were counted and marked and the number of transmigrated T cells that performed

diapedesis at a location that required to cross at least two different endothelial junctions were categorized as distantly transmigrating. For this individual transmigrated CD8⁺ T cells are traced back manually to their point of adhesion and crossed junctions are counted. If a cell passes more than two junctions before transmigrating it is counted as distant transmigration event. Distantly transmigrating T cells are given as percentage of all transmigrated T cells within an image series. For each experimental flow assay condition between 10 and 15 image series were recorded in parallel from the same flow channel. All series recorded were analyzed if possible.

Under Agarose Migration Assay

For assessment of T-cell motility in a confined environment, CD8⁺ T cells after 10 days of feeder stimulation and 12 hours of interleukin (IL-2, IL-7, and IL-15) treatment were collected and prestained. Cells from healthy donors were stained with Calcein Orange (Invitrogen, C34851) and patient-derived T cells with CMFDA (Invitrogen, C2925). After the staining procedure, T cells from patients and healthy donors were pooled resulting in three pairs of one healthy donor and one patient each. The paired cell solutions were then loaded into an under-agarose μ -Slide 8-Well chamber slide (Ibidi). The slide was coated with 2 μ g/mL fibronectin (Sigma), a thin layer of 0.5% agarose and had two 3 mm diameter holes at 2 mm distance, for loading of complete T-cell medium in one and 5×10^4 T cells in the other one. Cell migration was assessed using an Eclipse TE2000-E fully motorized inverted microscope (Nikon) and a 10x/0.45 NA objective, at 37 °C and 5% CO₂. FLASH4 CSU camera (Photometrics) and Metamorph software (Molecular Devices) were used for image acquisition during 3 hours at a rate of 1 image per minute. Cell motility parameters were assessed through semi-automated TrackMate tool from Fiji imaging software.²⁹

Human Cytotoxic T-Cell Degranulation Activity

The ability of expanded human CD8⁺ T cells to secrete lytic granules was assessed by CD107a (Thermo Scientific, Catalog Number 12-1079-42, LAMP1) surface staining. P815-GFP (ATCC) target cells were pre-incubated either with or without anti-CD3 antibody (OKT3, eBioscience) at the indicated concentrations. CD8⁺ T cells were mixed with target cells at a 2:1 ratio in 96-well U-bottom plates. Cells were briefly spun down and incubated in the presence of an anti-CD107a antibody for 4 hours. Following incubation, cells were analyzed using flow cytometry on a BD LSR Fortessa. All data were analyzed using FlowJo X (Treestar).

Murine T-Cell Proliferation Assay

Murine CD4⁺ and CD8⁺ T cells were purified from spleen and peripheral lymph nodes using Dynabeads™ DETACHaBEAD™ mouse CD4 Kit (12406D, Invitrogen) and CD8a⁺ T Cell Isolation Kit, mouse (Miltenyi 130-104-075). The cells were resuspended in RPMI 1640 medium containing 10% FCS, 100 U/ml penicillin, 100 µg/ml streptomycin and 100 µM 2-mercaptoethanol. For the proliferation assay, cells were seeded on 48-well plates coated with anti-CD3e (clone 145-2C11, BioLegend) and anti-CD28 (clone 37.51, BioLegend) antibodies and incubated at 37 °C, 5% CO₂ for 40 hours. For the last 16 hours of incubation 37 kBq [3H]-thymidine (PerkinElmer NET027X) was added in each well and incorporated radioactivity was measured with a scintillation counter.

ELISA and Intracellular Cytokine Measurement

For cytokine assays isolated murine CD4⁺ and CD8⁺ T cells were cultured on 1 µg/ml anti-CD3e (clone 145-2C11, BioLegend) and 1 µg/ml anti-CD28 (clone 37.51, BioLegend) antibody coated plates for 48 hours (CD8⁺) or 5 days (CD4⁺) followed by collecting cell supernatant. For detection of cytokines in cell culture supernatants the following ELISA Max mouse kits from Biolegend were used: interleukin-2 (431001), interferon-γ (IFN- γ) (430801), interleukin-4 (431101) and TNF-α (430901).

For intracellular cytokine measurement of human CD8⁺ T cells, 96-well high binding plates were coated with 1 µg/ml anti-CD3 and anti-CD28 antibodies in 100 µl PBS/well at 4°C overnight. Plates were washed with PBS, followed by seeding of patient- and healthy donor-derived expanded CD8⁺ T cells at 300,000 cells/ well in 100 µl RPMI 1640 supplemented with 10% fetal calf serum. After 48 hours of stimulation, Brefeldin A was added, and cells were incubated for another 5 hours. Surface staining was performed for 30 min on ice prior to fixation with BD Cytofix. After permeabilization with BD 1x Perm/Wash buffer, intracellular staining of cytokines was performed in BD 1x Perm/Wash buffer for 30 min on ice. BD LSR Fortessa was used for acquisition. The following antibodies were used: from BD Biosciences: CD3-APC-H7 (SK7), CD4-BV605 (RPA-T4), CD8-V500 (RPA-T8), TNF-α-PE (6401.1111); from Biozym Scientific: IL-2-PECy7 (MQ1-17H12), IFN-γ-FITC (4S.B3).

For intracellular cytokine measurement of human CD4⁺ T cells, 0.5–1x10⁶ PBMCs were stimulated with Phorbol 12-myristate 13-acetate (PMA, 0.2 μM) and ionomycin (1 μg/ml) in 200 μl RPMI 1640 supplemented with 10% fetal calf serum for 5 hours. During the final 2.5 hours of the stimulation Brefeldin A (Biozym Scientific, 420601) was added. Surface staining was performed for 15 min at 37°C prior to fixation and permeabilization with BD Cytofix/cytoperm. Intracellular staining of cytokines was performed in BD 1x Perm/Wash buffer for 20 min on ice. BD LSR Fortessa was used for acquisition. The following antibodies were used: CCR6-BV605 (G034E3) from Biolegend, 0.8μl CCR7-PE- CF594 (150503), CD3-APC-H7 (SK7), CD45RA-AF700 (HI100), CD8-V500 (RPA-T8), IL-4-APC (MP4-25D2) and CD25-PE (M-A251) all from BD Pharmingen, IFN-γ-FITC (4S.B3) and IL17-A-eFluor450 (eBio64DEC17) from eBiosciences and CD4-PECy7 (SFCI12T4D11) from Beckman Coulter.

To assess NLRP3 inflammasome activation, THP-1 cells were stimulated with either lipopolysaccharide (LPS) alone (1 μg/ml) or LPS + Nigericin (5 μM) in complete RPMI medium. For this, the cells were collected and washed with PBS (800 rpm, 5 min). Then, the LPS solution was added. After 4 hours of incubation, the cells were counted and plated at 100,000/ 100 μl in a 96-well plate. Subsequently, the Nigericin was added to the corresponding samples and the cells were incubated for another 4 hours. The plate was centrifuged, and the supernatant was frozen at -80°C. The Pyrin inflammasome activation was assessed by stimulating the cells with 50 ng/ml recombinant human IFN-γ (Eubio, rcyec-hifng), 20 ng/ml recombinant C. difficile Toxin B/TcdB Protein, CF (R&D Systems, 6246-GT-020) and 500 ng/ml Pam3CSK4 (InvivoGen, tlrl-pms) in complete RPMI medium for 24 hours. Supernatants were collected and frozen at -80°C. Cytokine measurements were performed as recommended by the manufacturer, using DuoSet ELISA Human total IL-18 kit (R&D Systems, DY318-05) and DuoSet ELISA Human IL-1β/IL-1F2 (R&D Systems, DY201-05).

2D-RP/RP Liquid Chromatography – Tandem Mass Spectrometry Analysis

Mass spectrometry analysis was performed on an Orbitrap Fusion Lumos mass spectrometer (ThermoFisher Scientific) coupled to an Ultimate 3000 nanoLC system (ThermoFisher Scientific) via a Nanospray Source (ThermoFisher Scientific). Peptide loading onto a trap column (PepMap 100 C18, 5 μm, 5 × 0.3 mm, ThermoFisher Scientific) at 10 μL/min using 0.1% TFA was followed

by separation on a C18 analytical column (2.0 μm particle size, 75 μm iDx500mm, ThermoFisher Scientific) at constant 50 °C (PRSO-V2 column oven, Sonation) using mobile phase A (0.4% formic acid in water) and mobile phase B (0.4% formic acid in 90% acetonitrile) and a four-step gradient over 97 minutes at a flow rate of 230 nL/min.

Mass spectrometer was operated in data-dependent acquisition mode (375–1650 m/z survey scan at 120 000 resolution, ‘standard’ AGC, maximum injection time 100 ms). Precursor ions were filtered (charge state 2-6, dynamic exclusion 60 s, ± 10 ppm window, monoisotopic precursor selection) and selected for data-dependent MS_n (ddMS_n) using 20 dependent scans (TopN approach) and an additional inclusion list. Isolation window was set to 1.6 Da, HCD collision energy to 30%, AGC target to ‘standard’, and maximum IT to 35 ms. Xcalibur Version 4.3.73.11 and Tune 3.4.3072.18 were used to operate the instrument.

Raw data files were processed using the Proteome Discoverer v.2.4.1.15 platform, with a TMT18plex quantification method selected: Sequest HT database search engine and Percolator validation software node were used with false discovery rate (FDR) set to 1%. A search against a full tryptic digestion of the human proteome (Canonical, reviewed, Uniprot), known contaminants, and an inclusion list of caspase peptides was performed, with a maximum of two allowable miscleavage sites. Methionine oxidation, N-terminal acetylation, methionine loss, and protein N-terminal acetylation with methionine loss were set as variable modifications, while carbamidomethylation of cysteine residues and tandem mass tag (TMT) 16-plex labeling of peptide N-termini and lysine residues were set as fixed modifications. Data were searched with mass tolerances of ± 10 ppm and ± 0.025 Da for the precursor and fragment ions, respectively. Both unique and razor peptides were used for TMT quantification. For reporter quantification a co-isolation threshold of 50% was used, and average reporter mass S/N threshold was set to 10. Correction of isotopic impurities was applied. Data were normalized to total peptide abundance to correct for experimental bias and scaled ‘on all average’. Protein ratios are directly calculated from the grouped protein abundances and tested statistically using an analysis of variance (ANOVA) hypothesis test.

Statistical Analysis

For statistical analysis of experimental data, appropriate statistical tests as indicated in the respective figure legends were performed using GraphPad Prism version 9.3.1. Data were displayed as mean \pm standard error of the mean (SEM) for individual experiments and as mean \pm standard deviation (SD) for combined representation of two or more experiments or if donors were pooled. More detailed statistical analysis of data shown in Figures 3 and 4 is outlined below. Figure 3B shows the mean \pm SD from two (Patient 4) or six (Patients 1 through 3) independent experiments. For the healthy donors, each datapoint is the average value of 2-4 individuals used in each experiment. For statistical analysis the values from each individual healthy donor were used. Figure 3C shows the mean \pm SD from three independent experiments. Each datapoint shows the average of two (control and *DOCK11* c.75dup) or three (*DOCK11* c.1718+5G \rightarrow A) individual clones. For statistical analysis the values from all individual clones were used. Figure 3D shows the mean \pm SD from three independent experiments. Each datapoint is the mean value of 5 imaging fields. For statistical analysis, values from all individual healthy donor values (n=9) were used. Figure 3E shows the mean \pm SD from three independent experiments. For statistical analysis, values from all individual healthy donor values (n=6) were used. Figure 3 F shows the mean \pm SD from four independent experiments. For the healthy donors, each datapoint is the average value of 2-3 individuals used in each experiment. For statistical analysis the average values from the pooled healthy donors were used. Figures 3G and 3H show the mean \pm SD from 3 individual mice. Figure 3I shows mean \pm SEM of one representative experiment from two independent experiments performed. Statistical analysis for Figures 3B-E were performed using a Mann-Whitney test, for Figures 3F-H using a two-way analysis of variance with a Šidák correction test for multiple comparison, and for Figure 3I using an unpaired Student's *t*-test. Figures 4B and 4C show the mean \pm SD from three independent experiments. Each datapoint is the average value of 10 samples, each containing pooled cells from 10 zebrafish embryos. For statistical analysis the average values from the pooled samples were used. Figure 4D shows the mean \pm SEM of one representative experiment from two independent experiments performed. Figure 4E shows the mean \pm SD from two to three independent experiments.

Supplementary Figures, Tables and Legends

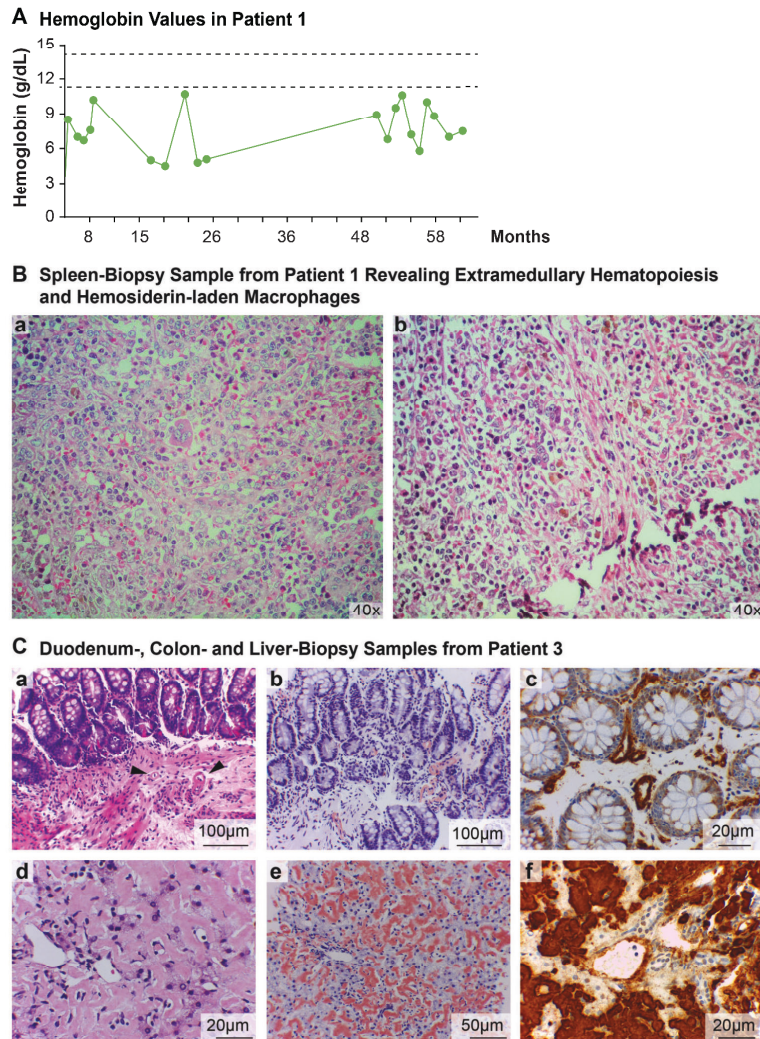


Figure S1. Longitudinal Hemoglobin Values and Stainings of Biopsy Samples from Patients

Panel A shows longitudinal hemoglobin values of Patient 1. Dashed lines indicate the reference range. Panel B shows spleen biopsy from Patient 1 stained with Hematoxylin and Eosin (HE) (40x) revealing spleen parenchyma with megakaryocyte in the center of picture (a), extramedullary hematopoiesis (a and b) and hemosiderin deposition (b). Panel C shows histology stains of duodenum, colon and liver biopsies from Patient 3. Duodenal mucosa, showing small vessels with seemingly rigid walls (a, black arrows), stained with HE (10x) (a) and with Congo Red (CR) (10x) (b) to reveal amyloid deposits. Amyloid A deposits revealed by Immunohistochemical (IHC) staining in the walls of vessels from the colonic mucosa (20x) (c). Hepatic tissue with severe deposit of amyloid material in sinusoidal spaces with marked compression of surrounded hepatocytes, HE (20x) (d), CR (10x) (e). IHC staining revealed Amyloid A as diffuse extracellular deposits in hepatic sinusoids (20x) (f).

Gating Scheme for Flow Cytometry Analysis of Human T- and B-Cell Subsets

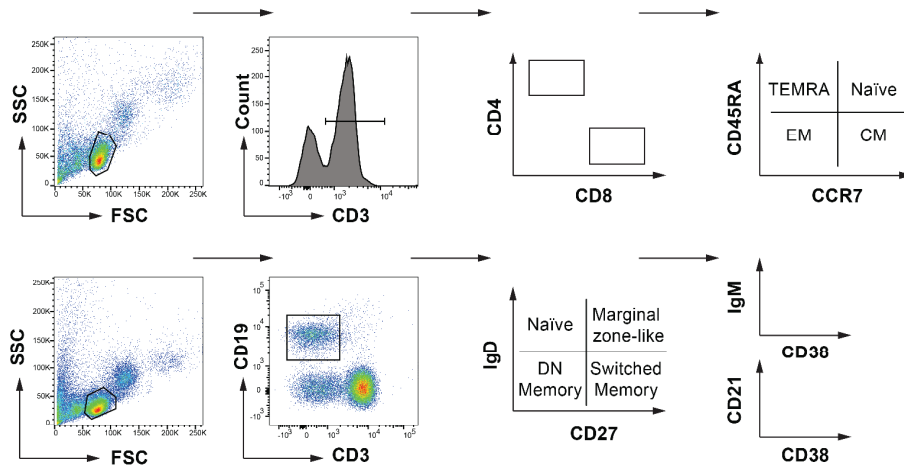


Figure S2. Flow Cytometry Analysis Gating of Human Immune-Cell Subsets

Gating scheme for immune-cell subset flow cytometry analysis of peripheral blood mononuclear cells obtained from patients and healthy donors. Representative flow cytometry plots and values are displayed in Figs. S3 and S4 and Table S5. SSC side scatter, FSC forward scatter, Ig immunoglobulin, CM central memory, EM effector memory, DN double negative.

Immunophenotyping Analysis of Human T-Cell, NK-Cell and Monocyte Subsets

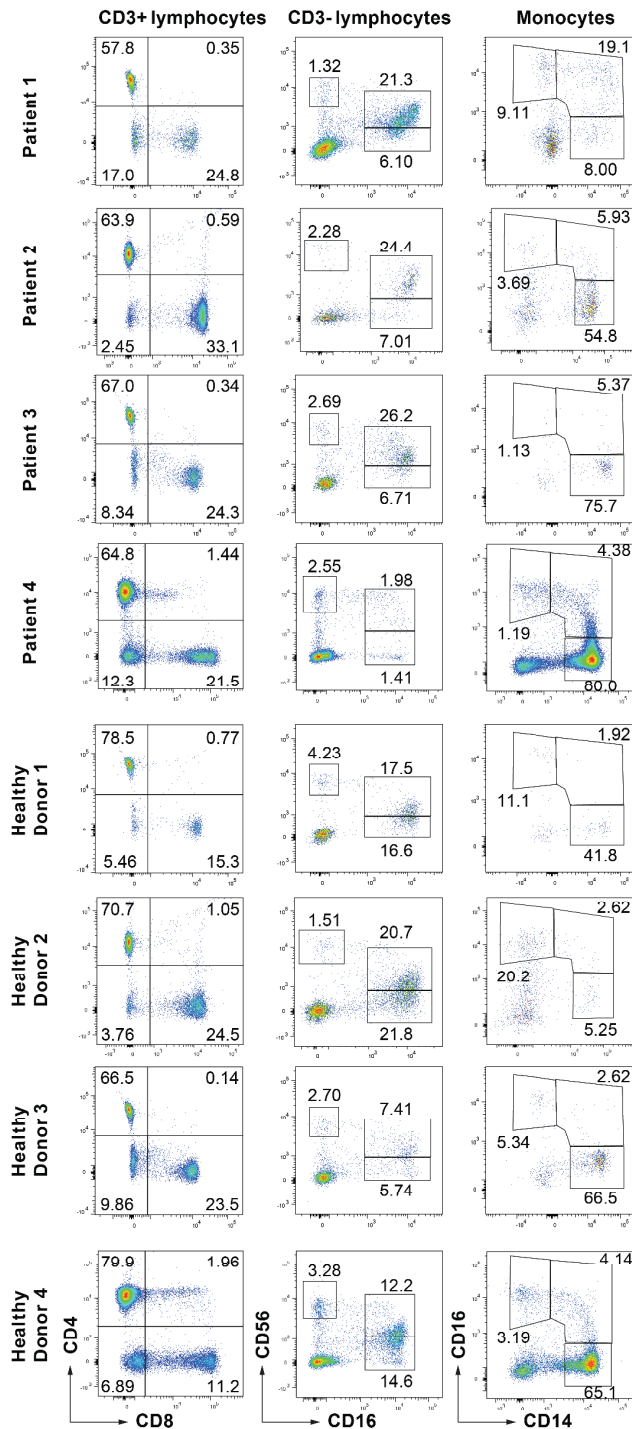


Figure S3. Immunophenotyping Analysis of Human T-Cell, NK-Cell and Monocyte Subsets

Flow cytometry plots of peripheral blood mononuclear cells obtained from patients and healthy donors reveal no major differences in CD4+ and CD8+ T-cell subsets among CD3+ cells. No remarkable differences in CD16+CD56-, CD16+CD56+ and CD16-CD56^{bright} NK-cell subsets among CD3- cells were found. No clear differences were observed for classical (CD14++CD16-), intermediate (CD14++CD16+) and non-classical (CD14-CD16++) monocyte subsets. For gating strategy see Fig. S2.

Immunophenotyping Analysis of Human B-Cell Subsets

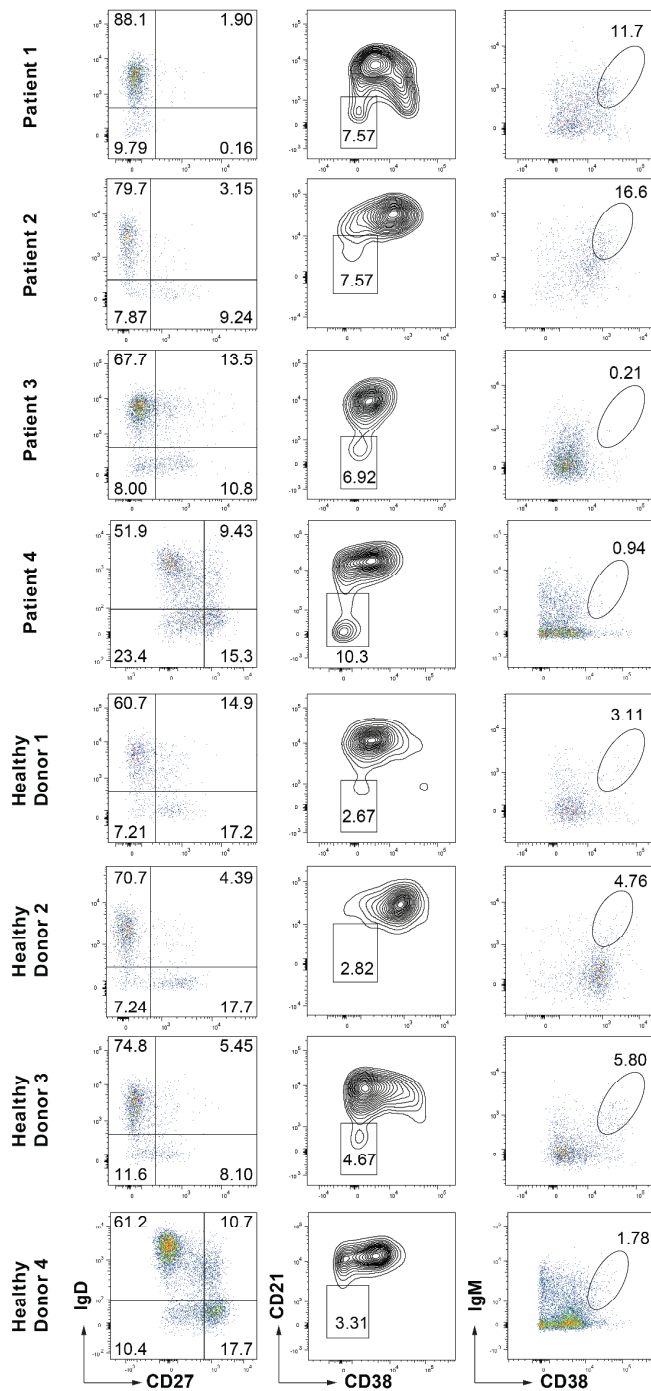


Figure S4. Immunophenotyping Analysis of Human B-cell Subsets

Representative flow cytometry plots of peripheral blood mononuclear cells obtained from patients and healthy donors reveal reduced marginal zone-like (CD27+IgD+) and switched memory (CD27+IgD-) CD3-CD19+ B cells for Patient 1, and slightly increased CD21^{low}CD38^{low} B cells (CD3-CD19+) in all patients. For gating strategy see Fig. S2. Ig immunoglobulin.

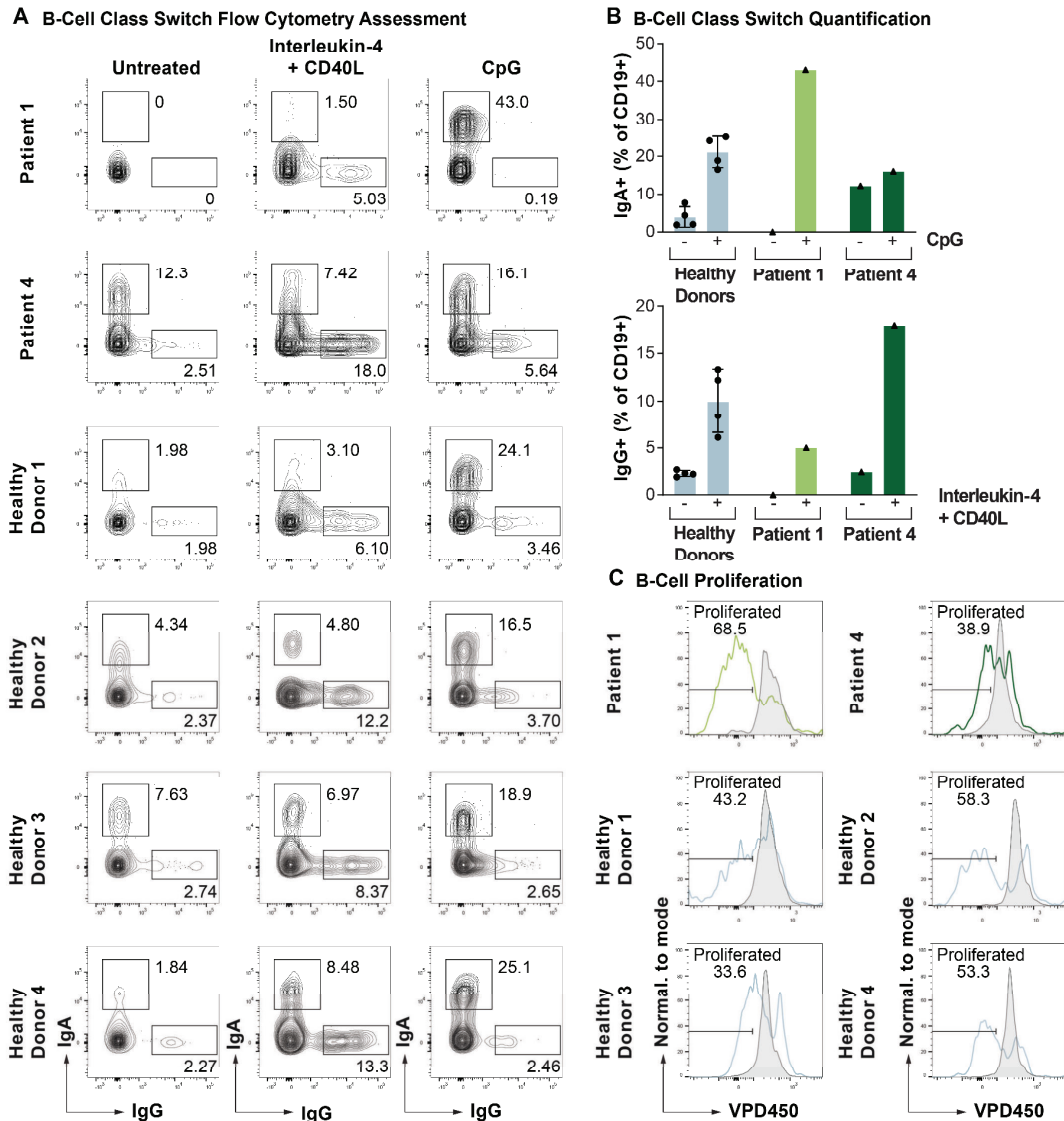


Figure S5. Evaluation of B-Cell Class-Switch Recombination and Proliferation

Representative flow cytometry plots (Panel A) and quantification (Panel B) revealing normal percentages of class-switched IgG⁺ and IgA⁺ CD3-CD19⁺ cells in response to 7-day stimulation (plus sign) with T-cell-dependent (CD40L + Interleukin-4) and -independent (CpG cytosine guanine dinucleotide) stimuli in Patients 1 and 4. The minus sign denotes no stimulation. Results are given as mean values, with standard deviations (I bars) derived from four healthy donors. Panel C shows representative flow cytometry plots showing normal percentage of proliferated B cells in response to CD40L + Interleukin-4 treatment measured by violet proliferation dye (VPD450) incorporation. Normal. denotes normalized. Ig immunoglobulin.

Whole-Exome Sequencing Filtering Strategy for Identification of Novel Rare Variants in Immune-related Genes

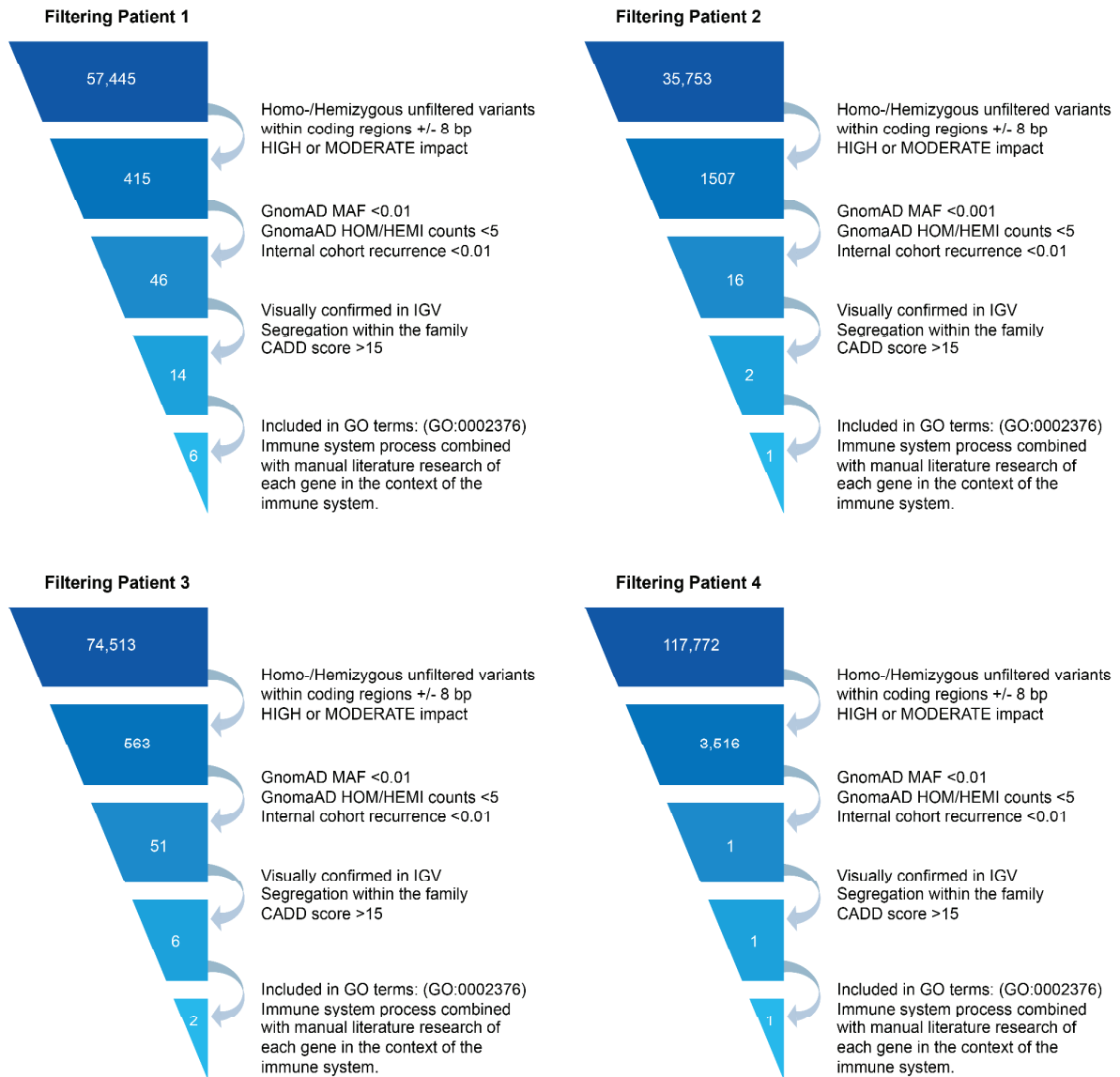


Figure S6. WES Filtering Strategy for Identification of Novel Rare Variants

Whole-exome sequencing (WES) strategies for Patients 1 through 4 for the identification of novel, rare variants in immune-related genes (see Tables S11-S14). MAF minor allele frequency in GnomAD, HOM/HEMI total homozygous or hemizygous counts in GnomAD, CADD Combined Annotation-Dependent Depletion, GO gene ontology.

A Sanger Sequencing Chromatograms of *DOCK11* gDNA

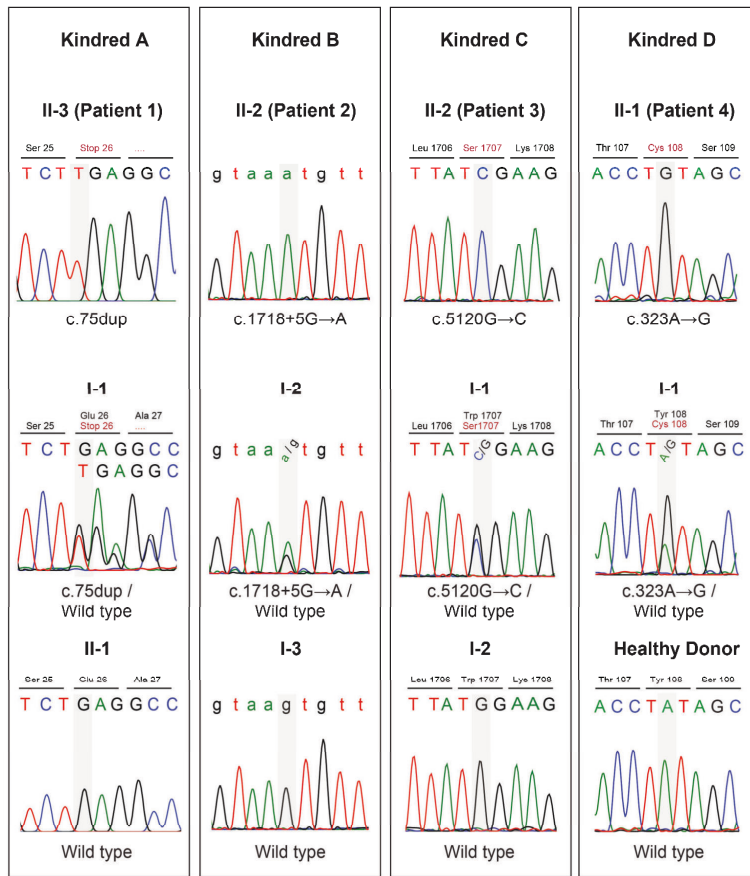
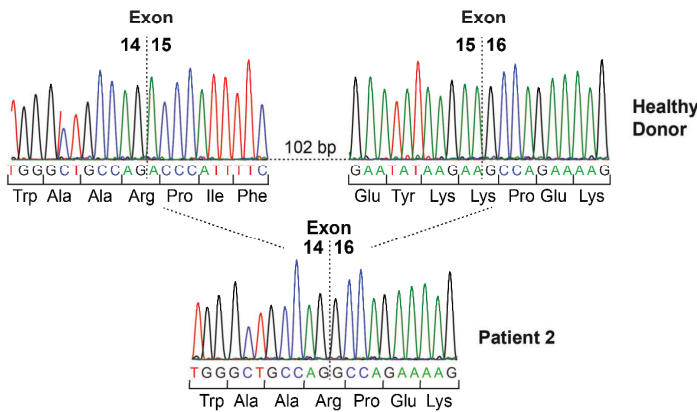


Figure S7. Evaluation of Identified *DOCK11* Germline Mutations

Panel A shows partial Sanger sequencing chromatogram of *DOCK11* alleles. Residues of patients' variants are highlighted in gray. Roman numerals indicate generations and Arabic numbers individuals within a generation (see Figure 1A). Panel B depicts Sanger sequencing chromatograms showing skipping of *DOCK11* exon 15 in fibroblast-derived cDNA from Patient 2 compared to a healthy donor. The encoded amino acid residues are depicted below each sequence in the three-letter code. bp base pairs, gDNA genomic DNA.

B Sanger Sequencing Chromatograms of *DOCK11* cDNA



A Assessment of Methylation Status of *AR* Locus to Determine X-Chromosome Inactivation

<i>AR</i> locus	Mother of P1	Mother of P2	Mother of P3	Mother of P4	Skewed control
<i>HpaII</i> (-)					
<i>HpaII</i> (+)					
XCI status	Not informative	13:87 skewed XCI	60:40 random XCI	52:48 random XCI	97:3 skewed XCI

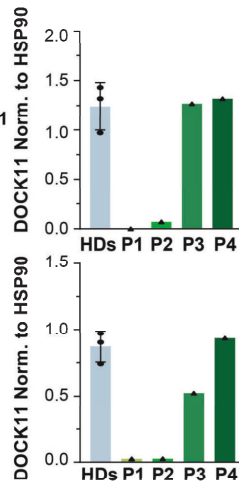
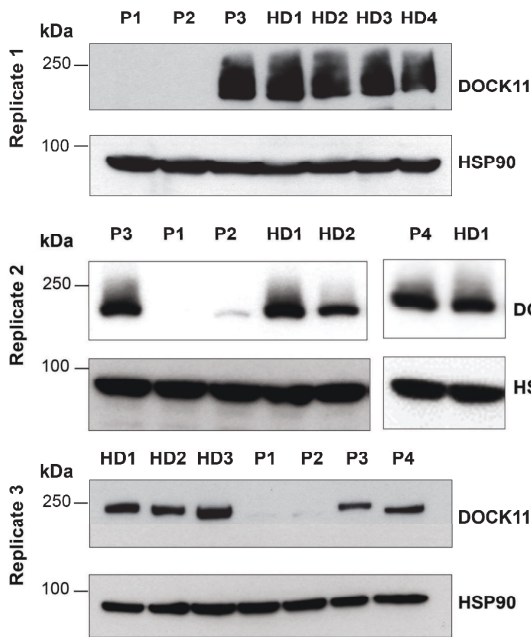
B Assessment of Methylation Status of *RP2* Locus to Determine X-Chromosome Inactivation

<i>RP2</i> locus	Mother of P1	Mother of P2
<i>HpaII</i> (-)		
<i>HpaII</i> (+)		
XCI status	49:51 random XCI	89:11 skewed XCI

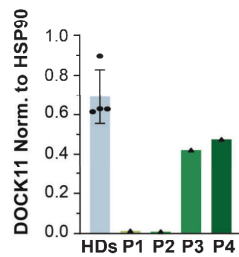
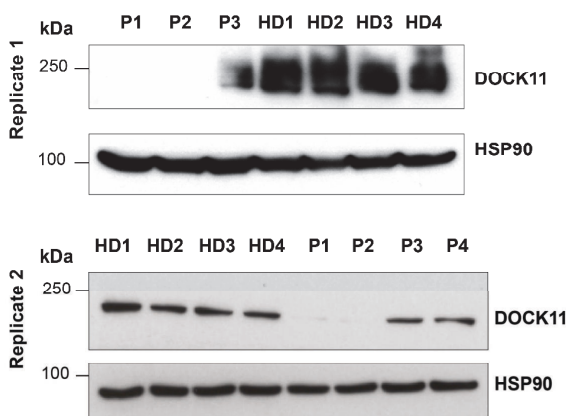
Figure S8. Assessment of X-chromosome Inactivation in Female Carriers

X-chromosome inactivation (XCI) was determined by analyzing the methylation status of the androgen receptor (*AR*) gene at Xq12 (Panel A) and/or the *RP2* activator of ARL3 GTPase (*RP2*) gene at Xp11.3 (Panel B) in leukocyte-derived DNA of mothers of Patients 1 through 4 (P1-P4) and a skewed female control. The *RP2* locus was investigated in the mother of Patient 1 because of homozygosity of the *AR* locus. The mother of Patient 2 was used as a skewed control for the *RP2* locus. Representative electropherograms show the different *AR* and/or *RP2* alleles. Predigestion of genomic DNA with (+) or without (-) *HpaII* is indicated. The ratio of the X-inactivation pattern (peak area of the shorter to longer allele) is given next to the electropherograms. The mother of Patient 2 showed a slightly skewed inactivation pattern for both tested loci. The other mothers showed a random pattern.

A DOCK11 Immunoblot of BLCLs



B DOCK11 Immunoblot of Expanded T Cells



C DOCK11 Immunoblot of Fibroblasts

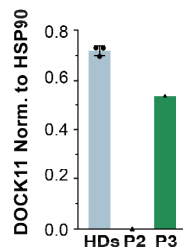
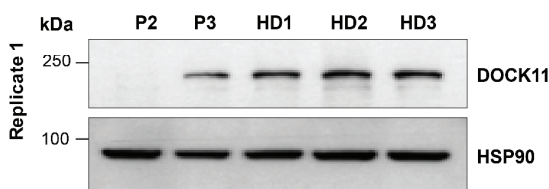


Figure S9. DOCK11 Expression in Different Cell Types

Panels A through C show immunoblot analysis of DOCK11 and HSP90 loading control in patient- (P) and healthy donor (HD)-derived lymphoblastoid cells (BLCLs) (Panel A), T cells (Panel B) and fibroblasts (Panel C) with the corresponding quantification of DOCK11 levels normalized (norm.) to HSP90, which reveal loss of DOCK11 protein expression in BLCLs and T cells from Patients 1 and 2 and remaining DOCK11 expression in Patients 3 and 4. Fibroblasts from Patient 2 show loss of DOCK11 protein expression. For each replicate, HD quantification results are given as mean values, with standard deviations (I bars) derived from multiple healthy donors. T-cell immunoblot replicate 2 (Panel B, bottom) is displayed in Figure 2A as representative immunoblot. PNGase F treatment was performed for BLCLs replicate 3 (A), T cells replicate 2 (B) and fibroblasts replicate 1 (C). Only immunoblots with discrete, clearly defined bands were quantified. kDa - kilo Dalton.

DOCK11 Immunoblot of Expanded T Cells

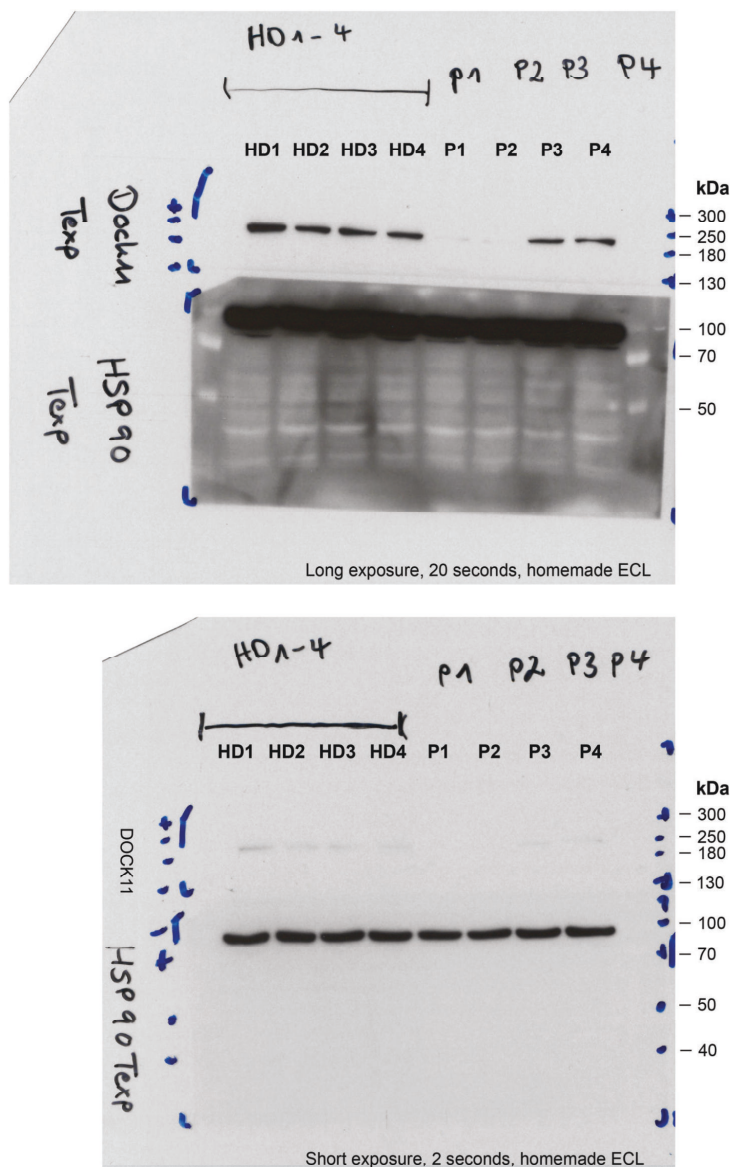
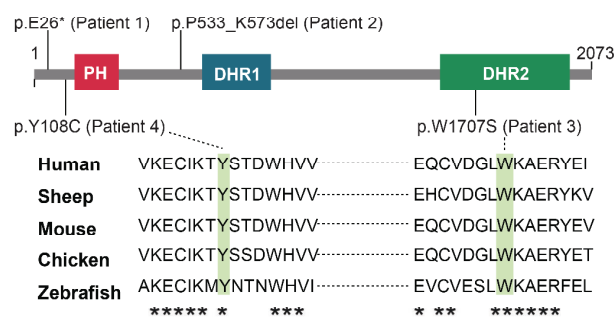


Figure S10. DOCK11 Expression in T Cells - Uncropped Immunoblot

Immunoblot analysis of DOCK11 and HSP90 loading control in T cells from patients (P) and healthy donors (HD), revealing loss of DOCK11 protein expression in T cells from Patients 1 and 2 and remaining DOCK11 expression in Patients 3 and 4. Parts of these blots are shown in Fig. 2A as representative immunoblots. Quantification is shown in Fig. S9B bottom (T cells replicate 2). kDa kilo Dalton, Texp expanded T cells.

A Mutations in DOCK11 Protein



B DOCK11 Protein Structure

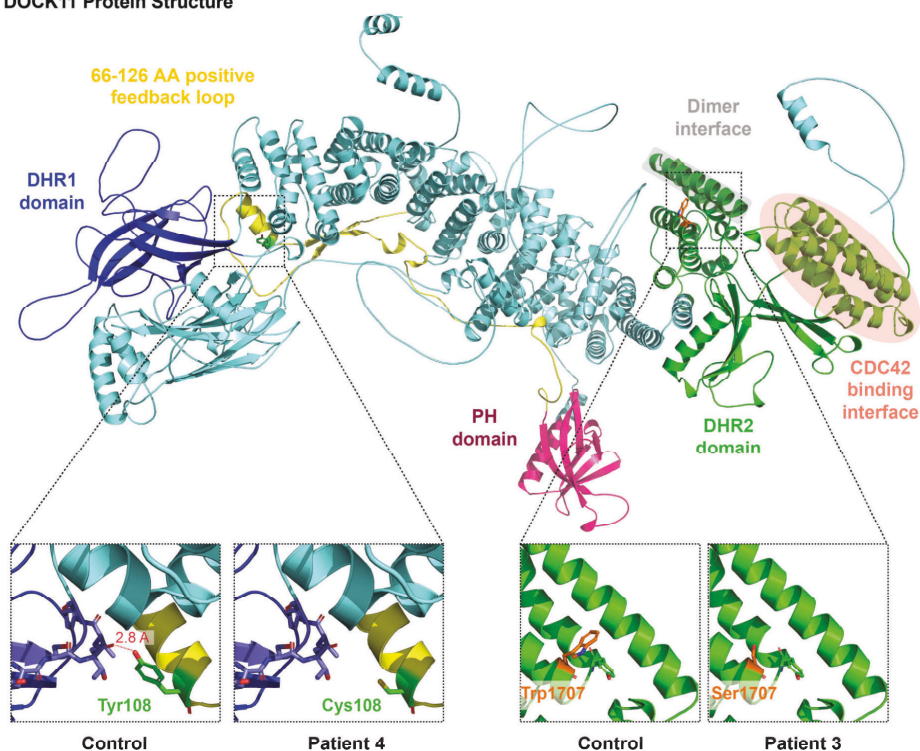


Figure S11. DOCK11 Protein Scheme with Identified Variants

Panel A displays a schematic illustration of the domain structure of DOCK11 indicating the position of the identified variants. Multiple sequence alignment shows conservation of Tyr108 and Trp1707 residues (highlighted in green) across eukaryotes. Highly conserved residues are marked by asterisks (*). Panel B depicts a 3D structural model of DOCK11 predicted by AlphaFold^{26,27} with a close-up view showing Tyr108 and Trp1707 residues, and the corresponding mutated residues of Patient 4 (Cys108) and Patient 3 (Ser1707). AA amino acids, DHR DOCK homology region, PH pleckstrin homology domain.

CDC42 Activation Assay in B Lymphoblastoid Cell Lines: Biological Replicates

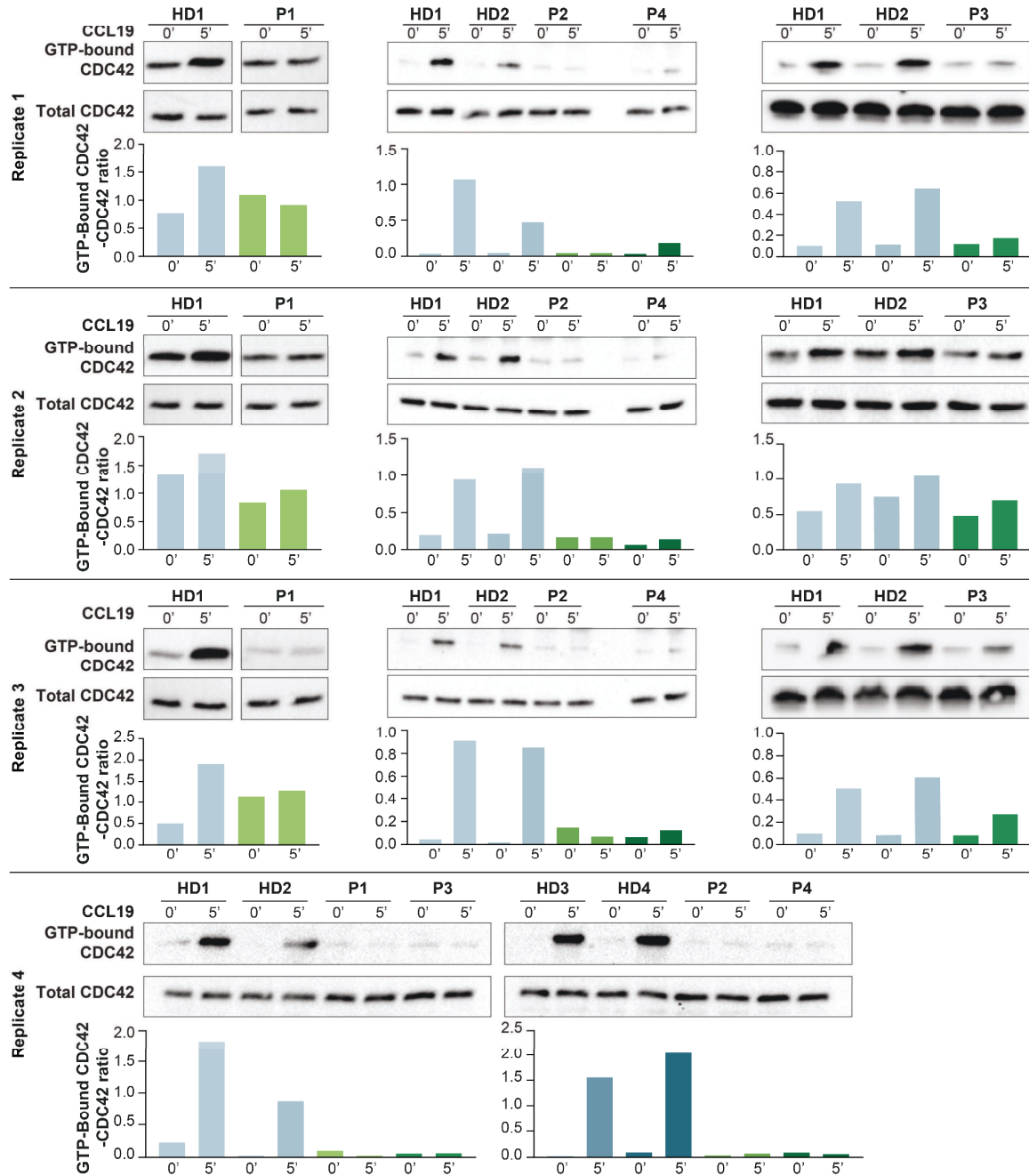


Figure S12. Assessment of CDC42 Activation in B Lymphoblastoid Cells

Immunoblot analysis reveals reduced GTP-bound (active) CDC42 in B lymphoblastoid cells from Patients 1 through 4 (P1-P4) on stimulation with CCL19 for 5 min (5') compared to healthy donors (HD). Displayed are immunoblots from four biological replicates and quantification. Displayed is the ratio of GTP-bound CDC42 to total CDC42 quantified using Fiji software. The fifth replicate is displayed as a representative immunoblot in Fig. 2D.

CDC42 Activation Assay in B Lymphoblastoid Cells

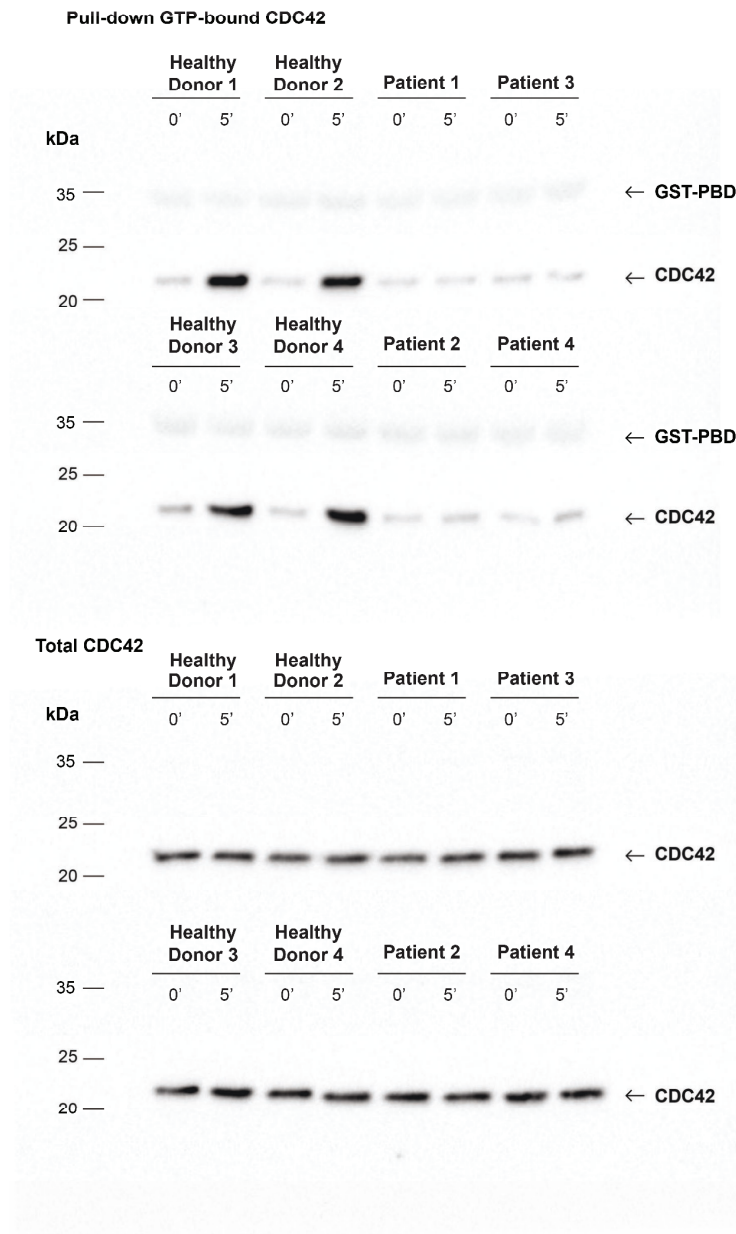


Figure S13. CDC42 Activation in B Lymphoblastoid Cells - Uncropped Immunoblot

Immunoblot analysis reveals reduced GTP-bound (active) CDC42 in B lymphoblastoid cells from Patients 1 through 4 (P1-P4) on stimulation with CCL19 for 5 min (5') compared to healthy donors (HD). Parts of these blots and quantification are shown in Fig. 2B as representative immunoblots. kDa kilo Dalton, GST-PBD GST-tagged Rac/Cdc42 (p21) binding domain (PBD) of the human p21 activated kinase 1 protein (PAK).

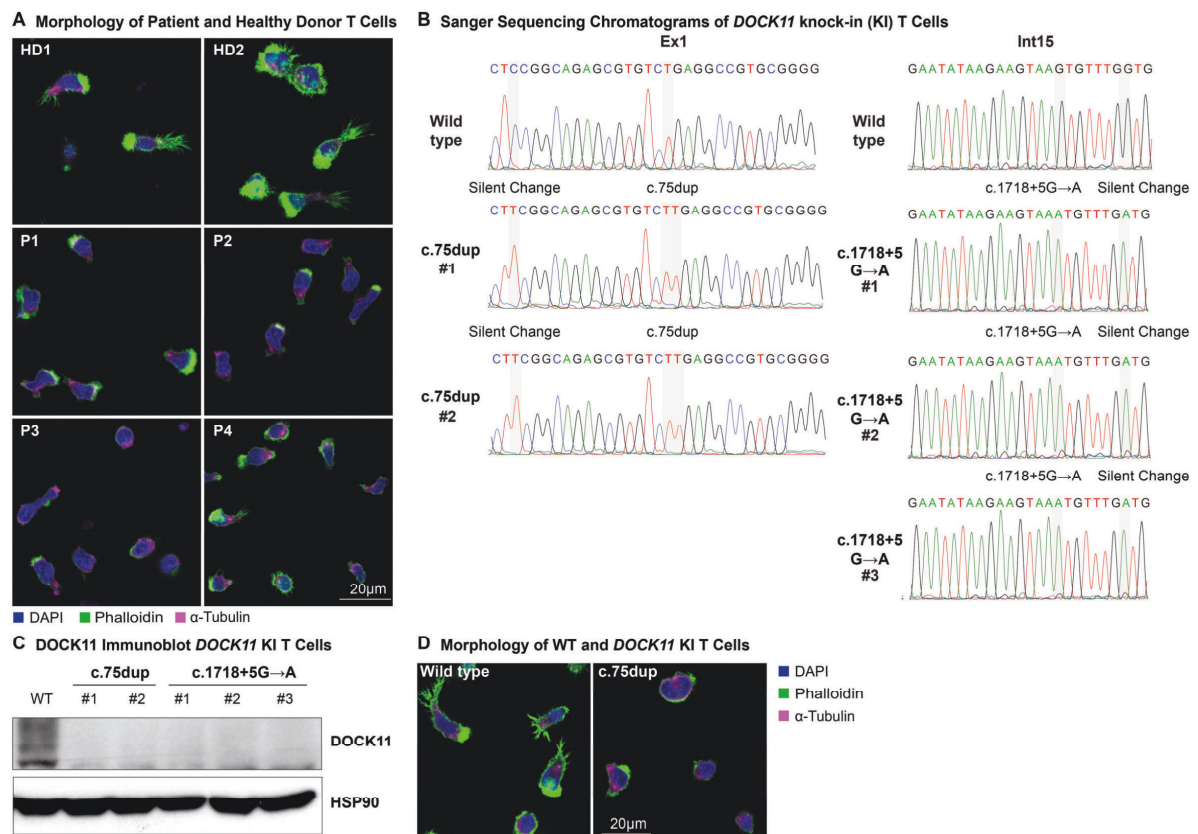


Figure S14. T-Cell Morphology in *DOCK11* Deficiency

Panel A shows representative images of T cells from healthy donors (HD) and patients (P) revealing distinct T-cell morphologic features on interaction with fibronectin. Magnification of Patient 1 and Healthy Donor 2 images are shown in Fig. 3A. Panel B displays partial Sanger sequencing chromatogram of CRISPR/Cas9-edited *DOCK11* knock-in (KI) T cells showing introduction of *DOCK11* variants from Patient 1 (c.75dup, 2 clones (#1 and #2) and Patient 2 (c.G1718+5G→A, 3 clones (#1, #2 and #3)) and silent changes (highlighted in gray) into wild-type (WT) control cells. Panel C shows loss of *DOCK11* protein expression in *DOCK11* knock-in compared to wild-type T cells analyzed by immunoblot. Anti-HSP90 antibody was used as loading control. Panel D shows representative images of wild-type and *DOCK11* c.75dup knock-in T cells on fibronectin-coated slides, corresponding to Fig. 3C.

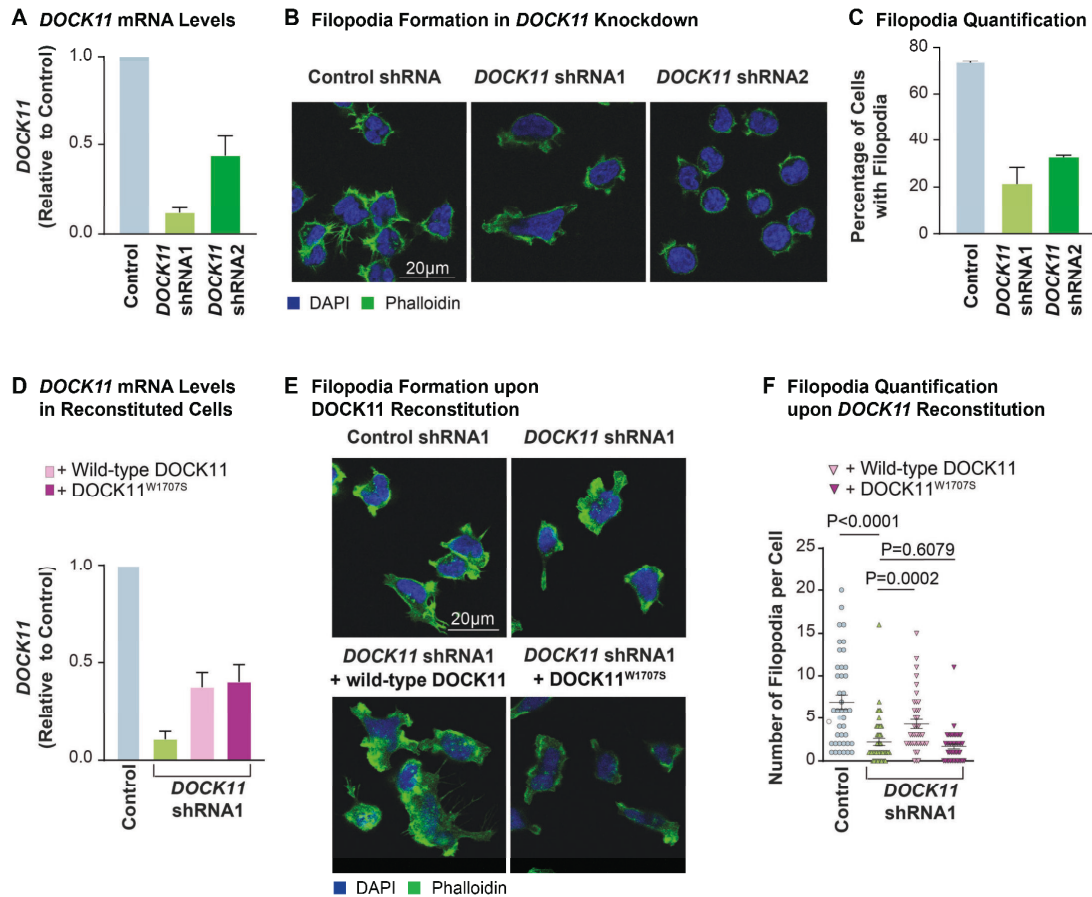


Figure S15. *DOCK11*-Knockdown in Jurkat T Cells Mimics Cell Shape Abnormalities of *DOCK11*-Deficient Patient Cells

Panel A shows quantitative PCR (qPCR) analysis of *DOCK11* expression in shRNA-mediated *DOCK11* knockdown and control Jurkat T cells normalized to a housekeeping gene and relative to control. Panel B shows representative images of Jurkat T cells spreading over fibronectin and Panel C the respective quantification. Panels D through F show *DOCK11* messenger RNA levels (Panel D), representative confocal microscopy images (Panel E) and respective quantification of number of filopodia per cell (Panel F) of control and *DOCK11* knockdown Jurkat T cells transduced or not with wild-type or c.5120G→C/p.W1707S mutant *DOCK11*-IRES-GFP. In Panels A, C and D, the results are given as mean values of multiple measurements, with standard errors (T bars). Data are representative of at least two independent experiments. Statistical analysis were performed with the use of a Mann–Whitney test.

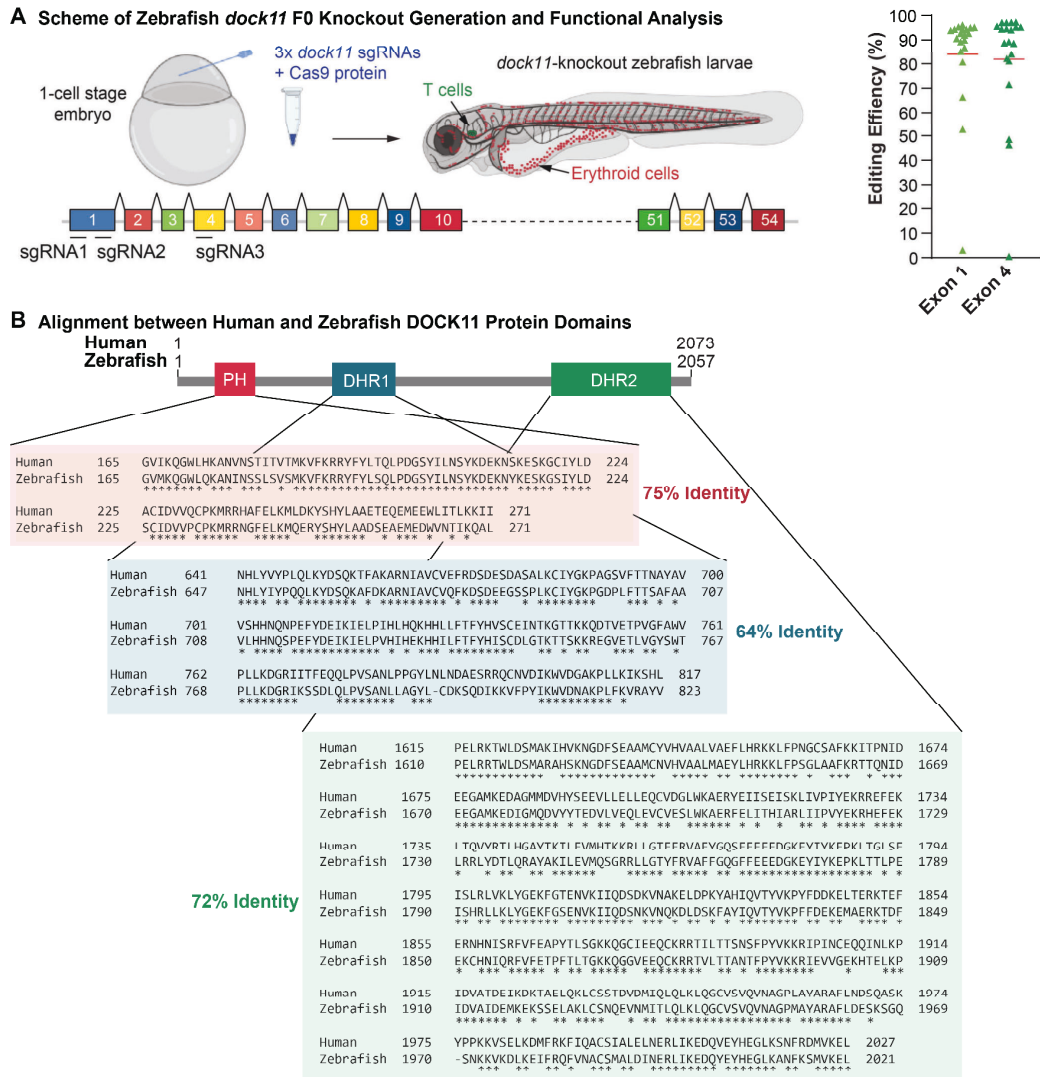


Figure S16. Generation of *dock11*-Knockout Zebrafish

Panel A shows a scheme of F0 *dock11*-knockout generation in *Danio rerio* using a combination of three single guide RNAs (sgRNAs) and Cas9 protein (top left). Arrows point to T-cell progenitors (green) and erythroid cells (red) in the zebrafish cartoon. Scheme of genomic *dock11* sequence with corresponding exons (Ex) showing the targeted exons by the three sgRNAs (bottom left). Quantification of *dock11* editing efficiency by capillary sequencing and tracking of indels by decomposition (TIDE) (right). Panel B shows alignment of the pleckstrin homology domain (PH) and the DOCK homology regions 1 and 2 (DHR1-2) domains between human DOCK11 and zebrafish Dock11, which display an overall 65% identity. *Conserved residues.

Classification of the Morphological Phenotype of Zebrafish *dock11* KO Embryos

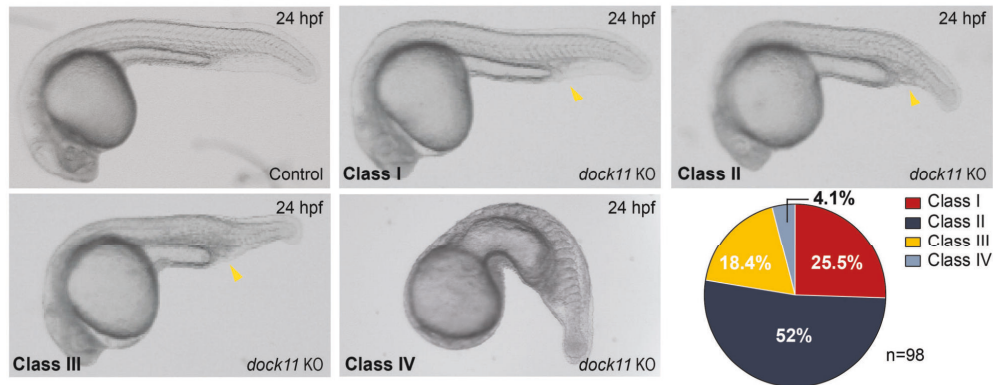


Figure S17. Evaluation of *dock11*-Knockout Zebrafish

Representative images of 24 hours postfertilization (hpf) control and *dock11*-knockout (KO) zebrafish embryos depicting four different morphological classes and respective quantification of 98 *dock11* KO zebrafish. Yellow arrowheads indicate intravascular blood accumulation predominantly at the tail region, adjacent and posterior to the yolk extension.

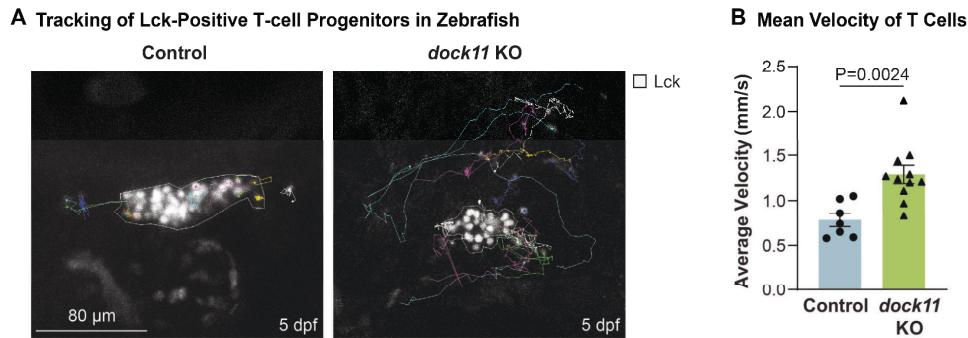


Figure S18. T-Cell Migration in *dock11*-Knockout Zebrafish

Panel A shows representative images (from Video S1 and Video S2) of the trajectories of T-cell progenitors migrating in the proximity of the developing thymus in the anterior part of 5 days postfertilization *lck:nlsmCherry* transgenic zebrafish embryos.³³ T-cell progenitors (Lck⁺ cells) were visualized by expression of mCherry in control and *dock11*-knockout (KO) embryos. Panel B shows quantification of the mean velocity of T-cell progenitors per embryo in control (blue; at least 11 cells/embryo were analyzed with a total number of 125 cells from 7 embryos) and *dock11*-knockout (green; at least 9 cells/embryo were analyzed with a total number of 291 cells from 12 embryos) *lck:mCherry* transgenic embryos.

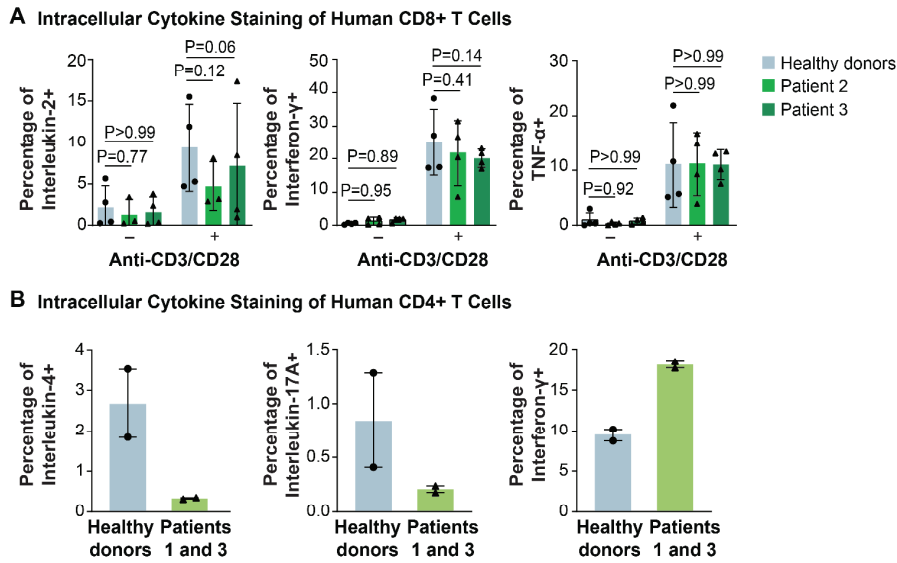
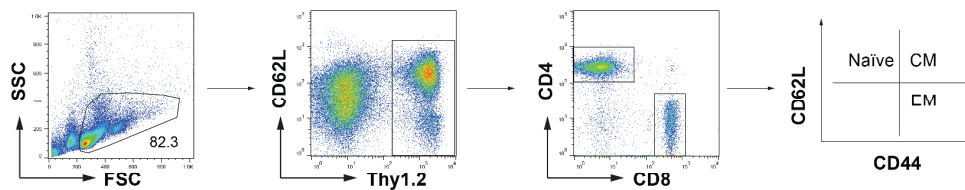


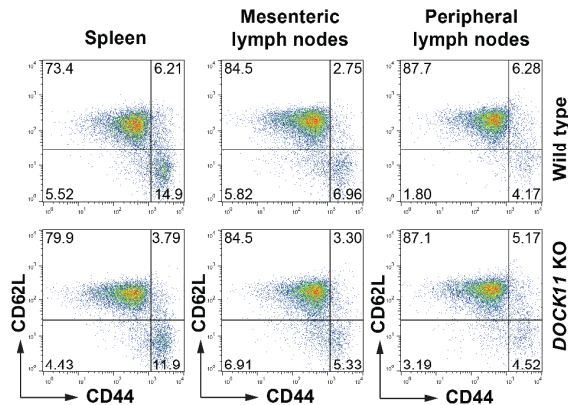
Figure S19. Cytokine Production in Human CD4+ and CD8+ T Cells

Panel A shows quantification of intracellular cytokine stainings (interleukin-2, interferon- γ and tumor necrosis factor α (TNF- α)) of CD8+ T cells from Patients 2 and 3 and pooled healthy donors (HDs) (mean of 2-3 HDs per datapoint) from 4 independent experiments displaying unaltered cytokine expression in patient-derived CD8+ T cells on anti-CD3/CD28 stimulation (plus sign). The minus sign denotes no stimulation. Results are given as mean values of multiple measurements, with standard deviations (I bars). Panel B shows quantification of intracellular cytokine stainings on stimulation of peripheral blood mononuclear cells with Phorbol 12-myristate 13-acetate and ionomycin revealing unaltered interleukin-17A, slightly reduced interleukin-4 and increased interferon- γ in CD4+CD25- memory T cells (based on CD45RA, CCR7 surface expression) from pooled Patients 1 and 3 and pooled healthy donors. Results are given as mean values, with standard errors (I bars).

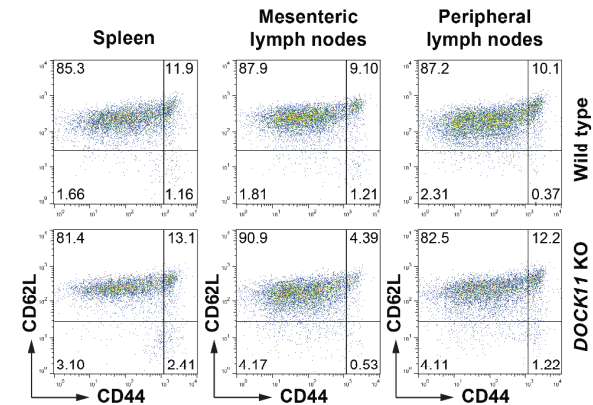
A Gating Scheme for Flow Cytometry Analysis of Murine T Cells



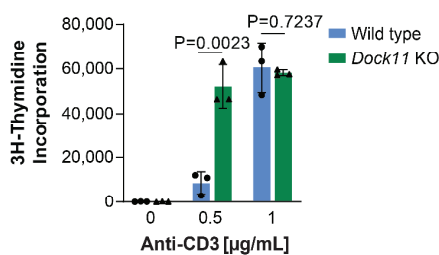
B Flow Cytometry Analysis of Murine CD4+ T Cell Subsets



C Flow Cytometry Analysis of Murine CD8+ T cell Subsets



D Proliferation Analysis of Murine CD4+ T Cells



E Proliferation Analysis of Murine CD8+ T Cells

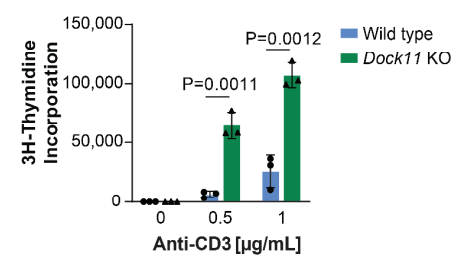
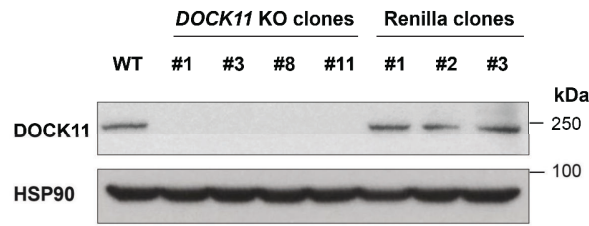


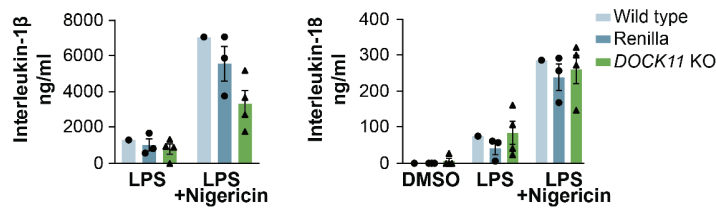
Figure S20. T-Cell Development and Proliferation in *Dock11*-Knockout Mice

Panel A shows gating scheme for immunophenotypic flow cytometry analysis of murine T cells. CD4+ (Panel B) and CD8+ (Panel C) naïve (CD62L+CD44-), central memory (CD62L+CD44+) and effector memory (CD62L-CD44+) T-cell subsets of *Dock11*-knockout (KO) and wild-type (WT) mice show no differences. Panel D and E show quantification of proliferation of CD4+ (Panel D) and CD8+ (Panel E) T cells from three *Dock11* KO and three WT mice stimulated with indicated concentrations of anti-CD3 antibody revealing increased proliferation of *Dock11* KO T cells compared to WT. Results are given as mean, with standard deviations (I bars). In Panels D and E, statistical analysis was performed with the use of an unpaired t-test. SSC side scatter, FSC forward scatter, CM central memory, EM effector memory.

A DOCK11 Expression in THP1 WT, Renilla and *DOCK11* KO Clones



B Cytokine Secretion upon NLRP3 Inflammasome Stimulation



C Cytokine Secretion upon Pysin Inflammasome Stimulation

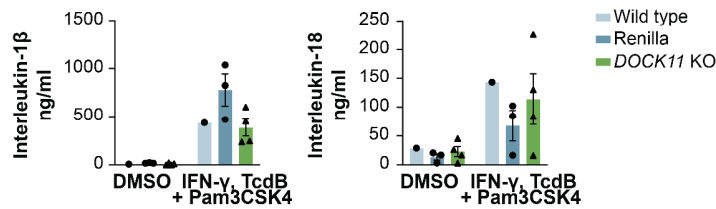


Figure S21. Normal Production of Cytokines by Human *DOCK11*-Deficient Monocyte-like Cells

Panel A shows immunoblot analysis of *DOCK11* in wild-type (WT), *DOCK11*-knockout (KO) and Renilla control human THP-1 cells displaying lack of protein expression in the KO cells. Anti-HSP90 antibody was used to control for equal loading. Panels B and C show ELISA measurements of interleukin-1 β and interleukin-18 cytokine levels in the supernatant of THP-1 cells stimulated with NLRP3 (Panel B) or Pysin (Panel C) inflammasome-inducing agents indicating comparable cytokine levels for *DOCK11* KO, WT and Renilla control THP-1 cells. Results are given as mean values, with standard errors (I bars). LPS lipopolysaccharide, DMSO dimethyl sulfoxide, TcdB *C. difficile* Toxin B. Pam3CSK4 denotes Pam3CysSerLys4, a synthetic triacylated lipopeptide.

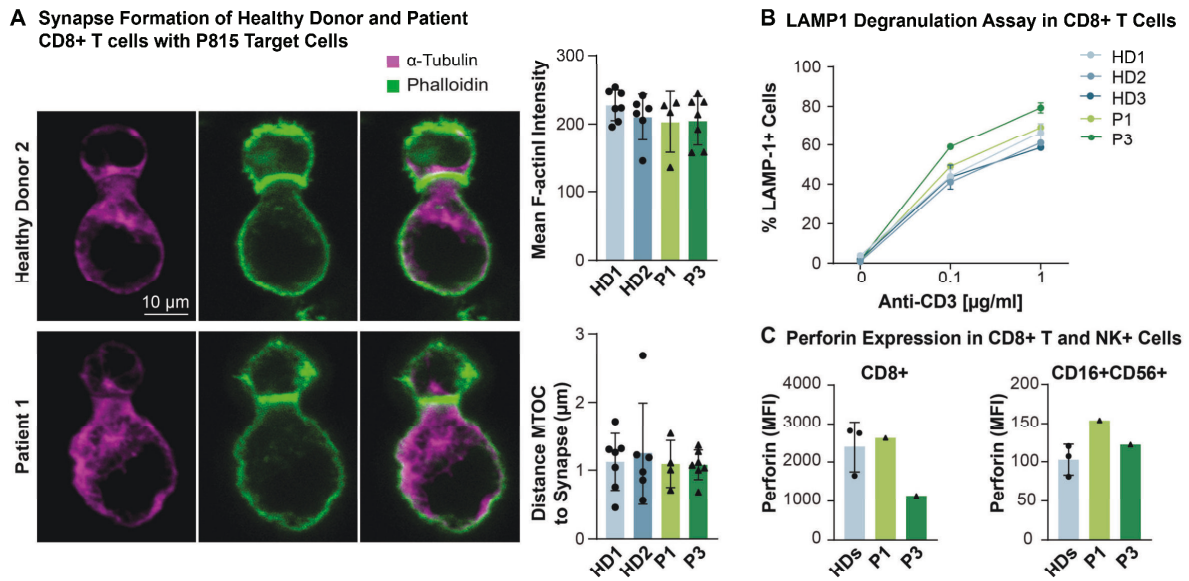
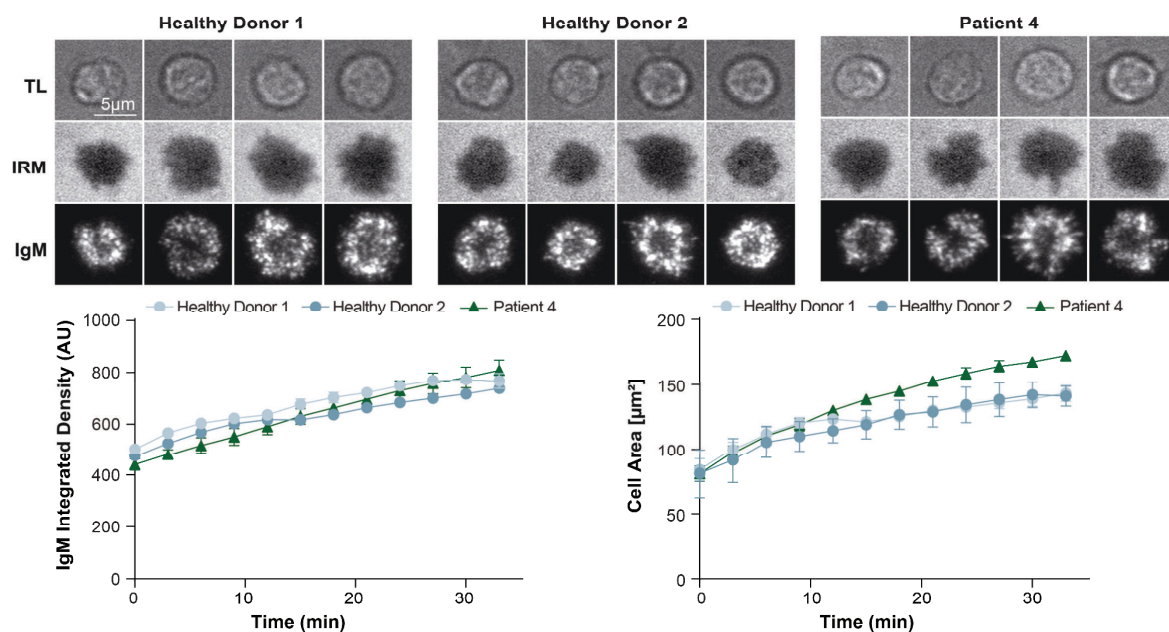


Figure S22. Human T-Cell Synapse Formation and Cytotoxicity

Panel A shows representative CD8+ T cell/ anti-CD3 antibody-coated P815 cell conjugates. Bar graphs display quantification of F-actin enrichment at the immune synapse (top graph) and polarization of the microtubule organization center (MTOC) (bottom graph). Results are given as mean, with standard deviations (I bars). Cells were stained with Phalloidin (green) and α -Tubulin antibody (purple). Panel B shows quantification of CD107a (LAMP-1) surface exposure in CD8+ T cells from patients (P) and healthy donors (HD) on exposure to anti-CD3 antibody-coated P815 cells at the indicated concentrations as a measure of cytotoxic T-cell degranulation from one representative experiment. LAMP-1 surface expression was assessed in two independent biological replicates. Panel C shows perforin expression in CD8+ T and CD16+CD56+ natural killer (NK) cells analyzed by flow cytometry. The results are given as mean from three healthy donors, with standard deviations (I bars). MFI - mean fluorescence intensity.

A Primary B-cell Synapse Assembly on Lipid Bilayers



B B Lymphoblastoid Cell Spreading and Activation on Coated Stimuli

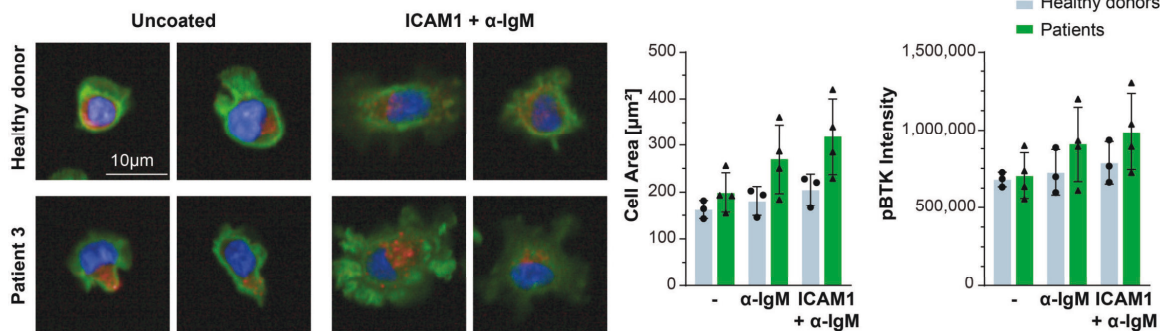


Figure S23. Human B-Cell Synapse Morphologic Features

Panel A shows four representative snapshots of mature primary B-cell synapses and quantification of cell area and integrated density of IgM accumulating over time. Results are given as mean values from 2 to 4 fields of view, with standard errors. Each value is based on a minimum of 295 cells. Panel B shows two representative images of B lymphoblastoid cell lines from one healthy donor (HD) and Patient 3 deposited in control wells (uncoated) or wells pre-coated with ICAM-1 + α -IgM. Cells were stained with DAPI (blue), Phalloidin (green) and anti-phosphorylated BTK antibody (red). Quantification of cell area and phosphorylated BTK intensity is shown for healthy donors (HD1-4) and the four patients (P1-P4). Cell area and intensity values were calculated across 3 replicate wells comprising a minimum of 165 cells per condition and the results are given as mean values, with standard deviations (I bars). The minus sign denotes no stimulation (uncoated wells). The results were confirmed in one independent experiment. TL - transmission light, IRM - interference reflection microscopy, Ig immunoglobulin.

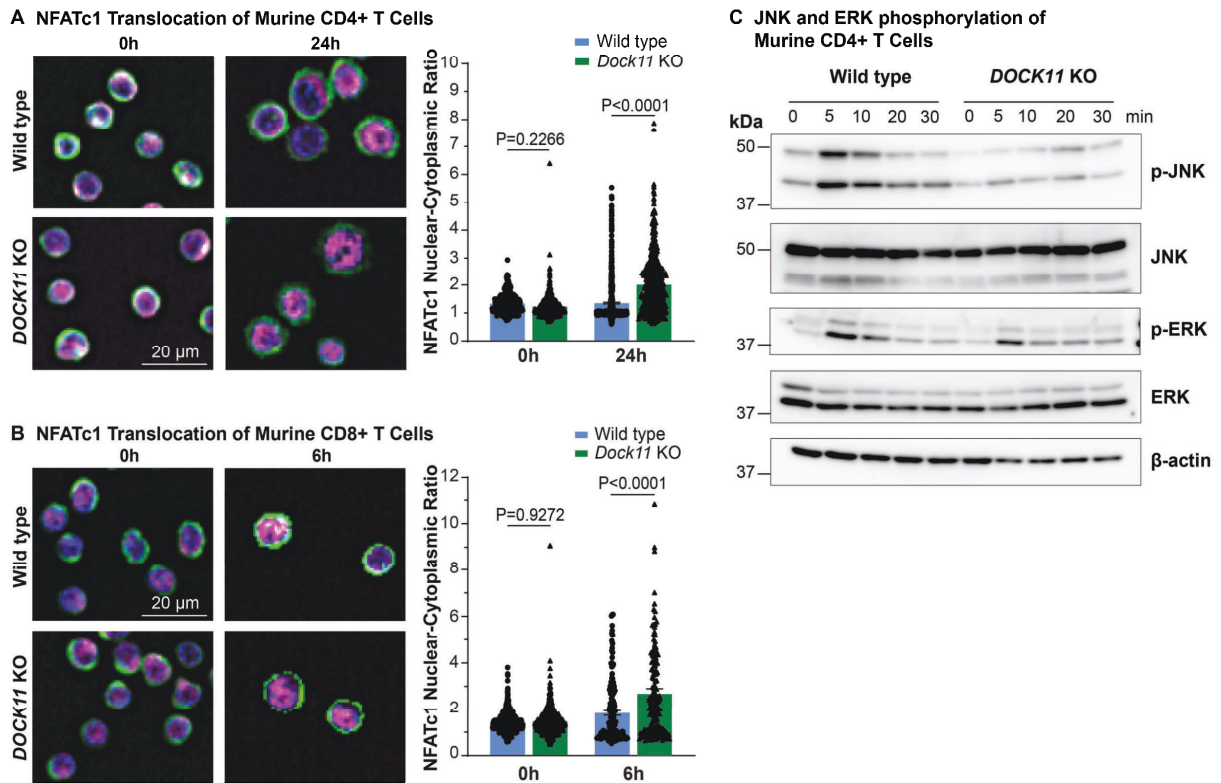


Figure S24. NFATc1 Nuclear Translocation in Murine CD4+ and CD8+ T Cells

Panels A and B show representative images of NFATc1 subcellular localization (left), and quantification of the NFATc1 nuclear-cytoplasmic ratio (right) of wild-type (WT) and *DoCK11*-knockout (KO) murine CD4+ (Panel A) and CD8+ (Panel B) T cells on stimulation with anti-CD3/CD28 antibodies for 24 (Panel A) or 6 (Panel B) hours, revealing increased NFATc1 nuclear translocation in *DoCK11* KO mice. Cells were stained with nuclear marker 4',6-diamidino-2-phenylindole (DAPI) (blue), Phalloidin (green) and NFATc1 (magenta). Results are shown as mean values, with standard errors (I bars). Panel C shows immunoblot analysis of JNK and ERK phosphorylation in CD4+ T cells from WT and *DoCK11* KO mice on stimulation with cross-linked anti-CD3 antibody for the indicated time points, revealing reduced JNK phosphorylation in *DoCK11* KO mice. Total JNK and ERK show no differences. Anti- β -actin was used as loading control. Data are representative of two (Panels A and B) or three (Panel C) independent replicates. In Panels A and B, statistical analysis were performed with the use of an ordinary analysis of variance with a Šidák correction test for multiple comparison. P phosphorylation, kDa kilo Dalton.

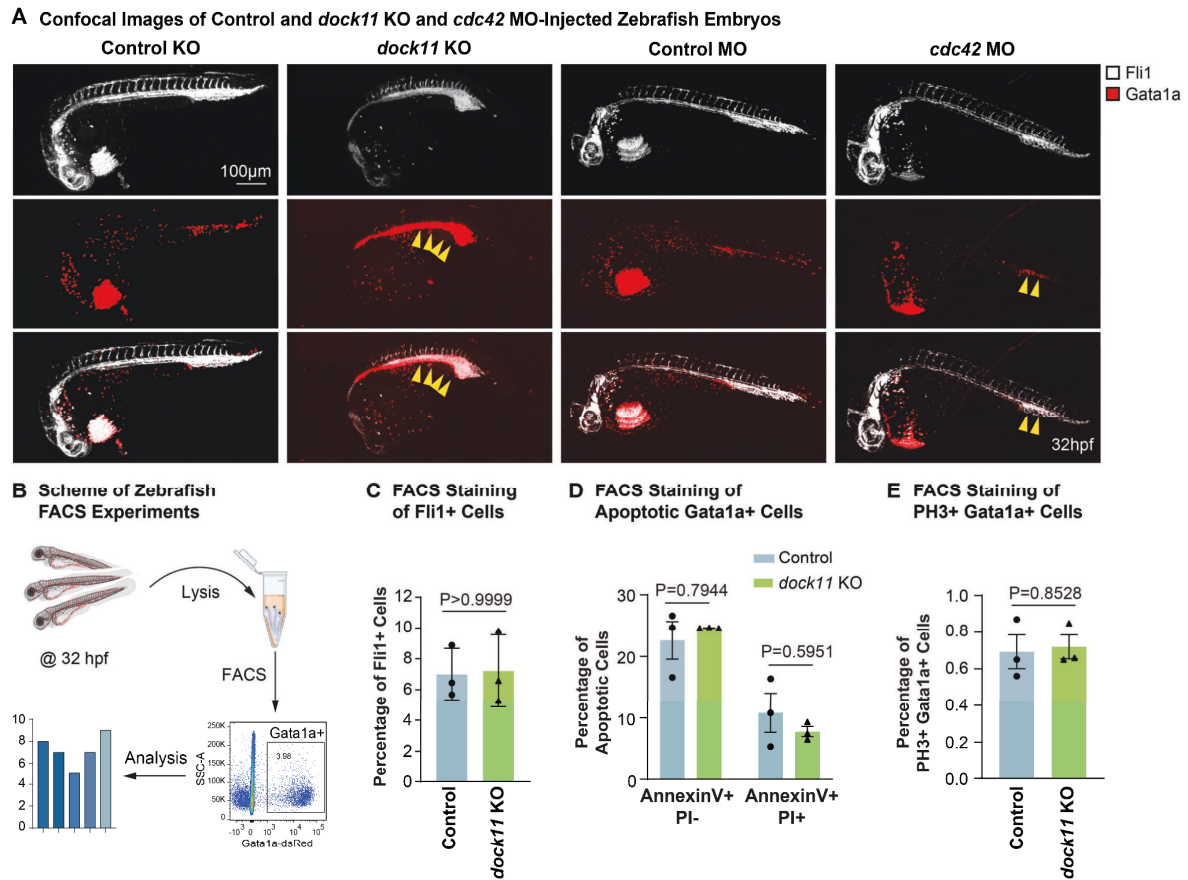


Figure S25. Evaluation of Gata1a-Positive Cells in *dock11*-Knockout Zebrafish

Panel A displays representative confocal images showing intravascular blood accumulation (yellow arrows) in *dock11*-knockout (KO) and *cdc42*-morpholino (MO) *fli1:GFP;gata1a:dsRed* transgenic embryos compared to their respective controls. Merged images are also shown in Fig. 4A. Panel B schematizes the workflow for the quantification of Gata1a⁺ and/or Fli1⁺ cells from *tg(fli1:GFP;gata1a:dsRed)* zebrafish embryos by flow cytometry. Panel C illustrates the quantification of Fli1⁺ cells by flow cytometry for 32 hours postfertilization (hpf) control and *dock11*-knockout (KO) embryos. Results are given as mean values from three independent experiments, with standard deviations (I bars). Panel D shows quantification of apoptosis of Gata1a⁺ cells from 3 days postfertilization (dpf) control and *dock11* KO zebrafish embryos measured by flow cytometry revealing similar levels of apoptosis in *dock11* KO compared to control embryos. Panel E shows flow cytometry analysis of PH3⁺Gata1a⁺ cells in 30 hpf, 4 dpf and 5 dpf control and *dock11* KO zebrafish embryos revealing similar percentages of mitotic (PH3⁺) cells in *dock11* KO compared to control embryos. In Panels D and E, the results are given as mean values, with standard errors (I bars). In Panels C and E, statistical analysis were performed with the use of a paired t test, and in Panel D using an ordinary analysis of variance with a Šidák correction test for multiple comparison. PI propidium iodide, PH3 phospho-histone H3.

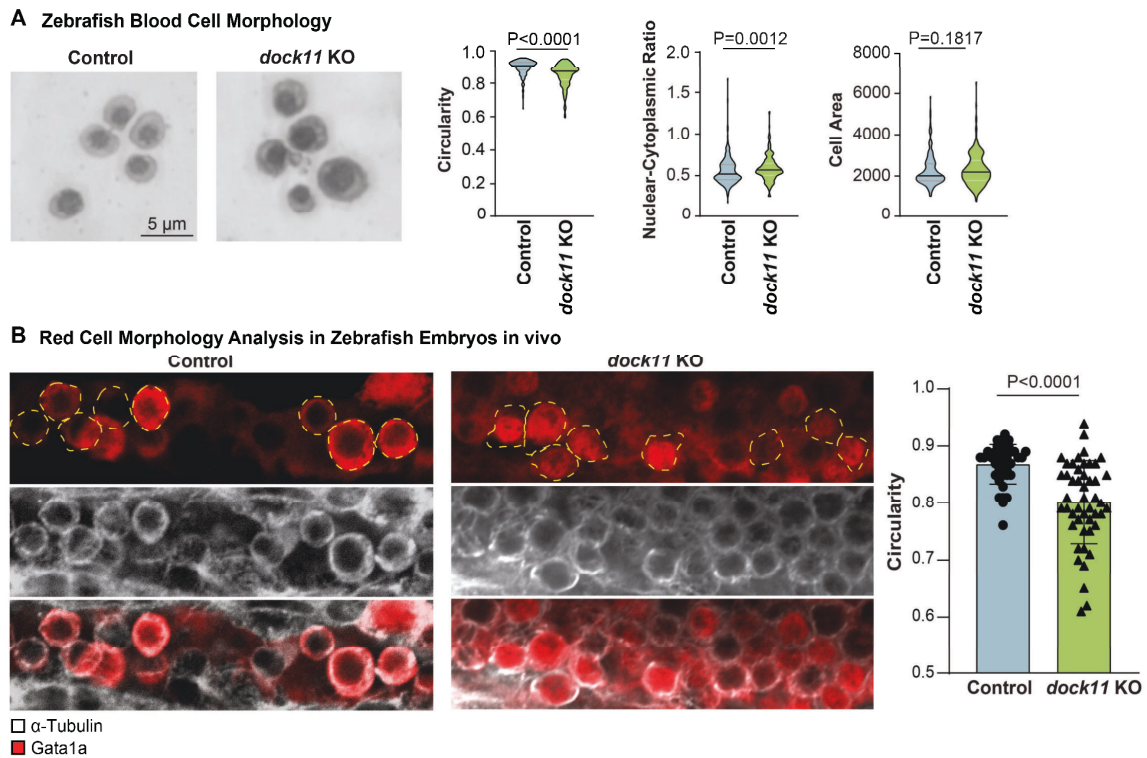
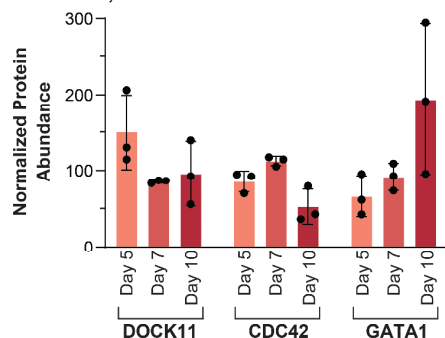


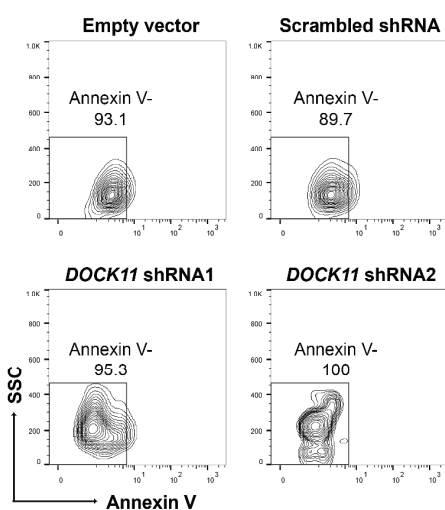
Figure S26. Morphologic features of Gata1a-Positive Cells in *dock11*-Knockout Zebrafish

Panel A shows representative images of stained cytopsin slides revealing altered blood cell morphologic features in *dock11*-knockout (KO) zebrafish compared to control at 48 hours postfertilization (hpf). Graphs show quantification of circularity, nuclear-cytoplasmic ratio and cell area. Representative violin plots from two independent experiments. Panel B shows representative confocal images of 48 hpf *gata1a:dsRed* transgenic embryos stained with anti- α -Tubulin and anti-RFP (for detection of Gata1a) antibodies and respective quantification depicting reduced circularity of Gata1a⁺ erythroid cells in *dock11*-knockout embryos. Results are given as mean values, with standard deviations (I bars). In Panels A and B, statistical analysis were performed with the use of a Mann–Whitney test. RFP red fluorescence protein.

A DOCK11, CDC42 and GATA1 Protein Levels During Erythroid Differentiation of CD34+ Cells



B Apoptosis during Erythroid Differentiation



C Delay during Erythroid Differentiation

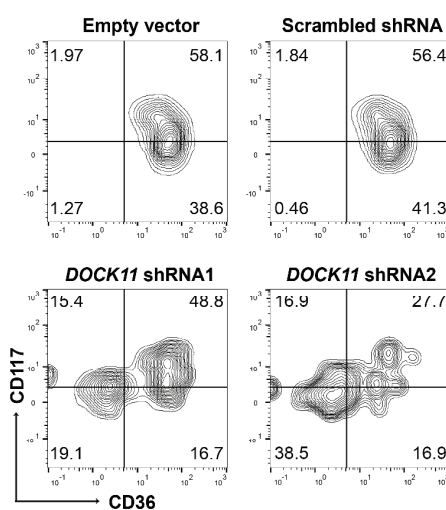


Figure S27. Evaluation of *dock11*-Knockout Zebrafish, *DOCK11*-Silenced Erythroid Cells

Panel A shows protein abundance of DOCK11, CDC42 and GATA1 from mass spectrometry analysis in healthy donor CD34⁺-derived erythroid cells after 5, 7 or 10 days of erythroid culture. Data were normalized to total peptide abundance to correct for experimental bias and scaled ‘on all average’. Panels B and C show assessment of human CD34⁺ cells during erythroid differentiation, which are transduced with empty, scrambled or *DOCK11* shRNA-containing pLKO.1-CMV-tGFP vectors at day 2 and sorted for GFP positive cells at day 5. Panel B shows representative flow cytometry plot of GFP⁺ cells stained with Annexin V after 10 days in erythroid culture, revealing no difference in apoptosis in *DOCK11*-silenced cells. Panel C shows representative flow cytometry plots of GFP⁺CD123⁻ cells stained with CD117 and CD36 after 7 days in erythroid culture, revealing a delay in erythroid differentiation in *DOCK11*-silenced cells. SSC side scatter.

Table S1. Extended Clinical Characterization of Female Carriers of *DOCK11* Variants

	Mother of Patient 1	Mother of Patient 3
WBC (cells$\times 10^3/\text{mm}^3$)	8.5	7.1
normal range	4.5 - 13.0	4.5 - 13.0
ALC (cells$\times 10^3/\text{mm}^3$)	n.a.	3.4
normal range	1.4 - 3.3	1.4 - 3.3
ANC (cells$\times 10^3/\text{mm}^3$)	n.a.	3.1
normal range	1.5 - 5.0	1.5 - 5.0
AMC (cells/mm^3)	n.a.	400
normal range	100 - 700	100 - 700
ATC (cells$\times 10^3/\text{mm}^3$)	n.a.	331
normal range	150 - 500	150 - 500
MPV	n.a.	6.3
normal range	7.0 - 12.0	7.0 - 12.0
RBC (cells $\times 10^6/\text{mm}^3$)	5.42	4.22
normal range	4.00-5.20	4.00-5.20
Hb (g/dL)	14.7	12.7
normal range	12.0-16.0	12.0-16.0
HCT (%)	n.a.	38.1
normal range	36.0 - 46.0	36.0 - 46.0
MCV (fl)	83.2	90
normal range	80.0 - 95.0	80.0 - 95.0
MCH (pg)	27.1	30.1
normal range	25.0 - 35.0	25.0 - 35.0
MCHC (g/dL)	n.a.	33.4
normal range	30.4 - 36.5	30.4 - 36.5
RDW-CV (%)	n.a.	12.4
normal range	11.5 - 18.0	11.5 - 18.0
ESR (mm 1h)	n.a.	6
normal range	< 15.0	< 15.0
		11.4
		4.5 - 13.0
		2.2
		1.4 - 3.3
		8.3 \uparrow
		1.5 - 5.0
		400
		100 - 700
		353
		150 - 500
		9
		7.0 - 12.0
		4.84
		4.00-5.20
		12.2
		12.0-16.0
		38
		36.0 - 46.0
		78
		80.0 - 95.0
		25.3
		25.0 - 35.0
		32.2
		30.4 - 36.5
		15.4
		11.5 - 18.0
		26.0
		< 15.0
		< 15.0
		10
		4.5 - 13.0
		3.6
		1.4 - 3.3
		5.4 \uparrow
		1.5 - 5.0
		500
		100 - 700
		463
		150 - 500
		9
		7.0 - 12.0
		4.5
		4.00-5.20
		12.2
		12.0-16.0
		36.6
		81
		80.0 - 95.0
		27.2
		25.0 - 35.0
		33.4
		30.4 - 36.5
		15.3
		11.5 - 18.0
		n.a.
		< 15.0

Table S1. Extended Laboratory Parameters of Female Carriers of Pathogenic *DOCK11* Variants

Analysis of absolute cell counts in peripheral blood and additional diagnostic markers were performed at the Mofid Children's Hospital, Shahid Beheshti University of Medical Sciences, Tehran, Iran and at Children Hospital Sant Joan de Déu, Barcelona, Spain. Reference values are taken from ref.^{34,35} or internal healthy donor cohorts. WBC whole blood cell count, ALC absolute lymphocyte count, ANC absolute neutrophil count, AMC absolute monocyte count, ATC absolute thrombocyte count, MPV mean platelet volume, RBC red blood cell count, Hb hemoglobin, HCT hematocrit, MCV mean corpuscular volume, MCH mean corpuscular hemoglobin, RDW-CV red cell distribution width - coefficient of variation, ESR erythrocyte sedimentation rate.

Table S2. Immunological Characteristics of Female Carriers				
	Mother of Patient 3		Mother of Patient 4	Reference range
CD4+T cells (%) [†]	79.2	80.3	84.4	28-64
CD8+T cells (%) [†]	12.8	13.1	10.4	12-40
CD16+CD56+ NK cells (% of CD3-)	5.73	8.63	4.02	n.a.
CD3+ TCRab (%)	88.7	90	n.a.	36-98
CD3+ TCRgd (%)	4.23	3.35	n.a.	0.83-11
DN (CD3+CD4-CD8-TcRab+) T cells (%) [†]	1.61	1.2	n.a.	0.57-5
CD4 Naïve (CD45RA+CCR7+) (%)	20.4	16.1	19.9	16-100
CD4 CM (CD45RA-CCR7+) (%)	59.5	67.7	56.9	18-95
CD4 EM (CD45RA-CCR7-) (%)	18.6	15.1	20.3	1-23
CD8 Naïve (CD45RA+CCR7+) (%)	28.4	32.5	25.1	6-100
CD8 CM (CD45RA-CCR7+) (%)	7.04	13.8	5	2-6
CD8 EM (CD45RA-CCR7-) (%)	38.3	30.8	34.7	1-100
CD8 TEMRA (CD45RA+CCR7-) (%)	26.3	22.9	35.2	4-92
CD19+ B cells (%) [‡]	15.1	11.1	9.53	7.2-11.2
Naïve B cells (IgD+CD27-)*	65.4	67.5	71.1	58.0-72.1
Switched-memory (IgD-CD27+) (%)*	16.3	15.2	13.2	9.2-18.9
Marginal (IgD+CD27+) (%)*	14.5	13.7	13.7	13.4-21.4
Transitional (IgM+CD38+) (%)*	1.85	3.12	8.58	n.a.
Plasmablasts (IgM-CD38 ^{high}) (%)*	1.11	2.08	1.14	n.a.
Plasmablasts (CD27 ^{high} CD38 ^{high}) (%)*	1.18	1.39	2.07	n.a.
CD21 ^{low} CD38 ^{low} B cells (%)*	3.38	3.14	2.31	1.8-4.7

Table S2. Immunological Characteristics of Female Carriers

Assessment of female carrier's peripheral blood lymphocyte subsets by flow cytometry. Values for three different time points are shown for mother of Patient 3. Adult reference values were taken from public data sets or internal healthy cohorts.³⁶⁻³⁸ Bold indicates values outside of the normal range. n.a. not available, † percentage of CD3+ lymphocytes. ‡ percentage of lymphocytes, * percentage of CD3-CD19+ B lymphocytes.

Table S3. Extended Laboratory Parameters of Patients 1 and 2 with DOCK11 Deficiency

Age	Patient 1							Patient 2		
	40 d	4m	8m	1y7m	4y8m	5y	2m	9m	2y10m	
WBC (cells$\times 10^3/\text{mm}^3$)	32.8	37.53	12.8	17.7	21.5	15.82	10.5	9.3	12.8	
normal range	5.0–19.5	6.0–17.5	6.0–17.5	6.0–17	5.5–15.5	5.0–14.5	5.0–19.5	6.0–17.5	5.5–15.5	
ALC (cells$\times 10^3/\text{mm}^3$)	n.a.	19.1	7.9	11.5	n.a.	n.a.	n.a.	4.1	n.a.	
normal range	2.5–16.5	4–13.5	4–10.5	3–9.5	2–8	1.3–7.0	2.5–16.5	4–10.5	2–8	
ANC (cells$\times 10^3/\text{mm}^3$)	n.a.	3.8	4.48	3.1	n.a.	n.a.	n.a.	2.6	n.a.	
normal range	1–9	1–8.5	1–8.5	1.5–8.5	1.5–8.5	1.7–7.5	1–9	1–8	1.5–8.5	
AMC (cells/mm^3)	n.a.	578	256	177	n.a.	n.a.	n.a.	1302	n.a.	
normal range	350–1365	300–875	300–875	300–850	275–775	275–775	350–1365	300–875	275–775	
ATC (cells$\times 10^3/\text{mm}^3$)	55	44	56	15	25	16	462	686	157	
normal range	150–450	150–450	150–450	150–450	150–450	150–450	150–450	150–450	150–450	
MPV (fl)	n.a.	n.a.	n.a.	n.a.	n.a.	16.1	n.a.	n.a.	n.a.	
normal range	6.5–10.0	6.5–10.0	6.5–10.0	6.5–10.0	6.5–10.0	6.5–10.0	6.5–10.0	6.5–10.0	6.5–10.0	
RBC (cells $\times 10^6/\text{mm}^3$)	1.79	1.79	3.01	1.86	2.3	3.25	5.1	4.2	3	
normal range	3.0–5.4	2.7–4.5	3.7–5.3	3.7–5.3	3.9–5.3	3.9–5.3	2.7–4.4	3.7–5.3	3.7–5.3	
Hb (g/dL)	5.2	3.6	7.6	4.5	5.8	8.2	13	10.2	7.9	
normal range	10.5–14.0	9.5–13.5	10.5–14	10.5–14	11.5–14.5	11.5–14.5	9.5–13.5	10.5–14	10.5–14	
HCT (%)	n.a.	12.2	23.3	15.7	19.2	26.9	42	33	25	
normal range	32–42	29–41	33–39	33–39	34–40	34–40	29–41	33–39	33–39	
MCV (fl)	66.5	68.2	77.4	84.4	82.4	82.8	83	79	85	
normal range	72–88	72–82	76–90	76–90	76–90	76–90	72–82	76–90	76–90	

Table S3. Extended Laboratory Parameters of Patients 1 and 2 with DOCK11 Deficiency									
Age	Patient 1					Patient 2			
	40 d	4m	8m	1y7m	4y8m	5y	2m	9m	2y10m
MCH (pg)	n.a.	20.1	25.25	22.58	24.9	25.4	26	25	27
normal range	26-34	25-35	23-31	23-31	24-30	24-30	26-34	23-31	24-30
MCHC (g/dL)	43.7	29.5	32.62	26.75	30.2	30.7	n.a.	n.a.	n.a.
normal range	29-37	30-36	30-36	30-36	32-36	32-36	29-37	30-36	32-36
Reticulocytes (%)	0.4	n.a.	0.3	n.a.	n.a.	n.a.	2.7	n.a.	n.a.
normal range	2.12-3.47	1.55-2.70	0.99-1.82	0.82-1.45	0.82-1.45	0.82-1.45	2.12-3.47	0.99-1.82	0.82-1.45
Hb reticulocytes (pg)	n.a.	n.a.	n.a.	n.a.	n.a.	n.a.	n.a.	n.a.	n.a.
normal range	29.5-32.8	29.5-32.8	29.5-32.8	29.5-32.8	29.5-32.8	29.5-32.8	29.5-32.8	29.5-32.8	29.5-32.8
RDW-CV (%)	n.a.	25.5	16.4	17.8	16.7	n.a.	n.a.	n.a.	n.a.
normal range	11.5-16.0	11.5-16.0	11.5-16.0	11.5-16.0	11.5-15.0	11.5-15.0	11.5-16.0	11.5-16.0	11.5-16.0
RBC morphology (microscopy)	Anisocytosis, Poikilocytosis, Hypochromia								
Leukoerythroblastosis	NRBCs, Pro- and meta-myelocytes								
Ferritin (ng/ml)	n.a.	243.8	n.a.	n.a.	n.a.	n.a.	n.a.	n.a.	n.a.
normal range	50-200	50-200	7-140	7-140	7-140	7-140	50-200	7-140	7-140
Iron (umol/L)	n.a.	n.a.	n.a.	n.a.	n.a.	n.a.	n.a.	n.a.	n.a.
normal range	10.74-30.43	10.74-30.43	10.74-30.43	10.74-30.43	10.74-30.43	10.74-30.43	10.74-30.43	10.74-30.43	10.74-30.43
Iron binding capacity (umol/L)	n.a.	n.a.	n.a.	n.a.	n.a.	n.a.	n.a.	n.a.	n.a.
normal range	50-120	50-120	50-120	50-120	50-120	50-120	50-120	50-120	50-120
Bilirubin T (mg/dL)	n.a.	n.a.	0.2	n.a.	n.a.	n.a.	n.a.	n.a.	0.2
normal range	0.1-1.2	0.1-1.2	0.1-1.2	0.1-1.2	0.1-1.2	0.1-1.2	0.1-1.2	0.1-1.2	0.1-1.2

Table S3. Extended Laboratory Parameters of Patients 1 and 2 with DOCK11 Deficiency

Age	Patient 1						Patient 2		
	40 d	4m	8m	1y7m	4y8m	5y	2m	9m	2y10m
ESR (mm/h)	n.a.	n.a.	15	n.a.	n.a.	n.a.	n.a.	n.a.	n.a.
normal range	<10	<10	<10	<10	<10	<10	<10	<10	<10
CRP (mg/L)	n.a.	n.a.	28	4	n.a.	n.a.	0.9	<0.4	0.7
normal range	<10	<10	<10	<10	<10	<10	<10	<10	<10
LDH (IU/L)	n.a.	349	n.a.	n.a.	n.a.	n.a.	275	n.a.	1028
normal range	500-920	500-920	500-920	500-920	470-900	470-900	500-920	500-920	500-920
Serum Amyloid A (mg/L)	n.a.	n.a.	n.a.	n.a.	n.a.	n.a.	n.a.	n.a.	n.a.
normal range	<6.5	<6.5	<6.5	<6.5	<6.5	<6.5	<6.5	<6.5	<6.5
Vitamin B12 pg/ml	n.a.	n.a.	n.a.	n.a.	n.a.	n.a.	n.a.	n.a.	n.a.
Normal range	211-946	211-946	211-946	211-946	211-946	211-946	211-946	211-946	211-946
Albumin (g/L)	n.a.	n.a.	n.a.	n.a.	n.a.	n.a.	n.a.	n.a.	24.7
normal range	28-50	39-51	39-51	37-55	37-55	37-55	28-50	39-51	37-55
Immunoglobulins									
IgG (mg/L)	n.a.	n.a.	2120	n.a.	n.a.	n.a.	n.a.	n.a.	6260
normal range	1770-5830	1730-8170	2180-9079	4250-10540	4640-12400	6350-12840	1770-5830	2180-9070	4420-11390
IgA (mg/L)	n.a.	n.a.	170	n.a.	n.a.	n.a.	n.a.	n.a.	1030
normal range	50-430	70-800	100-850	130-1160	220-1460	320-1910	50-430	130-1000	210-1050
IgM (mg/L)	n.a.	n.a.	440	n.a.	n.a.	n.a.	n.a.	n.a.	470
normal range	220-820	300-990	310-1160	440-1550	400-1800	440-1900	220-820	400-1590	440-1900
IgE (IU/mL)	n.a.	n.a.	0.1	n.a.	n.a.	n.a.	n.a.	n.a.	n.a.
normal range	<15	<15	<15	<60	<60	<60	<15	<15	<60

Table S3. Extended Laboratory Parameters of Patients 1 and 2 with DOCK11 Deficiency						
Age	Patient 1			Patient 2		
	40 d	4m	8m	1y7m	4y8m	5y
Autoantibodies	Direct and indirect Coombs tests: negative					
Nuclear antibodies (ANA), Neutrophil cytoplasmic antibodies (ANCA): all negative or within reference range.						

Table S3. Extended Laboratory Parameters of Patients 1 and 2 with DOCK11 Deficiency

Analysis of absolute cell counts in peripheral blood and additional diagnostic markers. The data were collected and analyzed at the Mofid Children's Hospital, Shahid Beheshti University of Medical Sciences, Tehran, Iran at the University Children's Hospital Oldenburg, Department of Neuropediatrics, Oldenburg, Germany. Reference values are taken from ref.^{34,35} or internal healthy donor cohorts. WBC whole blood cell count, ALC absolute lymphocyte count, ANC absolute neutrophil count, AMC absolute monocyte count, ATC absolute thrombocyte count, MPV mean platelet volume, RBC red blood cell count, Hb hemoglobin, HCT hematocrit, MCV mean corpuscular volume, MCH mean corpuscular hemoglobin, RDW-CV red cell distribution width - coefficient of variation, ESR erythrocyte sedimentation rate, CRP C-reactive protein, LDH lactate dehydrogenase, n.a. not available.

Table S4. Extended Laboratory Parameters of Patients 3 and 4 with DOCK11 Deficiency

Age	Patient 3					Patient 4					
	1y4m	3y4m	3y5m	3y6m	4y1m	2y0m	2y1m	2y2m	3y2m	4y2m	6y
WBC (cells $\times 10^3/\text{mm}^3$)	37	21.58	16.99	19.84	23.4	10.6	15.1	12.2	4.9	6.2	6.6
normal range	6.0–17.0	5.5–15.5	5.5–15.5	5.5–15.5	5.0–14.5	6.0–17.0	5.5–15.5	5.5–15.5	5.5–15.5	5.0–14.5	5.0–14.5
ALC (cells$\times 10^3/\text{mm}^3$)	6.8	12	4.9	5.7	10.5	n.a.	7.1	5.5	2.29	2.4	1.96
normal range	3.0–9.5	2–8	2–8	2–8	2–8	3.0–9.5	2–8	2–8	2–8	2–8	1.3–7.0
ANC (cells$\times 10^3/\text{mm}^3$)	27	5.8	10.1	13.3	8.7	n.a.	4.4	5.1	1.84	3.16	3.5
normal range	1.5–8.5	1.5–8.5	1.5–8.5	1.5–8.5	1.5–8.5	1.5–8.5	1.5–8.5	1.5–8.5	1.5–8.5	1.5–8.5	1.7–7.5
AMC (cells/mm^3)	2180	3600	1970	700	1900	n.a.	1510	1250	400	440	670
normal range	300–850	275–775	275–775	275–775	275–775	275–775	275–775	275–775	275–775	275–775	275–775
ATC (cells$\times 10^3/\text{mm}^3$)	n.a.	827	712	512	793	513	642	705	384	363	387
normal range	150–450	150–450	150–450	150–450	150–450	150–450	150–450	150–450	150–450	150–450	150–450
MPV (fl)	n.a.	n.a.	9.1	10.3	8.9	n.a.	n.a.	n.a.	n.a.	n.a.	n.a.
normal range	6.5–10.0	6.5–10.0	6.5–10.0	6.5–10.0	6.5–10.0	6.5–10.0	6.5–10.0	6.5–10.0	6.5–10.0	6.5–10.0	6.5–10.0
RBC (cells $\times 10^6/\text{mm}^3$)	n.a.	3.55	3.5	4.03	3.99	n/a	4.38	5.48	4.2	4.66	4.79
normal range	3.7–5.3	3.9–5.3	3.9–5.3	3.9–5.3	3.9–5.3	3.7–5.3	3.7–5.3	3.7–5.3	3.9–5.3	3.9–5.3	3.9–5.3
Hb (g/dL)	n.a.	10	9.8	9.3	9.2	9.67	8.06	11.76	11.92	12.09	12.89
normal range	10.5–14	11.5–14.5	11.5–14.5	11.5–14.5	11.5–14.5	10.5–14	10.5–14	10.5–14	11.5–14.5	11.5–14.5	11.5–14.5
HCT (%)	n.a.	30.2	32	29.8	31.1	n.a.	27	n.a.	33	36	38
normal range	33–39	34–40	34–40	34–40	34–40	33–39	33–39	33–39	34–40	34–40	34–40
MCV (fl)	n.a.	n.a.	90.4	73.9	78	n.a.	61	n.a.	78	76	79
normal range	76–90	76–90	76–90	76–90	76–90	76–90	76–90	76–90	76–90	76–90	76–90

Table S4. Extended Laboratory Parameters of Patients 3 and 4 with DOCK11 Deficiency

Age	Patient 3						Patient 4					
	1y4m	3y4m	3y5m	3y6m	4y1m		2y0m	2y1m	2y2m	3y2m	4y2m	6y
MCH (pg)	n.a.	n.a.	27.8	23.1	23.1	23.1	n.a.	18.4	n.a.	28.4	25.94	26.9
normal range	23-31	24-30	24-30	24-30	24-30	24-30	24-30	24-30	24-30	24-30	24-30	24-30
MCHC (g/dL)	n.a.	n.a.	30.7	31.2	29.7	29.7	n.a.	18.7	n.a.	22.7	21.1	21.2
normal range	30-36	32-36	32-36	32-36	32-36	32-36	32-36	32-36	32-36	32-36	32-36	32-36
Reticulocytes (%)	n.a.	n.a.	n.a.	n.a.	9.3	9.3	n.a.	n.a.	n.a.	n.a.	n.a.	n.a.
normal range	0.82-1.45	0.82-1.45	0.82-1.45	0.82-1.45	0.82-1.45	0.82-1.45	0.82-1.45	0.82-1.45	0.82-1.45	0.82-1.45	0.82-1.45	0.82-1.45
Hb reticulocytes (pg)	n.a.	n.a.	n.a.	n.a.	25.3	25.3	n.a.	n.a.	n.a.	n.a.	n.a.	n.a.
normal range	29.5-32.8	29.5-32.8	29.5-32.8	29.5-32.8	29.5-32.8	29.5-32.8	29.5-32.8	29.5-32.8	29.5-32.8	29.5-32.8	29.5-32.8	29.5-32.8
RDW-CV (%)	n.a.	n.a.	18	19.2	24.4	24.4	n.a.	15.2	n.a.	15.2	13.9	14.7
normal range	11.5-16.0	11.5-15.0	11.5-15.0	11.5-15.0	11.5-15.0	11.5-15.0	11.5-15.0	11.5-15.0	11.5-15.0	11.5-15.0	11.5-15.0	11.5-15.0
RBC morphology (microscopy)	Anisocytosis, Poikilocytosis, Hypochromia and Macrothrombocytes											
Leukoerythroblastosis	n.a.											
Ferritin (ng/ml)	n.a.	449	313	164	39.5	39.5	n.a.	5	14	22	15	28
normal range	7-140	7-140	7-140	7-140	7-140	7-140	7-140	7-140	7-140	7-140	7-140	7-140
Iron (umol/L)	n.a.	n.a.	n.a.	n.a.	4.1	4.1	n.a.	<2	n.a.	14	15	16
normal range	10.7-30.4	10.7-30.4	10.7-30.4	10.7-30.4	10.7-30.4	10.7-30.4	10.7-30.4	10.7-30.4	10.7-30.4	10.7-30.4	10.7-30.4	10.7-30.4
Iron binding capacity (umol/L)	n.a.	n.a.	n.a.	n.a.	n.a.	n.a.	n.a.	84	n.a.	66	82	72
normal range	50-120	50-120	50-120	50-120	50-120	50-120	50-120	50-120	50-120	50-120	50-120	50-120
Bilirubin T (mg/dL)	n.a.	0.21	0.16	0.03	n.a.	n.a.	n.a.	n.a.	n.a.	n.a.	n.a.	n.a.
normal range	0.1-1.2	0.1-1.2	0.1-1.2	0.1-1.2	0.1-1.2	0.1-1.2	0.1-1.2	0.1-1.2	0.1-1.2	0.1-1.2	0.1-1.2	0.1-1.2

Table S4. Extended Laboratory Parameters of Patients 3 and 4 with DOCK11 Deficiency

Age	Patient 3						Patient 4					
	1y4m	3y4m	3y5m	3y6m	4y1m		2y0m	2y1m	2y2m	3y2m	4y2m	6y
ESR (mm/h)	n.a.	n.a.	67	104	37		n.a.	15	6	n.a.	8	2
normal range	<10	<10	<10	<10	<10		<10	<10	<10	<10	<10	<10
CRP (mg/L)	245.8	96.2	26.7	25	16.2		0.2	0.4	<0.1	<0.1	n.a.	n.a.
normal range	<10	<10	<10	<10	<10		<10	<10	<10	<10	<10	<10
LDH (IU/L)	n.a.	346	254	305	1173		n.a.	n.a.	n.a.	n.a.	n.a.	n.a.
normal range	500-920	500-920	500-920	500-920	470-900		500-920	500-920	500-920	500-920	470-900	470-900
Serum Amyloid A (mg/L)	n.a.	n.a.	n.a.	n.a.	21		n.a.	n.a.	n.a.	n.a.	n.a.	n.a.
normal range	<6.5	<6.5	<6.5	<6.5	<6.5		<6.5	<6.5	<6.5	<6.5	<6.5	<6.5
Vitamin B12 pg/ml	n.a.	n.a.	293	n.a.	n.a.		n.a.	n.a.	n.a.	n.a.	n.a.	n.a.
Normal range	211-946	211-946	211-946	211-946	211-946		211-946	211-946	211-946	211-946	211-946	211-946
Albumin (g/L)	n.a.	18	n.a.	20	23		30	30	38	40	41	n.a.
normal range	37-55	37-55	37-55	37-55	37-55		37-55	37-55	37-55	37-55	37-55	37-55
Immunoglobulins												
IgG (mg/L)	n.a.	278	n.a.	1632	1085		n.a.	n.a.	5080	5530	n.a.	n.a.
normal range	4250-10540	4640-12400	4640-12400	4640-12400	4640-12400		4420-11390	4420-11390	4420-11390	4640-12400	4640-12400	635-1284
IgA (mg/L)	n.a.	114	124	47	145		n.a.	n.a.	1210	920	n.a.	n.a.
normal range	130-1160	220-1460	220-1460	220-1460	220-1460		210-1500	210-1500	210-1500	220-1460	220-1460	320-1910
IgM (mg/L)	n.a.	414	335	117	288		n.a.	n.a.	640	280	n.a.	n.a.
normal range	440-1550	400-1800	400-1800	400-1800	400-1800		430-1840	430-1840	430-1840	400-1800	400-1800	440-1900
IgE (IU/mL)	n.a.	n.a.	n.a.	n.a.	<1		n.a.	n.a.	176	n/a	n.a.	n.a.
normal range	<60	<60	<60	<60	<60		<60	<60	<60	<60	<60	<90

Table S4. Extended Laboratory Parameters of Patients 3 and 4 with DOCK11 Deficiency											
Age	Patient 3				Patient 4						
	1y4m	3y4m	3y5m	3y6m	4y1m	2y0m	2y1m	2y2m	3y2m	4y2m	6y
Autoantibodies tested	<p>Nuclear antibodies (ANA), neutrophil cytoplasmic antibodies (ANCA), double stranded DNA (dsDNA) antibodies, endomysial antibodies (EMA), tissue transglutaminase antibodies (tTG), glomerular basement membrane antibodies, thyroglobulin antibodies, thyroid peroxidase antibodies, centromere antibodies, mitochondrial, anti-LKM antibodies, smooth muscle antibodies, myeloperoxidase (MPO) antibodies, proteinase 3 antibodies: all negative or within reference range.</p>				<p>Insulin antibodies, glutamic acid decarboxylase 65-kilodalton isoform (GAD65) antibodies, tyrosine phosphatase-like protein insulinoma antigen 2 (IA2) antibodies, nuclear antibodies (ANA), double stranded DNA (dsDNA) antibodies, Smith (Sm) antibodies, nRNP antibody, Ro/SSA antibodies, LA/SSB antibodies, Scl-70 antibodies, Jo-1 antibodies, histone antibodies, nucleosome antibodies, centromere antibodies, ribosomal P antibodies, rheumatoid factor isotype IgG, IgA and IgM antibodies, Mi-2 antibodies, PM-Scl antibodies, Ku antibodies, PL-7 antibodies, PL-12 antibodies, smooth muscle antibodies, Actin antibodies, LKM1 antibodies, soluble liver antigen (SLA) antibodies, liver cytosol type 1 (LC1) antibodies, glycoprotein (gp) 210 antibodies, spot pattern (SP) antibodies, mitochondrial antibodies, mitochondrial M2 antibodies, thyroglobulin antibodies, thyroid peroxidase antibodies, neutrophil cytoplasmic antibodies (ANCA), proteinase 3 antibodies, myeloperoxidase (MPO) antibodies, cardiolipin antibodies (IgG, IgA, IgM), beta-2 glycoprotein 1 antibodies (IgA, IgM), deamidated gliadin antibodies (IgA, IgG), tissue transglutaminase antibodies (IgA, IgG), parietal cell antibodies, intrinsic factor antibodies, <i>Saccharomyces cerevisiae</i> antibodies (IgA, IgG), heart muscle antibodies, skeletal muscle antibodies, adrenal cortex antibodies.</p>						

Table S4. Extended Laboratory Parameters of Patients 3 and 4 with DOCK11 Deficiency

Analysis of absolute cell counts in peripheral blood and additional diagnostic markers. The data were collected and analyzed at the Virgen del Rocío University Children Hospital, Seville, the Children Hospital Sant Joan de Déu, Barcelona, Spain and the Radboud University Medical Center, Nijmegen, the Netherlands. Reference values are taken from ref.^{34,35} or internal healthy donor cohorts. WBC whole blood cell count, ALC absolute lymphocyte count, ANC absolute neutrophil count, AMC absolute monocyte count, ATC absolute thrombocyte count, MPV mean platelet volume, RBC red blood cell count, Hb hemoglobin, HCT hematocrit, MCV mean corpuscular volume, MCH mean corpuscular hemoglobin, RDW-CV red cell distribution width - coefficient of variation, ESR erythrocyte sedimentation rate, CRP C-reactive protein, LDH lactate dehydrogenase, n.a. not available.

Table S5. Immunological Characteristics of Patients with *DOCK11* Mutations

Age	Patient 1			Patient 2			Patient 3			Patient 4			Reference range		
	7m	2.5y	3y	3.5y	2.9y	3y	4y	4y	5y	5y	2y2m	6y10m	0-1y	2-3y	4-5y
CD4+ T cells (μ L)	4004	1045	n.a.	n.a.	n.a.	1751	6981	2064	n.a.	n.a.	2380	n.a.	1300-7000	500-2700	500-2700
CD8+ T cells (μ L)	1729	341	n.a.	n.a.	n.a.	1085	928	632	n.a.	n.a.	1640	n.a.	400-4100	200-1800	200-1800
CD19+ B cells (μ L)	1729	377	n.a.	n.a.	n.a.	728	1403	620	n.a.	n.a.	1010	n.a.	549-1225	670-1619	402-784
CD16+CD56+NK cells (μ L)	1001	3256	n.a.	n.a.	n.a.	n.a.	457	740	n.a.	n.a.	n.a.	n.a.	150-1330	150-810	180-510
NK-T cells (CD3+CD56+) (μ L)	n.a.	n.a.	n.a.	n.a.	n.a.	n.a.	n.a.	n.a.	n.a.	n.a.	690	n.a.	80-300	80-300	80-300
CD4+T cells (%) [†]	n.a.	57.8	44.1	63.9	63.9	39.45	81	55.1	67	43.0	58.0	64.8	25-86	25-66	25-66
CD8+T cells (%) [†]	n.a.	24.8	38.0	33.1	33.1	24.45	11.9	27.3	24.3	39.2	40.0	21.5	7-58	9-49	9-49
CD16+CD56+ NK cells (% of CD3-)	n.a.	21.3	7.71	24.4	24.4	n.a.	17.4	7.1	26.2	38.5	n.a.	1.98	3-24	5-23	6-21
CD3+ TCRab (%)	n.a.	50.5	88.2	97	97	n.a.	90.2	94.2	38.9	73.7	n.a.	86.5	46-88	31-100	31-100
CD3+ TCRgd (%)	n.a.	6.36	1.32	1.17	1.17	n.a.	2.99	5.7	7.98	11.7	n.a.	6.23	1-10	0.92-38	0.92-38
DN (CD3+CD4-CD8- TCRab+) T cells (%) [†]	n.a.	1.13	8.77	1.15	1.15	n.a.	1.06	n.a.	0.17	0.54	38	3.86	0.42-2	1-7	1-7
CD4 Naïve (CD45RA+CCR7+)	n.a.	49.9	64.8	78.2	78.2	n.a.	69.7	55	70.2	77.5	71	56.1	77-96	52-92	52-92
CD4 CM (CD45RA-CCR7+) (%)	n.a.	26.6	7.77	12.1	12.1	n.a.	16.1	20.5	17.5	9.61	10.8	24.2	7-22	15-56	15-56
CD4 EM (CD45RA-CRR7-) (%)	n.a.	17.0	6.74	7.28	7.28	n.a.	8.85	22.1	11.1	9.8	0.11	14.5	0.01-4	0.26-9	0.26-9
CD8 Naïve (CD45RA+CCR7+)	n.a.	55.7	77.8	94.8	94.8	n.a.	74.4	47	43.6	34.9	37.89	16.0	16-100	19-100	19-100
CD8 CM (CD45RA-CRR7+) (%)	n.a.	7.35	2.82	1.0	1.0	n.a.	4.93	4	11.3	15.7	2.75	1.15	2-6	1-9	1-9
CD8 EM (CD45RA-CRR7-) (%)	n.a.	15.6	4.87	1.18	1.18	n.a.	6.31	17.9	25	34.7	0.24	10.4	1-100	10-55	10-55
CD8 TEMRA (CD45RA+CCR7-) (%)	n.a.	21.3	14.5	3.03	3.03	n.a.	14.4	31.1	20.2	14.8	13.1	72.4	4-92	6-83	6-83
Tregs (CD4+CD25 ^{high} CD127-) (% of CD4+)	n.a.	5.86	4.2	n.a.	n.a.	n.a.	n.a.	6	n.a.	3.09	1.03	10.3	6-10	3-17	3-17
CD19+ B cells (%) [‡]	n.a.	16.1	6.15	3.09	3.09	14.97	15.6	5.4	22	11.3	18.8	9.34	10.2-18.5	16.5-25.8	13.4-21.1

Table S5. Immunological Characteristics of Patients with <i>DOCK11</i> Mutations															
Age	Patient 1			Patient 2			Patient 3			Patient 4		Reference range			
	7m	2.5y	3y	3.5y	2.9y	3y	4y	4y	5y	5y	6y10m	2y2m	0-1y	2-3y	4-5y
Naïve B cells (IgD+CD27-) (%)*	n.a.		88.1	83.3	79.7	91.24	76.8	78.9	67.7	83.3	69.14	51.9	90.9-96.2	83.4-90.1	76.3-84.9
Switched-memory (IgD-CD27+) (%)*	n.a.		0.16	0.0	9.24	3.4	10.9	11.7	10.8	6.85	6.51	15.3	0.1-1.9	1.5-4.1	3.3-7.4
Marginal (IgD+CD27+) (%)*	n.a.		1.9	0.75	3.15	2.65	5.4	4.5	13.5	2.72	4.72	9.43	1.6-4.1	4.1-6.9	4.1-9
Transitional (IgM+CD38+) (%)*	n.a.		11.7	10.3	16.6	14.45	5.69	1.3	0.21	8.08	0.13	0.94	7.2-20	3.1-12	3.1-12
Plasmablasts (IgM-CD38 ^{high}) (%)*	n.a.		2.43	2.05	0.29	0.21	2.38	4.2	0.56	0.31	2.27	3.97	0.2-4	0.6-4	0.6-4
Plasmablasts (CD27 ^{high} CD38 ^{high}) (%)*	n.a.		0.37	0.11	0.59	n.a.	0.62	n.a.	1.36	0.18	n.a.	3.85	0.1-4	0.1-4	0.1-4
CD21 ^{low} CD38 ^{low} B cells (%)*	n.a.		7.57	10.7	7.57	n.a.	4.0	7.3	6.92	3.42	2.33	10.3	0.3-4	1.8-3.6	1.8-5.2

Table S5. Immunological Characteristics of Patients with *DOCK11* Mutations

Assessment of patient-derived peripheral blood lymphocyte subsets by flow cytometry was performed at the indicated time points. Age-specific reference values were taken from public reference sets or internal healthy cohorts.³⁶⁻³⁸ Bold indicates values outside of the normal range. n.a. not available, † percentage of CD3+ lymphocytes. ‡ percentage of lymphocytes, * percentage of CD3-CD19+ B lymphocytes.

Gene	HGNC_ID	Chr	Genomic position (hg19)	REF/ALT	cDNA change	Amino acid change	GnomAD Allele frequency	CADD
<i>CFTR</i>	1884	7	117251664	A/G	ENST0000003084.6: c.3169A →G	p.Thr1057Ala	0.00003192	17.74

Table S6. Hemizygous/Homozygous Variants in Known IUIS Genes Identified by Trio Whole-Exome Sequencing in Patient 1

Pre-filtered for homo-/hemizygous variants in genes in the International Union of Immunological Societies (IUIS) classification 2022.³⁹ MAF GnomAD : <0.01, non-synonymous, within coding regions (+/- 8 bp), sorted by CADD score, GnomAD homo-/hemizygous counts: ≤5. The variant in *CFTR* was not considered pathogenic, because the clinical phenotype of the patient was not consistent with cystic fibrosis. Typical characteristics of cystic fibrosis, including chronic sinopulmonary disease, pancreatic insufficiency or chronic hepatic disease, were not reported in this patient.⁴⁰ The *CFTR* variant is listed in ClinVar as uncertain significance (Variation ID: 53668) and is absent in the CFTR2 database (<http://cftr2.org>) and the UMD-CFTR database.⁴¹ HGNC_ID HUGO Gene Nomenclature Committee identifier, Chr. Chromosome, REF/ALT Reference and alternative allele, respectively, CADD Combined Annotation Dependent Depletion.

Table S7. Heterozygous Variants in Known IUIS Genes Identified by Trio Whole-Exome Sequencing in Patient 1								
Gene	HGNC_ID	Chr	Genomic position (hg19)	REF/ALT	cDNA change	Amino acid change	GnomAD Allele frequency	CADD
<i>LIG1</i>	6598	19	48639012	G/C	ENST00000263274.7: c.1448C→G	p.Ala483Gly	n.a.	24
<i>KMT2D</i>	7133	12	49434493	G/A	ENST00000301067.7: c.7060C→T	p.Pro2354Ser	0.00004033	9.807
<i>CLCN7</i>	2025	16	1496726	A/G	ENST00000262318.8: c.2261-8T→C	n.a.	0.0000378	1.225
<i>COPG1</i>	2236	3	128976658	A/C	ENST00000314797.6: c.826A→C	p.Asn276His	n.a.	0.076

Table S7. Heterozygous Variants in Known IUIS Genes Identified by Trio Whole-Exome Sequencing in Patient 1

Pre-filtered for heterozygous variants in genes in the International Union of Immunological Societies (IUIS) classification 2022.³⁹ In **bold**, those inherited autosomal dominant. MAF GnomAD : <0.01, non-synonymous, within coding regions (+/- 8 bp), sorted by CADD score, GnomAD AC: ≤20. The variants in *LIG1*, *CLCN7* and *COPG1* were not considered pathogenic, because of the autosomal recessive mode of inheritance of the corresponding diseases. The variant in *KMT2D* was not considered pathogenic, because the patient did not display any characteristic features of Kabuki Syndrome, known to be caused by pathogenic mutations in *KMT2D*.⁴²⁻⁴⁴ Notably, a more stringent filtering for variants with CADD score >15 would have filtered out the variants in *KMT2D*, *CLCN7* and *COPG1*, respectively. HGNC_ID HUGO Gene Nomenclature Committee identifier, Chr. Chromosome, REF/ALT Reference and alternative allele, respectively, CADD Combined Annotation Dependent Depletion, n.a. not available.

Table S8. Hemizygous/Homozygous Variants in Known IUIS Genes Identified by Trio Whole-Exome Sequencing in Patient 3								
Gene	HGNC_ID	Chr	Genomic position (hg19)	REF/ALT	cDNA change	Amino acid change	GnomAD Allele frequency	CADD
<i>INO80</i>	26956	15	41277615	C/T	ENST00000361937.3: c.3842G→A	p.Arg1281Gln	0.001161 (2 hom)	26.5

Table S8. Hemizygous/Homozygous Variants in Known IUIS Genes Identified by Trio Whole-Exome Sequencing in Patient 3

Pre-filtered for homo-/hemizygous variants in genes in the International Union of Immunological Societies (IUIS) classification 2022.³⁹ MAF GnomAD : <0.01, non-synonymous, within coding regions (+/- 8 bp), sorted by Combined Annotation Dependent Depletion (CADD) score, GnomAD homo-/hemizygous counts: ≤5. The *INO80* variant was not considered pathogenic because of the strongly disparate clinical phenotype seen in the patient in this study, and because the characteristic features described for *INO80*-mutant patients including decreased frequencies of class-switched B cells were not observed in our index patient.⁴⁵ In Clinvar (Variation ID: 719735) this variant has been annotated as uncertain significance and likely benign. HGNC_ID HUGO Gene Nomenclature Committee identifier, Chr. Chromosome, REF/ALT Reference and alternative allele, respectively.

Table S9. Heterozygous Variants in Known IUIS Genes Identified by Trio Whole-Exome Sequencing in Patient 3									
Gene	HGNC_ID	Chr	Genomic position (hg19)	REF/ALT	cDNA change	Amino acid change	GnomAD Allele frequency	CADD	
<i>CFTR</i>	1884	7	117267591	C/T	ENST0000003084.6: c.3484C→T	p.Arg1162Ter	0.00005298	40	
<i>POLE</i>	9177	12	133226040	C/T	ENST00000320574.5: c.3857G→A	p.Arg1286His	0.00005469	32	
<i>KMT2D</i>	7133	12	49431112	G/C	ENST00000301067.7: c.10027C→G	p.Leu3343Val	n.a.	19.7	
<i>SAMHD1</i>	15925	20	35539668	C/T	ENST00000262878.4: c.1223G→A	p.Arg408His	0.000008137	1.295	
<i>NCF2</i>	7661	1	183543616	G/T	ENST00000367535.3: c.501+6C→A	n.a.	n.a.	0.382	

Table S9. Heterozygous Variants in Known IUIS Genes Identified by Trio Whole-Exome Sequencing in Patient 3

Pre-filtered for heterozygous variants in genes in the International Union of Immunological Societies (IUIS) classification 2022.³⁹ In **bold**, those inherited autosomal dominant. MAF GnomAD : <0.01, non-synonymous, within coding regions (+/- 8 bp), sorted by CADD score, GnomAD AC: ≤20. The variants in *CFTR*, *POLE*, *SAMHD1* and *NCF2* were not considered pathogenic, because of the autosomal recessive mode of inheritance of the corresponding diseases. The variant in *KMT2D* was not considered pathogenic, because the patient did not display any characteristic features of Kabuki Syndrome, known to be caused by pathogenic mutations in *KMT2D*.⁴²⁻⁴⁴ A more stringent filtering for variants with CADD score >15 would have filtered out the variants in *SAMHD1* and *NCF2*, respectively. HGNC_ID HUGO Gene Nomenclature Committee identifier, CHR Chromosome, POS Position in the chromosome (b37 assembly), REF Reference allele, ALT Alternative allele, gnomadAD_AF Minor allele frequency in GnomAD, nomadAD_AC Total allele counts in GnomAD, CADD Combined Annotation Dependent Depletion, n.a. not available.

Table S10. Heterozygous Variants in Known IUIS Genes Identified by Trio Whole-Exome Sequencing in Patient 4								
Gene	HGNC_ID	Chr	Genomic position (hg19)	REF/ALT	cDNA change	Amino acid change	GnomAD Allele frequency	CADD
<i>PIK3CG</i>	8978	7	106509167	T/A	ENST00000359195.3_1.1: c.1160T→A	p.Ile387Asn	n.a.	28.2
<i>KMT2D</i>	7133	12	49436060	G/A	ENST00000301067.11_2.1: c.5921C→T	p.Thr1974Met	0.00006589	27
<i>PLEKHM1</i>	19017	17	43531075	T/C	ENST00000430334.8_3.1: c.2143A→G	p.Ile715Val	0.00004001	0.039

Table S10. Heterozygous Variants in Known IUIS Genes Identified by Trio Whole-Exome Sequencing in Patient 4

Pre-filtered for heterozygous variants in genes in the International Union of Immunological Societies (IUIS) classification 2022.³⁹ In **bold**, those inherited autosomal dominant. MAF GnomAD : <0.01, non-synonymous, within coding regions (+/- 8 bp), sorted by CADD score, GnomAD AC: ≤20. The variants in *PIK3CG* and *PLEKHM1* were not considered pathogenic, because known disease-causing variants in these genes are inherited autosomal recessive. The variant in *KMT2D* was not considered pathogenic, because the patient did not display any characteristic features of Kabuki Syndrome, known to be caused by pathogenic mutations in *KMT2D*.⁴²⁻⁴⁴ A more stringent filtering for variants with CADD score >15 would have filtered out the variants in *PLEKHM1*. No hemizygous or homozygous variants in known IUIS genes were left after filtering. HGNC_ID HUGO Gene Nomenclature Committee identifier, CHR Chromosome, POS Position in the chromosome (b37 assembly), REF Reference allele, ALT Alternative allele, gnomadAD_AF Minor allele frequency in GnomAD, gnomadAD_AC Total allele counts in GnomAD, CADD Combined Annotation Dependent Depletion, n.a. not available.

Table S11. Hemizygous and Homozygous Variants Identified by Trio Whole-Exome Sequencing in Patient 1								
Gene	HGNC_ID	Chr	Genomic position (hg19)	REF/ALT	cDNA change	Amino acid change	GnomAD Allele frequency	CADD
Immune-related genes								
<i>DOCK11</i>	23483	X	117630009	-/T	ENST00000276202.7: c.75dup	p.Glu26Ter	n.a.	27.5
<i>CACNA1C</i>	1390	12	2706439	T/C	ENST00000347598.4: c.2837T→C	p.Ile946Thr	0.00002808	23.3
<i>KLRC4</i>	6377	12	10560364	T/G	ENST00000309384.1: c.365A→C	p.Glu122Ala	n.a.	22.5
<i>AC01</i>	1117	9	32450041	G/A	ENST00000309951.6: c.2602G→A	p.Asp868Asn	0.00003977	21.7
<i>SBN02</i>	29158	19	1119060	TCTC/T	ENST00000361757.3: c.1474_1476del	p.Glu492del	n.a.	21.3
<i>CFTR</i>	1884	7	117251664	A/G	ENST00000003084.6: c.3169A→G	p.Thr1057Ala	0.00003192	17.74
Non-Immune-related genes								
<i>TAF9B</i>	17306	X	77395075	C/G	ENST00000341864.5: c.34G→C	p.Ala12Pro	n.a.	33
<i>CDI63</i>	1631	12	7649556	G/A	ENST00000359156.4: c.952C→T	p.Arg318Ter	0.00000797	28.7
<i>DRP2</i>	3032	X	100493992	C/T	ENST00000395209.3: c.461C→T	p.Ser154Phe	n.a.	28.6
<i>ZNF862</i>	34519	7	149541750	C/T	ENST00000223210.4: c.61C→T	p.Leu21Phe	n.a.	27.6
<i>ARHGEF18</i>	17090	19	7516120	T/C	ENST00000359920.6: c.1259T→C	p.Val420Ala	n.a.	25.5
<i>ZNF556</i>	25669	19	2877887	G/A	ENST00000307635.2: c.931G→A	p.Gly311Arg	0.00001989	24.7
<i>VCP</i>	12666	9	35061053	C/T	ENST00000358901.6: c.1318G→A	p.Glu440Lys	n.a.	23.9
<i>C19orf26</i>	28617	19	1233443	C/T	ENST00000382477.2: c.1021G→A	p.Ala341Thr	n.a.	22.5

Table S11. Hemizygous and Homozygous Variants Identified by Trio Whole-Exome Sequencing in Patient 1

Variants with MAF < 0.01 and which were not excluded by segregation analysis are listed. Variants were prioritized due to absent/low expression of the encoded proteins in immune cells (*CACNA1C*, *AC01*, *SBN02*) or low/absent expression in B cells, CD4+ T cells and erythroid cells (*KLRC4*). The variant in *CFTR* was not considered pathogenic, because the patient's clinical phenotype was not consistent with cystic fibrosis. Typical characteristics of cystic fibrosis (chronic sinopulmonary disease, pancreatic insufficiency, chronic hepatic disease) were not reported.⁴⁰ The *CFTR* variant is listed in ClinVar as uncertain significance (Variation ID: 53668) and is absent in CFTR2 (<http://cftr2.org>) and UMD-CFTR databases.⁴¹ HGNC_ID HUGO Gene Nomenclature Committee identifier, Chr. Chromosome, REF/ALT Reference and alternative allele, respectively, CADD Combined Annotation Dependent Depletion, n.a. not available.

Table S12. Hemizygous and Homozygous Variants Identified by Trio Whole-Exome Sequencing in Patient 2								
Gene	HGNC_ID	Chr	Genomic position (hg19)	REF/ALT	cDNA change	Amino acid change	GnomAD Allele frequency	CADD
Immune-related genes								
<i>DOCK11</i>	23483	X	117718825	G/A	ENST00000276202.7: c.1718+5G→A	p.Pro533_Lys573del	n.a.	16.35
Non-Immune-related genes								
<i>NHS</i>	7820	X	17743947	A/C	ENST00000676302.1: c.1721A→C	p.His574Pro	n.a.	16.42

Table S12. Hemizygous and Homozygous Variants Identified by Trio Whole-Exome Sequencing in Patient 2

No other rare (MAF <0.01) homozygous variants were identified. Variants with MAF < 0.001 and which were not excluded by segregation analysis are listed. HGNC_ID HUGO Gene Nomenclature Committee identifier, Chr. Chromosome, REF/ALT Reference and alternative allele, respectively, CADD Combined Annotation Dependent Depletion, n.a. not available.

Table S13. Hemizygous and Homozygous Variants Identified by Trio Whole-Exome Sequencing in Patient 3								
Gene	HGNC_ID	Chr	Genomic position (hg19)	REF/ALT	cDNA change	Amino acid change	GnomAD Allele frequency	CADD
Immune-related genes								
<i>INO80</i>	26956	15	41277615	C/T	ENST00000361937.3: c.3842G→A	p.Arg1281Gln	0.001163 (2 hom)	29.70
<i>DOCK11</i>	23483	X	117805029	G/C	ENST00000276202.7: c.5120G→C	p.Trp1707Ser	n.a.	25.60
Non-Immune-related genes								
<i>TMEM237</i>	14432	2	202496888	C/T	ENST00000409883.2: c.439G→A	p.Val147Ile	0.0001828	23.4
<i>ZNF549</i>	26632	19	58049931	A/G	ENST00000376233.3: c.1559A→G	p.Gln520Arg	0.0003006	23.2
<i>AOXI</i>	553	2	201503018	A/G	ENST00000374700.2: c.2561A→G	p.Lys854Arg	0.001227	20.8
<i>DNAJC17</i>	25556	15	41066554	C/T	ENST00000220496.4: c.681G→A	p.Ala227Ala	0.00002844	15.46

Table S13. Hemizygous and Homozygous Variants Identified by Whole-Exome Sequencing in Patient 3

Variants with $MAF < 0.01$ and which were not excluded by segregation analysis are listed. The *INO80* variant was not considered pathogenic because of the strongly disparate clinical phenotype seen in the patient in this study, and because the characteristic features described for *INO80*-mutant patients including decreased frequencies of class-switched B cells were not observed in our index patient.⁴⁵ In Clinvar (Variation ID: 719735) this variant has been annotated as uncertain significance and likely benign. HGNC_ID HUGO Gene Nomenclature Committee identifier, Chr. Chromosome, REF/ALT Reference and alternative allele, respectively, CADD Combined Annotation Dependent Depletion, n.a. not available.

Table S14. Hemizygous and Homozygous Variants Identified by Trio Whole-Exome Sequencing in Patient 4								
Gene	HGNC_ID	Chr	Genomic position (hg19)	REF/ALT	cDNA change	Amino acid change	GnomAD Allele frequency	CADD
Immune-related genes								
<i>DOCK11</i>	23483	X	117677487	A/G	ENST00000276202.7: c.323A→G	p.Tyr108Cys	0.00001091	25

Table S14. Hemizygous and Homozygous Variants Identified by Whole-Exome Sequencing in Patient 4

No other rare (MAF <0.01) homozygous variants were identified. HGNC_ID HUGO Gene Nomenclature Committee identifier, Chr. Chromosome, REF/ALT Reference and alternative allele, respectively, CADD Combined Annotation Dependent Depletion.

Table S15. Evaluation of the Detected Variants in <i>DOCK11</i>	
<i>DOCK11</i> conservation evaluation	
Performed test	Score
CCDS Size (including canonical splice) (NM_144658.4)	6222
Number of unique protein-coding variants (gnomAD)	519 Missense, 20 pLoF
RVIS (Residual Variation Intolerance Score) ⁴⁶ Version 2 of <i>DOCK11</i>	-0.08 (47.26 % most intolerant)
LOEUF “loss-of-function observed/expected upper bound fraction” Score (gnomAD v2.1.1)	0.37
Haploinsufficiency Score (HI index) (DECIPHER) ⁴⁷	15.34% most intolerant
Expected SNVs pLOF (gnomAD)	78
Observed SNVs pLOF (gnomAD)	20
Mutation significance cutoff (MSC) for CADD¹⁹	
Mutation significance cutoff (MSC)	Confidence Interval
3.313	99%
11.507	95%
21.702	90%
Evaluation of the detected variants in <i>DOCK11</i> in exome variant databases (last accessed January 2023)	
Source	Found
125,748 exomes and 15,708 genomes from the Genome Aggregation Database (gnomAD v2.1.1) ¹⁵	no, except ENST00000276202.7:c.323A→G
14,559 individuals sequenced in NHLBI’s TOPMed program (Bravo) ⁴⁸	no
6,503 Exomes from NHLBI Exome Sequencing Project ⁴⁹	no
In-house collection of >1200 individuals (1058 exomes and 780 targeted enrichment screens)	no

Table S15. Evaluation of the Detected Variants in *DOCK11*

The *DOCK11* gene has a negative residual variation intolerance score, indicative of *DOCK11* being intolerant to genetic variation in the human population. The number of 'observed' nonsense variants in *DOCK11* was significantly lower than the number of 'expected' nonsense variants. The variants in Patients 1 through 3 (ENST00000276202.7:c.75dup, p.Glu26Ter; ENST00000276202.7:c.1718+5G→A, p.Pro533_Lys573del; ENST00000276202.7:c.5120G→C p.Trp1707Ser) are absent from public databases including GnomAD and BRAVO,^{15,48} and have not been previously reported. The *DOCK11* variant in Patient 4 (ENST00000276202.7:c.323A→G p.Tyr108Cys) is present in GnomAD at a very rare allelic frequency (0.00001091), with two other hemizygotes observed (last accession date 01/16/2023).

Supplementary Videos

Video S1. T-cell Migration in a 5 dpf Control Zebrafish Embryo

Representative time-lapse confocal microscopy movie showing the migration of fluorescently labeled T cells in the region around the thymus (anterior region) in a 5 days postfertilization (dpf) control *lck:nlsmCherry* transgenic zebrafish embryo. Lines correspond to the trajectories of the movement over time of Lck-positive T-cell progenitors.

<https://doi.org/10.5281/zenodo.8014043>

Video S2. T-cell Migration in a 5 dpf *dock11*-Knockout Zebrafish Embryo

Representative time-lapse confocal microscopy movie showing the migration of fluorescently labeled T cells in the region around the thymus (anterior region) in a 5 days postfertilization (dpf) *dock11*-knockout *lck:nlsmCherry* transgenic zebrafish embryo. Lines correspond to the trajectories of the movement over time of Lck-positive T-cell progenitors.

<https://doi.org/10.5281/zenodo.8014195>

Video S3. Blood Circulation in a 48 hpf Control Zebrafish Embryo

Representative time-lapse confocal microscopy movie showing the posterior region of a 48 hours postfertilization (hpf) control *fli1:GFP;gata1a:dsRed* double transgenic. Endothelial cells from the vasculature system are visualized in green, while blood cells are shown in red.

<https://doi.org/10.5281/zenodo.8014206>

Video S4. Blood Circulation in a 48 hpf *dock11*-Knockout Zebrafish Embryo

Representative time-lapse confocal microscopy movie showing the posterior region of a 48 hours postfertilization (hpf) *dock11*-knockout *fli1:GFP;gata1a:dsRed* double transgenic. Endothelial cells from the vasculature system are visualized in green, while blood cells are shown in red. White arrow points toward the accumulation of intravascular blood.

<https://doi.org/10.5281/zenodo.8014219>

Video S5. Dynamics of the Blood Circulation in 54 hpf Control Zebrafish Embryos

Representative confocal time lapses of the trunk region of a 54 hours postfertilization (hpf) control *fli1:GFP;gata1a:dsRed* double transgenic. Endothelial cells from the intersegmental vessels are visualized in green, while blood cells are shown in red.

<https://doi.org/10.5281/zenodo.8014225>

Video S6. Dynamics of the Blood Circulation in 54 hpf *dock11*-Knockout Zebrafish Embryos

Representative confocal time lapses of the trunk region of a 54 hours postfertilization (hpf) *dock11*-knockout *fli1:GFP;gata1a:dsRed* double transgenic. Endothelial cells from the intersegmental vessels are visualized in green, while blood cells are shown in red.

<https://doi.org/10.5281/zenodo.8014235>

Supplementary References

1. Buske OJ, Girdea M, Dumitriu S, et al. PhenomeCentral: a portal for phenotypic and genotypic matchmaking of patients with rare genetic diseases. *Hum Mutat* 2015;36(10):931-40. [PMID: 26251998]
2. Matsuda T, Yanase S, Takaoka A, Maruyama M. The immunosenescence-related gene *Zizimin2* is associated with early bone marrow B cell development and marginal zone B cell formation. *Immun Ageing* 2015;12:1. [PMID: 25729399]
3. Kimmel CB, Ballard WW, Kimmel SR, Ullmann B, Schilling TF. Stages of embryonic development of the zebrafish. *Dev Dyn* 1995;203(3):253-310. [PMID: 8589427]
4. Traver D, Paw BH, Poss KD, Penberthy WT, Lin S, Zon LI. Transplantation and in vivo imaging of multilineage engraftment in zebrafish bloodless mutants. *Nat Immunol* 2003;4(12):1238-46. [PMID: 14608381]
5. Lawson ND, Weinstein BM. In vivo imaging of embryonic vascular development using transgenic zebrafish. *Dev Biol* 2002;248(2):307-18. [PMID: 12167406]
6. Ewels P, Magnusson M, Lundin S, Käller M. MultiQC: summarize analysis results for multiple tools and samples in a single report. *Bioinformatics* 2016;32(19):3047-8. [PMID: 27312411]
7. Babraham Bioinformatics - FastQC A Quality Control tool for High Throughput Sequence Data. (<https://www.bioinformatics.babraham.ac.uk/projects/fastqc/>).
8. Van der Auwera GA, Carneiro MO, Hartl C, et al. From FastQ data to high confidence variant calls: the Genome Analysis Toolkit best practices pipeline. *Curr Protoc Bioinformatics* 2013;43(1110):11.10.1-11.10.33. [PMID: 25431634]
9. Girisha KM, Kortüm F, Shah H, et al. A novel multiple joint dislocation syndrome associated with a homozygous nonsense variant in the *EXOC6B* gene. *Eur J Hum Genet* 2016;24(8):1206-10. [PMID: 26669664]
10. Kortüm F, Caputo V, Bauer CK, et al. Mutations in *KCNH1* and *ATP6V1B2* cause Zimmermann-Laband syndrome. *Nat Genet* 2015;47(6):661-7. [PMID: 25915598]
11. McKenna A, Hanna M, Banks E, et al. The Genome Analysis Toolkit: a MapReduce framework for analyzing next-generation DNA sequencing data. *Genome Res* 2010;20(9):1297-303. [PMID: 20644199]
12. Wang K, Li M, Hakonarson H. ANNOVAR: functional annotation of genetic variants from high-throughput sequencing data. *Nucleic Acids Res* 2010;38(16):e164. [PMID: 20601685]
13. Salzer E, Cagdas D, Hons M, et al. *RASGRP1* deficiency causes immunodeficiency with impaired cytoskeletal dynamics. *Nat Immunol* 2016;17(12):1352-1360. [PMID: 27776107]
14. Ozen A, Comrie WA, Ardy RC, et al. *CD55* Deficiency, Early-Onset Protein-Losing Enteropathy, and Thrombosis. *N Engl J Med* 2017;377(1):52-61. [PMID: 28657829]
15. Karczewski KJ, Francioli LC, Tiao G, et al. The mutational constraint spectrum quantified from variation in 141,456 humans. *Nature* 2020;581(7809):434-443. [PMID: 32461654]
16. Sherry ST, Ward MH, Kholodov M, et al. dbSNP: the NCBI database of genetic variation. *Nucleic Acids Res* 2001;29(1):308-11. [PMID: 11125122]

17. Lelieveld SH, Reijnders MR, Pfundt R, et al. Meta-analysis of 2,104 trios provides support for 10 new genes for intellectual disability. *Nat Neurosci* 2016;19(9):1194-6. [PMID: 27479843]
18. Li H, Durbin R. Fast and accurate long-read alignment with Burrows-Wheeler transform. *Bioinformatics* 2010;26(5):589-95. [PMID: 20080505]
19. Kircher M, Witten DM, Jain P, O'Roak BJ, Cooper GM, Shendure J. A general framework for estimating the relative pathogenicity of human genetic variants. *Nat Genet* 2014;46(3):310-5. [PMID: 24487276]
20. van Rahden VA, Rau I, Fuchs S, et al. Clinical spectrum of females with HCCS mutation: from no clinical signs to a neonatal lethal form of the microphthalmia with linear skin defects (MLS) syndrome. *Orphanet J Rare Dis* 2014;9:53. [PMID: 24735900]
21. Machado FB, Machado FB, Faria MA, et al. 5meCpG epigenetic marks neighboring a primate-conserved core promoter short tandem repeat indicate X-chromosome inactivation. *PLoS One* 2014;9(7):e103714. [PMID: 25078280]
22. Brinkman EK, Chen T, Amendola M, van Steensel B. Easy quantitative assessment of genome editing by sequence trace decomposition. *Nucleic Acids Res* 2014;42(22):e168. [PMID: 25300484]
23. Kroll F, Powell GT, Ghosh M, et al. A simple and effective F0 knockout method for rapid screening of behaviour and other complex phenotypes. *Elife* 2021;10 [PMID: 33416493]
24. Choi SY, Chacon-Heszele MF, Huang L, et al. Cdc42 deficiency causes ciliary abnormalities and cystic kidneys. *J Am Soc Nephrol* 2013;24(9):1435-50. [PMID: 23766535]
25. Hermanson GT. *Bioconjugate Techniques: Third Edition*. 2013.
26. Varadi M, Anyango S, Deshpande M, et al. AlphaFold Protein Structure Database: massively expanding the structural coverage of protein-sequence space with high-accuracy models. *Nucleic Acids Research* 2021;50(D1):D439-D444. [PMID: 33958199]
27. Jumper J, Evans R, Pritzel A, et al. Highly accurate protein structure prediction with AlphaFold. *Nature* 2021;596(7873):583-589. [PMID: 34265844]
28. Pellegrin S, Mellor H. Rho GTPase Activation Assays. *Current Protocols in Cell Biology* 2008;38(1):14.8.1-14.8.19. [PMID: 18422222]
29. Schindelin J, Arganda-Carreras I, Frise E, et al. Fiji: an open-source platform for biological-image analysis. *Nat Methods* 2012;9(7):676-82. [PMID: 22743772]
30. Carpenter AE, Jones TR, Lamprecht MR, et al. CellProfiler: image analysis software for identifying and quantifying cell phenotypes. *Genome Biol* 2006;7(10):R100. [PMID: 17076895]
31. Salzer E, Zoghi S, Kiss MG, et al. The cytoskeletal regulator HEM1 governs B cell development and prevents autoimmunity. *Sci Immunol* 2020;5(49) [PMID: 32646852]
32. Schoppmeyer R, van Buul JD. Protocol to analyze transmigration of human cytotoxic T cells under physiological flow conditions in vitro. *STAR Protoc* 2022;3(3):101509. [PMID: 35776649]
33. Hess I, Boehm T. Intravital imaging of thymopoiesis reveals dynamic lympho-epithelial interactions. *Immunity* 2012;36(2):298-309. [PMID: 22342843]
34. Andropoulos DB. Appendix B: Pediatric Normal Laboratory Values. *Gregory's Pediatric Anesthesia* 2012:1300-1314.

35. Pediatric Reference Ranges. (https://www.healthcare.uiowa.edu/path_handbook/appendix/heme/pediatric_normals.html).
36. Garcia-Prat M, Álvarez-Sierra D, Aguiló-Cucurull A, et al. Extended immunophenotyping reference values in a healthy pediatric population. *Cytometry B Clin Cytom* 2019;96(3):223-233. [PMID: 30334372]
37. Schatorjé EJ, Gemen EF, Driessen GJ, Leuvenink J, van Hout RW, de Vries E. Paediatric reference values for the peripheral T cell compartment. *Scand J Immunol* 2012;75(4):436-44. [PMID: 22420532]
38. Morbach H, Eichhorn EM, Liese JG, Girschick HJ. Reference values for B cell subpopulations from infancy to adulthood. *Clin Exp Immunol* 2010;162(2):271-9. [PMID: 20854328]
39. Bousfiha A, Moundir A, Tangye SG, et al. The 2022 Update of IUIS Phenotypical Classification for Human Inborn Errors of Immunity. *J Clin Immunol* 2022;42(7):1508-1520. [PMID: 36198931]
40. Farrell PM, Rosenstein BJ, White TB, et al. Guidelines for diagnosis of cystic fibrosis in newborns through older adults: Cystic Fibrosis Foundation consensus report. *J Pediatr* 2008;153(2):S4-s14. [PMID: 18639722]
41. Bareil C, Thèze C, Bérout C, et al. UMD-CFTR: a database dedicated to CF and CFTR-related disorders. *Hum Mutat* 2010;31(9):1011-9. [PMID: 20607857]
42. Bögershausen N, Gatinois V, Riehmer V, et al. Mutation Update for Kabuki Syndrome Genes KMT2D and KDM6A and Further Delineation of X-Linked Kabuki Syndrome Subtype 2. *Hum Mutat* 2016;37(9):847-64. [PMID: 27302555]
43. Miyake N, Koshimizu E, Okamoto N, et al. MLL2 and KDM6A mutations in patients with Kabuki syndrome. *Am J Med Genet A* 2013;161a(9):2234-43. [PMID: 23913813]
44. Ng SB, Bigham AW, Buckingham KJ, et al. Exome sequencing identifies MLL2 mutations as a cause of Kabuki syndrome. *Nat Genet* 2010;42(9):790-3. [PMID: 20711175]
45. Kracker S, Di Virgilio M, Schwartzenruber J, et al. An inherited immunoglobulin class-switch recombination deficiency associated with a defect in the INO80 chromatin remodeling complex. *J Allergy Clin Immunol* 2015;135(4):998-1007.e6. [PMID: 25312759]
46. Petrovski S, Wang Q, Heinzen EL, Allen AS, Goldstein DB. Genic intolerance to functional variation and the interpretation of personal genomes. *PLoS Genet* 2013;9(8):e1003709. [PMID: 23990802]
47. Firth HV, Richards SM, Bevan AP, et al. DECIPHER: Database of Chromosomal Imbalance and Phenotype in Humans Using Ensembl Resources. *Am J Hum Genet* 2009;84(4):524-33. [PMID: 19344873]
48. Bravo. (<https://bravo.sph.umich.edu/freeze3a/hg19/>).
49. Exome Variant Server. (<https://evs.gs.washington.edu/EVS/>).

3. DISCUSSION

3.1 General Discussion

3.1.1 Study of IELs to dissect the role of actin regulators in immune cells

Defects in actin-regulatory proteins, underlying distinct inborn errors of immunity, have highlighted the role of actin dynamics in immune-cell function. Actin-related IELs comprise a group of clinically heterogeneous disorders that on a cellular level result in varying abnormalities of cell shape and cell function. The distinct molecular pathomechanisms underlying these so-called actinopathies may be explained by differences in subcellular localization, interaction partners, as well as cell type-specific expression (Dupré & Prunier, 2023; Moulding et al., 2013; Sprenkeler et al., 2021; Tangye et al., 2019).

RHO GTPases are key upstream regulators that orchestrate a plethora of effector molecules involved in remodeling the actin cytoskeleton. Moreover, numerous GEF, GAP and GDI proteins exist, which regulate the activity of these RHO GTPases in a cell type- and stimulus-dependent manner (Cherfils & Zeghouf, 2013; DerMardirossian & Bokoch, 2005; Etienne-Manneville & Hall, 2002; Gray et al., 2020).

Defects in the RHO GTPases RHOH, RAC2 and CDC42 have been shown to underly distinct immunodeficiencies with manifestations such as increased infection susceptibility, immune dysfunction and in the case of CDC42 also systemic features, including intellectual delay, growth retardation and facial dysmorphism (Crequer et al., 2012; Gernez et al., 2019; He et al., 2020; Hsu et al., 2019; Lam et al., 2019; Lougaris et al., 2019; Martinelli et al., 2018; Sharapova et al., 2019; Su & Orange, 2020; Szczawinska-Poplonyk et al., 2020; Takenouchi et al., 2015).

Additionally, prior to this publication, pathogenic mutations in the guanine nucleotide exchange factors *ARHGEF1* (encoding for RhoGEF1), *DEF6*, and in the two DOCK family members *DOCK2* and *DOCK8*, have been reported in patients with IELs (Alizadeh et al., 2018; Alroqi et al., 2017; Aydin et al., 2015; Biggs et al., 2017; Bouafia et al., 2019; Dobbs et al., 2015; Engelhardt et al., 2015; Serwas et al., 2019; Su, 2010; Zhang et al., 2009). Human DOCK2 and DEF6 deficiencies were first described by the Boztug group together with collaboration partners (Dobbs et al., 2015; Serwas et al., 2019). These guanine nucleotide exchange factors preferentially activate the small RHO GTPases RHOA (RhoGEF1), RAC1 (DOCK2 and DEF6) and CDC42 (DOCK8 and DEF6) (Bécart et al., 2008; Glaven et al., 1996; Gupta et al., 2003; Harada et al., 2012; Jaiswal et al., 2011; Mavrikis et al., 2004).

In addition to DOCK2 and DOCK8, other DOCK family members, for instance DOCK5, DOCK10 and DOCK11 are expressed in immune cells (Figure 7) and may have potential roles in immune-cell function. For instance, murine studies suggested a role for DOCK11 in immune-cell function. While these studies focused mainly on the role of DOCK11 in B-cell development and function (Matsuda et al., 2015; Sakamoto & Maruyama, 2020), its expression patterns suggested potential roles in additional immune cells (Abraham et al., 2015; Parrado, 2020). Prior to our study and a report by another group, which was published at the same time (Boussard et al., 2023), patients with pathogenic mutations in *DOCK11* had not yet been described and the role of DOCK11 for human disease had remained elusive.

Despite the growing number of immune defects due to mutations in actin-related proteins, these disorders are still rare. However, with the discovery of novel actinopathies and in-depth dissection of the underlying pathomechanisms, we progressively enhance our understanding of the role of actin remodeling in basic cellular processes and specific immune-cell functions.

We here identified hemizygous *DOCK11* mutations in four unrelated patients, presenting with immune dysregulation and anemia of unknown origin. In two patients, the mutations resulted in complete loss of DOCK11 protein expression. In line with the known role of DOCK11 as a CDC42 GEF (Lin et al., 2006), we observed impaired activation of CDC42 in B lymphoblastoid cells (BLCLs) from all patients. In parallel, Boussard et al, who reported 8 additional patients with immune dysregulation and early onset autoimmunity, harboring 7 distinct hemizygous mutations in *DOCK11*, showed reduced CDC42 activation in DOCK11-deficient platelets (Boussard et al., 2023).

3.1.2 DOCK11 deficiency - similarities and differences to the clinical phenotypes observed in patients with mutations in CDC42, DOCK2 or DOCK8

Interestingly, several of the manifestations reported here and in the study from Boussard et al. for patients carrying hemizygous *DOCK11* mutations are reminiscent of certain clinical features associated with mutations in CDC42, such as immune dysregulation, platelet defects and neuro-developmental abnormalities. In contrast, other manifestations seen in patients with *CDC42* mutations, such as facial abnormalities, neutropenia- and monocytopenia or hemophagocytic lymphohistiocytosis have not been observed in DOCK11-deficient patients (Gernez et al., 2019; Lam et al., 2019; Martinelli et al., 2018; Takenouchi et al., 2015). While two of the here described hemizygous mutations in *DOCK11* lead to loss of protein expression, complete loss-of-function of CDC42 is embryonically lethal (Chen et al., 2000), suggesting that DOCK11-mediated CDC42 activation is restricted to specific cell types or to a defined

subset of CDC42 functions. The distinct nature of hemizygous *DOCK11* mutations and heterozygous mutations in *CDC42*, some of which have been linked to aberrant localization or altered binding of regulators and downstream effectors, may further explain differences in the clinical phenotypes of these genetic defects (Bekhouche et al., 2020; El Masri & Delon, 2021; Martinelli et al., 2018; Nishitani-Isa et al., 2022; Su & Orange, 2020).

When comparing *DOCK11* deficiency to the previously described defects in *DOCK2* and *DOCK8*, there are both overlapping as well as divergent clinical and cellular features. Pathogenic mutations in *DOCK2* and *DOCK8* cause distinct combined immunodeficiency disorders with bacterial and viral recurrent infections and T-cell lymphopenia (Alizadeh et al., 2018; Dobbs et al., 2015; Engelhardt et al., 2015; Moens et al., 2019; Su, 2010; Zhang et al., 2009). While recurrent infections, although less severe, are also present in patients with pathogenic *DOCK11* mutations, we did not observe T-cell lymphopenia.

As an additional clinical feature, autoimmunity is commonly observed in *DOCK8*-deficient patients, but not in *DOCK2* deficiency (Dobbs et al., 2015; Engelhardt et al., 2015; Su, 2010; Zhang et al., 2009). The *DOCK11*-deficient patients reported in this study showed no clinical autoimmune features nor the presence of autoantibodies, despite testing for a large panel of autoantibodies. However, the study by Boussard and Delage et al. (Boussard et al., 2023) found autoantibodies in all 8 patients and linked hemizygous mutations in *DOCK11* to various autoimmune manifestations, including autoimmune cytopenia and systemic lupus erythematosus. Comparison of the two cohorts showed that the median age of onset in the patients presenting with autoimmunity was 5 years, while patients in our cohort all showed an early-onset disease manifestation before the age of 2 years. Additionally, three out of four patients in our cohort died during childhood, whereas the patients from the study of Boussard et al. have a current median age of 17 (Boussard et al., 2023). Hence, we speculate that some *DOCK11*-deficient patients may develop signs of autoimmunity later in life. Interestingly, an increase in CD21^{low} B cells, which has previously been associated with autoimmune diseases, was observed in patients from both cohorts (Boussard et al., 2023). Larger cohort studies will be necessary to define the prevalence of autoimmunity in *DOCK11* deficiency. Collectively, these data imply that regular monitoring of autoantibodies or other signs of autoimmunity should be performed in patients with pathogenic *DOCK11* mutations, to be able to respond timely and adjust the treatment strategy if needed.

Overall, the *DOCK11*-deficient patients in our study presented with a more immune dysregulation and autoinflammatory/autoimmune phenotype rather than a classical immunodeficiency. This has an impact on the treatment strategies, as clinicians need to finely

balance the administration of immunosuppressants to counteract hyperinflammation, while at the same time this may increase the patient's susceptibility to infections. Based on our study and the additional patients described by Boussard et al., there is a broad clinical spectrum with many organ-specific manifestations in DOCK11 deficiency, implicating the need for distinct therapeutic options for individual patients. Moreover, early diagnosis, purely based on clinical manifestations, seems difficult. Instead, a combination of both genetic assessment as well as functional assessment of a potential DOCK11 defect may be required. As a first step, one could predict the pathogenicity of a variant identified by whole exome, whole genome or Sanger sequencing based on several parameters. Criteria for variant assessment include the minor allele frequency in population databases, such as the Genome Aggregation Database (gnomAD), the type of mutation (nonsense, frameshift, splice-site or missense; exonic or intronic), and whether the variant is located in a functional domain (Casanova et al., 2014; Gudmundsson et al., 2022; Karczewski et al., 2020; Kircher et al., 2014; Richards et al., 2015; Vorsteveld et al., 2021). Conservation of the altered residue, as well as information regarding epigenetic or post-translational modification should also be considered. Several bioinformatic tools, such as CADD, PolyPhen and SIFT, are taking such criteria into consideration in order to score the deleteriousness of a given mutation, thereby aiding variant prioritization (Adzhubei et al., 2010; Kircher et al., 2014; Ng & Henikoff, 2003). In a second step, we suggest investigating the effect of a given variant on DOCK11 expression as well as function, for instance through assessment of CDC42 activation.

3.1.3 DOCK proteins fine-tune lymphocyte morphology and migration - novel insights from DOCK11 deficiency

On a cellular level, DOCK2 and DOCK8 deficiencies have been linked to defects in B- and T-cell synapse assembly and T- and NK-cell cytotoxicity (Dobbs et al., 2015; Le Floc'h et al., 2013; Randall et al., 2011; Sakai et al., 2013; Sanui et al., 2003; Ushijima et al., 2018; Wang et al., 2017). The findings from this study do not indicate a clear role for DOCK11 in B- and T-cell synapse assembly, or in T- and NK-cell cytotoxicity. However, given the fine-tuned regulation of RHO GTPase signaling, other experimental conditions, for instance different time points or stimuli, may still reveal a role of DOCK11 in these cellular processes.

Interestingly, lymphocyte migration is affected by defects in all three DOCK family members; however, the type of migration shown to be impaired differs. While DOCK8 deficiency induces cell shattering during T- and NK-cell migration in a confined environment, a cell death process termed cytothripsis (Zhang et al., 2014), lack of DOCK2 impaired lamellipodia formation and lateral migration over endothelial cells, lymphocyte chemotaxis as well as migration in

peripheral lymph nodes (Fukui et al., 2001; Nishikimi et al., 2013; Nombela-Arrieta et al., 2004; Nombela-Arrieta et al., 2007; Shulman et al., 2006). While we did not observe defects in lamellipodia formation, T cells from DOCK11-deficient patients showed impaired filopodia formation. In line with a described role for filopodia in transendothelial migration (Ridley, 2011; Shulman et al., 2009), we observed a reduced capacity of effector T cells from patients to migrate over TNF- α stimulated human umbilical vein endothelial cells (HUVEC) cells.

Migration in a confined environment, as assessed in an under-agarose migration assay, did not affect cell integrity, but revealed that lack of DOCK11 function leads to increased T-cell velocity. This defect was also recapitulated in a zebrafish *dock11*-knockout model, confirming a critical role of DOCK11 in T-cell migration *in vivo*. Using a different type of migration assay, Boussard et al. also observed increased T-cell migration speed in confined channels (Boussard et al., 2023). Filopodia have been suggested to play a role in sensing extracellular matrix topography and stiffness (Chan & Odde, 2008; Jacquemet et al., 2015; D. Lee et al., 2012). Whether the increased migration speed is linked to impaired filopodia formation and hence reduced interaction with the extracellular matrix or surrounding cells, remains to be determined. As a consequence of these two types of migration defects, DOCK11-deficient T lymphocytes may show reduced entry of inflamed tissue. Moreover, in combination with impaired target recognition this could result on one hand in reduced capacity to fight infection, while on the other hand hyperactive T cells may release cytokines in an unrestricted fashion, thereby contributing to systemic inflammation and tissue destruction.

3.1.4 Distinct roles of CDC42 GEFs in T-cell cytokine production

Although both DOCK8 and DOCK11 are known to regulate CDC42 activity, defects in these two proteins cause distinct defects in lymphocyte migration. In addition, our data point towards variant roles of DOCK8 and DOCK11 in regulating T-cell activation and cytokine production. While defects in DOCK8 have been linked to reduced T-cell proliferation and a bias towards Th2 cytokines (Tangye et al., 2017; Zhang et al., 2009), lack of DOCK11 resulted in increased T-cell proliferation and increased production of the Th1 cytokines, IL-2 and IFN- γ , while levels of the Th2 cytokine IL-4 were slightly reduced. These findings suggest that DOCK8 and DOCK11 execute their guanine nucleotide exchange factor function towards CDC42 in a non-redundant fashion.

Indeed RHO GTPases, including CDC42, are known to mediate a multiplicity of functions that are orchestrated by a vast set of regulators with distinct recruitment and activation properties (Jaffe & Hall, 2005). For CDC42, nearly 25 GEFs have been described in mammalian cells

(Pichaud et al., 2019; Thompson et al., 2021). These different GEFs may modulate specific aspects of CDC42 function in a non-redundant manner through specific activation of CDC42 in a cell type-, stimuli- and localization-dependent manner. For instance, different GEFs have distinct protein domains that allow binding to specific lipids or other proteins and can thereby differentially regulate the spatiotemporal activation of CDC42 and its downstream effectors (Jaffe & Hall, 2005). The pleckstrin homology domain, which enables binding to specific phosphatidylinositol lipids present on intracellular membranes, is present in DOCK11 but not DOCK8, which could account for a distinct pattern of CDC42 activation. Beyond the intrinsic differences in the ability of DOCK8 and DOCK11 to regulate CDC42 activity, these two GEFs may harbor distinct specificities towards additional RHO GTPases.

Interestingly, our hypothesis that DOCK11 regulates T-cell proliferation and cytokine production following TCR stimulation through its CDC42 GEF function, is supported by previous data showing that CDC42 negatively regulates effector T-cell proliferation and IL-2 and IFN- γ production by CD4⁺ T cells (Guo et al., 2010; Guo et al., 2011). However, the role of CDC42 in T-cell signaling seems to be different between thymocytes and effector cells. For instance, it has been shown that CDC42 is essential for the positive selection of CD4⁺CD8⁺ double-positive cells, as well as proliferation and MAPK signaling during thymopoiesis (Guo et al., 2010; Guo et al., 2011). Whether these variant roles of CDC42 in different T-cell subsets can be explained for instance by varying expression or function of DOCK11 and other GEFs, like DOCK8, remains to be determined.

The remarkable differences in T-cell cytokine production in DOCK8 and DOCK11 deficiencies highlight the complexity of RHO GTPase regulation. Differences in experimental settings may be overcome by high-throughput techniques allowing side-by-side comparison of T cells derived from patients with various defects.

3.1.5 DOCK11 as a novel negative regulator of TCR signaling

TCR signaling strength has been suggested to influence cytokine production and Th subset differentiation (Bhattacharyya & Feng, 2020; Constant et al., 1995; Tubo & Jenkins, 2014; Yamane & Paul, 2013). In the context of actin regulators, altered TCR signaling strength is often considered to be a consequence of changes in T-cell synapse formation, a process heavily dependent on actin dynamics (reviewed in (Dupré et al., 2021; Dustin & Cooper, 2000)). Surprisingly, we did not observe overt changes in immune synapse formation in DOCK11-deficient T cells. Hence, our data suggest that DOCK11 regulates actin remodeling in the context of filopodia formation, but not T-cell synapse formation. Therefore, we speculated that

DOCK11 might regulate cytokine production not through an actin-dependent mechanism at the T-cell synapse interface, but perhaps by modulating TCR-induced signaling pathways and the resulting transcriptional activity. Indeed, we found that both murine and human T cells lacking DOCK11 show increased nuclear translocation of the transcription factor NFATc1, known to regulate the production of various cytokines, including IL-2, IFN- γ and IL-4, following TCR ligation (Hermann-Kleiter & Baier, 2010; Macian, 2005; Vaeth & Feske, 2018). While DOCK11 had not been previously linked to NFATc1 activity, studies in non-immune cells have suggested a potential link between CDC42 and NFAT proteins. For instance, in human mammary epithelial cells Wnt-5a/Yes/Cdc42 signaling has been suggested to negatively regulate Wnt-5a/Ca²⁺-induced NFATc2 activity (Dejmek et al., 2006). In line with an inhibitory role of CDC42 for NFAT translocation, CDC42 has been proposed to antagonize calcineurin-mediated NFAT activation through JNK signaling thereby reducing hypertrophy and hence the risk for heart failure (Maillet et al., 2009). In contrast, defects in the CDC42 GEF DEF6, also known as SWAP-70-like adapter of T cells (SLAT), have been linked to reduced NFATc2 nuclear translocation and IL-2 production amenable to rescue with constitutively active CDC42 (Feau et al., 2013), indicating a positive role of CDC42 in NFATc2 activity. These studies suggested that CDC42 may have opposing roles in different cell types and variant impact on distinct NFAT isoforms.

Given that JNK, a known downstream effector of CDC42 (Bagrodia et al., 1995; Coso et al., 1995), was shown to specifically inhibit calcineurin-mediated phosphorylation of NFATc1 in T cells (Chow et al., 2000), we hypothesized that DOCK11 might inhibit NFATc1 through CDC42-induced activation of JNK (Figure 8). Indeed, in line with the impaired CDC42 activation, DOCK11 deficiency led to impaired JNK phosphorylation.

There is contradictory data regarding CDC42-mediated regulation of JNK phosphorylation in mature T and T progenitor cells. While in CDC42-deficient thymocytes increased JNK as well as ERK phosphorylation has been observed, another study showed reduced JNK phosphorylation in CDC42-deficient T cells displaying a hyperactivated phenotype (Guo et al., 2010; Guo et al., 2011). However, while the aberrant activation in the latter study was suggested to be caused by increased ERK phosphorylation, potentially due to impaired CDC42/JNK-mediated ERK inhibition (Guo et al., 2010), we did not find alteration in ERK phosphorylation in DOCK11-deficient effector T cells. Alternatively, Guo et al. also speculated that CDC42 might negatively regulate ERK activity in a JNK-independent manner. Based on this hypothesis and the findings from our study, DOCK11 might regulate the CDC42/JNK axis specifically, without affecting CDC42-mediated regulation of ERK. The observed differences in ERK activation could also be connected to the differentiation status of the T cells used

(naive vs effector T cell) and distinct roles of DOCK11 in these T-cell subsets. While lack of CDC42 leads to reduced naïve T cells and increased effector and effector memory T cells, we did not observe major alteration in T-cell subsets in both DOCK11-deficient humans and mice. These data further support the hypothesis that DOCK11 may be less important for CDC42 function during development, while being critical during the T-cell effector response.

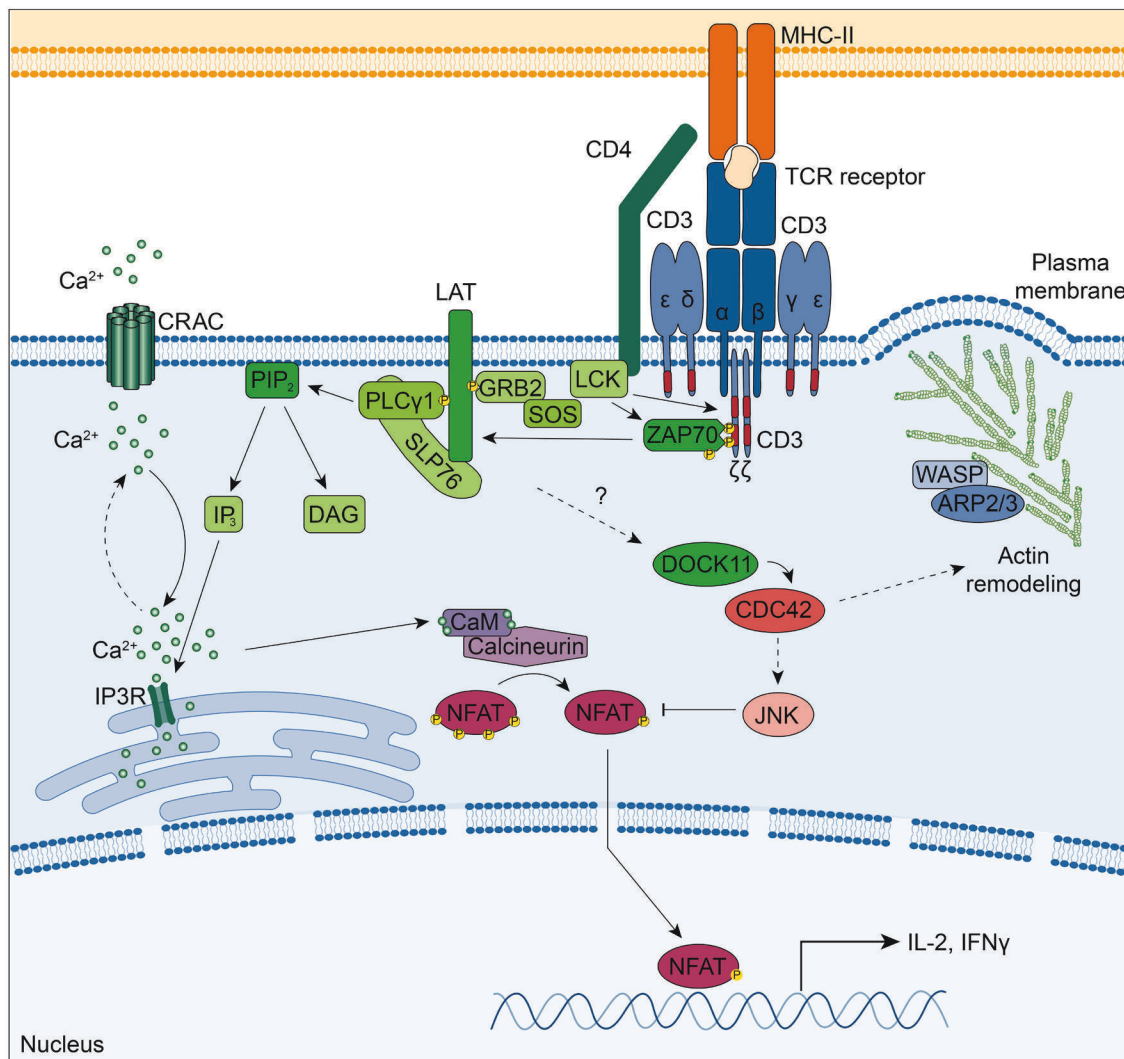


Figure 8. Model of DOCK11-mediated regulation of cytokine production

Schematic illustration of DOCK11-mediated regulation of cytokine production based on our current findings. Upon TCR-ligation DOCK11 induces CDC42 activation resulting in JNK phosphorylation. Activated JNK inhibits NFAT translocation and thus NFAT-mediated transcriptional control of T-cell cytokines, including IL-2 and IFN- γ . Figure adapted from (Bhattacharyya & Feng, 2020; Gaud et al., 2018).

In conclusion, while we could show that DOCK11 is critical for lymphocyte morphology and migration, we unexpectedly identified DOCK11 as a novel negative regulator of TCR-induced signaling.

3.1.6 Dissecting the origin of anemia in DOCK11 deficiency

Given the predominant expression of DOCK11 in immune cells, a role of human DOCK11 in immune cells, as reported in this paper, had never been previously shown, but was suspected. More surprisingly, we also found a DOCK11-intrinsic role in erythroid morphology and differentiation.

There are different causes of anemia in pediatric diseases (reviewed in (Gallagher, 2022)). The mean corpuscular volume can give a hint towards the underlying cause. For instance, iron deficiency and thalassemia usually cause microcytic anemia (Gallagher, 2022; Massey, 1992). In contrast, an increased mean corpuscular volume (macrocytic anemia) may be an indication for megaloblastic anemia, caused by lack of vitamin B12 or folic acid, a bone marrow failure syndrome or hypothyroidism (Fiesco-Roa et al., 2019; Gallagher, 2022; Myers et al., 2020; Socha et al., 2020; Ulirsch et al., 2018). Normocytic anemia, which we observed in patients with DOCK11 deficiency in our study, is commonly associated with anemia of chronic disease, acute inflammation, or conditions that lead to hemolysis of red blood cells, such as autoimmune hemolytic anemia (AIHA) or inherited erythrocyte membrane defects (Berentsen & Barcellini, 2021; Gallagher, 2022; Go et al., 2017; Phillips & Henderson, 2018). Another important parameter for clinical diagnosis is the reticulocyte count that indicates whether the body responds to blood loss or hemolysis with increased erythropoiesis.

In the context of IEIs, anemia is most commonly associated with an overt immune reaction against self, leading to autoimmune hemolytic anemia (Cunningham-Rundles, 2002; Seidel, 2014). The best evidence for AIHA is the presence of autoantibodies directed against red blood cells (Berentsen & Barcellini, 2021; Go et al., 2017). However, while anemia and anisocytosis of unknown origin was reported in all DOCK11-deficient patients, at least in our cohort we did not find evidence for autoimmune-mediated destruction of red blood cells. Neither autoantibodies directed against RBCs nor other autoantibodies were found in the patients studied. Instead, we observed erythroid hypoplasia in a bone marrow smear from patient 1 who displayed severe transfusion-dependent anemia. Our hypothesis that DOCK11 deficiency leads to reduced formation of erythrocyte progenitors was further underlined by reduced cell growth and enhanced cell death upon short hairpin RNA (shRNA)-mediated knockdown of *DOCK11* in CD34⁺ cells and subsequent erythrocyte differentiation in liquid

culture. Moreover, we found reduced Gata1⁺ erythroid cell numbers and altered erythrocyte morphology in a *dock11*-knockout zebrafish model. Given that it takes 3-4 weeks for fully mature T and B cells to arise in zebrafish (Lam et al., 2004; Trede et al., 2004), these data suggest that DOCK11 deficiency can cause anemia independent of the presence of mature lymphocytes, which could potentially drive an autoimmune reaction.

The exact mechanism by which DOCK11 regulates erythropoiesis remains to be determined. Given that the anemia in *dock11*-knockout zebrafish was amenable to rescue with constitutively active CDC42, indicates that DOCK11 regulates erythropoiesis in a CDC42-dependent manner. Compellingly, previous studies have implicated CDC42 in various steps during erythrocyte development. For instance, inducible deletion of *Cdc42* in mouse bone marrow led to myeloid hyperproliferation accompanied by reduced erythropoiesis (Yang et al., 2007). Mechanistically, the alterations in myelopoiesis and erythropoiesis were linked to changes in gene expression of myeloid- and erythroid-promoting genes including increased expression of PU.1, C/EBP1 α , and Gfi-1 and downregulation of GATA-2 (Yang et al., 2007). Interestingly, also increased CDC42 activity upon lack of Cdc42GAP resulted in anemia and reduction of HSPCs and erythroid progenitor cells, suggesting that CDC42 activity has to be finely balanced to ensure normal erythropoiesis (Wang et al., 2006). In addition to controlling the early steps of erythroid development, CDC42 has also been shown to regulate actomyosin-mediated contraction during enucleation of erythroblasts at the terminal differentiation stages (Ubukawa et al., 2020). Since in our *in vitro* experiment shRNA-mediated knockdown of *DOCK11* in CD34⁺ cells led to a significant reduction in cell growth during erythroid differentiation, we did not obtain large enough numbers of DOCK11-deficient terminally differentiated erythroblasts to assess whether DOCK11 may also play a role in nuclear extrusion. It will be of future interest to determine whether DOCK11-mediated CDC42 activation is restricted to specific stages of erythropoiesis.

In addition to autoimmune-mediated destruction or reduced erythropoiesis, anemia can also be caused by enhanced eradication of red blood cells in the spleen (Da Costa et al., 2013; Motulsky et al., 1958). Splenomegaly, a potential indicator for enhanced destruction of red blood cells in the spleen, was reported in 2 out of 4 patients in our cohort. In patient 1, the extent of splenomegaly was so large that it impeded the walking capabilities of the patient. Consequently, a splenectomy was performed. As the patient deceased 2 days later, it remains unclear if the splenectomy would have improved the anemia.

While our data suggest an erythroid intrinsic role for DOCK11 in regulating erythropoiesis and none of our patients showed clear signs of autoimmunity, autoantibodies directed against red

blood cells were detected in some of the patients in the study by Boussard et al. (Boussard et al., 2023). This divergence raises the question whether there are certain risk factors which enhance the probability for development of autoimmunity, for instance differences in Treg function. Interestingly, Boussard et al. show reduced STAT5B activation upon IL-2 stimulation of T cells, and defects in IL-2 receptor signaling have previously been implicated in autoimmune disease. We did not observe differences in Treg numbers in the DOCK11-deficient patients, and due to limitations in patient material we did not explore Treg function. However, we did report increased levels of IL-2 in effector T cells upon TCR stimulation. If or to what extent an increased level of IL-2 production may influence the IL-2/STAT5 signaling defect in regulatory T cells remains to be determined.

Overall, considering the findings from both studies, we propose a multifactorial cause of anemia in patients with DOCK11 deficiency, which may differ amongst individuals with germline *DOCK11* defects.

In addition to the here described role of DOCK11 in erythroid development, another DOCK family member, DOCK4 has also previously been linked to altered erythropoiesis and dysplastic erythrocyte morphology (Sundaravel et al., 2015; Sundaravel et al., 2019). In myelodysplastic syndromes, reduced DOCK4 expression due to chromosome 7 deletions was associated with erythroid dysplasia and anemia (Sundaravel et al., 2015). The study proposed that the observed dysplasia is a consequence of disrupted F-actin due to impaired RAC1 activation. Furthermore, it has been suggested that DOCK4 acts as a negative regulator of LYN kinase, SHP1 and SHIP1 and that as a consequence of reduced DOCK4 expression, HSCs show enhanced migration at the expense of erythroid differentiation (Sundaravel et al., 2019). In line with previous work showing that SHP1 phosphatase negatively regulates erythropoiesis (Bittorf et al., 1999; Sharlow et al., 1997; Wickrema et al., 1999), the study by Sundaravel et al, showed that pharmacological inhibition of SHP1 rescued the erythroid differentiation impairment caused by reduced DOCK4 expression (Sundaravel et al., 2019). Whether DOCK11 deficiency also disrupts F-actin dynamics in erythrocytes as a consequence of disturbed CDC42 activity and similar to DOCK4 acts as a negative regulator of certain kinases will be an interesting field for future research.

3.2 Conclusion and Future Prospects

In summary, we have identified distinct rare hemizygous mutations in *DOCK11* in four patients from four unrelated families with early-onset immune dysregulation and anemia of unknown origin. Based on DOCK11 expression in hematopoietic cells and a previously identified role of

DOCK11 in B-cell development and function (Matsuda et al., 2015; Sakamoto & Maruyama, 2020), we speculated that the predicted pathogenic *DOCK11* variants are interesting candidates for further investigation. Using patient material, as well as CRISPR-edited cell lines we could show that the identified mutations in *DOCK11* impair CDC42 activation and result in aberrant lymphocyte morphology, confirming their pathogenicity. Given that little was known about DOCK11 function in T lymphocytes, we further dissected the functional phenotype of DOCK11-deficient T cells. Interestingly, in line with the role of DOCK11 and its downstream effector CDC42 in actin remodeling, DOCK11 impairment reduced transendothelial migration of effector T cells, while enhancing migration speed in a confined environment. Unexpectedly, we did not find overt alterations in T-cell synapse formation. Instead, using both patient T cells, as well as T cells derived from *Dock11*-knockout mice, we uncovered a previously unknown role of DOCK11 in negatively regulating TCR-induced signaling. Our mechanistic studies suggest a hitherto unknown DOCK11/CDC42/JNK signaling axis affecting NFATc1 translocation and downstream cytokine production in T lymphocytes (Figure 8). Additionally, based on the anemia phenotype in patients with DOCK11 deficiency, we assessed the impact of DOCK11 defects on erythroid morphology and development. While anemia in IEIs has frequently been linked to autoimmune-driven destruction of erythrocytes, we could reveal an erythroid intrinsic role of DOCK11 critical for normal erythropoiesis.

In summary, we uncovered novel roles for DOCK11 in various hematopoietic cells and showed its implication in human disease. Nevertheless, many questions remain, which may be addressed in the future to provide a more detailed picture of DOCK11 deficiency. While our studies focused on dissecting the role of DOCK11 in T lymphocytes and erythroid cells, future studies may explore the role of DOCK11 in additional hematopoietic cells, including monocytes/macrophages, which show high expression of *DOCK11* (Figure 7). While we did not observe changes in cytokine production in monocyte-like THP-1 cells lacking DOCK11, a study of murine bone marrow derived macrophages has suggested a role for DOCK11 in macrophage chemotaxis (Namekata et al., 2020). Moreover, similar to what has been shown recently in murine *Dock11*-KO B cells (Sakabe et al., 2012; Sugiyama et al., 2022), DOCK11 may also play a role in toll-like-receptor signaling in myeloid cells.

Moreover, we have not explored the potential causes of the delayed developmental delay present in patient 2. Although only reported for one out of four patients, this clinical phenotype may suggest a role for DOCK11 in cells of the nervous system, for instance inhibitory neurons, which also show high expression of *DOCK11* (Figure 7). This hypothesis is further supported by the findings that many patients carrying CDC42 mutations display syndromic neurodevelopmental manifestations (Martinelli et al., 2018; Takenouchi et al., 2015) and that

CDC42 has previously been shown to play a role in neurite outgrow (Miyamoto et al., 2007; Sarner et al., 2000). Interestingly, most DOCK family members, apart from DOCK11, have been linked to neurological disease, and their function in cells of the nervous system has been studied to varying degrees. In case future studies will identify additional patients with neurodevelopmental manifestations that carry *DOCK11* mutations, it will be of particular interest to investigate DOCK11 function in neuronal cells, for instance by using iPSC-derived neurons (Freel et al., 2020; Mariani et al., 2015).

In general, while the findings from our as well as previous studies highlight the role of DOCK11 in activating CDC42 and downstream effectors, upstream regulators of DOCK11 activity remain poorly understood. Our data, showing impaired CDC42 activation in response to CCL19 stimulation in DOCK11-deficient BLCLs, suggests that DOCK11 is activated downstream of CCR7 receptor engagement. Moreover, DOCK11 has been suggested to be phosphorylated in response to TCR stimulation (Locard-Paulet et al., 2020; Tan et al., 2017) and we could show altered T-cell function in DOCK11-deficient T cells following TCR engagement. Similarly, DOCK2 has been shown to exert its RAC1-activating function in response to both CCR7 and TCR stimulation (Gollmer et al., 2009; Sanui et al., 2003). DOCK2 requires engulfment and cell motility 1 (ELMO1) for its GEF function and it has been suggested that phosphorylation of DOCK2 and ELMO1 may induce the release of the DOCK2-ELMO1 complex from its auto-inhibited state, and promoting an active conformation required for RAC1 activation (Chang et al., 2020). Whether DOCK11-mediated CDC42 activation also depends on prior phosphorylation events and which upstream kinases and other interacting proteins could be involved in this regulation, will be an interesting field for future studies.

Eventually, the findings from this study may contribute to developing personalized treatment options. A next step could be to explore small molecule drugs, which target the above discussed signaling pathways. Emapalumab, an interferon gamma (IFN- γ)–blocking antibody, which successfully improved the symptoms of one patient carrying a *CDC42* missense variant (Lam et al., 2019), could be a candidate drug. Given the increased levels of the pro-inflammatory cytokine IFN- γ produced by T cells derived from one DOCK11-deficient patient or from the *DOCK11*-knockout mice in response to TCR stimulation, suggests that this drug may help to reduce the inflammatory symptoms of patients with DOCK11 deficiency. Moreover, given the underlying monogenic cause and the observed clear defect in hematopoietic cells, HSCT is a valuable option for DOCK11 deficiency. To date there are a only few rare diseases for which a gene therapy has been approved, including severe aromatic L-amino acid decarboxylase deficiency, spinal muscular atrophy, severe combined immunodeficiency and beta-thalassemia (Arabi et al., 2022; Glascock et al., 2017; Hoggatt,

2016; Hoy, 2019; Keam, 2022; Ma et al., 2020; Mahajan, 2019; Ottesen, 2017; Schimmer & Breazzano, 2016; Stirnadel-Farrant et al., 2018). However, the gene therapy field is rapidly developing and may provide another treatment option for DOCK11 deficiency in the future.

4. MATERIALS AND METHODS

Corresponding materials and methods are described in detail within the published manuscript in Chapter 2.

5. REFERENCES

- Abraham, S., Scarcia, M., Bagshaw, R. D., McMahon, K., Grant, G., Harvey, T., Yeo, M., Esteves, F. O. G., Thygesen, H. H., Jones, P. F., Speirs, V., Hanby, A. M., Selby, P. J., Loriger, M., Dear, T. N., Pawson, T., Marshall, C. J., & Mavria, G. (2015). A Rac/Cdc42 exchange factor complex promotes formation of lateral filopodia and blood vessel lumen morphogenesis. *Nat Commun*, 6, 7286. <https://doi.org/10.1038/ncomms8286>
- Adriani, M., Aoki, J., Horai, R., Thornton, A. M., Konno, A., Kirby, M., Anderson, S. M., Siegel, R. M., Candotti, F., & Schwartzberg, P. L. (2007). Impaired in vitro regulatory T cell function associated with Wiskott-Aldrich syndrome. *Clin Immunol*, 124(1), 41-48. <https://doi.org/10.1016/j.clim.2007.02.001>
- Adzhubei, I. A., Schmidt, S., Peshkin, L., Ramensky, V. E., Gerasimova, A., Bork, P., Kondrashov, A. S., & Sunyaev, S. R. (2010). A method and server for predicting damaging missense mutations. *Nat Methods*, 7(4), 248-249. <https://doi.org/10.1038/nmeth0410-248>
- Aganna, E., Martinon, F., Hawkins, P. N., Ross, J. B., Swan, D. C., Booth, D. R., Lachmann, H. J., Bybee, A., Gaudet, R., Woo, P., Feighery, C., Cotter, F. E., Thome, M., Hitman, G. A., Tschopp, J., & McDermott, M. F. (2002). Association of mutations in the NALP3/CIAS1/PYPAF1 gene with a broad phenotype including recurrent fever, cold sensitivity, sensorineural deafness, and AA amyloidosis. *Arthritis Rheum*, 46(9), 2445-2452. <https://doi.org/10.1002/art.10509>
- Ahmed, S., Goh, W. I., & Bu, W. (2010). I-BAR domains, IRSp53 and filopodium formation. *Semin Cell Dev Biol*, 21(4), 350-356. <https://doi.org/10.1016/j.semcdb.2009.11.008>
- Akashi, K., Traver, D., Miyamoto, T., & Weissman, I. L. (2000). A clonogenic common myeloid progenitor that gives rise to all myeloid lineages. *Nature*, 404(6774), 193-197. <https://doi.org/10.1038/35004599>
- Aksentijevich, I., Nowak, M., Mallah, M., Chae, J. J., Watford, W. T., Hofmann, S. R., Stein, L., Russo, R., Goldsmith, D., Dent, P., Rosenberg, H. F., Austin, F., Remmers, E. F., Balow, J. E., Jr., Rosenzweig, S., Komarow, H., Shoham, N. G., Wood, G., Jones, J., . . . Goldbach-Mansky, R. (2002). De novo CIAS1 mutations, cytokine activation, and evidence for genetic heterogeneity in patients with neonatal-onset multisystem inflammatory disease (NOMID): a new member of the expanding family of pyrin-associated autoinflammatory diseases. *Arthritis Rheum*, 46(12), 3340-3348. <https://doi.org/10.1002/art.10688>
- Aksentijevich, I., Putnam, C. D., Remmers, E. F., Mueller, J. L., Le, J., Kolodner, R. D., Moak, Z., Chuang, M., Austin, F., Goldbach-Mansky, R., Hoffman, H. M., & Kastner, D. L. (2007). The clinical continuum of cryopyrinopathies: novel CIAS1 mutations in North American patients and a new cryopyrin model. *Arthritis Rheum*, 56(4), 1273-1285. <https://doi.org/10.1002/art.22491>
- Akula, M. K., Shi, M., Jiang, Z., Foster, C. E., Miao, D., Li, A. S., Zhang, X., Gavin, R. M., Forde, S. D., Germain, G., Carpenter, S., Rosadini, C. V., Gritsman, K., Chae, J. J., Hampton, R., Silverman, N., Gravallese, E. M., Kagan, J. C., Fitzgerald, K. A., . . . Wang, D. (2016). Control of the innate immune response by the mevalonate pathway. *Nat Immunol*, 17(8), 922-929. <https://doi.org/10.1038/ni.3487>
- Albert, M. H., Notarangelo, L. D., & Ochs, H. D. (2011). Clinical spectrum, pathophysiology and treatment of the Wiskott-Aldrich syndrome. *Curr Opin Hematol*, 18(1), 42-48. <https://doi.org/10.1097/MOH.0b013e32834114bc>
- Aldrich, R. A., Steinberg, A. G., & Campbell, D. C. (1954). Pedigree demonstrating a sex-linked recessive condition characterized by draining ears, eczematoid dermatitis and bloody diarrhea. *Pediatrics*, 13(2), 133-139.
- Alizadeh, Z., Mazinani, M., Shakerian, L., Nabavi, M., & Fazlollahi, M. R. (2018). DOCK2 Deficiency in a Patient with Hyper IgM Phenotype. *J Clin Immunol*, 38(1), 10-12. <https://doi.org/10.1007/s10875-017-0468-5>

- Alkhaury, O. K., Abolhassani, H., Rezaei, N., Fang, M., Andersen, K. K., Chavoshzadeh, Z., Mohammadzadeh, I., El-Rajab, M. A., Massaad, M., Chou, J., Aghamohammadi, A., Geha, R. S., & Hammarström, L. (2016). Spectrum of Phenotypes Associated with Mutations in LRBA. *J Clin Immunol*, *36*(1), 33-45. <https://doi.org/10.1007/s10875-015-0224-7>
- Alroqi, F. J., Charbonnier, L. M., Keles, S., Ghandour, F., Mouawad, P., Sabouneh, R., Mohammed, R., Almutairi, A., Chou, J., Massaad, M. J., Geha, R. S., Baz, Z., & Chatila, T. A. (2017). DOCK8 Deficiency Presenting as an IPEX-Like Disorder. *J Clin Immunol*, *37*(8), 811-819. <https://doi.org/10.1007/s10875-017-0451-1>
- An, X., Debnath, G., Guo, X., Liu, S., Lux, S. E., Baines, A., Gratzer, W., & Mohandas, N. (2005). Identification and functional characterization of protein 4.1R and actin-binding sites in erythrocyte beta spectrin: regulation of the interactions by phosphatidylinositol-4,5-bisphosphate. *Biochemistry*, *44*(31), 10681-10688. <https://doi.org/10.1021/bi047331z>
- An, X., Salomao, M., Guo, X., Gratzer, W., & Mohandas, N. (2007). Tropomyosin modulates erythrocyte membrane stability. *Blood*, *109*(3), 1284-1288. <https://doi.org/10.1182/blood-2006-07-036954>
- Andrianantoandro, E., & Pollard, T. D. (2006). Mechanism of actin filament turnover by severing and nucleation at different concentrations of ADF/cofilin. *Mol Cell*, *24*(1), 13-23. <https://doi.org/10.1016/j.molcel.2006.08.006>
- Arabi, F., Mansouri, V., & Ahmadbeigi, N. (2022). Gene therapy clinical trials, where do we go? An overview. *Biomed Pharmacother*, *153*, 113324. <https://doi.org/10.1016/j.biopha.2022.113324>
- Ardavín, C. (2003). Origin, precursors and differentiation of mouse dendritic cells. *Nat Rev Immunol*, *3*(7), 582-590. <https://doi.org/10.1038/nri1127>
- Avagyan, S., & Zon, L. I. (2016). Fish to Learn: Insights into Blood Development and Blood Disorders from Zebrafish Hematopoiesis. *Hum Gene Ther*, *27*(4), 287-294. <https://doi.org/10.1089/hum.2016.024>
- Aydin, S. E., Kilic, S. S., Aytakin, C., Kumar, A., Porras, O., Kainulainen, L., Kostyuchenko, L., Genel, F., Kutukculer, N., Karaca, N., Gonzalez-Granado, L., Abbott, J., Al-Zahrani, D., Rezaei, N., Baz, Z., Thiel, J., Ehl, S., Marodi, L., Orange, J. S., . . . inborn errors working party of, E. (2015). DOCK8 deficiency: clinical and immunological phenotype and treatment options - a review of 136 patients. *J Clin Immunol*, *35*(2), 189-198. <https://doi.org/10.1007/s10875-014-0126-0>
- Bagrodia, S., Dérijard, B., Davis, R. J., & Cerione, R. A. (1995). Cdc42 and PAK-mediated signaling leads to Jun kinase and p38 mitogen-activated protein kinase activation. *J Biol Chem*, *270*(47), 27995-27998. <https://doi.org/10.1074/jbc.270.47.27995>
- Bamshad, M. J., Ng, S. B., Bigham, A. W., Tabor, H. K., Emond, M. J., Nickerson, D. A., & Shendure, J. (2011). Exome sequencing as a tool for Mendelian disease gene discovery. *Nat Rev Genet*, *12*(11), 745-755. <https://doi.org/10.1038/nrg3031>
- Banerjee, P. P., & Orange, J. S. (2010). Quantitative measurement of F-actin accumulation at the NK cell immunological synapse. *J Immunol Methods*, *355*(1-2), 1-13. <https://doi.org/10.1016/j.jim.2010.02.003>
- Barry, M., & Bleackley, R. C. (2002). Cytotoxic T lymphocytes: all roads lead to death. *Nat Rev Immunol*, *2*(6), 401-409. <https://doi.org/10.1038/nri819>
- Bécart, S., Balancio, A. J., Charvet, C., Feau, S., Sedwick, C. E., & Altman, A. (2008). Tyrosine-phosphorylation-dependent translocation of the SLAT protein to the immunological synapse is required for NFAT transcription factor activation. *Immunity*, *29*(5), 704-719. <https://doi.org/10.1016/j.immuni.2008.08.015>
- Beemiller, P., & Krummel, M. F. (2013). Regulation of T-cell receptor signaling by the actin cytoskeleton and poroelastic cytoplasm. *Immunol Rev*, *256*(1), 148-159. <https://doi.org/10.1111/imr.12120>
- Bekhouche, B., Tourville, A., Ravichandran, Y., Tacine, R., Abrami, L., Dussiot, M., Khau-Dancasius, A., Boccara, O., Khirat, M., Mangeney, M., Dingli, F., Loew, D., Boëda, B., Jordan, P., Molina, T. J., Bellon, N., Fraitag, S., Hadj-Rabia, S., Blanche, S., . . . Delon, J. (2020). A toxic palmitoylation of Cdc42 enhances NF-κB signaling and drives a

- severe autoinflammatory syndrome. *J Allergy Clin Immunol*, 146(5), 1201-1204.e1208. <https://doi.org/10.1016/j.jaci.2020.03.020>
- Ben-Shmuel, A., Sabag, B., Biber, G., & Barda-Saad, M. (2021). The Role of the Cytoskeleton in Regulating the Natural Killer Cell Immune Response in Health and Disease: From Signaling Dynamics to Function. *Front Cell Dev Biol*, 9, 609532. <https://doi.org/10.3389/fcell.2021.609532>
- Bennett, C. L., Christie, J., Ramsdell, F., Brunkow, M. E., Ferguson, P. J., Whitesell, L., Kelly, T. E., Saulsbury, F. T., Chance, P. F., & Ochs, H. D. (2001). The immune dysregulation, polyendocrinopathy, enteropathy, X-linked syndrome (IPEX) is caused by mutations of FOXP3. *Nat Genet*, 27(1), 20-21. <https://doi.org/10.1038/83713>
- Bennett, C. M., Kanki, J. P., Rhodes, J., Liu, T. X., Paw, B. H., Kieran, M. W., Langenau, D. M., Delahaye-Brown, A., Zon, L. I., Fleming, M. D., & Look, A. T. (2001). Myelopoiesis in the zebrafish, *Danio rerio*. *Blood*, 98(3), 643-651. <https://doi.org/10.1182/blood.v98.3.643>
- Berentsen, S., & Barcellini, W. (2021). Autoimmune Hemolytic Anemias. *N Engl J Med*, 385(15), 1407-1419. <https://doi.org/10.1056/NEJMra2033982>
- Bettelli, E., Dastrange, M., & Oukka, M. (2005). Foxp3 interacts with nuclear factor of activated T cells and NF-kappa B to repress cytokine gene expression and effector functions of T helper cells. *Proc Natl Acad Sci U S A*, 102(14), 5138-5143. <https://doi.org/10.1073/pnas.0501675102>
- Bhattacharyya, N. D., & Feng, C. G. (2020). Regulation of T Helper Cell Fate by TCR Signal Strength. *Front Immunol*, 11, 624. <https://doi.org/10.3389/fimmu.2020.00624>
- Biggs, C. M., Keles, S., & Chatila, T. A. (2017). DOCK8 deficiency: Insights into pathophysiology, clinical features and management. *Clin Immunol*, 181, 75-82. <https://doi.org/10.1016/j.clim.2017.06.003>
- Bittorf, T., Seiler, J., Zhang, Z., Jaster, R., & Brock, J. (1999). SHP1 protein tyrosine phosphatase negatively modulates erythroid differentiation and suppression of apoptosis in J2E erythroleukemic cells. *Biol Chem*, 380(10), 1201-1209. <https://doi.org/10.1515/bc.1999.152>
- Blumenthal, D., & Burkhardt, J. K. (2020). Multiple actin networks coordinate mechanotransduction at the immunological synapse. *J Cell Biol*, 219(2). <https://doi.org/10.1083/jcb.201911058>
- Bode, S. F., Lehmborg, K., Maul-Pavicic, A., Vraetz, T., Janka, G., Stadt, U. Z., & Ehl, S. (2012). Recent advances in the diagnosis and treatment of hemophagocytic lymphohistiocytosis. *Arthritis Res Ther*, 14(3), 213. <https://doi.org/10.1186/ar3843>
- Borrego-Diaz, E., Kerff, F., Lee, S. H., Ferron, F., Li, Y., & Dominguez, R. (2006). Crystal structure of the actin-binding domain of alpha-actinin 1: evaluating two competing actin-binding models. *J Struct Biol*, 155(2), 230-238. <https://doi.org/10.1016/j.jsb.2006.01.013>
- Bos, J. L., Rehmann, H., & Wittinghofer, A. (2007). GEFs and GAPs: critical elements in the control of small G proteins. *Cell*, 129(5), 865-877. <https://doi.org/10.1016/j.cell.2007.05.018>
- Bouafia, A., Lofek, S., Bruneau, J., Chentout, L., Lamrini, H., Trinquand, A., Deau, M. C., Heurtier, L., Meignin, V., Picard, C., Macintyre, E., Alibeu, O., Bras, M., Molina, T. J., Cavazzana, M., André-Schmutz, I., Durandy, A., Fischer, A., Oksenhendler, E., & Kracker, S. (2019). Loss of ARHGEF1 causes a human primary antibody deficiency. *J Clin Invest*, 129(3), 1047-1060. <https://doi.org/10.1172/jci120572>
- Bouma, G., Carter, N. A., Recher, M., Malinova, D., Adriani, M., Notarangelo, L. D., Burns, S. O., Mauri, C., & Thrasher, A. J. (2014). Exacerbated experimental arthritis in Wiskott-Aldrich syndrome protein deficiency: modulatory role of regulatory B cells. *Eur J Immunol*, 44(9), 2692-2702. <https://doi.org/10.1002/eji.201344245>
- Bousfiha, A., Moundir, A., Tangye, S. G., Picard, C., Jeddane, L., Al-Herz, W., Rundles, C. C., Franco, J. L., Holland, S. M., Klein, C., Morio, T., Oksenhendler, E., Puel, A., Puck, J., Seppänen, M. R. J., Somech, R., Su, H. C., Sullivan, K. E., Torgerson, T. R., & Meyts, I. (2022). The 2022 Update of IUIS Phenotypical Classification for Human Inborn Errors

- of Immunity. *J Clin Immunol*, 42(7), 1508-1520. <https://doi.org/10.1007/s10875-022-01352-z>
- Boussard, C., Delage, L., Gajardo, T., Kauskot, A., Batignes, M., Goudin, N., Stolzenberg, M. C., Brunaud, C., Panikulam, P., Riller, Q., Moya-Nilges, M., Solarz, J., Reperant, C., Durel, B., Bordet, J. C., Pellé, O., Lebreton, C., Magerus-Chatinet, A., Pirabakaran, V., . . . Rieux-Laucat, F. (2023). DOCK11 deficiency in patients with X-linked actinopathy and autoimmunity. *Blood*. <https://doi.org/10.1182/blood.2022018486>
- Bouso, P. (2008). T-cell activation by dendritic cells in the lymph node: lessons from the movies. *Nat Rev Immunol*, 8(9), 675-684. <https://doi.org/10.1038/nri2379>
- Broderick, M. J., & Winder, S. J. (2005). Spectrin, alpha-actinin, and dystrophin. *Adv Protein Chem*, 70, 203-246. [https://doi.org/10.1016/s0065-3233\(05\)70007-3](https://doi.org/10.1016/s0065-3233(05)70007-3)
- Brugnera, E., Haney, L., Grimsley, C., Lu, M., Walk, S. F., Tosello-Trampont, A. C., Macara, I. G., Madhani, H., Fink, G. R., & Ravichandran, K. S. (2002). Unconventional Rac-GEF activity is mediated through the Dock180-ELMO complex. *Nat Cell Biol*, 4(8), 574-582. <https://doi.org/10.1038/ncb824>
- Buccioli, G., Pillay, B., Casas-Martin, J., Delafontaine, S., Proesmans, M., Lorent, N., Coolen, J., Tousseyn, T., Bossuyt, X., Ma, C. S., Schrijvers, R., Tangye, S. G., Moens, L., & Meyts, I. (2020). Systemic Inflammation and Myelofibrosis in a Patient with Takenouchi-Kosaki Syndrome due to CDC42 Tyr64Cys Mutation. *J Clin Immunol*, 40(4), 567-570. <https://doi.org/10.1007/s10875-020-00742-5>
- Burns, S. O., Zараfov, A., & Thrasher, A. J. (2017). Primary immunodeficiencies due to abnormalities of the actin cytoskeleton. *Curr Opin Hematol*, 24(1), 16-22. <https://doi.org/10.1097/moh.0000000000000296>
- Burridge, K., & Guilluy, C. (2016). Focal adhesions, stress fibers and mechanical tension. *Exp Cell Res*, 343(1), 14-20. <https://doi.org/10.1016/j.yexcr.2015.10.029>
- Butler, B., & Cooper, J. A. (2009). Distinct roles for the actin nucleators Arp2/3 and hDia1 during NK-mediated cytotoxicity. *Curr Biol*, 19(22), 1886-1896. <https://doi.org/10.1016/j.cub.2009.10.029>
- Calvez, R., Lafouresse, F., De Meester, J., Galy, A., Valitutti, S., & Dupre, L. (2011). The Wiskott-Aldrich syndrome protein permits assembly of a focused immunological synapse enabling sustained T-cell receptor signaling. *Haematologica*, 96(10), 1415-1423. <https://doi.org/10.3324/haematol.2011.040204>
- Campi, G., Varma, R., & Dustin, M. L. (2005). Actin and agonist MHC-peptide complex-dependent T cell receptor microclusters as scaffolds for signaling. *J Exp Med*, 202(8), 1031-1036. <https://doi.org/10.1084/jem.20051182>
- A candidate gene for familial Mediterranean fever. (1997). *Nat Genet*, 17(1), 25-31. <https://doi.org/10.1038/ng0997-25>
- Candotti, F. (2018). Clinical Manifestations and Pathophysiological Mechanisms of the Wiskott-Aldrich Syndrome. *J Clin Immunol*, 38(1), 13-27. <https://doi.org/10.1007/s10875-017-0453-z>
- Canna, S. W., de Jesus, A. A., Gouni, S., Brooks, S. R., Marrero, B., Liu, Y., DiMattia, M. A., Zaal, K. J., Sanchez, G. A., Kim, H., Chapelle, D., Plass, N., Huang, Y., Villarino, A. V., Biancotto, A., Fleisher, T. A., Duncan, J. A., O'Shea, J. J., Benseler, S., . . . Goldbach-Mansky, R. (2014). An activating NLRC4 inflammasome mutation causes autoinflammation with recurrent macrophage activation syndrome. *Nat Genet*, 46(10), 1140-1146. <https://doi.org/10.1038/ng.3089>
- Cantor, A. B., & Orkin, S. H. (2002). Transcriptional regulation of erythropoiesis: an affair involving multiple partners. *Oncogene*, 21(21), 3368-3376. <https://doi.org/10.1038/sj.onc.1205326>
- Carman, C. V., Sage, P. T., Sciuto, T. E., de la Fuente, M. A., Geha, R. S., Ochs, H. D., Dvorak, H. F., Dvorak, A. M., & Springer, T. A. (2007). Transcellular diapedesis is initiated by invasive podosomes. *Immunity*, 26(6), 784-797. <https://doi.org/10.1016/j.immuni.2007.04.015>
- Carradice, D., & Lieschke, G. J. (2008). Zebrafish in hematology: sushi or science? *Blood*, 111(7), 3331-3342. <https://doi.org/10.1182/blood-2007-10-052761>

- Casanova, J. L., Conley, M. E., Seligman, S. J., Abel, L., & Notarangelo, L. D. (2014). Guidelines for genetic studies in single patients: lessons from primary immunodeficiencies. *J Exp Med*, 211(11), 2137-2149. <https://doi.org/10.1084/jem.20140520>
- Castiello, M. C., Bosticardo, M., Pala, F., Catucci, M., Chamberlain, N., van Zelm, M. C., Driessen, G. J., Pac, M., Bernatowska, E., Scaramuzza, S., Aiuti, A., Sauer, A. V., Traggiai, E., Meffre, E., Villa, A., & van der Burg, M. (2014). Wiskott-Aldrich Syndrome protein deficiency perturbs the homeostasis of B-cell compartment in humans. *J Autoimmun*, 50(100), 42-50. <https://doi.org/10.1016/j.jaut.2013.10.006>
- Castro, C. N., Rosenzweig, M., Carapito, R., Shahrooei, M., Konantz, M., Khan, A., Miao, Z., Gross, M., Tranchant, T., Radosavljevic, M., Paul, N., Stemmlen, T., Pitoiset, F., Hirschler, A., Nespola, B., Molitor, A., Rolli, V., Pichot, A., Faletti, L. E., . . . Bahram, S. (2020). NCKAP1L defects lead to a novel syndrome combining immunodeficiency, lymphoproliferation, and hyperinflammation. *J Exp Med*, 217(12). <https://doi.org/10.1084/jem.20192275>
- Caudy, A. A., Reddy, S. T., Chatila, T., Atkinson, J. P., & Verbsky, J. W. (2007). CD25 deficiency causes an immune dysregulation, polyendocrinopathy, enteropathy, X-linked-like syndrome, and defective IL-10 expression from CD4 lymphocytes. *J Allergy Clin Immunol*, 119(2), 482-487. <https://doi.org/10.1016/j.jaci.2006.10.007>
- Chae, J. J., Park, Y. H., Park, C., Hwang, I. Y., Hoffmann, P., Kehrl, J. H., Aksentijevich, I., & Kastner, D. L. (2015). Connecting two pathways through Ca²⁺ signaling: NLRP3 inflammasome activation induced by a hypermorphic PLCG2 mutation. *Arthritis Rheumatol*, 67(2), 563-567. <https://doi.org/10.1002/art.38961>
- Chan, C. E., & Odde, D. J. (2008). Traction dynamics of filopodia on compliant substrates. *Science*, 322(5908), 1687-1691. <https://doi.org/10.1126/science.1163595>
- Chan, M. M., Wooden, J. M., Tsang, M., Gilligan, D. M., Hirehallur, S. D., Finney, G. L., Rynes, E., Maccoss, M., Ramirez, J. A., Park, H., & Iritani, B. M. (2013). Hematopoietic protein-1 regulates the actin membrane skeleton and membrane stability in murine erythrocytes. *PLoS One*, 8(2), e54902. <https://doi.org/10.1371/journal.pone.0054902>
- Chang, L., Yang, J., Jo, C. H., Boland, A., Zhang, Z., McLaughlin, S. H., Abu-Thuraia, A., Killoran, R. C., Smith, M. J., Côté, J. F., & Barford, D. (2020). Structure of the DOCK2-ELMO1 complex provides insights into regulation of the auto-inhibited state. *Nat Commun*, 11(1), 3464. <https://doi.org/10.1038/s41467-020-17271-9>
- Chemin, K., Gerstner, C., & Malmström, V. (2019). Effector Functions of CD4+ T Cells at the Site of Local Autoimmune Inflammation-Lessons From Rheumatoid Arthritis. *Front Immunol*, 10, 353. <https://doi.org/10.3389/fimmu.2019.00353>
- Chen, A. T., & Zon, L. I. (2009). Zebrafish blood stem cells. *J Cell Biochem*, 108(1), 35-42. <https://doi.org/10.1002/jcb.22251>
- Chen, F., Ma, L., Parrini, M. C., Mao, X., Lopez, M., Wu, C., Marks, P. W., Davidson, L., Kwiatkowski, D. J., Kirchhausen, T., Orkin, S. H., Rosen, F. S., Mayer, B. J., Kirschner, M. W., & Alt, F. W. (2000). Cdc42 is required for PIP(2)-induced actin polymerization and early development but not for cell viability. *Curr Biol*, 10(13), 758-765. [https://doi.org/10.1016/s0960-9822\(00\)00571-6](https://doi.org/10.1016/s0960-9822(00)00571-6)
- Chen, L., & Flies, D. B. (2013). Molecular mechanisms of T cell co-stimulation and co-inhibition. *Nat Rev Immunol*, 13(4), 227-242. <https://doi.org/10.1038/nri3405>
- Chereau, D., Kerff, F., Graceffa, P., Grabarek, Z., Langsetmo, K., & Dominguez, R. (2005). Actin-bound structures of Wiskott-Aldrich syndrome protein (WASP)-homology domain 2 and the implications for filament assembly. *Proc Natl Acad Sci U S A*, 102(46), 16644-16649. <https://doi.org/10.1073/pnas.0507021102>
- Cherfils, J., & Zoghoufi, M. (2013). Regulation of small GTPases by GEFs, GAPs, and GDIs. *Physiol Rev*, 93(1), 269-309. <https://doi.org/10.1152/physrev.00003.2012>
- Chhabra, E. S., & Higgs, H. N. (2007). The many faces of actin: matching assembly factors with cellular structures. *Nat Cell Biol*, 9(10), 1110-1121. <https://doi.org/10.1038/ncb1007-1110>

- Chi, X., Li, Y., & Qiu, X. (2020). V(D)J recombination, somatic hypermutation and class switch recombination of immunoglobulins: mechanism and regulation. *Immunology*, *160*(3), 233-247. <https://doi.org/10.1111/imm.13176>
- Chou, H. C., Antón, I. M., Holt, M. R., Curcio, C., Lanzardo, S., Worth, A., Burns, S., Thrasher, A. J., Jones, G. E., & Calle, Y. (2006). WIP regulates the stability and localization of WASP to podosomes in migrating dendritic cells. *Curr Biol*, *16*(23), 2337-2344. <https://doi.org/10.1016/j.cub.2006.10.037>
- Chow, C. W., Dong, C., Flavell, R. A., & Davis, R. J. (2000). c-Jun NH(2)-terminal kinase inhibits targeting of the protein phosphatase calcineurin to NFATc1. *Mol Cell Biol*, *20*(14), 5227-5234. <https://doi.org/10.1128/mcb.20.14.5227-5234.2000>
- Chrzanowska-Wodnicka, M., & Burridge, K. (1996). Rho-stimulated contractility drives the formation of stress fibers and focal adhesions. *J Cell Biol*, *133*(6), 1403-1415. <https://doi.org/10.1083/jcb.133.6.1403>
- Collison, L. W., Workman, C. J., Kuo, T. T., Boyd, K., Wang, Y., Vignali, K. M., Cross, R., Sehy, D., Blumberg, R. S., & Vignali, D. A. (2007). The inhibitory cytokine IL-35 contributes to regulatory T-cell function. *Nature*, *450*(7169), 566-569. <https://doi.org/10.1038/nature06306>
- Consortium, T. I. F. (1997). Ancient Missense Mutations in a New Member of the RoRet Gene Family Are Likely to Cause Familial Mediterranean Fever. *Cell*, *90*(4), 797-807. [https://doi.org/https://doi.org/10.1016/S0092-8674\(00\)80539-5](https://doi.org/https://doi.org/10.1016/S0092-8674(00)80539-5)
- Constant, S., Pfeiffer, C., Woodard, A., Pasqualini, T., & Bottomly, K. (1995). Extent of T cell receptor ligation can determine the functional differentiation of naive CD4+ T cells. *J Exp Med*, *182*(5), 1591-1596. <https://doi.org/10.1084/jem.182.5.1591>
- Cook, S. A., Comrie, W. A., Poli, M. C., Similuk, M., Oler, A. J., Faruqi, A. J., Kuhns, D. B., Yang, S., Vargas-Hernández, A., Carisey, A. F., Fournier, B., Anderson, D. E., Price, S., Smelkinson, M., Abou Chahla, W., Forbes, L. R., Mace, E. M., Cao, T. N., Coban-Akdemir, Z. H., . . . Lenardo, M. J. (2020). HEM1 deficiency disrupts mTORC2 and F-actin control in inherited immunodysregulatory disease. *Science*, *369*(6500), 202-207. <https://doi.org/10.1126/science.aay5663>
- Cooper, J. A. (2002). Actin dynamics: tropomyosin provides stability. *Curr Biol*, *12*(15), R523-525. [https://doi.org/10.1016/s0960-9822\(02\)01028-x](https://doi.org/10.1016/s0960-9822(02)01028-x)
- Coppola, S., Insalaco, A., Zara, E., Di Rocco, M., Marafon, D. P., Spadaro, F., Pannone, L., Farina, L., Pasquini, L., Martinelli, S., De Benedetti, F., & Tartaglia, M. (2022). Mutations at the C-terminus of CDC42 cause distinct hematopoietic and autoinflammatory disorders. *J Allergy Clin Immunol*, *150*(1), 223-228. <https://doi.org/10.1016/j.jaci.2022.01.024>
- Coso, O. A., Chiariello, M., Yu, J. C., Teramoto, H., Crespo, P., Xu, N., Miki, T., & Gutkind, J. S. (1995). The small GTP-binding proteins Rac1 and Cdc42 regulate the activity of the JNK/SAPK signaling pathway. *Cell*, *81*(7), 1137-1146. [https://doi.org/10.1016/s0092-8674\(05\)80018-2](https://doi.org/10.1016/s0092-8674(05)80018-2)
- Costagliola, G., Peroni, D. G., & Consolini, R. (2022). Beyond Infections: New Warning Signs for Inborn Errors of Immunity in Children. *Front Pediatr*, *10*, 855445. <https://doi.org/10.3389/fped.2022.855445>
- Côté, J. F., Motoyama, A. B., Bush, J. A., & Vuori, K. (2005). A novel and evolutionarily conserved PtdIns(3,4,5)P3-binding domain is necessary for DOCK180 signalling. *Nat Cell Biol*, *7*(8), 797-807. <https://doi.org/10.1038/ncb1280>
- Côté, J. F., & Vuori, K. (2002). Identification of an evolutionarily conserved superfamily of DOCK180-related proteins with guanine nucleotide exchange activity. *J Cell Sci*, *115*(Pt 24), 4901-4913. <https://doi.org/10.1242/jcs.00219>
- Cotta-de-Almeida, V., Dupré, L., Guipouy, D., & Vasconcelos, Z. (2015). Signal Integration during T Lymphocyte Activation and Function: Lessons from the Wiskott-Aldrich Syndrome. *Front Immunol*, *6*, 47. <https://doi.org/10.3389/fimmu.2015.00047>
- Covacu, R., Philip, H., Jaronen, M., Almeida, J., Kenison, J. E., Darko, S., Chao, C. C., Yaari, G., Louzoun, Y., Carmel, L., Douek, D. C., Efroni, S., & Quintana, F. J. (2016). System-wide Analysis of the T Cell Response. *Cell Rep*, *14*(11), 2733-2744. <https://doi.org/10.1016/j.celrep.2016.02.056>

- Crawford, G., Enders, A., Gileadi, U., Stankovic, S., Zhang, Q., Lambe, T., Crockford, T. L., Lockstone, H. E., Freeman, A., Arkwright, P. D., Smart, J. M., Ma, C. S., Tangye, S. G., Goodnow, C. C., Cerundolo, V., Godfrey, D. I., Su, H. C., Randall, K. L., & Cornwall, R. J. (2013). DOCK8 is critical for the survival and function of NKT cells. *Blood*, *122*(12), 2052-2061. <https://doi.org/10.1182/blood-2013-02-482331>
- Crequer, A., Troeger, A., Patin, E., Ma, C. S., Picard, C., Pedergrana, V., Fieschi, C., Lim, A., Abhyankar, A., Gineau, L., Mueller-Fleckenstein, I., Schmidt, M., Taieb, A., Krueger, J., Abel, L., Tangye, S. G., Orth, G., Williams, D. A., Casanova, J. L., & Jouanguy, E. (2012). Human RHOH deficiency causes T cell defects and susceptibility to EV-HPV infections. *J Clin Invest*, *122*(9), 3239-3247. <https://doi.org/10.1172/jci62949>
- Crotty, S. (2014). T follicular helper cell differentiation, function, and roles in disease. *Immunity*, *41*(4), 529-542. <https://doi.org/10.1016/j.immuni.2014.10.004>
- Cunningham-Rundles, C. (2002). Hematologic complications of primary immune deficiencies. *Blood Rev*, *16*(1), 61-64. <https://doi.org/10.1054/blre.2001.0185>
- Cyster, J. G., & Allen, C. D. C. (2019). B Cell Responses: Cell Interaction Dynamics and Decisions. *Cell*, *177*(3), 524-540. <https://doi.org/10.1016/j.cell.2019.03.016>
- Da Costa, L., Galimand, J., Fenneteau, O., & Mohandas, N. (2013). Hereditary spherocytosis, elliptocytosis, and other red cell membrane disorders. *Blood Rev*, *27*(4), 167-178. <https://doi.org/10.1016/j.blre.2013.04.003>
- Davidson, A. J., & Zon, L. I. (2004). The 'definitive' (and 'primitive') guide to zebrafish hematopoiesis. *Oncogene*, *23*(43), 7233-7246. <https://doi.org/10.1038/sj.onc.1207943>
- De Meester, J., Calvez, R., Valitutti, S., & Dupré, L. (2010). The Wiskott-Aldrich syndrome protein regulates CTL cytotoxicity and is required for efficient killing of B cell lymphoma targets. *J Leukoc Biol*, *88*(5), 1031-1040. <https://doi.org/10.1189/jlb.0410197>
- de Noronha, S., Hardy, S., Sinclair, J., Blundell, M. P., Strid, J., Schulz, O., Zwirner, J., Jones, G. E., Katz, D. R., Kinnon, C., & Thrasher, A. J. (2005). Impaired dendritic-cell homing in vivo in the absence of Wiskott-Aldrich syndrome protein. *Blood*, *105*(4), 1590-1597. <https://doi.org/10.1182/blood-2004-06-2332>
- Dejmek, J., Säfholm, A., Kamp Nielsen, C., Andersson, T., & Leandersson, K. (2006). Wnt-5a/Ca²⁺-induced NFAT activity is counteracted by Wnt-5a/Yes-Cdc42-casein kinase 1 α signaling in human mammary epithelial cells. *Mol Cell Biol*, *26*(16), 6024-6036. <https://doi.org/10.1128/mcb.02354-05>
- DerMardirossian, C., & Bokoch, G. M. (2005). GDIs: central regulatory molecules in Rho GTPase activation. *Trends Cell Biol*, *15*(7), 356-363. <https://doi.org/10.1016/j.tcb.2005.05.001>
- Derry, J. M., Ochs, H. D., & Francke, U. (1994). Isolation of a novel gene mutated in Wiskott-Aldrich syndrome. *Cell*, *78*(4), 635-644. [https://doi.org/10.1016/0092-8674\(94\)90528-2](https://doi.org/10.1016/0092-8674(94)90528-2)
- Dias, J., Gumenyuk, M., Kang, H., Vodyanik, M., Yu, J., Thomson, J. A., & Slukvin, II. (2011). Generation of red blood cells from human induced pluripotent stem cells. *Stem Cells Dev*, *20*(9), 1639-1647. <https://doi.org/10.1089/scd.2011.0078>
- Dobbs, K., Dominguez Conde, C., Zhang, S. Y., Parolini, S., Audry, M., Chou, J., Haapaniemi, E., Keles, S., Bilic, I., Okada, S., Massaad, M. J., Rounioja, S., Alwahadneh, A. M., Serwas, N. K., Capuder, K., Ciftci, E., Felgentreff, K., Ohsumi, T. K., Pedergrana, V., . . . Notarangelo, L. D. (2015). Inherited DOCK2 Deficiency in Patients with Early-Onset Invasive Infections. *N Engl J Med*, *372*(25), 2409-2422. <https://doi.org/10.1056/NEJMoa1413462>
- Dorfleutner, A., & Stehlik, C. (2016). A dRAStic RHOAblock of Pyrin inflammasome activation. *Nat Immunol*, *17*(8), 900-902. <https://doi.org/10.1038/ni.3511>
- Dowds, T. A., Masumoto, J., Zhu, L., Inohara, N., & Núñez, G. (2004). Cryopyrin-induced interleukin 1 β secretion in monocytic cells: enhanced activity of disease-associated mutants and requirement for ASC. *J Biol Chem*, *279*(21), 21924-21928. <https://doi.org/10.1074/jbc.M401178200>
- Drenth, J. P., Cuisset, L., Grateau, G., Vasseur, C., van de Velde-Visser, S. D., de Jong, J. G., Beckmann, J. S., van der Meer, J. W., & Delpech, M. (1999). Mutations in the gene encoding mevalonate kinase cause hyper-IgD and periodic fever syndrome.

- International Hyper-IgD Study Group. *Nat Genet*, 22(2), 178-181. <https://doi.org/10.1038/9696>
- Driever, W., Solnica-Krezel, L., Schier, A. F., Neuhauss, S. C., Malicki, J., Stemple, D. L., Stainier, D. Y., Zwartkruis, F., Abdelilah, S., Rangini, Z., Belak, J., & Boggs, C. (1996). A genetic screen for mutations affecting embryogenesis in zebrafish. *Development*, 123, 37-46. <https://doi.org/10.1242/dev.123.1.37>
- Dupré, L., Aiuti, A., Trifari, S., Martino, S., Saracco, P., Bordignon, C., & Roncarolo, M. G. (2002). Wiskott-Aldrich syndrome protein regulates lipid raft dynamics during immunological synapse formation. *Immunity*, 17(2), 157-166. [https://doi.org/10.1016/s1074-7613\(02\)00360-6](https://doi.org/10.1016/s1074-7613(02)00360-6)
- Dupré, L., Boztug, K., & Pfajfer, L. (2021). Actin Dynamics at the T Cell Synapse as Revealed by Immune-Related Actinopathies. *Front Cell Dev Biol*, 9, 665519. <https://doi.org/10.3389/fcell.2021.665519>
- Dupré, L., & Prunier, G. (2023). Deciphering actin remodelling in immune cells through the prism of actin-related inborn errors of immunity. *Eur J Cell Biol*, 102(1), 151283. <https://doi.org/10.1016/j.ejcb.2022.151283>
- Dustin, M. L. (2007). Cell adhesion molecules and actin cytoskeleton at immune synapses and kinapses. *Curr Opin Cell Biol*, 19(5), 529-533. <https://doi.org/10.1016/j.ceb.2007.08.003>
- Dustin, M. L. (2008). T-cell activation through immunological synapses and kinapses. *Immunol Rev*, 221, 77-89. <https://doi.org/10.1111/j.1600-065X.2008.00589.x>
- Dustin, M. L. (2009). Modular design of immunological synapses and kinapses. *Cold Spring Harb Perspect Biol*, 1(1), a002873. <https://doi.org/10.1101/cshperspect.a002873>
- Dustin, M. L., & Cooper, J. A. (2000). The immunological synapse and the actin cytoskeleton: molecular hardware for T cell signaling. *Nat Immunol*, 1(1), 23-29. <https://doi.org/10.1038/76877>
- Edwards, D. C., Sanders, L. C., Bokoch, G. M., & Gill, G. N. (1999). Activation of LIM-kinase by Pak1 couples Rac/Cdc42 GTPase signalling to actin cytoskeletal dynamics. *Nat Cell Biol*, 1(5), 253-259. <https://doi.org/10.1038/12963>
- Edwards, M., Zwolak, A., Schafer, D. A., Sept, D., Dominguez, R., & Cooper, J. A. (2014). Capping protein regulators fine-tune actin assembly dynamics. *Nat Rev Mol Cell Biol*, 15(10), 677-689. <https://doi.org/10.1038/nrm3869>
- El Masri, R., & Delon, J. (2021). RHO GTPases: from new partners to complex immune syndromes. *Nat Rev Immunol*, 21(8), 499-513. <https://doi.org/10.1038/s41577-021-00500-7>
- Engelhardt, K. R., Gertz, M. E., Keles, S., Schaffer, A. A., Sigmund, E. C., Glocker, C., Saghafi, S., Pourpak, Z., Ceja, R., Sassi, A., Graham, L. E., Massaad, M. J., Mellouli, F., Ben-Mustapha, I., Khemiri, M., Kilic, S. S., Etzioni, A., Freeman, A. F., Thiel, J., . . . Grimbacher, B. (2015). The extended clinical phenotype of 64 patients with dedicator of cytokinesis 8 deficiency. *J Allergy Clin Immunol*, 136(2), 402-412. <https://doi.org/10.1016/j.jaci.2014.12.1945>
- Etienne-Manneville, S., & Hall, A. (2002). Rho GTPases in cell biology. *Nature*, 420(6916), 629-635. <https://doi.org/10.1038/nature01148>
- Fagerholm, S. C., Guenther, C., Lloret Asens, M., Savinko, T., & Uotila, L. M. (2019). Beta2-Integrins and Interacting Proteins in Leukocyte Trafficking, Immune Suppression, and Immunodeficiency Disease. *Front Immunol*, 10, 254. <https://doi.org/10.3389/fimmu.2019.00254>
- Fang, D., & Zhu, J. (2017). Dynamic balance between master transcription factors determines the fates and functions of CD4 T cell and innate lymphoid cell subsets. *J Exp Med*, 214(7), 1861-1876. <https://doi.org/10.1084/jem.20170494>
- Fealey, M. E., Horn, B., Coffman, C., Miller, R., Lin, A. Y., Thompson, A. R., Schramel, J., Groth, E., Hinderliter, A., Cembran, A., & Thomas, D. D. (2018). Dynamics of Dystrophin's Actin-Binding Domain. *Biophys J*, 115(3), 445-454. <https://doi.org/10.1016/j.bpj.2018.05.039>

- Feau, S., Schoenberger, S. P., Altman, A., & Beart, S. (2013). SLAT regulates CD8+ T cell clonal expansion in a Cdc42- and NFAT1-dependent manner. *J Immunol*, *190*(1), 174-183. <https://doi.org/10.4049/jimmunol.1201685>
- Fiesco-Roa, M. O., Giri, N., McReynolds, L. J., Best, A. F., & Alter, B. P. (2019). Genotype-phenotype associations in Fanconi anemia: A literature review. *Blood Rev*, *37*, 100589. <https://doi.org/10.1016/j.blre.2019.100589>
- Filipovich, A. H. (2009). Hemophagocytic lymphohistiocytosis (HLH) and related disorders. *Hematology Am Soc Hematol Educ Program*, 127-131. <https://doi.org/10.1182/asheducation-2009.1.127>
- Fischer, K. D., Kong, Y. Y., Nishina, H., Tedford, K., Marengère, L. E., Kozieradzki, I., Sasaki, T., Starr, M., Chan, G., Gardener, S., Nghiem, M. P., Bouchard, D., Barbacid, M., Bernstein, A., & Penninger, J. M. (1998). Vav is a regulator of cytoskeletal reorganization mediated by the T-cell receptor. *Curr Biol*, *8*(10), 554-562. [https://doi.org/10.1016/s0960-9822\(98\)70224-6](https://doi.org/10.1016/s0960-9822(98)70224-6)
- Fitzgerald, K. A., & Kagan, J. C. (2020). Toll-like Receptors and the Control of Immunity. *Cell*, *180*(6), 1044-1066. <https://doi.org/10.1016/j.cell.2020.02.041>
- Fleire, S. J., Goldman, J. P., Carrasco, Y. R., Weber, M., Bray, D., & Batista, F. D. (2006). B cell ligand discrimination through a spreading and contraction response. *Science*, *312*(5774), 738-741. <https://doi.org/10.1126/science.1123940>
- Fliedner, T. M., Graessle, D., Paulsen, C., & Reimers, K. (2002). Structure and function of bone marrow hemopoiesis: mechanisms of response to ionizing radiation exposure. *Cancer Biother Radiopharm*, *17*(4), 405-426. <https://doi.org/10.1089/108497802760363204>
- Flinn, A. M., & Gennery, A. R. (2022). Primary immune regulatory disorders: Undiagnosed needles in the haystack? *Orphanet J Rare Dis*, *17*(1), 99. <https://doi.org/10.1186/s13023-022-02249-1>
- Föger, N., Rangell, L., Danilenko, D. M., & Chan, A. C. (2006). Requirement for coronin 1 in T lymphocyte trafficking and cellular homeostasis. *Science*, *313*(5788), 839-842. <https://doi.org/10.1126/science.1130563>
- Fontenot, J. D., Gavin, M. A., & Rudensky, A. Y. (2003). Foxp3 programs the development and function of CD4+CD25+ regulatory T cells. *Nat Immunol*, *4*(4), 330-336. <https://doi.org/10.1038/ni904>
- Fowler, V. M. (2013). The human erythrocyte plasma membrane: a Rosetta Stone for decoding membrane-cytoskeleton structure. *Curr Top Membr*, *72*, 39-88. <https://doi.org/10.1016/b978-0-12-417027-8.00002-7>
- Franchi, L., Eigenbrod, T., & Núñez, G. (2009). Cutting edge: TNF-alpha mediates sensitization to ATP and silica via the NLRP3 inflammasome in the absence of microbial stimulation. *J Immunol*, *183*(2), 792-796. <https://doi.org/10.4049/jimmunol.0900173>
- Fraser, J. H., Rincón, M., McCoy, K. D., & Le Gros, G. (1999). CTLA4 ligation attenuates AP-1, NFAT and NF-kappaB activity in activated T cells. *Eur J Immunol*, *29*(3), 838-844. [https://doi.org/10.1002/\(sici\)1521-4141\(199903\)29:03<838::Aid-immu838>3.0.Co;2-p](https://doi.org/10.1002/(sici)1521-4141(199903)29:03<838::Aid-immu838>3.0.Co;2-p)
- Freel, B. A., Sheets, J. N., & Francis, K. R. (2020). iPSC modeling of rare pediatric disorders. *J Neurosci Methods*, *332*, 108533. <https://doi.org/10.1016/j.jneumeth.2019.108533>
- Freiberg, B. A., Kupfer, H., Maslanik, W., Delli, J., Kappler, J., Zaller, D. M., & Kupfer, A. (2002). Staging and resetting T cell activation in SMACs. *Nat Immunol*, *3*(10), 911-917. <https://doi.org/10.1038/ni836>
- Fritz, R. D., & Pertz, O. (2016). The dynamics of spatio-temporal Rho GTPase signaling: formation of signaling patterns. *F1000Res*, *5*. <https://doi.org/10.12688/f1000research.7370.1>
- Fujimi, A., Matsunaga, T., Kobune, M., Kawano, Y., Nagaya, T., Tanaka, I., Iyama, S., Hayashi, T., Sato, T., Miyanishi, K., Sagawa, T., Sato, Y., Takimoto, R., Takayama, T., Kato, J., Gasa, S., Sakai, H., Tsuchida, E., Ikebuchi, K., . . . Niitsu, Y. (2008). Ex vivo large-scale generation of human red blood cells from cord blood CD34+ cells by co-culturing with macrophages. *Int J Hematol*, *87*(4), 339-350. <https://doi.org/10.1007/s12185-008-0062-y>

- Fukui, Y., Hashimoto, O., Sanui, T., Oono, T., Koga, H., Abe, M., Inayoshi, A., Noda, M., Oike, M., Shirai, T., & Sasazuki, T. (2001). Haematopoietic cell-specific CDM family protein DOCK2 is essential for lymphocyte migration. *Nature*, *412*(6849), 826-831. <https://doi.org/10.1038/35090591>
- Gallagher, P. G. (2022). Anemia in the pediatric patient. *Blood*, *140*(6), 571-593. <https://doi.org/10.1182/blood.2020006479>
- Gambineri, E., Ciullini Mannurita, S., Hagin, D., Vignoli, M., Anover-Sombke, S., DeBoer, S., Segundo, G. R. S., Allenspach, E. J., Favre, C., Ochs, H. D., & Torgerson, T. R. (2018). Clinical, Immunological, and Molecular Heterogeneity of 173 Patients With the Phenotype of Immune Dysregulation, Polyendocrinopathy, Enteropathy, X-Linked (IPEX) Syndrome. *Front Immunol*, *9*, 2411. <https://doi.org/10.3389/fimmu.2018.02411>
- Gao, W., Yang, J., Liu, W., Wang, Y., & Shao, F. (2016). Site-specific phosphorylation and microtubule dynamics control Pysin inflammasome activation. *Proc Natl Acad Sci U S A*, *113*(33), E4857-4866. <https://doi.org/10.1073/pnas.1601700113>
- Garcia-Mata, R., Boulter, E., & Burridge, K. (2011). The 'invisible hand': regulation of RHO GTPases by RHOGDIs. *Nat Rev Mol Cell Biol*, *12*(8), 493-504. <https://doi.org/10.1038/nrm3153>
- García-Serna, A. M., Alcaraz-García, M. J., Ruiz-Lafuente, N., Sebastián-Ruiz, S., Martínez, C. M., Moya-Quiles, M. R., Minguela, A., García-Alonso, A. M., Martín-Orozco, E., & Parrado, A. (2016). Dock10 regulates CD23 expression and sustains B-cell lymphopoiesis in secondary lymphoid tissue. *Immunobiology*, *221*(12), 1343-1350. <https://doi.org/10.1016/j.imbio.2016.07.015>
- Gaud, G., Lesourne, R., & Love, P. E. (2018). Regulatory mechanisms in T cell receptor signalling. *Nat Rev Immunol*, *18*(8), 485-497. <https://doi.org/10.1038/s41577-018-0020-8>
- Gavin, M. A., Rasmussen, J. P., Fontenot, J. D., Vasta, V., Manganiello, V. C., Beavo, J. A., & Rudensky, A. Y. (2007). Foxp3-dependent programme of regulatory T-cell differentiation. *Nature*, *445*(7129), 771-775. <https://doi.org/10.1038/nature05543>
- Gerasimčik, N., He, M., Baptista, M. A. P., Severinson, E., & Westerberg, L. S. (2017). Deletion of Dock10 in B Cells Results in Normal Development but a Mild Deficiency upon In Vivo and In Vitro Stimulations. *Front Immunol*, *8*, 491. <https://doi.org/10.3389/fimmu.2017.00491>
- Germain, R. N. (2002). T-cell development and the CD4-CD8 lineage decision. *Nat Rev Immunol*, *2*(5), 309-322. <https://doi.org/10.1038/nri798>
- Gernez, Y., de Jesus, A. A., Alsaleem, H., Macaubas, C., Roy, A., Lovell, D., Jagadeesh, K. A., Alehashemi, S., Erdman, L., Grimley, M., Talarico, S., Bacchetta, R., Lewis, D. B., Canna, S. W., Laxer, R. M., Mellins, E. D., Goldbach-Mansky, R., & Weinacht, K. G. (2019). Severe autoinflammation in 4 patients with C-terminal variants in cell division control protein 42 homolog (CDC42) successfully treated with IL-1beta inhibition. *J Allergy Clin Immunol*, *144*(4), 1122-1125 e1126. <https://doi.org/10.1016/j.jaci.2019.06.017>
- Giarratana, M. C., Kobari, L., Lapillonne, H., Chalmers, D., Kiger, L., Cynober, T., Marden, M. C., Wajcman, H., & Douay, L. (2005). Ex vivo generation of fully mature human red blood cells from hematopoietic stem cells. *Nat Biotechnol*, *23*(1), 69-74. <https://doi.org/10.1038/nbt1047>
- Gluscock, J., Lenz, M., Hobby, K., & Jarecki, J. (2017). Cure SMA and our patient community celebrate the first approved drug for SMA. *Gene Ther*, *24*(9), 498-500. <https://doi.org/10.1038/gt.2017.39>
- Glaven, J. A., Whitehead, I. P., Nomanbhoy, T., Kay, R., & Cerione, R. A. (1996). Lfc and Lsc oncoproteins represent two new guanine nucleotide exchange factors for the Rho GTP-binding protein. *J Biol Chem*, *271*(44), 27374-27381. <https://doi.org/10.1074/jbc.271.44.27374>
- Go, R. S., Winters, J. L., & Kay, N. E. (2017). How I treat autoimmune hemolytic anemia. *Blood*, *129*(22), 2971-2979. <https://doi.org/10.1182/blood-2016-11-693689>
- Godin, I. (2016). 8 - Ontogeny of the Hematopoietic System. In R. Baldock, J. Bard, D. R. Davidson, & G. Morriss-Kay (Eds.), *Kaufman's Atlas of Mouse Development*

- Supplement* (pp. 111-120). Academic Press.
<https://doi.org/https://doi.org/10.1016/B978-0-12-800043-4.00008-7>
- Gokhin, D. S., & Fowler, V. M. (2016). Feisty filaments: actin dynamics in the red blood cell membrane skeleton. *Curr Opin Hematol*, 23(3), 206-214.
<https://doi.org/10.1097/moh.0000000000000227>
- Gollmer, K., Asperti-Boursin, F., Tanaka, Y., Okkenhaug, K., Vanhaesebroeck, B., Peterson, J. R., Fukui, Y., Donnadieu, E., & Stein, J. V. (2009). CCL21 mediates CD4+ T-cell costimulation via a DOCK2/Rac-dependent pathway. *Blood*, 114(3), 580-588.
<https://doi.org/10.1182/blood-2009-01-200923>
- Gómez del Arco, P., Martínez-Martínez, S., Maldonado, J. L., Ortega-Pérez, I., & Redondo, J. M. (2000). A role for the p38 MAP kinase pathway in the nuclear shuttling of NFATp. *J Biol Chem*, 275(18), 13872-13878. <https://doi.org/10.1074/jbc.275.18.13872>
- Goode, B. L., & Eck, M. J. (2007). Mechanism and function of formins in the control of actin assembly. *Annu Rev Biochem*, 76, 593-627.
<https://doi.org/10.1146/annurev.biochem.75.103004.142647>
- Gorman, J. A., Babich, A., Dick, C. J., Schoon, R. A., Koenig, A., Gomez, T. S., Burkhardt, J. K., & Billadeau, D. D. (2012). The cytoskeletal adaptor protein IQGAP1 regulates TCR-mediated signaling and filamentous actin dynamics. *J Immunol*, 188(12), 6135-6144.
<https://doi.org/10.4049/jimmunol.1103487>
- Gotoh, K., Tanaka, Y., Nishikimi, A., Inayoshi, A., Enjoji, M., Takayanagi, R., Sasazuki, T., & Fukui, Y. (2008). Differential requirement for DOCK2 in migration of plasmacytoid dendritic cells versus myeloid dendritic cells. *Blood*, 111(6), 2973-2976.
<https://doi.org/10.1182/blood-2007-09-112169>
- Gotoh, K., Tanaka, Y., Nishikimi, A., Nakamura, R., Yamada, H., Maeda, N., Ishikawa, T., Hoshino, K., Uruno, T., Cao, Q., Higashi, S., Kawaguchi, Y., Enjoji, M., Takayanagi, R., Kaisho, T., Yoshikai, Y., & Fukui, Y. (2010). Selective control of type I IFN induction by the Rac activator DOCK2 during TLR-mediated plasmacytoid dendritic cell activation. *J Exp Med*, 207(4), 721-730. <https://doi.org/10.1084/jem.20091776>
- Goudouris, E. S. (2021). Immunodeficiencies: non-infectious manifestations. *J Pediatr (Rio J)*, 97 Suppl 1(Suppl 1), S24-s33. <https://doi.org/10.1016/j.jpeds.2020.10.004>
- Graf, T., & Enver, T. (2009). Forcing cells to change lineages. *Nature*, 462(7273), 587-594.
<https://doi.org/10.1038/nature08533>
- Grandemange, S., Sanchez, E., Louis-Plence, P., Tran Mau-Them, F., Bessis, D., Coubes, C., Frouin, E., Seyger, M., Girard, M., Puechberty, J., Costes, V., Rodière, M., Carbasse, A., Jeziorski, E., Portales, P., Sarrabay, G., Mondain, M., Jorgensen, C., Apparailly, F., . . . Geneviève, D. (2017). A new autoinflammatory and autoimmune syndrome associated with NLRP1 mutations: NAIAD (NLRP1-associated autoinflammation with arthritis and dyskeratosis). *Ann Rheum Dis*, 76(7), 1191-1198.
<https://doi.org/10.1136/annrheumdis-2016-210021>
- Gray, J. L., von Delft, F., & Brennan, P. E. (2020). Targeting the Small GTPase Superfamily through Their Regulatory Proteins. *Angew Chem Int Ed Engl*, 59(16), 6342-6366.
<https://doi.org/10.1002/anie.201900585>
- Gudmundsson, S., Singer-Berk, M., Watts, N. A., Phu, W., Goodrich, J. K., Solomonson, M., Rehm, H. L., MacArthur, D. G., & O'Donnell-Luria, A. (2022). Variant interpretation using population databases: Lessons from gnomAD. *Hum Mutat*, 43(8), 1012-1030.
<https://doi.org/10.1002/humu.24309>
- Guo, F., Hildeman, D., Tripathi, P., Velu, C. S., Grimes, H. L., & Zheng, Y. (2010). Coordination of IL-7 receptor and T-cell receptor signaling by cell-division cycle 42 in T-cell homeostasis. *Proc Natl Acad Sci U S A*, 107(43), 18505-18510.
<https://doi.org/10.1073/pnas.1010249107>
- Guo, F., Zhang, S., Tripathi, P., Mattner, J., Phelan, J., Sproles, A., Mo, J., Wills-Karp, M., Grimes, H. L., Hildeman, D., & Zheng, Y. (2011). Distinct roles of Cdc42 in thymopoiesis and effector and memory T cell differentiation. *PLoS One*, 6(3), e18002.
<https://doi.org/10.1371/journal.pone.0018002>
- Gupta, S., Fanzo, J. C., Hu, C., Cox, D., Jang, S. Y., Lee, A. E., Greenberg, S., & Pernis, A. B. (2003). T cell receptor engagement leads to the recruitment of IBP, a novel guanine

- nucleotide exchange factor, to the immunological synapse. *J Biol Chem*, 278(44), 43541-43549. <https://doi.org/10.1074/jbc.M308960200>
- Guram, K., Kim, S. S., Wu, V., Sanders, P. D., Patel, S., Schoenberger, S. P., Cohen, E. E. W., Chen, S. Y., & Sharabi, A. B. (2019). A Threshold Model for T-Cell Activation in the Era of Checkpoint Blockade Immunotherapy. *Front Immunol*, 10, 491. <https://doi.org/10.3389/fimmu.2019.00491>
- Habibi, S., Zaki-Dizaji, M., Rafiemanesh, H., Lo, B., Jamee, M., Gámez-Díaz, L., Salami, F., Kamali, A. N., Mohammadi, H., Abolhassani, H., Yazdani, R., Aghamohammadi, A., Anaya, J. M., & Azizi, G. (2019). Clinical, Immunologic, and Molecular Spectrum of Patients with LPS-Responsive Beige-Like Anchor Protein Deficiency: A Systematic Review. *J Allergy Clin Immunol Pract*, 7(7), 2379-2386.e2375. <https://doi.org/10.1016/j.jaip.2019.04.011>
- Haire, R. N., Rast, J. P., Litman, R. T., & Litman, G. W. (2000). Characterization of three isotypes of immunoglobulin light chains and T-cell antigen receptor alpha in zebrafish. *Immunogenetics*, 51(11), 915-923. <https://doi.org/10.1007/s002510000229>
- Ham, H., Guerrier, S., Kim, J., Schoon, R. A., Anderson, E. L., Hamann, M. J., Lou, Z., & Billadeau, D. D. (2013). Deducator of cytokinesis 8 interacts with talin and Wiskott-Aldrich syndrome protein to regulate NK cell cytotoxicity. *J Immunol*, 190(7), 3661-3669. <https://doi.org/10.4049/jimmunol.1202792>
- Harada, Y., Tanaka, Y., Terasawa, M., Pieczyk, M., Habiro, K., Katakai, T., Hanawa-Suetsugu, K., Kukimoto-Niino, M., Nishizaki, T., Shirouzu, M., Duan, X., Uruno, T., Nishikimi, A., Sanematsu, F., Yokoyama, S., Stein, J. V., Kinashi, T., & Fukui, Y. (2012). DOCK8 is a Cdc42 activator critical for interstitial dendritic cell migration during immune responses. *Blood*, 119(19), 4451-4461. <https://doi.org/10.1182/blood-2012-01-407098>
- Harlan, J. E., Hajduk, P. J., Yoon, H. S., & Fesik, S. W. (1994). Pleckstrin homology domains bind to phosphatidylinositol-4,5-bisphosphate. *Nature*, 371(6493), 168-170. <https://doi.org/10.1038/371168a0>
- Harty, J. T., & Badovinac, V. P. (2008). Shaping and reshaping CD8+ T-cell memory. *Nat Rev Immunol*, 8(2), 107-119. <https://doi.org/10.1038/nri2251>
- Hayakawa, M., Kitagawa, H., Miyazawa, K., Kitagawa, M., & Kikugawa, K. (2005). The FWD1/beta-TrCP-mediated degradation pathway establishes a 'turning off switch' of a Cdc42 guanine nucleotide exchange factor, FGD1. *Genes Cells*, 10(3), 241-251. <https://doi.org/10.1111/j.1365-2443.2005.00834.x>
- He, T., Huang, Y., Ling, J., & Yang, J. (2020). A New Patient with NOCARH Syndrome Due to CDC42 Defect. *J Clin Immunol*, 40(4), 571-575. <https://doi.org/10.1007/s10875-020-00786-7>
- Heasman, S. J., & Ridley, A. J. (2008). Mammalian Rho GTPases: new insights into their functions from in vivo studies. *Nat Rev Mol Cell Biol*, 9(9), 690-701. <https://doi.org/10.1038/nrm2476>
- Heasman, S. J., & Ridley, A. J. (2010). Multiple roles for RhoA during T cell transendothelial migration. *Small GTPases*, 1(3), 174-179. <https://doi.org/10.4161/sgtp.1.3.14724>
- Helft, J., Anjos-Afonso, F., van der Veen, A. G., Chakravarty, P., Bonnet, D., & Reis e Sousa, C. (2017). Dendritic Cell Lineage Potential in Human Early Hematopoietic Progenitors. *Cell Rep*, 20(3), 529-537. <https://doi.org/10.1016/j.celrep.2017.06.075>
- Hermann-Kleiter, N., & Baier, G. (2010). NFAT pulls the strings during CD4+ T helper cell effector functions. *Blood*, 115(15), 2989-2997. <https://doi.org/10.1182/blood-2009-10-233585>
- Hirose, S., Takayama, N., Nakamura, S., Nagasawa, K., Ochi, K., Hirata, S., Yamazaki, S., Yamaguchi, T., Otsu, M., Sano, S., Takahashi, N., Sawaguchi, A., Ito, M., Kato, T., Nakauchi, H., & Eto, K. (2013). Immortalization of erythroblasts by c-MYC and BCL-XL enables large-scale erythrocyte production from human pluripotent stem cells. *Stem Cell Reports*, 1(6), 499-508. <https://doi.org/10.1016/j.stemcr.2013.10.010>
- Hodge, R. G., & Ridley, A. J. (2016). Regulating Rho GTPases and their regulators. *Nat Rev Mol Cell Biol*, 17(8), 496-510. <https://doi.org/10.1038/nrm.2016.67>
- Hoffman, H. M., Mueller, J. L., Broide, D. H., Wanderer, A. A., & Kolodner, R. D. (2001). Mutation of a new gene encoding a putative pyrin-like protein causes familial cold

- autoinflammatory syndrome and Muckle-Wells syndrome. *Nat Genet*, 29(3), 301-305. <https://doi.org/10.1038/ng756>
- Hoggatt, J. (2016). Gene Therapy for "Bubble Boy" Disease. *Cell*, 166(2), 263. <https://doi.org/10.1016/j.cell.2016.06.049>
- Holsinger, L. J., Graef, I. A., Swat, W., Chi, T., Bautista, D. M., Davidson, L., Lewis, R. S., Alt, F. W., & Crabtree, G. R. (1998). Defects in actin-cap formation in Vav-deficient mice implicate an actin requirement for lymphocyte signal transduction. *Curr Biol*, 8(10), 563-572. [https://doi.org/10.1016/s0960-9822\(98\)70225-8](https://doi.org/10.1016/s0960-9822(98)70225-8)
- Hori, S., Nomura, T., & Sakaguchi, S. (2003). Control of regulatory T cell development by the transcription factor Foxp3. *Science*, 299(5609), 1057-1061. <https://doi.org/10.1126/science.1079490>
- Houmadi, R., Guipouy, D., Rey-Barroso, J., Vasconcelos, Z., Cornet, J., Manghi, M., Destainville, N., Valitutti, S., Allart, S., & Dupré, L. (2018). The Wiskott-Aldrich Syndrome Protein Contributes to the Assembly of the LFA-1 Nanocluster Belt at the Lytic Synapse. *Cell Rep*, 22(4), 979-991. <https://doi.org/10.1016/j.celrep.2017.12.088>
- Houten, S. M., Kuis, W., Duran, M., de Koning, T. J., van Royen-Kerkhof, A., Romeijn, G. J., Frenkel, J., Dorland, L., de Barse, M. M., Huijbers, W. A., Rijkers, G. T., Waterham, H. R., Wanders, R. J., & Poll-The, B. T. (1999). Mutations in MVK, encoding mevalonate kinase, cause hyperimmunoglobulinaemia D and periodic fever syndrome. *Nat Genet*, 22(2), 175-177. <https://doi.org/10.1038/9691>
- Hoy, S. M. (2019). Onasemnogene Apeparovvec: First Global Approval. *Drugs*, 79(11), 1255-1262. <https://doi.org/10.1007/s40265-019-01162-5>
- Hsu, A. P., Donkó, A., Arrington, M. E., Swamydas, M., Fink, D., Das, A., Escobedo, O., Bonagura, V., Szabolcs, P., Steinberg, H. N., Bergerson, J., Skoskiewicz, A., Makhija, M., Davis, J., Foruraghi, L., Palmer, C., Fuleihan, R. L., Church, J. A., Bhandoola, A., . . . Holland, S. M. (2019). Dominant activating RAC2 mutation with lymphopenia, immunodeficiency, and cytoskeletal defects. *Blood*, 133(18), 1977-1988. <https://doi.org/10.1182/blood-2018-11-886028>
- Huang, X., Shah, S., Wang, J., Ye, Z., Dowe, S. N., Tsang, K. M., Mendelsohn, L. G., Kato, G. J., Kickler, T. S., & Cheng, L. (2014). Extensive ex vivo expansion of functional human erythroid precursors established from umbilical cord blood cells by defined factors. *Mol Ther*, 22(2), 451-463. <https://doi.org/10.1038/mt.2013.201>
- Imam, T., Park, S., Kaplan, M. H., & Olson, M. R. (2018). Effector T Helper Cell Subsets in Inflammatory Bowel Diseases. *Front Immunol*, 9, 1212. <https://doi.org/10.3389/fimmu.2018.01212>
- Ivanovs, A., Rybtsov, S., Ng, E. S., Stanley, E. G., Elefanty, A. G., & Medvinsky, A. (2017). Human haematopoietic stem cell development: from the embryo to the dish. *Development*, 144(13), 2323-2337. <https://doi.org/10.1242/dev.134866>
- Ivanovs, A., Rybtsov, S., Welch, L., Anderson, R. A., Turner, M. L., & Medvinsky, A. (2011). Highly potent human hematopoietic stem cells first emerge in the intraembryonic aorta-gonad-mesonephros region. *J Exp Med*, 208(12), 2417-2427. <https://doi.org/10.1084/jem.20111688>
- Iwasaki, A., & Medzhitov, R. (2010). Regulation of adaptive immunity by the innate immune system. *Science*, 327(5963), 291-295. <https://doi.org/10.1126/science.1183021>
- Iwasaki, H., & Akashi, K. (2007). Myeloid lineage commitment from the hematopoietic stem cell. *Immunity*, 26(6), 726-740. <https://doi.org/10.1016/j.immuni.2007.06.004>
- Jabara, H. H., McDonald, D. R., Janssen, E., Massaad, M. J., Ramesh, N., Borzutzky, A., Rauter, I., Benson, H., Schneider, L., Baxi, S., Recher, M., Notarangelo, L. D., Wakim, R., Dbaibo, G., Dasouki, M., Al-Herz, W., Barlan, I., Baris, S., Kutukculer, N., . . . Geha, R. S. (2012). DOCK8 functions as an adaptor that links TLR-MyD88 signaling to B cell activation. *Nat Immunol*, 13(6), 612-620. <https://doi.org/10.1038/ni.2305>
- Jacobelli, J., Chmura, S. A., Buxton, D. B., Davis, M. M., & Krummel, M. F. (2004). A single class II myosin modulates T cell motility and stopping, but not synapse formation. *Nat Immunol*, 5(5), 531-538. <https://doi.org/10.1038/ni1065>

- Jacquemet, G., Hamidi, H., & Ivaska, J. (2015). Filopodia in cell adhesion, 3D migration and cancer cell invasion. *Curr Opin Cell Biol*, 36, 23-31. <https://doi.org/10.1016/j.ceb.2015.06.007>
- Jaffe, A. B., & Hall, A. (2005). Rho GTPases: biochemistry and biology. *Annu Rev Cell Dev Biol*, 21, 247-269. <https://doi.org/10.1146/annurev.cellbio.21.020604.150721>
- Jaiswal, M., Gremer, L., Dvorsky, R., Haeusler, L. C., Cirstea, I. C., Uhlenbrock, K., & Ahmadian, M. R. (2011). Mechanistic insights into specificity, activity, and regulatory elements of the regulator of G-protein signaling (RGS)-containing Rho-specific guanine nucleotide exchange factors (GEFs) p115, PDZ-RhoGEF (PRG), and leukemia-associated RhoGEF (LARG). *J Biol Chem*, 286(20), 18202-18212. <https://doi.org/10.1074/jbc.M111.226431>
- Jamilloux, Y., Magnotti, F., Belot, A., & Henry, T. (2018). The pyrin inflammasome: from sensing RhoA GTPases-inhibiting toxins to triggering autoinflammatory syndromes. *Pathog Dis*, 76(3). <https://doi.org/10.1093/femspd/fty020>
- Janka, G. E. (2007). Hemophagocytic syndromes. *Blood Rev*, 21(5), 245-253. <https://doi.org/10.1016/j.blre.2007.05.001>
- Janka, G. E., & Lehmborg, K. (2013). Hemophagocytic lymphohistiocytosis: pathogenesis and treatment. *Hematology Am Soc Hematol Educ Program*, 2013, 605-611. <https://doi.org/10.1182/asheducation-2013.1.605>
- Janssen, E., & Geha, R. S. (2019). Primary immunodeficiencies caused by mutations in actin regulatory proteins. *Immunol Rev*, 287(1), 121-134. <https://doi.org/10.1111/imr.12716>
- Janssen, E., Kumari, S., Tohme, M., Ullas, S., Barrera, V., Tas, J. M., Castillo-Rama, M., Bronson, R. T., Usmani, S. M., Irvine, D. J., Mempel, T. R., & Geha, R. S. (2017). DOCK8 enforces immunological tolerance by promoting IL-2 signaling and immune synapse formation in Tregs. *JCI Insight*, 2(19). <https://doi.org/10.1172/jci.insight.94298>
- Janssen, E., Morbach, H., Ullas, S., Bannock, J. M., Massad, C., Menard, L., Barlan, I., Lefranc, G., Su, H., Dasouki, M., Al-Herz, W., Keles, S., Chatila, T., Geha, R. S., & Meffre, E. (2014). Deducator of cytokinesis 8-deficient patients have a breakdown in peripheral B-cell tolerance and defective regulatory T cells. *J Allergy Clin Immunol*, 134(6), 1365-1374. <https://doi.org/10.1016/j.jaci.2014.07.042>
- Ji, P., Jayapal, S. R., & Lodish, H. F. (2008). Enucleation of cultured mouse fetal erythroblasts requires Rac GTPases and mDia2. *Nat Cell Biol*, 10(3), 314-321. <https://doi.org/10.1038/ncb1693>
- Jing, L., & Zon, L. I. (2011). Zebrafish as a model for normal and malignant hematopoiesis. *Dis Model Mech*, 4(4), 433-438. <https://doi.org/10.1242/dmm.006791>
- Josefowicz, S. Z., Lu, L. F., & Rudensky, A. Y. (2012). Regulatory T cells: mechanisms of differentiation and function. *Annu Rev Immunol*, 30, 531-564. <https://doi.org/10.1146/annurev.immunol.25.022106.141623>
- Kalfa, T. A., Pushkaran, S., Mohandas, N., Hartwig, J. H., Fowler, V. M., Johnson, J. F., Joiner, C. H., Williams, D. A., & Zheng, Y. (2006). Rac GTPases regulate the morphology and deformability of the erythrocyte cytoskeleton. *Blood*, 108(12), 3637-3645. <https://doi.org/10.1182/blood-2006-03-005942>
- Kalinichenko, A., Perinetti Casoni, G., Dupré, L., Trotta, L., Huemer, J., Galgano, D., German, Y., Haladik, B., Pazmandi, J., Thian, M., Yüce Petronczki, Ö., Chiang, S. C., Taskinen, M., Hekkala, A., Kauppila, S., Lindgren, O., Tapiainen, T., Kraakman, M. J., Vetterranta, K., . . . Boztug, K. (2021). RhoG deficiency abrogates cytotoxicity of human lymphocytes and causes hemophagocytic lymphohistiocytosis. *Blood*, 137(15), 2033-2045. <https://doi.org/10.1182/blood.2020008738>
- Karczewski, K. J., Francioli, L. C., Tiao, G., Cummings, B. B., Alfoldi, J., Wang, Q., Collins, R. L., Laricchia, K. M., Ganna, A., Birnbaum, D. P., Gauthier, L. D., Brand, H., Solomonson, M., Watts, N. A., Rhodes, D., Singer-Berk, M., England, E. M., Seaby, E. G., Kosmicki, J. A., . . . MacArthur, D. G. (2020). The mutational constraint spectrum quantified from variation in 141,456 humans. *Nature*, 581(7809), 434-443. <https://doi.org/10.1038/s41586-020-2308-7>
- Karlsson, M., Zhang, C., Méar, L., Zhong, W., Digre, A., Katona, B., Sjöstedt, E., Butler, L., Odeberg, J., Dusart, P., Edfors, F., Oksvold, P., von Feilitzen, K., Zwahlen, M., Arif, M.,

- Altay, O., Li, X., Ozcan, M., Mardinoglu, A., . . . Lindskog, C. (2021). A single-cell type transcriptomics map of human tissues. *Sci Adv*, 7(31). <https://doi.org/10.1126/sciadv.abh2169>
- Katagiri, K., Katakai, T., Ebisuno, Y., Ueda, Y., Okada, T., & Kinashi, T. (2009). Mst1 controls lymphocyte trafficking and interstitial motility within lymph nodes. *Embo j*, 28(9), 1319-1331. <https://doi.org/10.1038/emboj.2009.82>
- Kaustio, M., Nayebzadeh, N., Hinttala, R., Tapiainen, T., Åström, P., Mamia, K., Perna, N., Lehtonen, J., Glumoff, V., Rahikkala, E., Honkila, M., Olsén, P., Hassinen, A., Polso, M., Al Sukaiti, N., Al Shekaili, J., Al Kindi, M., Al Hashmi, N., Almusa, H., . . . Saarela, J. (2021). Loss of DIAPH1 causes SCBMS, combined immunodeficiency, and mitochondrial dysfunction. *J Allergy Clin Immunol*, 148(2), 599-611. <https://doi.org/10.1016/j.jaci.2020.12.656>
- Keam, S. J. (2022). Eladocagene Exuparvovec: First Approval. *Drugs*, 82(13), 1427-1432. <https://doi.org/10.1007/s40265-022-01775-3>
- Kearney, C. J., Randall, K. L., & Oliaro, J. (2017). DOCK8 regulates signal transduction events to control immunity. *Cell Mol Immunol*, 14(5), 406-411. <https://doi.org/10.1038/cmi.2017.9>
- Khan, A. A., Hanada, T., Mohseni, M., Jeong, J. J., Zeng, L., Gaetani, M., Li, D., Reed, B. C., Speicher, D. W., & Chishti, A. H. (2008). Dematin and adducin provide a novel link between the spectrin cytoskeleton and human erythrocyte membrane by directly interacting with glucose transporter-1. *J Biol Chem*, 283(21), 14600-14609. <https://doi.org/10.1074/jbc.M707818200>
- Khattri, R., Cox, T., Yasayko, S. A., & Ramsdell, F. (2003). An essential role for Scurfin in CD4+CD25+ T regulatory cells. *Nat Immunol*, 4(4), 337-342. <https://doi.org/10.1038/ni909>
- Kim, A. S., Kakalis, L. T., Abdul-Manan, N., Liu, G. A., & Rosen, M. K. (2000). Autoinhibition and activation mechanisms of the Wiskott-Aldrich syndrome protein. *Nature*, 404(6774), 151-158. <https://doi.org/10.1038/35004513>
- Kim, M. L., Chae, J. J., Park, Y. H., De Nardo, D., Stirzaker, R. A., Ko, H. J., Tye, H., Cengia, L., DiRago, L., Metcalf, D., Roberts, A. W., Kastner, D. L., Lew, A. M., Lyras, D., Kile, B. T., Croker, B. A., & Masters, S. L. (2015). Aberrant actin depolymerization triggers the pyrin inflammasome and autoinflammatory disease that is dependent on IL-18, not IL-1beta. *J Exp Med*, 212(6), 927-938. <https://doi.org/10.1084/jem.20142384>
- Kircher, M., Witten, D. M., Jain, P., O'Roak, B. J., Cooper, G. M., & Shendure, J. (2014). A general framework for estimating the relative pathogenicity of human genetic variants. *Nat Genet*, 46(3), 310-315. <https://doi.org/10.1038/ng.2892>
- Klee, C. B., Ren, H., & Wang, X. (1998). Regulation of the calmodulin-stimulated protein phosphatase, calcineurin. *J Biol Chem*, 273(22), 13367-13370. <https://doi.org/10.1074/jbc.273.22.13367>
- Klein, L., Kyewski, B., Allen, P. M., & Hogquist, K. A. (2014). Positive and negative selection of the T cell repertoire: what thymocytes see (and don't see). *Nat Rev Immunol*, 14(6), 377-391. <https://doi.org/10.1038/nri3667>
- Kobayashi, S., Shirai, T., Kiyokawa, E., Mochizuki, N., Matsuda, M., & Fukui, Y. (2001). Membrane recruitment of DOCK180 by binding to PtdIns(3,4,5)P3. *Biochem J*, 354(Pt 1), 73-78. <https://doi.org/10.1042/0264-6021:3540073>
- Kolhatkar, N. S., Scharping, N. E., Sullivan, J. M., Jacobs, H. M., Schwartz, M. A., Khim, S., Notarangelo, L. D., Thrasher, A. J., Rawlings, D. J., & Jackson, S. W. (2015). B-cell intrinsic TLR7 signals promote depletion of the marginal zone in a murine model of Wiskott-Aldrich syndrome. *Eur J Immunol*, 45(10), 2773-2779. <https://doi.org/10.1002/eji.201545644>
- Kondo, M., Weissman, I. L., & Akashi, K. (1997). Identification of clonogenic common lymphoid progenitors in mouse bone marrow. *Cell*, 91(5), 661-672. [https://doi.org/10.1016/s0092-8674\(00\)80453-5](https://doi.org/10.1016/s0092-8674(00)80453-5)
- Koshino, I., Mohandas, N., & Takakuwa, Y. (2012). Identification of a novel role for dematin in regulating red cell membrane function by modulating spectrin-actin interaction. *J Biol Chem*, 287(42), 35244-35250. <https://doi.org/10.1074/jbc.M111.305441>

- Krause, M., & Gautreau, A. (2014). Steering cell migration: lamellipodium dynamics and the regulation of directional persistence. *Nat Rev Mol Cell Biol*, *15*(9), 577-590. <https://doi.org/10.1038/nrm3861>
- Kress, H., Stelzer, E. H., Holzer, D., Buss, F., Griffiths, G., & Rohrbach, A. (2007). Filopodia act as phagocytic tentacles and pull with discrete steps and a load-dependent velocity. *Proc Natl Acad Sci U S A*, *104*(28), 11633-11638. <https://doi.org/10.1073/pnas.0702449104>
- Krishnan, K., & Moens, P. D. J. (2009). Structure and functions of profilins. *Biophys Rev*, *1*(2), 71-81. <https://doi.org/10.1007/s12551-009-0010-y>
- Krishnaswamy, J. K., Singh, A., Gowthaman, U., Wu, R., Gorrepati, P., Sales Nascimento, M., Gallman, A., Liu, D., Rhebergen, A. M., Calabro, S., Xu, L., Ranney, P., Srivastava, A., Ranson, M., Gorham, J. D., McCaw, Z., Kleeberger, S. R., Heinz, L. X., Müller, A. C., . . . Eisenbarth, S. C. (2015). Coincidental loss of DOCK8 function in NLRP10-deficient and C3H/HeJ mice results in defective dendritic cell migration. *Proc Natl Acad Sci U S A*, *112*(10), 3056-3061. <https://doi.org/10.1073/pnas.1501554112>
- Kritikou, J. S., Dahlberg, C. I., Baptista, M. A., Wagner, A. K., Banerjee, P. P., Gwalani, L. A., Poli, C., Panda, S. K., Kärre, K., Kaech, S. M., Wermeling, F., Andersson, J., Orange, J. S., Brauner, H., & Westerberg, L. S. (2016). IL-2 in the tumor microenvironment is necessary for Wiskott-Aldrich syndrome protein deficient NK cells to respond to tumors in vivo. *Sci Rep*, *6*, 30636. <https://doi.org/10.1038/srep30636>
- Krummel, M. F., & Allison, J. P. (1996). CTLA-4 engagement inhibits IL-2 accumulation and cell cycle progression upon activation of resting T cells. *J Exp Med*, *183*(6), 2533-2540. <https://doi.org/10.1084/jem.183.6.2533>
- Kuehn, H. S., Ouyang, W., Lo, B., Deenick, E. K., Niemela, J. E., Avery, D. T., Schickel, J. N., Tran, D. Q., Stoddard, J., Zhang, Y., Frucht, D. M., Dumitriu, B., Scheinberg, P., Folio, L. R., Frein, C. A., Price, S., Koh, C., Heller, T., Seroogy, C. M., . . . Uzel, G. (2014). Immune dysregulation in human subjects with heterozygous germline mutations in CTLA4. *Science*, *345*(6204), 1623-1627. <https://doi.org/10.1126/science.1255904>
- Kuhlman, P. A., Hughes, C. A., Bennett, V., & Fowler, V. M. (1996). A new function for adducin. Calcium/calmodulin-regulated capping of the barbed ends of actin filaments. *J Biol Chem*, *271*(14), 7986-7991. <https://doi.org/10.1074/jbc.271.14.7986>
- Kuijk, L. M., Beekman, J. M., Koster, J., Waterham, H. R., Frenkel, J., & Coffey, P. J. (2008). HMG-CoA reductase inhibition induces IL-1beta release through Rac1/PI3K/PKB-dependent caspase-1 activation. *Blood*, *112*(9), 3563-3573. <https://doi.org/10.1182/blood-2008-03-144667>
- Kulkarni, K., Yang, J., Zhang, Z., & Barford, D. (2011). Multiple factors confer specific Cdc42 and Rac protein activation by dedicator of cytokinesis (DOCK) nucleotide exchange factors. *J Biol Chem*, *286*(28), 25341-25351. <https://doi.org/10.1074/jbc.M111.236455>
- Kulkeaw, K., Inoue, T., Ishitani, T., Nakanishi, Y., Zon, L. I., & Sugiyama, D. (2018). Purification of zebrafish erythrocytes as a means of identifying a novel regulator of haematopoiesis. *Br J Haematol*, *180*(3), 420-431. <https://doi.org/10.1111/bjh.15048>
- Kulkeaw, K., & Sugiyama, D. (2012). Zebrafish erythropoiesis and the utility of fish as models of anemia. *Stem Cell Res Ther*, *3*(6), 55. <https://doi.org/10.1186/scrt146>
- Kumari, S., Curado, S., Mayya, V., & Dustin, M. L. (2014). T cell antigen receptor activation and actin cytoskeleton remodeling. *Biochim Biophys Acta*, *1838*(2), 546-556. <https://doi.org/10.1016/j.bbamem.2013.05.004>
- Kunimura, K., Uruno, T., & Fukui, Y. (2020). DOCK family proteins: key players in immune surveillance mechanisms. *Int Immunol*, *32*(1), 5-15. <https://doi.org/10.1093/intimm/dxz067>
- Kunisaki, Y., Nishikimi, A., Tanaka, Y., Takii, R., Noda, M., Inayoshi, A., Watanabe, K., Sanematsu, F., Sasazuki, T., Sasaki, T., & Fukui, Y. (2006). DOCK2 is a Rac activator that regulates motility and polarity during neutrophil chemotaxis. *J Cell Biol*, *174*(5), 647-652. <https://doi.org/10.1083/jcb.200602142>
- Kurita, R., Suda, N., Sudo, K., Miharada, K., Hiroyama, T., Miyoshi, H., Tani, K., & Nakamura, Y. (2013). Establishment of immortalized human erythroid progenitor cell lines able to

- produce enucleated red blood cells. *PLoS One*, 8(3), e59890. <https://doi.org/10.1371/journal.pone.0059890>
- Lafouresse, F., Cotta-de-Almeida, V., Malet-Engra, G., Galy, A., Valitutti, S., & Dupré, L. (2012). Wiskott-Aldrich syndrome protein controls antigen-presenting cell-driven CD4+ T-cell motility by regulating adhesion to intercellular adhesion molecule-1. *Immunology*, 137(2), 183-196. <https://doi.org/10.1111/j.1365-2567.2012.03620.x>
- Lam, M. T., Coppola, S., Krumbach, O. H. F., Prencipe, G., Insalaco, A., Cifaldi, C., Brigida, I., Zara, E., Scala, S., Di Cesare, S., Martinelli, S., Di Rocco, M., Pascarella, A., Niceta, M., Pantaleoni, F., Ciolfi, A., Netter, P., Carisey, A. F., Diehl, M., . . . Tartaglia, M. (2019). A novel disorder involving dyshematopoiesis, inflammation, and HLH due to aberrant CDC42 function. *J Exp Med*, 216(12), 2778-2799. <https://doi.org/10.1084/jem.20190147>
- Lam, S. H., Chua, H. L., Gong, Z., Lam, T. J., & Sin, Y. M. (2004). Development and maturation of the immune system in zebrafish, *Danio rerio*: a gene expression profiling, in situ hybridization and immunological study. *Dev Comp Immunol*, 28(1), 9-28. [https://doi.org/10.1016/s0145-305x\(03\)00103-4](https://doi.org/10.1016/s0145-305x(03)00103-4)
- Langenau, D. M., Ferrando, A. A., Traver, D., Kutok, J. L., Hezel, J. P., Kanki, J. P., Zon, L. I., Look, A. T., & Trede, N. S. (2004). In vivo tracking of T cell development, ablation, and engraftment in transgenic zebrafish. *Proc Natl Acad Sci U S A*, 101(19), 7369-7374. <https://doi.org/10.1073/pnas.0402248101>
- Lanzi, G., Moratto, D., Vairo, D., Masneri, S., Delmonte, O., Paganini, T., Parolini, S., Tabellini, G., Mazza, C., Savoldi, G., Montin, D., Martino, S., Tovo, P., Pessach, I. M., Massaad, M. J., Ramesh, N., Porta, F., Plebani, A., Notarangelo, L. D., . . . Giliani, S. (2012). A novel primary human immunodeficiency due to deficiency in the WASP-interacting protein WIP. *J Exp Med*, 209(1), 29-34. <https://doi.org/10.1084/jem.20110896>
- Le Floc'h, A., Tanaka, Y., Bantilan, N. S., Voisinne, G., Altan-Bonnet, G., Fukui, Y., & Huse, M. (2013). Annular PIP3 accumulation controls actin architecture and modulates cytotoxicity at the immunological synapse. *J Exp Med*, 210(12), 2721-2737. <https://doi.org/10.1084/jem.20131324>
- LeBien, T. W., & Tedder, T. F. (2008). B lymphocytes: how they develop and function. *Blood*, 112(5), 1570-1580. <https://doi.org/10.1182/blood-2008-02-078071>
- Lee, D., Fong, K. P., King, M. R., Brass, L. F., & Hammer, D. A. (2012). Differential dynamics of platelet contact and spreading. *Biophys J*, 102(3), 472-482. <https://doi.org/10.1016/j.bpj.2011.10.056>
- Lee, G. S., Subramanian, N., Kim, A. I., Aksentijevich, I., Goldbach-Mansky, R., Sacks, D. B., Germain, R. N., Kastner, D. L., & Chae, J. J. (2012). The calcium-sensing receptor regulates the NLRP3 inflammasome through Ca²⁺ and cAMP. *Nature*, 492(7427), 123-127. <https://doi.org/10.1038/nature11588>
- Lee, P. P., Lobato-Marquez, D., Pramanik, N., Sirianni, A., Daza-Cajigal, V., Rivers, E., Cavazza, A., Bouma, G., Moulding, D., Hultenby, K., Westerberg, L. S., Hollinshead, M., Lau, Y. L., Burns, S. O., Mostowy, S., Bajaj-Elliott, M., & Thrasher, A. J. (2017). Wiskott-Aldrich syndrome protein regulates autophagy and inflammasome activity in innate immune cells. *Nat Commun*, 8(1), 1576. <https://doi.org/10.1038/s41467-017-01676-0>
- Lemmon, M. A. (2007). Pleckstrin homology (PH) domains and phosphoinositides. *Biochem Soc Symp*(74), 81-93. <https://doi.org/10.1042/bss0740081>
- Li, X., & Bennett, V. (1996). Identification of the spectrin subunit and domains required for formation of spectrin/adducin/actin complexes. *J Biol Chem*, 271(26), 15695-15702. <https://doi.org/10.1074/jbc.271.26.15695>
- Li, X., Matsuoka, Y., & Bennett, V. (1998). Adducin preferentially recruits spectrin to the fast growing ends of actin filaments in a complex requiring the MARCKS-related domain and a newly defined oligomerization domain. *J Biol Chem*, 273(30), 19329-19338. <https://doi.org/10.1074/jbc.273.30.19329>
- Lieschke, G. J., & Currie, P. D. (2007). Animal models of human disease: zebrafish swim into view. *Nat Rev Genet*, 8(5), 353-367. <https://doi.org/10.1038/nrg2091>

- Lin, B., & Goldbach-Mansky, R. (2022). Pathogenic insights from genetic causes of autoinflammatory inflammasomopathies and interferonopathies. *J Allergy Clin Immunol*, 149(3), 819-832. <https://doi.org/10.1016/j.jaci.2021.10.027>
- Lin, Q., Yang, W., Baird, D., Feng, Q., & Cerione, R. A. (2006). Identification of a DOCK180-related guanine nucleotide exchange factor that is capable of mediating a positive feedback activation of Cdc42. *J Biol Chem*, 281(46), 35253-35262. <https://doi.org/10.1074/jbc.M606248200>
- Lin, W., Haribhai, D., Relland, L. M., Truong, N., Carlson, M. R., Williams, C. B., & Chatila, T. A. (2007). Regulatory T cell development in the absence of functional Foxp3. *Nat Immunol*, 8(4), 359-368. <https://doi.org/10.1038/ni1445>
- Linder, S., Nelson, D., Weiss, M., & Aepfelbacher, M. (1999). Wiskott-Aldrich syndrome protein regulates podosomes in primary human macrophages. *Proc Natl Acad Sci U S A*, 96(17), 9648-9653. <https://doi.org/10.1073/pnas.96.17.9648>
- Lo, B., Zhang, K., Lu, W., Zheng, L., Zhang, Q., Kanellopoulou, C., Zhang, Y., Liu, Z., Fritz, J. M., Marsh, R., Husami, A., Kissell, D., Nortman, S., Chaturvedi, V., Haines, H., Young, L. R., Mo, J., Filipovich, A. H., Bleesing, J. J., . . . Jordan, M. B. (2015). AUTOIMMUNE DISEASE. Patients with LRBA deficiency show CTLA4 loss and immune dysregulation responsive to abatacept therapy. *Science*, 349(6246), 436-440. <https://doi.org/10.1126/science.aaa1663>
- Locard-Paulet, M., Voisinne, G., Froment, C., Goncalves Menoita, M., Ounoughene, Y., Girard, L., Gregoire, C., Mori, D., Martinez, M., Luche, H., Garin, J., Malissen, M., Burlet-Schiltz, O., Malissen, B., Gonzalez de Peredo, A., & Roncagalli, R. (2020). LymphoAtlas: a dynamic and integrated phosphoproteomic resource of TCR signaling in primary T cells reveals ITSN2 as a regulator of effector functions. *Mol Syst Biol*, 16(7), e9524. <https://doi.org/10.15252/msb.20209524>
- López-Nevado, M., González-Granado, L. I., Ruiz-García, R., Pleguezuelo, D., Cabrera-Marante, O., Salmón, N., Blanco-Lobo, P., Domínguez-Pinilla, N., Rodríguez-Pena, R., Sebastián, E., Cruz-Rojo, J., Olbrich, P., Ruiz-Contreras, J., Paz-Artal, E., Neth, O., & Allende, L. M. (2021). Primary Immune Regulatory Disorders With an Autoimmune Lymphoproliferative Syndrome-Like Phenotype: Immunologic Evaluation, Early Diagnosis and Management. *Front Immunol*, 12, 671755. <https://doi.org/10.3389/fimmu.2021.671755>
- Lougaris, V., Chou, J., Beano, A., Wallace, J. G., Baronio, M., Gazzurelli, L., Lorenzini, T., Moratto, D., Tabellini, G., Parolini, S., Seleman, M., Stafstrom, K., Xu, H., Harris, C., Geha, R. S., & Plebani, A. (2019). A monoallelic activating mutation in RAC2 resulting in a combined immunodeficiency. *J Allergy Clin Immunol*, 143(4), 1649-1653.e1643. <https://doi.org/10.1016/j.jaci.2019.01.001>
- Loughran, S. J., Haas, S., Wilkinson, A. C., Klein, A. M., & Brand, M. (2020). Lineage commitment of hematopoietic stem cells and progenitors: insights from recent single cell and lineage tracing technologies. *Exp Hematol*, 88, 1-6. <https://doi.org/10.1016/j.exphem.2020.07.002>
- Lux, S. E. t. (2016). Anatomy of the red cell membrane skeleton: unanswered questions. *Blood*, 127(2), 187-199. <https://doi.org/10.1182/blood-2014-12-512772>
- Lyons, S. E., Lawson, N. D., Lei, L., Bennett, P. E., Weinstein, B. M., & Liu, P. P. (2002). A nonsense mutation in zebrafish gata1 causes the bloodless phenotype in vlad tepes. *Proc Natl Acad Sci U S A*, 99(8), 5454-5459. <https://doi.org/10.1073/pnas.082695299>
- Ma, C. C., Wang, Z. L., Xu, T., He, Z. Y., & Wei, Y. Q. (2020). The approved gene therapy drugs worldwide: from 1998 to 2019. *Biotechnol Adv*, 40, 107502. <https://doi.org/10.1016/j.biotechadv.2019.107502>
- Macian, F. (2005). NFAT proteins: key regulators of T-cell development and function. *Nat Rev Immunol*, 5(6), 472-484. <https://doi.org/10.1038/nri1632>
- Maekawa, M., Ishizaki, T., Boku, S., Watanabe, N., Fujita, A., Iwamatsu, A., Obinata, T., Ohashi, K., Mizuno, K., & Narumiya, S. (1999). Signaling from Rho to the actin cytoskeleton through protein kinases ROCK and LIM-kinase. *Science*, 285(5429), 895-898. <https://doi.org/10.1126/science.285.5429.895>

- Mahajan, R. (2019). Onasemnogene Apeparovec for Spinal Muscular Atrophy: The Costlier Drug Ever. *Int J Appl Basic Med Res*, 9(3), 127-128. https://doi.org/10.4103/ijabmr.IJABMR_190_19
- Maillard, M. H., Cotta-de-Almeida, V., Takeshima, F., Nguyen, D. D., Michetti, P., Nagler, C., Bhan, A. K., & Snapper, S. B. (2007). The Wiskott-Aldrich syndrome protein is required for the function of CD4(+)CD25(+)Foxp3(+) regulatory T cells. *J Exp Med*, 204(2), 381-391. <https://doi.org/10.1084/jem.20061338>
- Maillet, M., Lynch, J. M., Sanna, B., York, A. J., Zheng, Y., & Molkenkin, J. D. (2009). Cdc42 is an antihypertrophic molecular switch in the mouse heart. *J Clin Invest*, 119(10), 3079-3088. <https://doi.org/10.1172/jci37694>
- Malik, H. S., & Bliska, J. B. (2020). The pyrin inflammasome and the Yersinia effector interaction. *Immunol Rev*, 297(1), 96-107. <https://doi.org/10.1111/imr.12907>
- Mandey, S. H., Kuijk, L. M., Frenkel, J., & Waterham, H. R. (2006). A role for geranylgeranylation in interleukin-1beta secretion. *Arthritis Rheum*, 54(11), 3690-3695. <https://doi.org/10.1002/art.22194>
- Manz, M. G., Traver, D., Miyamoto, T., Weissman, I. L., & Akashi, K. (2001). Dendritic cell potentials of early lymphoid and myeloid progenitors. *Blood*, 97(11), 3333-3341. <https://doi.org/10.1182/blood.v97.11.3333>
- Mariani, J., Coppola, G., Zhang, P., Abyzov, A., Provini, L., Tomasini, L., Amenduni, M., Szekely, A., Palejev, D., Wilson, M., Gerstein, M., Grigorenko, E. L., Chawarska, K., Pelphrey, K. A., Howe, J. R., & Vaccarino, F. M. (2015). FOXG1-Dependent Dysregulation of GABA/Glutamate Neuron Differentiation in Autism Spectrum Disorders. *Cell*, 162(2), 375-390. <https://doi.org/10.1016/j.cell.2015.06.034>
- Martín-Cófreces, N. B., Vicente-Manzanares, M., & Sánchez-Madrid, F. (2018). Adhesive Interactions Delineate the Topography of the Immune Synapse. *Front Cell Dev Biol*, 6, 149. <https://doi.org/10.3389/fcell.2018.00149>
- Martinelli, R., Zeiger, A. S., Whitfield, M., Sciuto, T. E., Dvorak, A., Van Vliet, K. J., Greenwood, J., & Carman, C. V. (2014). Probing the biomechanical contribution of the endothelium to lymphocyte migration: diapedesis by the path of least resistance. *J Cell Sci*, 127(Pt 17), 3720-3734. <https://doi.org/10.1242/jcs.148619>
- Martinelli, S., Krumbach, O. H. F., Pantaleoni, F., Coppola, S., Amin, E., Pannone, L., Nouri, K., Farina, L., Dvorsky, R., Lepri, F., Buchholzer, M., Konopatzki, R., Walsh, L., Payne, K., Pierpont, M. E., Vergano, S. S., Langley, K. G., Larsen, D., Farwell, K. D., . . . Mirzaa, G. M. (2018). Functional Dysregulation of CDC42 Causes Diverse Developmental Phenotypes. *Am J Hum Genet*, 102(2), 309-320. <https://doi.org/10.1016/j.ajhg.2017.12.015>
- Massey, A. C. (1992). Microcytic anemia. Differential diagnosis and management of iron deficiency anemia. *Med Clin North Am*, 76(3), 549-566. [https://doi.org/10.1016/s0025-7125\(16\)30339-x](https://doi.org/10.1016/s0025-7125(16)30339-x)
- Masters, S. L., Simon, A., Aksentijevich, I., & Kastner, D. L. (2009). Horror aut inflammaticus: the molecular pathophysiology of autoinflammatory disease (*). *Annu Rev Immunol*, 27, 621-668. <https://doi.org/10.1146/annurev.immunol.25.022106.141627>
- Matalon, O., Ben-Shmuel, A., Kivelevitz, J., Sabag, B., Fried, S., Joseph, N., Noy, E., Biber, G., & Barda-Saad, M. (2018). Actin retrograde flow controls natural killer cell response by regulating the conformation state of SHP-1. *Embo j*, 37(5). <https://doi.org/10.15252/emboj.201696264>
- Matsuda, T., Yanase, S., Takaoka, A., & Maruyama, M. (2015). The immunosenescence-related gene Zizimin2 is associated with early bone marrow B cell development and marginal zone B cell formation. *Immun Ageing*, 12, 1. <https://doi.org/10.1186/s12979-015-0028-x>
- Matsudaira, P. (1994). Actin crosslinking proteins at the leading edge. *Semin Cell Biol*, 5(3), 165-174. <https://doi.org/10.1006/scel.1994.1021>
- Mattila, P. K., & Lappalainen, P. (2008). Filopodia: molecular architecture and cellular functions. *Nat Rev Mol Cell Biol*, 9(6), 446-454. <https://doi.org/10.1038/nrm2406>

- Mavrakis, K. J., McKinlay, K. J., Jones, P., & Sablitzky, F. (2004). DEF6, a novel PH-DH-like domain protein, is an upstream activator of the Rho GTPases Rac1, Cdc42, and RhoA. *Exp Cell Res*, 294(2), 335-344. <https://doi.org/10.1016/j.yexcr.2003.12.004>
- McCoy, K. D., Hermans, I. F., Fraser, J. H., Le Gros, G., & Ronchese, F. (1999). Cytotoxic T lymphocyte-associated antigen 4 (CTLA-4) can regulate dendritic cell-induced activation and cytotoxicity of CD8(+) T cells independently of CD4(+) T cell help. *J Exp Med*, 189(7), 1157-1162. <https://doi.org/10.1084/jem.189.7.1157>
- Medvinsky, A., & Dzierzak, E. (1996). Definitive hematopoiesis is autonomously initiated by the AGM region. *Cell*, 86(6), 897-906. [https://doi.org/10.1016/s0092-8674\(00\)80165-8](https://doi.org/10.1016/s0092-8674(00)80165-8)
- Meeker, N. D., Smith, A. C., Frazer, J. K., Bradley, D. F., Rudner, L. A., Love, C., & Trede, N. S. (2010). Characterization of the zebrafish T cell receptor beta locus. *Immunogenetics*, 62(1), 23-29. <https://doi.org/10.1007/s00251-009-0407-6>
- Mehidi, A., Rossier, O., Schaks, M., Chazeau, A., Binamé, F., Remorino, A., Coppey, M., Karatas, Z., Sibarita, J. B., Rottner, K., Moreau, V., & Giannone, G. (2019). Transient Activations of Rac1 at the Lamellipodium Tip Trigger Membrane Protrusion. *Curr Biol*, 29(17), 2852-2866.e2855. <https://doi.org/10.1016/j.cub.2019.07.035>
- Meller, N., Irani-Tehrani, M., Ratnikov, B. I., Paschal, B. M., & Schwartz, M. A. (2004). The novel Cdc42 guanine nucleotide exchange factor, zizimin1, dimerizes via the Cdc42-binding CZH2 domain. *J Biol Chem*, 279(36), 37470-37476. <https://doi.org/10.1074/jbc.M404535200>
- Meller, N., Merlot, S., & Guda, C. (2005). CZH proteins: a new family of Rho-GEFs. *J Cell Sci*, 118(Pt 21), 4937-4946. <https://doi.org/10.1242/jcs.02671>
- Mellor, H. (2010). The role of formins in filopodia formation. *Biochim Biophys Acta*, 1803(2), 191-200. <https://doi.org/10.1016/j.bbamcr.2008.12.018>
- Mesin, L., Ersching, J., & Vitorica, G. D. (2016). Germinal Center B Cell Dynamics. *Immunity*, 45(3), 471-482. <https://doi.org/10.1016/j.immuni.2016.09.001>
- Metcalf, D. (1998). Lineage commitment and maturation in hematopoietic cells: the case for extrinsic regulation. *Blood*, 92(2), 345-347; discussion 352.
- Meyen, D., Tarbashevich, K., Banisch, T. U., Wittwer, C., Reichman-Fried, M., Maugis, B., Grimaldi, C., Messerschmidt, E. M., & Raz, E. (2015). Dynamic filopodia are required for chemokine-dependent intracellular polarization during guided cell migration in vivo. *Elife*, 4. <https://doi.org/10.7554/eLife.05279>
- Meyts, I., Bosch, B., Bolze, A., Boisson, B., Itan, Y., Belkadi, A., Pedergrana, V., Moens, L., Picard, C., Cobat, A., Bossuyt, X., Abel, L., & Casanova, J. L. (2016). Exome and genome sequencing for inborn errors of immunity. *J Allergy Clin Immunol*, 138(4), 957-969. <https://doi.org/10.1016/j.jaci.2016.08.003>
- Miao, R., Lim, V. Y., Kothapalli, N., Ma, Y., Fossati, J., Zehentmeier, S., Sun, R., & Pereira, J. P. (2020). Hematopoietic Stem Cell Niches and Signals Controlling Immune Cell Development and Maintenance of Immunological Memory. *Front Immunol*, 11, 600127. <https://doi.org/10.3389/fimmu.2020.600127>
- Mikkola, H. K., & Orkin, S. H. (2006). The journey of developing hematopoietic stem cells. *Development*, 133(19), 3733-3744. <https://doi.org/10.1242/dev.02568>
- Miyamoto, Y., Yamauchi, J., Sanbe, A., & Tanoue, A. (2007). Dock6, a Dock-C subfamily guanine nucleotide exchanger, has the dual specificity for Rac1 and Cdc42 and regulates neurite outgrowth. *Exp Cell Res*, 313(4), 791-804. <https://doi.org/10.1016/j.yexcr.2006.11.017>
- Mizesko, M. C., Banerjee, P. P., Monaco-Shawver, L., Mace, E. M., Bernal, W. E., Sawalle-Belohradsky, J., Belohradsky, B. H., Heinz, V., Freeman, A. F., Sullivan, K. E., Holland, S. M., Torgerson, T. R., Al-Herz, W., Chou, J., Hanson, I. C., Albert, M. H., Geha, R. S., Renner, E. D., & Orange, J. S. (2013). Defective actin accumulation impairs human natural killer cell function in patients with dedicator of cytokinesis 8 deficiency. *J Allergy Clin Immunol*, 131(3), 840-848. <https://doi.org/10.1016/j.jaci.2012.12.1568>
- Miziorko, H. M. (2011). Enzymes of the mevalonate pathway of isoprenoid biosynthesis. *Arch Biochem Biophys*, 505(2), 131-143. <https://doi.org/10.1016/j.abb.2010.09.028>

- Mizuno, K. (2013). Signaling mechanisms and functional roles of cofilin phosphorylation and dephosphorylation. *Cell Signal*, 25(2), 457-469. <https://doi.org/10.1016/j.cellsig.2012.11.001>
- Moens, L., Gouwy, M., Bosch, B., Pastukhov, O., Nieto-Patlàn, A., Siler, U., Bucciol, G., Mekahli, D., Vermeulen, F., Desmet, L., Maebe, S., Flipts, H., Corveleyn, A., Moshous, D., Philippet, P., Tangye, S. G., Boisson, B., Casanova, J. L., Florkin, B., . . . Meyts, I. (2019). Human DOCK2 Deficiency: Report of a Novel Mutation and Evidence for Neutrophil Dysfunction. *J Clin Immunol*, 39(3), 298-308. <https://doi.org/10.1007/s10875-019-00603-w>
- Moens, L., & Tangye, S. G. (2014). Cytokine-Mediated Regulation of Plasma Cell Generation: IL-21 Takes Center Stage. *Front Immunol*, 5, 65. <https://doi.org/10.3389/fimmu.2014.00065>
- Moignard, V., Macaulay, I. C., Swiers, G., Buettner, F., Schütte, J., Calero-Nieto, F. J., Kinston, S., Joshi, A., Hannah, R., Theis, F. J., Jacobsen, S. E., de Bruijn, M. F., & Göttgens, B. (2013). Characterization of transcriptional networks in blood stem and progenitor cells using high-throughput single-cell gene expression analysis. *Nat Cell Biol*, 15(4), 363-372. <https://doi.org/10.1038/ncb2709>
- Mooren, O. L., Li, J., Nawas, J., & Cooper, J. A. (2014). Endothelial cells use dynamic actin to facilitate lymphocyte transendothelial migration and maintain the monolayer barrier. *Mol Biol Cell*, 25(25), 4115-4129. <https://doi.org/10.1091/mbc.E14-05-0976>
- Morales-Tirado, V., Johannson, S., Hanson, E., Howell, A., Zhang, J., Siminovitch, K. A., & Fowell, D. J. (2004). Cutting edge: selective requirement for the Wiskott-Aldrich syndrome protein in cytokine, but not chemokine, secretion by CD4+ T cells. *J Immunol*, 173(2), 726-730. <https://doi.org/10.4049/jimmunol.173.2.726>
- Moreau, H. D., Lemaître, F., Garrod, K. R., Garcia, Z., Lennon-Duménil, A. M., & Bousso, P. (2015). Signal strength regulates antigen-mediated T-cell deceleration by distinct mechanisms to promote local exploration or arrest. *Proc Natl Acad Sci U S A*, 112(39), 12151-12156. <https://doi.org/10.1073/pnas.1506654112>
- Morimoto, A., Nakazawa, Y., & Ishii, E. (2016). Hemophagocytic lymphohistiocytosis: Pathogenesis, diagnosis, and management. *Pediatr Int*, 58(9), 817-825. <https://doi.org/10.1111/ped.13064>
- Morrison, S. J., & Scadden, D. T. (2014). The bone marrow niche for haematopoietic stem cells. *Nature*, 505(7483), 327-334. <https://doi.org/10.1038/nature12984>
- Motulsky, A. G., Casserl, F., Giblett, E. R., Broun, G. O., Jr., & Finch, C. A. (1958). Anemia and the spleen. *N Engl J Med*, 259(25), 1215-1219 concl. <https://doi.org/10.1056/nejm195812182592506>
- Moulding, D. A., Record, J., Malinova, D., & Thrasher, A. J. (2013). Actin cytoskeletal defects in immunodeficiency. *Immunol Rev*, 256(1), 282-299. <https://doi.org/10.1111/imr.12114>
- Mullins, R. D., Heuser, J. A., & Pollard, T. D. (1998). The interaction of Arp2/3 complex with actin: nucleation, high affinity pointed end capping, and formation of branching networks of filaments. *Proc Natl Acad Sci U S A*, 95(11), 6181-6186. <https://doi.org/10.1073/pnas.95.11.6181>
- Mulloy, J. C., Cancelas, J. A., Filippi, M. D., Kalfa, T. A., Guo, F., & Zheng, Y. (2010). Rho GTPases in hematopoiesis and hemopathies. *Blood*, 115(5), 936-947. <https://doi.org/10.1182/blood-2009-09-198127>
- Murray, P. J., & Wynn, T. A. (2011). Protective and pathogenic functions of macrophage subsets. *Nat Rev Immunol*, 11(11), 723-737. <https://doi.org/10.1038/nri3073>
- Myers, K. C., Furutani, E., Weller, E., Siegele, B., Galvin, A., Arsenault, V., Alter, B. P., Boulad, F., Bueso-Ramos, C., Burroughs, L., Castillo, P., Connelly, J., Davies, S. M., DiNardo, C. D., Hanif, I., Ho, R. H., Karras, N., Manalang, M., McReynolds, L. J., . . . Shimamura, A. (2020). Clinical features and outcomes of patients with Shwachman-Diamond syndrome and myelodysplastic syndrome or acute myeloid leukaemia: a multicentre, retrospective, cohort study. *Lancet Haematol*, 7(3), e238-e246. [https://doi.org/10.1016/s2352-3026\(19\)30206-6](https://doi.org/10.1016/s2352-3026(19)30206-6)

- Nag, S., Larsson, M., Robinson, R. C., & Burtnick, L. D. (2013). Gelsolin: the tail of a molecular gymnast. *Cytoskeleton (Hoboken)*, *70*(7), 360-384. <https://doi.org/10.1002/cm.21117>
- Nakamura, M., Verboon, J. M., & Parkhurst, S. M. (2017). Prepatterning by RhoGEFs governs Rho GTPase spatiotemporal dynamics during wound repair. *J Cell Biol*, *216*(12), 3959-3969. <https://doi.org/10.1083/jcb.201704145>
- Namekata, K., Guo, X., Kimura, A., Azuchi, Y., Kitamura, Y., Harada, C., & Harada, T. (2020). Roles of the DOCK-D family proteins in a mouse model of neuroinflammation. *J Biol Chem*, *295*(19), 6710-6720. <https://doi.org/10.1074/jbc.RA119.010438>
- Nemazee, D. (2017). Mechanisms of central tolerance for B cells. *Nat Rev Immunol*, *17*(5), 281-294. <https://doi.org/10.1038/nri.2017.19>
- Ng, P. C., & Henikoff, S. (2003). SIFT: Predicting amino acid changes that affect protein function. *Nucleic Acids Res*, *31*(13), 3812-3814. <https://doi.org/10.1093/nar/gkg509>
- Nikolich-Zugich, J., Slifka, M. K., & Messaoudi, I. (2004). The many important facets of T-cell repertoire diversity. *Nat Rev Immunol*, *4*(2), 123-132. <https://doi.org/10.1038/nri1292>
- Nishikimi, A., Fukuhara, H., Su, W., Hongu, T., Takasuga, S., Mihara, H., Cao, Q., Sanematsu, F., Kanai, M., Hasegawa, H., Tanaka, Y., Shibasaki, M., Kanaho, Y., Sasaki, T., Frohman, M. A., & Fukui, Y. (2009). Sequential regulation of DOCK2 dynamics by two phospholipids during neutrophil chemotaxis. *Science*, *324*(5925), 384-387. <https://doi.org/10.1126/science.1170179>
- Nishikimi, A., Kukimoto-Niino, M., Yokoyama, S., & Fukui, Y. (2013). Immune regulatory functions of DOCK family proteins in health and disease. *Exp Cell Res*, *319*(15), 2343-2349. <https://doi.org/10.1016/j.yexcr.2013.07.024>
- Nishikimi, A., Meller, N., Uekawa, N., Isobe, K., Schwartz, M. A., & Maruyama, M. (2005). Zizimin2: a novel, DOCK180-related Cdc42 guanine nucleotide exchange factor expressed predominantly in lymphocytes. *FEBS Lett*, *579*(5), 1039-1046. <https://doi.org/10.1016/j.febslet.2005.01.006>
- Nishitani-Isa, M., Mukai, K., Honda, Y., Nihira, H., Tanaka, T., Shibata, H., Kodama, K., Hiejima, E., Izawa, K., Kawasaki, Y., Osawa, M., Katata, Y., Onodera, S., Watanabe, T., Uchida, T., Kure, S., Takita, J., Ohara, O., Saito, M. K., . . . Yasumi, T. (2022). Trapping of CDC42 C-terminal variants in the Golgi drives pyrin inflammasome hyperactivation. *J Exp Med*, *219*(6). <https://doi.org/10.1084/jem.20211889>
- Nombela-Arrieta, C., Lacalle, R. A., Montoya, M. C., Kunisaki, Y., Megías, D., Marqués, M., Carrera, A. C., Mañes, S., Fukui, Y., Martínez, A. C., & Stein, J. V. (2004). Differential requirements for DOCK2 and phosphoinositide-3-kinase gamma during T and B lymphocyte homing. *Immunity*, *21*(3), 429-441. <https://doi.org/10.1016/j.immuni.2004.07.012>
- Nombela-Arrieta, C., Mempel, T. R., Soriano, S. F., Mazo, I., Wymann, M. P., Hirsch, E., Martínez, A. C., Fukui, Y., von Andrian, U. H., & Stein, J. V. (2007). A central role for DOCK2 during interstitial lymphocyte motility and sphingosine-1-phosphate-mediated egress. *J Exp Med*, *204*(3), 497-510. <https://doi.org/10.1084/jem.20061780>
- Normand, S., Massonnet, B., Delwail, A., Favot, L., Cuisset, L., Grateau, G., Morel, F., Silvain, C., & Lecron, J. C. (2009). Specific increase in caspase-1 activity and secretion of IL-1 family cytokines: a putative link between mevalonate kinase deficiency and inflammation. *Eur Cytokine Netw*, *20*(3), 101-107. <https://doi.org/10.1684/ecn.2009.0163>
- Notarangelo, L. D., Uzel, G., & Rao, V. K. (2019). Primary immunodeficiencies: novel genes and unusual presentations. *Hematology Am Soc Hematol Educ Program*, *2019*(1), 443-448. <https://doi.org/10.1182/hematology.2019000051>
- Nunes-Santos, C. J., Kuehn, H., Boast, B., Hwang, S., Kuhns, D. B., Stoddard, J., Niemela, J. E., Fink, D. L., Pittaluga, S., Abu-Asab, M., Davies, J. S., Barr, V. A., Kawai, T., Delmonte, O. M., Bosticardo, M., Garofalo, M., Carneiro-Sampaio, M., Somech, R., Gharagozlou, M., . . . Rosenzweig, S. D. (2023). Inherited ARPC5 mutations cause an actinopathy impairing cell motility and disrupting cytokine signaling. *Nat Commun*, *14*(1), 3708. <https://doi.org/10.1038/s41467-023-39272-0>

- Ochs, H. D., Slichter, S. J., Harker, L. A., Von Behrens, W. E., Clark, R. A., & Wedgwood, R. J. (1980). The Wiskott-Aldrich syndrome: studies of lymphocytes, granulocytes, and platelets. *Blood*, *55*(2), 243-252.
- Ohkura, N., Kitagawa, Y., & Sakaguchi, S. (2013). Development and maintenance of regulatory T cells. *Immunity*, *38*(3), 414-423. <https://doi.org/10.1016/j.immuni.2013.03.002>
- Olivier, E. N., Qiu, C., Velho, M., Hirsch, R. E., & Bouhassira, E. E. (2006). Large-scale production of embryonic red blood cells from human embryonic stem cells. *Exp Hematol*, *34*(12), 1635-1642. <https://doi.org/10.1016/j.exphem.2006.07.003>
- Olson, B. M., Sullivan, J. A., & Burlingham, W. J. (2013). Interleukin 35: a key mediator of suppression and the propagation of infectious tolerance. *Front Immunol*, *4*, 315. <https://doi.org/10.3389/fimmu.2013.00315>
- Orange, J. S., Ramesh, N., Remold-O'Donnell, E., Sasahara, Y., Koopman, L., Byrne, M., Bonilla, F. A., Rosen, F. S., Geha, R. S., & Strominger, J. L. (2002). Wiskott-Aldrich syndrome protein is required for NK cell cytotoxicity and colocalizes with actin to NK cell-activating immunologic synapses. *Proc Natl Acad Sci U S A*, *99*(17), 11351-11356. <https://doi.org/10.1073/pnas.162376099>
- Orkin, S. H. (2000). Diversification of haematopoietic stem cells to specific lineages. *Nat Rev Genet*, *1*(1), 57-64. <https://doi.org/10.1038/35049577>
- Orkin, S. H., & Zon, L. I. (2008). Hematopoiesis: an evolving paradigm for stem cell biology. *Cell*, *132*(4), 631-644. <https://doi.org/10.1016/j.cell.2008.01.025>
- Ottesen, E. W. (2017). ISS-N1 makes the First FDA-approved Drug for Spinal Muscular Atrophy. *Transl Neurosci*, *8*, 1-6. <https://doi.org/10.1515/tnsci-2017-0001>
- Paik, E. J., & Zon, L. I. (2010). Hematopoietic development in the zebrafish. *Int J Dev Biol*, *54*(6-7), 1127-1137. <https://doi.org/10.1387/ijdb.093042ep>
- Palm, N. W., & Medzhitov, R. (2009). Pattern recognition receptors and control of adaptive immunity. *Immunol Rev*, *227*(1), 221-233. <https://doi.org/10.1111/j.1600-065X.2008.00731.x>
- Pandiyan, P., Zheng, L., Ishihara, S., Reed, J., & Lenardo, M. J. (2007). CD4+CD25+Foxp3+ regulatory T cells induce cytokine deprivation-mediated apoptosis of effector CD4+ T cells. *Nat Immunol*, *8*(12), 1353-1362. <https://doi.org/10.1038/ni1536>
- Papa, R., Penco, F., Volpi, S., & Gattorno, M. (2020). Actin Remodeling Defects Leading to Autoinflammation and Immune Dysregulation. *Front Immunol*, *11*, 604206. <https://doi.org/10.3389/fimmu.2020.604206>
- Park, H., Staehling-Hampton, K., Appleby, M. W., Brunkow, M. E., Habib, T., Zhang, Y., Ramsdell, F., Liggitt, H. D., Freie, B., Tsang, M., Carlson, G., Friend, S., Frevert, C., & Iritani, B. M. (2008). A point mutation in the murine Hem1 gene reveals an essential role for Hematopoietic protein 1 in lymphopoiesis and innate immunity. *J Exp Med*, *205*(12), 2899-2913. <https://doi.org/10.1084/jem.20080340>
- Park, J. H., Lee, K. H., Jeon, B., Ochs, H. D., Lee, J. S., Gee, H. Y., Seo, S., Geum, D., Piccirillo, C. A., Eisenhut, M., van der Vliet, H. J., Lee, J. M., Kronbichler, A., Ko, Y., & Shin, J. I. (2020). Immune dysregulation, polyendocrinopathy, enteropathy, X-linked (IPEX) syndrome: A systematic review. *Autoimmun Rev*, *19*(6), 102526. <https://doi.org/10.1016/j.autrev.2020.102526>
- Park, Y. H., Wood, G., Kastner, D. L., & Chae, J. J. (2016). Pyrin inflammasome activation and RhoA signaling in the autoinflammatory diseases FMF and HIDS. *Nat Immunol*, *17*(8), 914-921. <https://doi.org/10.1038/ni.3457>
- Parker, M. P., & Peterson, K. R. (2018). Mouse Models of Erythropoiesis and Associated Diseases. *Methods Mol Biol*, *1698*, 37-65. https://doi.org/10.1007/978-1-4939-7428-3_3
- Parrado, A. (2020). Expression of DOCK9 and DOCK11 Analyzed with Commercial Antibodies: Focus on Regulation of Mutually Exclusive First Exon Isoforms. *Antibodies (Basel)*, *9*(3). <https://doi.org/10.3390/antib9030027>
- Paul, A. S., & Pollard, T. D. (2009). Review of the mechanism of processive actin filament elongation by formins. *Cell Motil Cytoskeleton*, *66*(8), 606-617. <https://doi.org/10.1002/cm.20379>

- Pertz, O. (2010). Spatio-temporal Rho GTPase signaling - where are we now? *J Cell Sci*, 123(Pt 11), 1841-1850. <https://doi.org/10.1242/jcs.064345>
- Pevny, L., Simon, M. C., Robertson, E., Klein, W. H., Tsai, S. F., D'Agati, V., Orkin, S. H., & Costantini, F. (1991). Erythroid differentiation in chimaeric mice blocked by a targeted mutation in the gene for transcription factor GATA-1. *Nature*, 349(6306), 257-260. <https://doi.org/10.1038/349257a0>
- Pfajfer, L., Mair, N. K., Jiménez-Heredia, R., Genel, F., Gulez, N., Ardeniz, Ö., Hoeger, B., Bal, S. K., Madritsch, C., Kalinichenko, A., Chandra Ardy, R., Gerçeker, B., Rey-Barroso, J., Ijspeert, H., Tangye, S. G., Simonitsch-Klupp, I., Huppa, J. B., van der Burg, M., Dupré, L., & Boztug, K. (2018). Mutations affecting the actin regulator WD repeat-containing protein 1 lead to aberrant lymphoid immunity. *J Allergy Clin Immunol*, 142(5), 1589-1604.e1511. <https://doi.org/10.1016/j.jaci.2018.04.023>
- Pfajfer, L., Seidel, M. G., Houmadi, R., Rey-Barroso, J., Hirschmugl, T., Salzer, E., Antón, I. M., Urban, C., Schwinger, W., Boztug, K., & Dupré, L. (2017). WIP deficiency severely affects human lymphocyte architecture during migration and synapse assembly. *Blood*, 130(17), 1949-1953. <https://doi.org/10.1182/blood-2017-04-777383>
- Phillips, J., & Henderson, A. C. (2018). Hemolytic Anemia: Evaluation and Differential Diagnosis. *Am Fam Physician*, 98(6), 354-361.
- Pichaud, F., Walther, R. F., & Nunes de Almeida, F. (2019). Regulation of Cdc42 and its effectors in epithelial morphogenesis. *J Cell Sci*, 132(10). <https://doi.org/10.1242/jcs.217869>
- Pollard, T. D. (2016). Actin and Actin-Binding Proteins. *Cold Spring Harb Perspect Biol*, 8(8). <https://doi.org/10.1101/cshperspect.a018226>
- Pollard, T. D., & Borisy, G. G. (2003). Cellular motility driven by assembly and disassembly of actin filaments. *Cell*, 112(4), 453-465. [https://doi.org/10.1016/s0092-8674\(03\)00120-x](https://doi.org/10.1016/s0092-8674(03)00120-x)
- Pollard, T. D., & Cooper, J. A. (2009). Actin, a central player in cell shape and movement. *Science*, 326(5957), 1208-1212. <https://doi.org/10.1126/science.1175862>
- Prakriya, M., Feske, S., Gwack, Y., Srikanth, S., Rao, A., & Hogan, P. G. (2006). Orai1 is an essential pore subunit of the CRAC channel. *Nature*, 443(7108), 230-233. <https://doi.org/10.1038/nature05122>
- Premkumar, L., Bobkov, A. A., Patel, M., Jaroszewski, L., Bankston, L. A., Stec, B., Vuori, K., Côté, J. F., & Liddington, R. C. (2010). Structural basis of membrane targeting by the Dock180 family of Rho family guanine exchange factors (Rho-GEFs). *J Biol Chem*, 285(17), 13211-13222. <https://doi.org/10.1074/jbc.M110.102517>
- Putney, J. W. (2011). Origins of the concept of store-operated calcium entry. *Front Biosci (Schol Ed)*, 3(3), 980-984. <https://doi.org/10.2741/202>
- Qi, H. (2016). T follicular helper cells in space-time. *Nat Rev Immunol*, 16(10), 612-625. <https://doi.org/10.1038/nri.2016.94>
- Randall, K. L., Chan, S. S., Ma, C. S., Fung, I., Mei, Y., Yabas, M., Tan, A., Arkwright, P. D., Al Suwairi, W., Lugo Reyes, S. O., Yamazaki-Nakashimada, M. A., Garcia-Cruz Mde, L., Smart, J. M., Picard, C., Okada, S., Jouanguy, E., Casanova, J. L., Lambe, T., Cornall, R. J., . . . Goodnow, C. C. (2011). DOCK8 deficiency impairs CD8 T cell survival and function in humans and mice. *J Exp Med*, 208(11), 2305-2320. <https://doi.org/10.1084/jem.20110345>
- Randall, K. L., Lambe, T., Johnson, A. L., Treanor, B., Kucharska, E., Domaschenz, H., Whittle, B., Tze, L. E., Enders, A., Crockford, T. L., Bouriez-Jones, T., Alston, D., Cyster, J. G., Lenardo, M. J., Mackay, F., Deenick, E. K., Tangye, S. G., Chan, T. D., Camidge, T., . . . Goodnow, C. C. (2009). Dock8 mutations cripple B cell immunological synapses, germinal centers and long-lived antibody production. *Nat Immunol*, 10(12), 1283-1291. <https://doi.org/10.1038/ni.1820>
- Ransom, D. G., Haffter, P., Odenthal, J., Brownlie, A., Vogelsang, E., Kelsh, R. N., Brand, M., van Eeden, F. J., Furutani-Seiki, M., Granato, M., Hammerschmidt, M., Heisenberg, C. P., Jiang, Y. J., Kane, D. A., Mullins, M. C., & Nüsslein-Volhard, C. (1996). Characterization of zebrafish mutants with defects in embryonic hematopoiesis. *Development*, 123, 311-319. <https://doi.org/10.1242/dev.123.1.311>

- Rao, J. N., Madasu, Y., & Dominguez, R. (2014). Mechanism of actin filament pointed-end capping by tropomodulin. *Science*, *345*(6195), 463-467. <https://doi.org/10.1126/science.1256159>
- Raskov, H., Orhan, A., Christensen, J. P., & Gögenur, I. (2021). Cytotoxic CD8(+) T cells in cancer and cancer immunotherapy. *Br J Cancer*, *124*(2), 359-367. <https://doi.org/10.1038/s41416-020-01048-4>
- Raza, Y., Salman, H., & Luberto, C. (2021). Sphingolipids in Hematopoiesis: Exploring Their Role in Lineage Commitment. *Cells*, *10*(10). <https://doi.org/10.3390/cells10102507>
- Recher, M., Burns, S. O., de la Fuente, M. A., Volpi, S., Dahlberg, C., Walter, J. E., Moffitt, K., Mathew, D., Honke, N., Lang, P. A., Patrizi, L., Falet, H., Keszei, M., Mizui, M., Csizmadia, E., Candotti, F., Nadeau, K., Bouma, G., Delmonte, O. M., . . . Notarangelo, L. D. (2012). B cell-intrinsic deficiency of the Wiskott-Aldrich syndrome protein (WASp) causes severe abnormalities of the peripheral B-cell compartment in mice. *Blood*, *119*(12), 2819-2828. <https://doi.org/10.1182/blood-2011-09-379412>
- Ren, A., Yin, W., Miller, H., Westerberg, L. S., Candotti, F., Park, C. S., Lee, P., Gong, Q., Chen, Y., & Liu, C. (2021). Novel Discoveries in Immune Dysregulation in Inborn Errors of Immunity. *Front Immunol*, *12*, 725587. <https://doi.org/10.3389/fimmu.2021.725587>
- Richards, S., Aziz, N., Bale, S., Bick, D., Das, S., Gastier-Foster, J., Grody, W. W., Hegde, M., Lyon, E., Spector, E., Voelkerding, K., & Rehm, H. L. (2015). Standards and guidelines for the interpretation of sequence variants: a joint consensus recommendation of the American College of Medical Genetics and Genomics and the Association for Molecular Pathology. *Genet Med*, *17*(5), 405-424. <https://doi.org/10.1038/gim.2015.30>
- Ridley, A. J. (2011). Life at the leading edge. *Cell*, *145*(7), 1012-1022. <https://doi.org/10.1016/j.cell.2011.06.010>
- Ridley, A. J., Paterson, H. F., Johnston, C. L., Diekmann, D., & Hall, A. (1992). The small GTP-binding protein rac regulates growth factor-induced membrane ruffling. *Cell*, *70*(3), 401-410. [https://doi.org/10.1016/0092-8674\(92\)90164-8](https://doi.org/10.1016/0092-8674(92)90164-8)
- Rieger, M. A., & Schroeder, T. (2009). Analyzing cell fate control by cytokines through continuous single cell biochemistry. *J Cell Biochem*, *108*(2), 343-352. <https://doi.org/10.1002/jcb.22273>
- Rieger, M. A., & Schroeder, T. (2012). Hematopoiesis. *Cold Spring Harb Perspect Biol*, *4*(12). <https://doi.org/10.1101/cshperspect.a008250>
- Rivas, F. V., O'Keefe, J. P., Alegre, M. L., & Gajewski, T. F. (2004). Actin cytoskeleton regulates calcium dynamics and NFAT nuclear duration. *Mol Cell Biol*, *24*(4), 1628-1639. <https://doi.org/10.1128/mcb.24.4.1628-1639.2004>
- Rivers, E., Hong, Y., Bajaj-Elliott, M., Worth, A., & Thrasher, A. J. (2021). IL-18: A potential inflammation biomarker in Wiskott-Aldrich syndrome. *Eur J Immunol*, *51*(5), 1285-1288. <https://doi.org/10.1002/eji.202049024>
- Roberts, A. E., Allanson, J. E., Tartaglia, M., & Gelb, B. D. (2013). Noonan syndrome. *Lancet*, *381*(9863), 333-342. [https://doi.org/10.1016/s0140-6736\(12\)61023-x](https://doi.org/10.1016/s0140-6736(12)61023-x)
- Rocamora-Reverte, L., Melzer, F. L., Würzner, R., & Weinberger, B. (2020). The Complex Role of Regulatory T Cells in Immunity and Aging. *Front Immunol*, *11*, 616949. <https://doi.org/10.3389/fimmu.2020.616949>
- Romagnani, S. (1997). The Th1/Th2 paradigm. *Immunol Today*, *18*(6), 263-266. [https://doi.org/10.1016/s0167-5699\(97\)80019-9](https://doi.org/10.1016/s0167-5699(97)80019-9)
- Romberg, N., Al Moussawi, K., Nelson-Williams, C., Stiegler, A. L., Loring, E., Choi, M., Overton, J., Meffre, E., Khokha, M. K., Huttner, A. J., West, B., Podoltsev, N. A., Boggon, T. J., Kazmierczak, B. I., & Lifton, R. P. (2014). Mutation of NLRC4 causes a syndrome of enterocolitis and autoinflammation. *Nat Genet*, *46*(10), 1135-1139. <https://doi.org/10.1038/ng.3066>
- Rossman, K. L., Der, C. J., & Sondek, J. (2005). GEF means go: turning on RHO GTPases with guanine nucleotide-exchange factors. *Nat Rev Mol Cell Biol*, *6*(2), 167-180. <https://doi.org/10.1038/nrm1587>
- Rouiller, I., Xu, X. P., Amann, K. J., Egile, C., Nickell, S., Nicastro, D., Li, R., Pollard, T. D., Volkmann, N., & Hanein, D. (2008). The structural basis of actin filament branching by

- the Arp2/3 complex. *J Cell Biol*, 180(5), 887-895. <https://doi.org/10.1083/jcb.200709092>
- Sage, P. T., Varghese, L. M., Martinelli, R., Sciuto, T. E., Kamei, M., Dvorak, A. M., Springer, T. A., Sharpe, A. H., & Carman, C. V. (2012). Antigen recognition is facilitated by invadosome-like protrusions formed by memory/effector T cells. *J Immunol*, 188(8), 3686-3699. <https://doi.org/10.4049/jimmunol.1102594>
- Sakabe, I., Asai, A., Iijima, J., & Maruyama, M. (2012). Age-related guanine nucleotide exchange factor, mouse Zizimin2, induces filopodia in bone marrow-derived dendritic cells. *Immun Ageing*, 9, 2. <https://doi.org/10.1186/1742-4933-9-2>
- Sakaguchi, S., Yamaguchi, T., Nomura, T., & Ono, M. (2008). Regulatory T cells and immune tolerance. *Cell*, 133(5), 775-787. <https://doi.org/10.1016/j.cell.2008.05.009>
- Sakai, Y., Tanaka, Y., Yanagihara, T., Watanabe, M., Duan, X., Terasawa, M., Nishikimi, A., Sanematsu, F., & Fukui, Y. (2013). The Rac activator DOCK2 regulates natural killer cell-mediated cytotoxicity in mice through the lytic synapse formation. *Blood*, 122(3), 386-393. <https://doi.org/10.1182/blood-2012-12-475897>
- Sakamoto, A., & Maruyama, M. (2020). Contribution of DOCK11 to the Expansion of Antigen-Specific Populations among Germinal Center B Cells. *Immunohorizons*, 4(9), 520-529. <https://doi.org/10.4049/immunohorizons.2000048>
- Sakamoto, A., Matsuda, T., Kawaguchi, K., Takaoka, A., & Maruyama, M. (2017). Involvement of Zizimin2/3 in the age-related defect of peritoneal B-1a cells as a source of anti-bacterial IgM. *Int Immunol*, 29(9), 431-438. <https://doi.org/10.1093/intimm/dxx054>
- Sakata, D., Taniguchi, H., Yasuda, S., Adachi-Morishima, A., Hamazaki, Y., Nakayama, R., Miki, T., Minato, N., & Narumiya, S. (2007). Impaired T lymphocyte trafficking in mice deficient in an actin-nucleating protein, mDia1. *J Exp Med*, 204(9), 2031-2038. <https://doi.org/10.1084/jem.20062647>
- Salomao, M., Zhang, X., Yang, Y., Lee, S., Hartwig, J. H., Chasis, J. A., Mohandas, N., & An, X. (2008). Protein 4.1R-dependent multiprotein complex: new insights into the structural organization of the red blood cell membrane. *Proc Natl Acad Sci U S A*, 105(23), 8026-8031. <https://doi.org/10.1073/pnas.0803225105>
- Salzer, E., Cagdas, D., Hons, M., Mace, E. M., Garncarz, W., Petronczki Ö, Y., Platzer, R., Pfajfer, L., Bilic, I., Ban, S. A., Willmann, K. L., Mukherjee, M., Supper, V., Hsu, H. T., Banerjee, P. P., Sinha, P., McClanahan, F., Zlabinger, G. J., Pickl, W. F., . . . Boztug, K. (2016). RASGRP1 deficiency causes immunodeficiency with impaired cytoskeletal dynamics. *Nat Immunol*, 17(12), 1352-1360. <https://doi.org/10.1038/ni.3575>
- Salzer, E., Zoghi, S., Kiss, M. G., Kage, F., Rashkova, C., Stahnke, S., Haimel, M., Platzer, R., Caldera, M., Ardy, R. C., Hoeger, B., Block, J., Medgyesi, D., Sin, C., Shahkarami, S., Kain, R., Ziaee, V., Hammerl, P., Bock, C., . . . Boztug, K. (2020). The cytoskeletal regulator HEM1 governs B cell development and prevents autoimmunity. *Sci Immunol*, 5(49). <https://doi.org/10.1126/sciimmunol.abc3979>
- Sanui, T., Inayoshi, A., Noda, M., Iwata, E., Oike, M., Sasazuki, T., & Fukui, Y. (2003). DOCK2 is essential for antigen-induced translocation of TCR and lipid rafts, but not PKC-theta and LFA-1, in T cells. *Immunity*, 19(1), 119-129. [https://doi.org/10.1016/s1074-7613\(03\)00169-9](https://doi.org/10.1016/s1074-7613(03)00169-9)
- Saoudi, A., Kassem, S., Dejean, A., & Gaud, G. (2014). Rho-GTPases as key regulators of T lymphocyte biology. *Small GTPases*, 5. <https://doi.org/10.4161/sgtp.28208>
- Sarner, S., Kozma, R., Ahmed, S., & Lim, L. (2000). Phosphatidylinositol 3-kinase, Cdc42, and Rac1 act downstream of Ras in integrin-dependent neurite outgrowth in N1E-115 neuroblastoma cells. *Mol Cell Biol*, 20(1), 158-172. <https://doi.org/10.1128/mcb.20.1.158-172.2000>
- Sasahara, Y., Rachid, R., Byrne, M. J., de la Fuente, M. A., Abraham, R. T., Ramesh, N., & Geha, R. S. (2002). Mechanism of recruitment of WASP to the immunological synapse and of its activation following TCR ligation. *Mol Cell*, 10(6), 1269-1281. [https://doi.org/10.1016/s1097-2765\(02\)00728-1](https://doi.org/10.1016/s1097-2765(02)00728-1)
- Schaks, M., Döring, H., Kage, F., Steffen, A., Klünemann, T., Blankenfeldt, W., Stradal, T., & Rottner, K. (2021). RhoG and Cdc42 can contribute to Rac-dependent lamellipodia

- formation through WAVE regulatory complex-binding. *Small GTPases*, 12(2), 122-132. <https://doi.org/10.1080/21541248.2019.1657755>
- Schimmer, J., & Breazzano, S. (2016). Investor Outlook: Rising from the Ashes; GSK's European Approval of Strimvelis for ADA-SCID. *Hum Gene Ther Clin Dev*, 27(2), 57-61. <https://doi.org/10.1089/humc.2016.29010.ind>
- Schnoor, M. (2015). Endothelial actin-binding proteins and actin dynamics in leukocyte transendothelial migration. *J Immunol*, 194(8), 3535-3541. <https://doi.org/10.4049/jimmunol.1403250>
- Schroder, K., & Tschopp, J. (2010). The inflammasomes. *Cell*, 140(6), 821-832. <https://doi.org/10.1016/j.cell.2010.01.040>
- Schubert, D., Bode, C., Kenefeck, R., Hou, T. Z., Wing, J. B., Kennedy, A., Bulashevskaya, A., Petersen, B. S., Schäffer, A. A., Grüning, B. A., Unger, S., Frede, N., Baumann, U., Witte, T., Schmidt, R. E., Dueckers, G., Niehues, T., Seneviratne, S., Kanariou, M., . . . Grimbacher, B. (2014). Autosomal dominant immune dysregulation syndrome in humans with CTLA4 mutations. *Nat Med*, 20(12), 1410-1416. <https://doi.org/10.1038/nm.3746>
- Schwab, C., Gabrysch, A., Olbrich, P., Patiño, V., Warnatz, K., Wolff, D., Hoshino, A., Kobayashi, M., Imai, K., Takagi, M., Dybedal, I., Haddock, J. A., Sansom, D. M., Lucena, J. M., Seidl, M., Schmitt-Graeff, A., Reiser, V., Emmerich, F., Frede, N., . . . Grimbacher, B. (2018). Phenotype, penetrance, and treatment of 133 cytotoxic T-lymphocyte antigen 4-insufficient subjects. *J Allergy Clin Immunol*, 142(6), 1932-1946. <https://doi.org/10.1016/j.jaci.2018.02.055>
- Schwinger, W., Urban, C., Ulreich, R., Sperl, D., Karastaneva, A., Strenger, V., Lackner, H., Boztug, K., Albert, M. H., Benesch, M., & Seidel, M. G. (2018). The Phenotype and Treatment of WIP Deficiency: Literature Synopsis and Review of a Patient With Pre-transplant Serial Donor Lymphocyte Infusions to Eliminate CMV. *Front Immunol*, 9, 2554. <https://doi.org/10.3389/fimmu.2018.02554>
- Seidel, J. A., Otsuka, A., & Kabashima, K. (2018). Anti-PD-1 and Anti-CTLA-4 Therapies in Cancer: Mechanisms of Action, Efficacy, and Limitations. *Front Oncol*, 8, 86. <https://doi.org/10.3389/fonc.2018.00086>
- Seidel, M. G. (2014). Autoimmune and other cytopenias in primary immunodeficiencies: pathomechanisms, novel differential diagnoses, and treatment. *Blood*, 124(15), 2337-2344. <https://doi.org/10.1182/blood-2014-06-583260>
- Serwas, N. K., Hoeger, B., Ardy, R. C., Stulz, S. V., Sui, Z., Memaran, N., Meeths, M., Krolo, A., Yüce Petronczki, Ö., Pfajfer, L., Hou, T. Z., Halliday, N., Santos-Valente, E., Kalinichenko, A., Kennedy, A., Mace, E. M., Mukherjee, M., Tesi, B., Schrenpf, A., . . . Boztug, K. (2019). Human DEF6 deficiency underlies an immunodeficiency syndrome with systemic autoimmunity and aberrant CTLA-4 homeostasis. *Nat Commun*, 10(1), 3106. <https://doi.org/10.1038/s41467-019-10812-x>
- Shah, K., Al-Haidari, A., Sun, J., & Kazi, J. U. (2021). T cell receptor (TCR) signaling in health and disease. *Signal Transduct Target Ther*, 6(1), 412. <https://doi.org/10.1038/s41392-021-00823-w>
- Sharapova, S. O., Haapaniemi, E., Sakovich, I. S., Kostyuchenko, L. V., Donkó, A., Dulau-Florea, A., Malko, O., Bondarenko, A. V., Stegantseva, M. V., Leto, T. L., Uygun, V., Karasu, G. T., Holland, S. M., Hsu, A. P., & Aleinikova, O. V. (2019). Heterozygous activating mutation in RAC2 causes infantile-onset combined immunodeficiency with susceptibility to viral infections. *Clin Immunol*, 205, 1-5. <https://doi.org/10.1016/j.clim.2019.05.003>
- Sharfe, N., Dadi, H. K., Shahar, M., & Roifman, C. M. (1997). Human immune disorder arising from mutation of the alpha chain of the interleukin-2 receptor. *Proc Natl Acad Sci U S A*, 94(7), 3168-3171. <https://doi.org/10.1073/pnas.94.7.3168>
- Sharlow, E. R., Pacifici, R., Crouse, J., Batac, J., Todokoro, K., & Wojchowski, D. M. (1997). Hematopoietic cell phosphatase negatively regulates erythropoietin-induced hemoglobinization in erythroleukemic SKT6 cells. *Blood*, 90(6), 2175-2187.
- Shi, L. (2013). Dock protein family in brain development and neurological disease. *Commun Integr Biol*, 6(6), e26839. <https://doi.org/10.4161/cib.26839>

- Shiraishi, A., Uruno, T., Sanematsu, F., Ushijima, M., Sakata, D., Hara, T., & Fukui, Y. (2017). DOCK8 Protein Regulates Macrophage Migration through Cdc42 Protein Activation and LRAP35a Protein Interaction. *J Biol Chem*, 292(6), 2191-2202. <https://doi.org/10.1074/jbc.M116.736306>
- Shortman, K., & Liu, Y. J. (2002). Mouse and human dendritic cell subtypes. *Nat Rev Immunol*, 2(3), 151-161. <https://doi.org/10.1038/nri746>
- Shulman, Z., Pasvolsky, R., Woolf, E., Grabovsky, V., Feigelson, S. W., Erez, N., Fukui, Y., & Alon, R. (2006). DOCK2 regulates chemokine-triggered lateral lymphocyte motility but not transendothelial migration. *Blood*, 108(7), 2150-2158. <https://doi.org/10.1182/blood-2006-04-017608>
- Shulman, Z., Shinder, V., Klein, E., Grabovsky, V., Yeger, O., Geron, E., Montresor, A., Bolomini-Vittori, M., Feigelson, S. W., Kirchhausen, T., Laudanna, C., Shakhar, G., & Alon, R. (2009). Lymphocyte crawling and transendothelial migration require chemokine triggering of high-affinity LFA-1 integrin. *Immunity*, 30(3), 384-396. <https://doi.org/10.1016/j.immuni.2008.12.020>
- Simon, K. L., Anderson, S. M., Garabedian, E. K., Moratto, D., Sokolic, R. A., & Candotti, F. (2014). Molecular and phenotypic abnormalities of B lymphocytes in patients with Wiskott-Aldrich syndrome. *J Allergy Clin Immunol*, 133(3), 896-899.e894. <https://doi.org/10.1016/j.jaci.2013.08.050>
- Skinner, O. P., Jurczyk, J., Baker, P. J., Masters, S. L., Rios Wilks, A. G., Clearwater, M. S., Robertson, A. A. B., Schroder, K., Mehr, S., Munoz, M. A., & Rogers, M. J. (2019). Lack of protein prenylation promotes NLRP3 inflammasome assembly in human monocytes. *J Allergy Clin Immunol*, 143(6), 2315-2317.e2313. <https://doi.org/10.1016/j.jaci.2019.02.013>
- Smith-Garvin, J. E., Koretzky, G. A., & Jordan, M. S. (2009). T cell activation. *Annu Rev Immunol*, 27, 591-619. <https://doi.org/10.1146/annurev.immunol.021908.132706>
- Snapper, S. B., Meelu, P., Nguyen, D., Stockton, B. M., Bozza, P., Alt, F. W., Rosen, F. S., von Andrian, U. H., & Klein, C. (2005). WASP deficiency leads to global defects of directed leukocyte migration in vitro and in vivo. *J Leukoc Biol*, 77(6), 993-998. <https://doi.org/10.1189/jlb.0804444>
- Socha, D. S., DeSouza, S. I., Flagg, A., Sekeres, M., & Rogers, H. J. (2020). Severe megaloblastic anemia: Vitamin deficiency and other causes. *Cleve Clin J Med*, 87(3), 153-164. <https://doi.org/10.3949/ccjm.87a.19072>
- Song, K. H., Kwon, K. W., Choi, J. C., Jung, J., Park, Y., Suh, K. Y., & Doh, J. (2014). T cells sense biophysical cues using lamellipodia and filopodia to optimize intraluminal path finding. *Integr Biol (Camb)*, 6(4), 450-459. <https://doi.org/10.1039/c4ib00021h>
- Song, Y., Shan, L., Gbyli, R., Liu, W., Fu, X., Wang, X., Qin, A., Patel, A., Gao, Y., Tebaldi, T., Biancon, G., Urbonas, D., Alderman, J., Halene, S., & Flavell, R. (2019). In Vivo reconstruction of Human Erythropoiesis with Circulating Mature Human RBCs in Humanized Liver Mistrg Mice. *Blood*, 134(Supplement_1), 338-338. <https://doi.org/10.1182/blood-2019-130701>
- Spiering, D., & Hodgson, L. (2011). Dynamics of the Rho-family small GTPases in actin regulation and motility. *Cell Adh Migr*, 5(2), 170-180. <https://doi.org/10.4161/cam.5.2.14403>
- Sprenkeler, E. G. G., Webbers, S. D. S., & Kuijpers, T. W. (2021). When Actin is Not Actin' Like It Should: A New Category of Distinct Primary Immunodeficiency Disorders. *J Innate Immun*, 13(1), 3-25. <https://doi.org/10.1159/000509717>
- Springer, T. A. (1990). Adhesion receptors of the immune system. *Nature*, 346(6283), 425-434. <https://doi.org/10.1038/346425a0>
- Standing, A. S., Malinova, D., Hong, Y., Record, J., Moulding, D., Blundell, M. P., Nowak, K., Jones, H., Omoyinmi, E., Gilmour, K. C., Medlar, A., Stanescu, H., Kleta, R., Anderson, G., Nanthapaisal, S., Gomes, S. M., Klein, N., Eleftheriou, D., Thrasher, A. J., & Brogan, P. A. (2017). Autoinflammatory periodic fever, immunodeficiency, and thrombocytopenia (PFIT) caused by mutation in actin-regulatory gene WDR1. *J Exp Med*, 214(1), 59-71. <https://doi.org/10.1084/jem.20161228>

- Stanford, S. M., Rapini, N., & Bottini, N. (2012). Regulation of TCR signalling by tyrosine phosphatases: from immune homeostasis to autoimmunity. *Immunology*, *137*(1), 1-19. <https://doi.org/10.1111/j.1365-2567.2012.03591.x>
- Stepp, S. E., Dufourcq-Lagelouse, R., Le Deist, F., Bhawan, S., Certain, S., Mathew, P. A., Henter, J. I., Bennett, M., Fischer, A., de Saint Basile, G., & Kumar, V. (1999). Perforin gene defects in familial hemophagocytic lymphohistiocytosis. *Science*, *286*(5446), 1957-1959. <https://doi.org/10.1126/science.286.5446.1957>
- Stinchcombe, J. C., Majorovits, E., Bossi, G., Fuller, S., & Griffiths, G. M. (2006). Centrosome polarization delivers secretory granules to the immunological synapse. *Nature*, *443*(7110), 462-465. <https://doi.org/10.1038/nature05071>
- Stirnadel-Farrant, H., Kudari, M., Garman, N., Imrie, J., Chopra, B., Giannelli, S., Gabaldo, M., Corti, A., Zancan, S., Aiuti, A., Cicalese, M. P., Batta, R., Appleby, J., Davinelli, M., & Ng, P. (2018). Gene therapy in rare diseases: the benefits and challenges of developing a patient-centric registry for Strimvelis in ADA-SCID. *Orphanet J Rare Dis*, *13*(1), 49. <https://doi.org/10.1186/s13023-018-0791-9>
- Streb, H., Irvine, R. F., Berridge, M. J., & Schulz, I. (1983). Release of Ca²⁺ from a nonmitochondrial intracellular store in pancreatic acinar cells by inositol-1,4,5-trisphosphate. *Nature*, *306*(5938), 67-69. <https://doi.org/10.1038/306067a0>
- Su, H. C. (2010). Deducator of cytokinesis 8 (DOCK8) deficiency. *Curr Opin Allergy Clin Immunol*, *10*(6), 515-520. <https://doi.org/10.1097/ACI.0b013e32833fd718>
- Su, H. C., & Orange, J. S. (2020). The Growing Spectrum of Human Diseases Caused by Inherited CDC42 Mutations. *J Clin Immunol*, *40*(4), 551-553. <https://doi.org/10.1007/s10875-020-00785-8>
- Suárez-Fueyo, A., Bradley, S. J., & Tsokos, G. C. (2016). T cells in Systemic Lupus Erythematosus. *Curr Opin Immunol*, *43*, 32-38. <https://doi.org/10.1016/j.coi.2016.09.001>
- Sugiyama, Y., Fujiwara, M., Sakamoto, A., Tsushima, H., Nishikimi, A., & Maruyama, M. (2022). The immunosenescence-related factor DOCK11 is involved in secondary immune responses of B cells. *Immun Ageing*, *19*(1), 2. <https://doi.org/10.1186/s12979-021-00259-4>
- Sundaravel, S., Duggan, R., Bhagat, T., Ebenezer, D. L., Liu, H., Yu, Y., Bartenstein, M., Unnikrishnan, M., Karmakar, S., Liu, T. C., Torregroza, I., Quenon, T., Anastasi, J., McGraw, K. L., Pellagatti, A., Boulwood, J., Yajnik, V., Artz, A., Le Beau, M. M., . . . Wickrema, A. (2015). Reduced DOCK4 expression leads to erythroid dysplasia in myelodysplastic syndromes. *Proc Natl Acad Sci U S A*, *112*(46), E6359-6368. <https://doi.org/10.1073/pnas.1516394112>
- Sundaravel, S., Kuo, W. L., Jeong, J. J., Choudhary, G. S., Gordon-Mitchell, S., Liu, H., Bhagat, T. D., McGraw, K. L., Gurbuxani, S., List, A. F., Verma, A., & Wickrema, A. (2019). Loss of Function of DOCK4 in Myelodysplastic Syndromes Stem Cells is Restored by Inhibitors of DOCK4 Signaling Networks. *Clin Cancer Res*, *25*(18), 5638-5649. <https://doi.org/10.1158/1078-0432.Ccr-19-0924>
- Swanson, K. V., Deng, M., & Ting, J. P. (2019). The NLRP3 inflammasome: molecular activation and regulation to therapeutics. *Nat Rev Immunol*, *19*(8), 477-489. <https://doi.org/10.1038/s41577-019-0165-0>
- Szczawinska-Poplonyk, A., Ploski, R., Bernatowska, E., & Pac, M. (2020). A Novel CDC42 Mutation in an 11-Year Old Child Manifesting as Syndromic Immunodeficiency, Autoinflammation, Hemophagocytic Lymphohistiocytosis, and Malignancy: A Case Report. *Front Immunol*, *11*, 318. <https://doi.org/10.3389/fimmu.2020.00318>
- Takenawa, T., & Miki, H. (2001). WASP and WAVE family proteins: key molecules for rapid rearrangement of cortical actin filaments and cell movement. *J Cell Sci*, *114*(Pt 10), 1801-1809. <https://doi.org/10.1242/jcs.114.10.1801>
- Takenouchi, T., Kosaki, R., Niizuma, T., Hata, K., & Kosaki, K. (2015). Macrothrombocytopenia and developmental delay with a de novo CDC42 mutation: Yet another locus for thrombocytopenia and developmental delay. *Am J Med Genet A*, *167A*(11), 2822-2825. <https://doi.org/10.1002/ajmg.a.37275>

- Talaat, R. M., Mohamed, S. F., Bassyouni, I. H., & Raouf, A. A. (2015). Th1/Th2/Th17/Treg cytokine imbalance in systemic lupus erythematosus (SLE) patients: Correlation with disease activity. *Cytokine*, 72(2), 146-153. <https://doi.org/10.1016/j.cyto.2014.12.027>
- Tan, H., Yang, K., Li, Y., Shaw, T. I., Wang, Y., Blanco, D. B., Wang, X., Cho, J. H., Wang, H., Rankin, S., Guy, C., Peng, J., & Chi, H. (2017). Integrative Proteomics and Phosphoproteomics Profiling Reveals Dynamic Signaling Networks and Bioenergetics Pathways Underlying T Cell Activation. *Immunity*, 46(3), 488-503. <https://doi.org/10.1016/j.immuni.2017.02.010>
- Tanaka, Y., Hamano, S., Gotoh, K., Murata, Y., Kunisaki, Y., Nishikimi, A., Takii, R., Kawaguchi, M., Inayoshi, A., Masuko, S., Himeno, K., Sasazuki, T., & Fukui, Y. (2007). T helper type 2 differentiation and intracellular trafficking of the interleukin 4 receptor-alpha subunit controlled by the Rac activator Dock2. *Nat Immunol*, 8(10), 1067-1075. <https://doi.org/10.1038/ni1506>
- Tangye, S. G., Al-Herz, W., Bousfiha, A., Cunningham-Rundles, C., Franco, J. L., Holland, S. M., Klein, C., Morio, T., Oksenhendler, E., Picard, C., Puel, A., Puck, J., Seppänen, M. R. J., Somech, R., Su, H. C., Sullivan, K. E., Torgerson, T. R., & Meyts, I. (2022). Human Inborn Errors of Immunity: 2022 Update on the Classification from the International Union of Immunological Societies Expert Committee. *J Clin Immunol*, 42(7), 1473-1507. <https://doi.org/10.1007/s10875-022-01289-3>
- Tangye, S. G., Buccioli, G., Casas-Martin, J., Pillay, B., Ma, C. S., Moens, L., & Meyts, I. (2019). Human inborn errors of the actin cytoskeleton affecting immunity: way beyond WAS and WIP. *Immunol Cell Biol*, 97(4), 389-402. <https://doi.org/10.1111/imcb.12243>
- Tangye, S. G., Pillay, B., Randall, K. L., Avery, D. T., Phan, T. G., Gray, P., Ziegler, J. B., Smart, J. M., Peake, J., Arkwright, P. D., Hambleton, S., Orange, J., Goodnow, C. C., Uzel, G., Casanova, J. L., Lugo Reyes, S. O., Freeman, A. F., Su, H. C., & Ma, C. S. (2017). Deducator of cytokinesis 8-deficient CD4(+) T cells are biased to a TH2 effector fate at the expense of TH1 and TH17 cells. *J Allergy Clin Immunol*, 139(3), 933-949. <https://doi.org/10.1016/j.jaci.2016.07.016>
- Tartaglia, M., & Gelb, B. D. (2010). Disorders of dysregulated signal traffic through the RAS-MAPK pathway: phenotypic spectrum and molecular mechanisms. *Ann N Y Acad Sci*, 1214, 99-121. <https://doi.org/10.1111/j.1749-6632.2010.05790.x>
- Taylor, M. D., Sadhukhan, S., Kottangada, P., Ramgopal, A., Sarkar, K., D'Silva, S., Selvakumar, A., Candotti, F., & Vyas, Y. M. (2010). Nuclear role of WASp in the pathogenesis of dysregulated TH1 immunity in human Wiskott-Aldrich syndrome. *Sci Transl Med*, 2(37), 37ra44. <https://doi.org/10.1126/scitranslmed.3000813>
- Teft, W. A., Kirchhof, M. G., & Madrenas, J. (2006). A molecular perspective of CTLA-4 function. *Annu Rev Immunol*, 24, 65-97. <https://doi.org/10.1146/annurev.immunol.24.021605.090535>
- The French FMF Consortium, Bernot, A., Clepet, C., Dasilva, C., Devaud, C., Petit, J.-L., Caloustian, C., Cruaud, C., Samson, D., Pulcini, F., Weissenbach, J., Heilig, R., Notanicola, C., Domingo, C., Rozenbaum, M., Benchetrit, E., Topaloglu, R., Dewalle, M., Dross, C., . . . Grateau, G. (1997). A candidate gene for familial Mediterranean fever. *Nature Genetics*, 17(1), 25-31. <https://doi.org/10.1038/ng0997-25>
- The International FMF Consortium. (1997). Ancient missense mutations in a new member of the RoRet gene family are likely to cause familial Mediterranean fever. *Cell*, 90(4), 797-807. [https://doi.org/10.1016/s0092-8674\(00\)80539-5](https://doi.org/10.1016/s0092-8674(00)80539-5)
- Thisse, C., & Zon, L. I. (2002). Organogenesis--heart and blood formation from the zebrafish point of view. *Science*, 295(5554), 457-462. <https://doi.org/10.1126/science.1063654>
- Thome, M., Charton, J. E., Pelzer, C., & Hailfinger, S. (2010). Antigen receptor signaling to NF-kappaB via CARMA1, BCL10, and MALT1. *Cold Spring Harb Perspect Biol*, 2(9), a003004. <https://doi.org/10.1101/cshperspect.a003004>
- Thompson, A. P., Bitsina, C., Gray, J. L., von Delft, F., & Brennan, P. E. (2021). RHO to the DOCK for GDP disembarking: Structural insights into the DOCK GTPase nucleotide exchange factors. *J Biol Chem*, 296, 100521. <https://doi.org/10.1016/j.jbc.2021.100521>
- Thrasher, A. J., & Burns, S. O. (2010). WASP: a key immunological multitasker. *Nat Rev Immunol*, 10(3), 182-192. <https://doi.org/10.1038/nri2724>

- Thumkeo, D., Katsura, Y., Nishimura, Y., Kanchanawong, P., Tohyama, K., Ishizaki, T., Kitajima, S., Takahashi, C., Hirata, T., Watanabe, N., Krummel, M. F., & Narumiya, S. (2020). mDia1/3-dependent actin polymerization spatiotemporally controls LAT phosphorylation by Zap70 at the immune synapse. *Sci Adv*, 6(1), eaay2432. <https://doi.org/10.1126/sciadv.aay2432>
- Tian, Y., Xu, J., Feng, S., He, S., Zhao, S., Zhu, L., Jin, W., Dai, Y., Luo, L., Qu, J. Y., & Wen, Z. (2017). The first wave of T lymphopoiesis in zebrafish arises from aorta endothelium independent of hematopoietic stem cells. *J Exp Med*, 214(11), 3347-3360. <https://doi.org/10.1084/jem.20170488>
- Tivol, E. A., Borriello, F., Schweitzer, A. N., Lynch, W. P., Bluestone, J. A., & Sharpe, A. H. (1995). Loss of CTLA-4 leads to massive lymphoproliferation and fatal multiorgan tissue destruction, revealing a critical negative regulatory role of CTLA-4. *Immunity*, 3(5), 541-547. [https://doi.org/10.1016/1074-7613\(95\)90125-6](https://doi.org/10.1016/1074-7613(95)90125-6)
- Trakarnsanga, K., Griffiths, R. E., Wilson, M. C., Blair, A., Satchwell, T. J., Meinders, M., Cogan, N., Kupzig, S., Kurita, R., Nakamura, Y., Toyne, A. M., Anstee, D. J., & Frayne, J. (2017). An immortalized adult human erythroid line facilitates sustainable and scalable generation of functional red cells. *Nat Commun*, 8, 14750. <https://doi.org/10.1038/ncomms14750>
- Traver, D., Akashi, K., Manz, M., Merad, M., Miyamoto, T., Engleman, E. G., & Weissman, I. L. (2000). Development of CD8alpha-positive dendritic cells from a common myeloid progenitor. *Science*, 290(5499), 2152-2154. <https://doi.org/10.1126/science.290.5499.2152>
- Treanor, B., Depoil, D., Bruckbauer, A., & Batista, F. D. (2011). Dynamic cortical actin remodeling by ERM proteins controls BCR microcluster organization and integrity. *J Exp Med*, 208(5), 1055-1068. <https://doi.org/10.1084/jem.20101125>
- Treanor, B., Depoil, D., Gonzalez-Granja, A., Barral, P., Weber, M., Dushek, O., Bruckbauer, A., & Batista, F. D. (2010). The membrane skeleton controls diffusion dynamics and signaling through the B cell receptor. *Immunity*, 32(2), 187-199. <https://doi.org/10.1016/j.immuni.2009.12.005>
- Trede, N. S., Langenau, D. M., Traver, D., Look, A. T., & Zon, L. I. (2004). The use of zebrafish to understand immunity. *Immunity*, 20(4), 367-379. [https://doi.org/10.1016/s1074-7613\(04\)00084-6](https://doi.org/10.1016/s1074-7613(04)00084-6)
- Trifari, S., Sitia, G., Aiuti, A., Scaramuzza, S., Marangoni, F., Guidotti, L. G., Martino, S., Saracco, P., Notarangelo, L. D., Roncarolo, M. G., & Dupre, L. (2006). Defective Th1 cytokine gene transcription in CD4+ and CD8+ T cells from Wiskott-Aldrich syndrome patients. *J Immunol*, 177(10), 7451-7461. <https://doi.org/10.4049/jimmunol.177.10.7451>
- Tube, N. J., & Jenkins, M. K. (2014). TCR signal quantity and quality in CD4(+) T cell differentiation. *Trends Immunol*, 35(12), 591-596. <https://doi.org/10.1016/j.it.2014.09.008>
- Tuzlak, S., Dejean, A. S., Iannacone, M., Quintana, F. J., Waisman, A., Ginhoux, F., Korn, T., & Becher, B. (2021). Repositioning T(H) cell polarization from single cytokines to complex help. *Nat Immunol*, 22(10), 1210-1217. <https://doi.org/10.1038/s41590-021-01009-w>
- Tybulewicz, V. L., & Henderson, R. B. (2009). Rho family GTPases and their regulators in lymphocytes. *Nat Rev Immunol*, 9(9), 630-644. <https://doi.org/10.1038/nri2606>
- Ubukawa, K., Goto, T., Asanuma, K., Sasaki, Y., Guo, Y. M., Kobayashi, I., Sawada, K., Wakui, H., & Takahashi, N. (2020). Cdc42 regulates cell polarization and contractile actomyosin rings during terminal differentiation of human erythroblasts. *Sci Rep*, 10(1), 11806. <https://doi.org/10.1038/s41598-020-68799-1>
- Ulirsch, J. C., Verboon, J. M., Kazerounian, S., Guo, M. H., Yuan, D., Ludwig, L. S., Handsaker, R. E., Abdulhay, N. J., Fiorini, C., Genovese, G., Lim, E. T., Cheng, A., Cummings, B. B., Chao, K. R., Beggs, A. H., Genetti, C. A., Sieff, C. A., Newburger, P. E., Niewiadomska, E., . . . Gazda, H. T. (2018). The Genetic Landscape of Diamond-Blackfan Anemia. *Am J Hum Genet*, 103(6), 930-947. <https://doi.org/10.1016/j.ajhg.2018.10.027>

- Ushijima, M., Uruno, T., Nishikimi, A., Sanematsu, F., Kamikaseda, Y., Kunimura, K., Sakata, D., Okada, T., & Fukui, Y. (2018). The Rac Activator DOCK2 Mediates Plasma Cell Differentiation and IgG Antibody Production. *Front Immunol*, 9, 243. <https://doi.org/10.3389/fimmu.2018.00243>
- Vaeth, M., & Feske, S. (2018). NFAT control of immune function: New Frontiers for an Abiding Trooper. *F1000Res*, 7, 260. <https://doi.org/10.12688/f1000research.13426.1>
- Vaeth, M., Yang, J., Yamashita, M., Zee, I., Eckstein, M., Knosp, C., Kaufmann, U., Karoly Jani, P., Lacruz, R. S., Flockerzi, V., Kacs Kovics, I., Prakriya, M., & Feske, S. (2017). ORAI2 modulates store-operated calcium entry and T cell-mediated immunity. *Nat Commun*, 8, 14714. <https://doi.org/10.1038/ncomms14714>
- Valitutti, S., Dessing, M., Aktories, K., Gallati, H., & Lanzavecchia, A. (1995). Sustained signaling leading to T cell activation results from prolonged T cell receptor occupancy. Role of T cell actin cytoskeleton. *J Exp Med*, 181(2), 577-584. <https://doi.org/10.1084/jem.181.2.577>
- van Buul, J. D., & Hordijk, P. L. (2004). Signaling in leukocyte transendothelial migration. *Arterioscler Thromb Vasc Biol*, 24(5), 824-833. <https://doi.org/10.1161/01.ATV.0000122854.76267.5c>
- Verboon, J. M., Mahmut, D., Kim, A. R., Nakamura, M., Abdulhay, N. J., Nandakumar, S. K., Gupta, N., Akie, T. E., Geddis, A. E., Manes, B., Kapp, M. E., Hofmann, I., Gabriel, S. B., Klein, D. E., Williams, D. A., Frangoul, H. A., Parkhurst, S. M., Crane, G. M., Cantor, A. B., & Sankaran, V. G. (2020). Infantile Myelofibrosis and Myeloproliferation with CDC42 Dysfunction. *J Clin Immunol*, 40(4), 554-566. <https://doi.org/10.1007/s10875-020-00778-7>
- Verboon, J. M., Sugumar, B., & Parkhurst, S. M. (2015). Wiskott-Aldrich syndrome proteins in the nucleus: aWASH with possibilities. *Nucleus*, 6(5), 349-359. <https://doi.org/10.1080/19491034.2015.1086051>
- Vicente-Manzanares, M., & Sánchez-Madrid, F. (2004). Role of the cytoskeleton during leukocyte responses. *Nat Rev Immunol*, 4(2), 110-122. <https://doi.org/10.1038/nri1268>
- Vignjevic, D., Kojima, S., Aratyn, Y., Danciu, O., Svitkina, T., & Borisy, G. G. (2006). Role of fascin in filopodial protrusion. *J Cell Biol*, 174(6), 863-875. <https://doi.org/10.1083/jcb.200603013>
- Vivier, E., Tomasello, E., Baratin, M., Walzer, T., & Ugolini, S. (2008). Functions of natural killer cells. *Nat Immunol*, 9(5), 503-510. <https://doi.org/10.1038/ni1582>
- Vonna, L., Wiedemann, A., Aepfelbacher, M., & Sackmann, E. (2007). Micromechanics of filopodia mediated capture of pathogens by macrophages. *Eur Biophys J*, 36(2), 145-151. <https://doi.org/10.1007/s00249-006-0118-y>
- Vorsteveld, E. E., Hoischen, A., & van der Made, C. I. (2021). Next-Generation Sequencing in the Field of Primary Immunodeficiencies: Current Yield, Challenges, and Future Perspectives. *Clin Rev Allergy Immunol*, 61(2), 212-225. <https://doi.org/10.1007/s12016-021-08838-5>
- Voskoboinik, I., Smyth, M. J., & Trapani, J. A. (2006). Perforin-mediated target-cell death and immune homeostasis. *Nat Rev Immunol*, 6(12), 940-952. <https://doi.org/10.1038/nri1983>
- Voskoboinik, I., & Trapani, J. A. (2013). Perforinopathy: a spectrum of human immune disease caused by defective perforin delivery or function. *Front Immunol*, 4, 441. <https://doi.org/10.3389/fimmu.2013.00441>
- Waite, A. L., Schaner, P., Hu, C., Richards, N., Balci-Peynircioglu, B., Hong, A., Fox, M., & Gumucio, D. L. (2009). Pyrin and ASC co-localize to cellular sites that are rich in polymerizing actin. *Exp Biol Med (Maywood)*, 234(1), 40-52. <https://doi.org/10.3181/0806-rm-184>
- Walker, L. S., & Sansom, D. M. (2011). The emerging role of CTLA4 as a cell-extrinsic regulator of T cell responses. *Nat Rev Immunol*, 11(12), 852-863. <https://doi.org/10.1038/nri3108>
- Walunas, T. L., Lenschow, D. J., Bakker, C. Y., Linsley, P. S., Freeman, G. J., Green, J. M., Thompson, C. B., & Bluestone, J. A. (1994). CTLA-4 can function as a negative

- regulator of T cell activation. *Immunity*, 1(5), 405-413. [https://doi.org/10.1016/1074-7613\(94\)90071-x](https://doi.org/10.1016/1074-7613(94)90071-x)
- Wan, F., Hu, C. B., Ma, J. X., Gao, K., Xiang, L. X., & Shao, J. Z. (2016). Characterization of $\gamma\delta$ T Cells from Zebrafish Provides Insights into Their Important Role in Adaptive Humoral Immunity. *Front Immunol*, 7, 675. <https://doi.org/10.3389/fimmu.2016.00675>
- Wang, D., Ye, Z., Wei, W., Yu, J., Huang, L., Zhang, H., & Yue, J. (2021). Capping protein regulates endosomal trafficking by controlling F-actin density around endocytic vesicles and recruiting RAB5 effectors. *Elife*, 10. <https://doi.org/10.7554/eLife.65910>
- Wang, J., Xu, L., Shaheen, S., Liu, S., Zheng, W., Sun, X., Li, Z., & Liu, W. (2017). Growth of B Cell Receptor Microclusters Is Regulated by PIP(2) and PIP(3) Equilibrium and Dock2 Recruitment and Activation. *Cell Rep*, 21(9), 2541-2557. <https://doi.org/10.1016/j.celrep.2017.10.117>
- Wang, L., Yang, L., Filippi, M. D., Williams, D. A., & Zheng, Y. (2006). Genetic deletion of Cdc42GAP reveals a role of Cdc42 in erythropoiesis and hematopoietic stem/progenitor cell survival, adhesion, and engraftment. *Blood*, 107(1), 98-105. <https://doi.org/10.1182/blood-2005-05-2171>
- Ward, S. G. (2009). Millipede-like lymphocyte crawling: feeling the way with filopodia. *Immunity*, 30(3), 315-317. <https://doi.org/10.1016/j.immuni.2009.03.002>
- Watanabe, S., De Zan, T., Ishizaki, T., Yasuda, S., Kamijo, H., Yamada, D., Aoki, T., Kiyonari, H., Kaneko, H., Shimizu, R., Yamamoto, M., Goshima, G., & Narumiya, S. (2013). Loss of a Rho-regulated actin nucleator, mDia2, impairs cytokinesis during mouse fetal erythropoiesis. *Cell Rep*, 5(4), 926-932. <https://doi.org/10.1016/j.celrep.2013.10.021>
- Waterhouse, P., Penninger, J. M., Timms, E., Wakeham, A., Shahinian, A., Lee, K. P., Thompson, C. B., Griesser, H., & Mak, T. W. (1995). Lymphoproliferative disorders with early lethality in mice deficient in Ctla-4. *Science*, 270(5238), 985-988. <https://doi.org/10.1126/science.270.5238.985>
- Weinreb, C., Rodriguez-Fraticelli, A., Camargo, F. D., & Klein, A. M. (2020). Lineage tracing on transcriptional landscapes links state to fate during differentiation. *Science*, 367(6479). <https://doi.org/10.1126/science.aaw3381>
- Weinstein, B. M., Schier, A. F., Abdelilah, S., Malicki, J., Solnica-Krezel, L., Stemple, D. L., Stainier, D. Y., Zwartkruis, F., Driever, W., & Fishman, M. C. (1996). Hematopoietic mutations in the zebrafish. *Development*, 123, 303-309. <https://doi.org/10.1242/dev.123.1.303>
- Wickrema, A., Chen, F., Namin, F., Yi, T., Ahmad, S., Uddin, S., Chen, Y. H., Feldman, L., Stock, W., Hoffman, R., & Platanius, L. C. (1999). Defective expression of the SHP-1 phosphatase in polycythemia vera. *Exp Hematol*, 27(7), 1124-1132. [https://doi.org/10.1016/s0301-472x\(99\)00043-0](https://doi.org/10.1016/s0301-472x(99)00043-0)
- Wildin, R. S., Ramsdell, F., Peake, J., Faravelli, F., Casanova, J. L., Buist, N., Levy-Lahad, E., Mazzella, M., Goulet, O., Perroni, L., Bricarelli, F. D., Byrne, G., McEuen, M., Proll, S., Appleby, M., & Brunkow, M. E. (2001). X-linked neonatal diabetes mellitus, enteropathy and endocrinopathy syndrome is the human equivalent of mouse scurfy. *Nat Genet*, 27(1), 18-20. <https://doi.org/10.1038/83707>
- Wildin, R. S., Smyk-Pearson, S., & Filipovich, A. H. (2002). Clinical and molecular features of the immunodysregulation, polyendocrinopathy, enteropathy, X linked (IPEX) syndrome. *J Med Genet*, 39(8), 537-545. <https://doi.org/10.1136/jmg.39.8.537>
- Wiskott, A. (1937). Familiarer angeborener Morbus Werlhofii? *Monatsschr Kinderheilkd*, 68, 212-216.
- Wülfing, C., Bauch, A., Crabtree, G. R., & Davis, M. M. (2000). The vav exchange factor is an essential regulator in actin-dependent receptor translocation to the lymphocyte-antigen-presenting cell interface. *Proc Natl Acad Sci U S A*, 97(18), 10150-10155. <https://doi.org/10.1073/pnas.97.18.10150>
- Xing, Y., & Hogquist, K. A. (2012). T-cell tolerance: central and peripheral. *Cold Spring Harb Perspect Biol*, 4(6). <https://doi.org/10.1101/cshperspect.a006957>
- Xu, H., Yang, J., Gao, W., Li, L., Li, P., Zhang, L., Gong, Y. N., Peng, X., Xi, J. J., Chen, S., Wang, F., & Shao, F. (2014). Innate immune sensing of bacterial modifications of Rho

- GTPases by the Pyrin inflammasome. *Nature*, 513(7517), 237-241. <https://doi.org/10.1038/nature13449>
- Yamamura, K., Uruno, T., Shiraishi, A., Tanaka, Y., Ushijima, M., Nakahara, T., Watanabe, M., Kido-Nakahara, M., Tsuge, I., Furue, M., & Fukui, Y. (2017). The transcription factor EPAS1 links DOCK8 deficiency to atopic skin inflammation via IL-31 induction. *Nat Commun*, 8, 13946. <https://doi.org/10.1038/ncomms13946>
- Yamane, H., & Paul, W. E. (2013). Early signaling events that underlie fate decisions of naive CD4(+) T cells toward distinct T-helper cell subsets. *Immunol Rev*, 252(1), 12-23. <https://doi.org/10.1111/imr.12032>
- Yamashiro, S., Gokhin, D. S., Kimura, S., Nowak, R. B., & Fowler, V. M. (2012). Tropomodulins: pointed-end capping proteins that regulate actin filament architecture in diverse cell types. *Cytoskeleton (Hoboken)*, 69(6), 337-370. <https://doi.org/10.1002/cm.21031>
- Yang, J., Zhang, Z., Roe, S. M., Marshall, C. J., & Barford, D. (2009). Activation of Rho GTPases by DOCK exchange factors is mediated by a nucleotide sensor. *Science*, 325(5946), 1398-1402. <https://doi.org/10.1126/science.1174468>
- Yang, L., Wang, L., Kalfa, T. A., Cancelas, J. A., Shang, X., Pushkaran, S., Mo, J., Williams, D. A., & Zheng, Y. (2007). Cdc42 critically regulates the balance between myelopoiesis and erythropoiesis. *Blood*, 110(12), 3853-3861. <https://doi.org/10.1182/blood-2007-03-079582>
- Zhang, H., Schaff, U. Y., Green, C. E., Chen, H., Sarantos, M. R., Hu, Y., Wara, D., Simon, S. I., & Lowell, C. A. (2006). Impaired integrin-dependent function in Wiskott-Aldrich syndrome protein-deficient murine and human neutrophils. *Immunity*, 25(2), 285-295. <https://doi.org/10.1016/j.immuni.2006.06.014>
- Zhang, J., Shehabeldin, A., da Cruz, L. A., Butler, J., Somani, A. K., McGavin, M., Koziaradzki, I., dos Santos, A. O., Nagy, A., Grinstein, S., Penninger, J. M., & Siminovitch, K. A. (1999). Antigen receptor-induced activation and cytoskeletal rearrangement are impaired in Wiskott-Aldrich syndrome protein-deficient lymphocytes. *J Exp Med*, 190(9), 1329-1342. <https://doi.org/10.1084/jem.190.9.1329>
- Zhang, Q., Davis, J. C., Lamborn, I. T., Freeman, A. F., Jing, H., Favreau, A. J., Matthews, H. F., Davis, J., Turner, M. L., Uzel, G., Holland, S. M., & Su, H. C. (2009). Combined immunodeficiency associated with DOCK8 mutations. *N Engl J Med*, 361(21), 2046-2055. <https://doi.org/10.1056/NEJMoa0905506>
- Zhang, Q., Dove, C. G., Hor, J. L., Murdock, H. M., Strauss-Albee, D. M., Garcia, J. A., Mandl, J. N., Grodick, R. A., Jing, H., Chandler-Brown, D. B., Lenardo, T. E., Crawford, G., Matthews, H. F., Freeman, A. F., Cornall, R. J., Germain, R. N., Mueller, S. N., & Su, H. C. (2014). DOCK8 regulates lymphocyte shape integrity for skin antiviral immunity. *J Exp Med*, 211(13), 2549-2566. <https://doi.org/10.1084/jem.20141307>
- Zhang, W., & Liu, H. T. (2002). MAPK signal pathways in the regulation of cell proliferation in mammalian cells. *Cell Res*, 12(1), 9-18. <https://doi.org/10.1038/sj.cr.7290105>
- Zhang, Y., Chen, M., & Chen, C. (2021). Using the Zebrafish as a Genetic Model to Study Erythropoiesis. *Int J Mol Sci*, 22(19). <https://doi.org/10.3390/ijms221910475>
- Zheng, D., Liwinski, T., & Elinav, E. (2020). Inflammasome activation and regulation: toward a better understanding of complex mechanisms. *Cell Discov*, 6, 36. <https://doi.org/10.1038/s41421-020-0167-x>
- Zhou, Q., Lee, G. S., Brady, J., Datta, S., Katan, M., Sheikh, A., Martins, M. S., Bunney, T. D., Santich, B. H., Moir, S., Kuhns, D. B., Long Priel, D. A., Ombrello, A., Stone, D., Ombrello, M. J., Khan, J., Milner, J. D., Kastner, D. L., & Aksentijevich, I. (2012). A hypermorphic missense mutation in PLCG2, encoding phospholipase C γ 2, causes a dominantly inherited autoinflammatory disease with immunodeficiency. *Am J Hum Genet*, 91(4), 713-720. <https://doi.org/10.1016/j.ajhg.2012.08.006>
- Zicha, D., Allen, W. E., Brickell, P. M., Kinnon, C., Dunn, G. A., Jones, G. E., & Thrasher, A. J. (1998). Chemotaxis of macrophages is abolished in the Wiskott-Aldrich syndrome. *Br J Haematol*, 101(4), 659-665. <https://doi.org/10.1046/j.1365-2141.1998.00767.x>
- Zon, L. I. (1995). Developmental biology of hematopoiesis. *Blood*, 86(8), 2876-2891.

6. CURRICULUM VITAE

Personal data

Address	Staudgasse 11/25 1180 Vienna
Mobile	+43-670-6036646
E-Mail	block_jana@gmx.de
Date, place of birth	05.07.1992, Bonn, Germany
Nationality	German

Education

10/2014 – 5/2017	Albert Ludwig University, Freiburg, Germany Master of Science Molecular Medicine Final grade: 1.1 (in a scale from 1 to 6; 1.0 is best)
10/2011 - 7/2014	Albert Ludwig University, Freiburg, Germany Bachelor of Science Molecular Medicine Final grade: 1.2 (in a scale from 1 to 6; 1.0 is best)
2002 - 2011	Secondary school Tannenbusch-Gymnasium, Bonn, Germany Abitur Final grade: 1.0 (in a scale from 1 to 6; 1.0 is best)

Professional experience/ internships

09/2017 - present	PhD student at the St. Anna Children's Cancer Research Institute (CCRI), the Ludwig Boltzmann Institute for Rare and Undiagnosed Diseases and the CeMM Research Center for Molecular Medicine of the Austrian Academy of Sciences, Vienna, Austria Laboratory Prof. Dr. Kaan Boztug, Immune Deficiency, Cancer Predisposition & Precision Oncology
11/2016 - 05/2017	Master thesis "Regulation of the expression of the serum and glucocorticoid-regulated kinase 1 in <i>Caenorhabditis elegans</i> " at the Faculty of Biology of the Albert Ludwigs University of Freiburg, Germany Laboratory Prof. Dr. Ralf Baumeister, Bioinformatics and Molecular Genetics, Supervisor Dr. Wolfgang Maier

02 - 08/2016	Research assistant in the clinical studies department of the Center for Chronic Immunodeficiency (CCI), Freiburg, Germany Study coordinator Prof. Dr. Stephan Ehl
04/2015 - 07/2015 and 04/2014 - 07/2014	Internship and bachelor thesis "HIV gene therapy using TALE- and CRISPR-based transcription factors" at Center for Chronic Immunodeficiency, Freiburg, Germany Laboratory Dr. Claudio Mussolino, Genome and Epigenome Engineering
03/2012 - 08/2013	Internship and following employment as research assistant at the Institute of Molecular Medicine und Cell Research, Freiburg, Germany Laboratory Prof. Dr. Andreas Hecht, Molecular mechanisms of cancer cell invasion
06 - 07/2011	Internship at the Life and Medical Sciences (LIMES) Institute, Bonn Germany Laboratory Prof. Dr. Joachim Schultze

Additional Skills/Achievements

Fellowships	DOC Fellowship of the Austrian Academy of Sciences (03/2020 – 02/2022)
Conference Presentations	<p>2019: Poster at EU-LIFE Scientific Meeting, 'Signalling & Gene Regulation in Health & Disease', Babraham Institute, Cambridge, UK</p> <p>2019: Poster at 15th Annual Young Scientist Association (YSA) PhD Symposium, Medical University of Vienna, Vienna, Austria</p> <p>2019: Poster at 3rd Harald von Boehmer Midwinter Conference (MWC), 'Advances in Immunobiology', Seefeld, Austria</p> <p>2018: Oral presentation at the 18th Biennial Meeting of The European Society for Immunodeficiencies, Lisbon, Portugal</p>
Software	MS Office, Adobe Illustrator, Prsim, Fiji/ Image J, CellProfiler, Zeiss ZEN, SnapGene, FlowJo; Search engines: UCSC, Ensembl, BLAST, NCBI
Languages	German (native language) English (full professional proficiency) Spanish (elementary proficiency)

Publications

Block J, Rashkova C, Castanon I, Zoghi S, Platon J, Ardy RC, Fujiwara M, Chaves B, Schoppmeyer R, van der Made CI, Jimenez Heredia R, Harms FL, Alavi S, Alsina L, Sanchez Moreno P, Ávila Polo R, Cabrera-Pérez R, Kostel Bal S, Pfajfer L, Ransmayr B, Mautner AK, Kondo R, Tinnacher A, Caldera M, Schuster M, Domínguez Conde C, Platzer R, Salzer E, Boyer T, Brunner HG, Nooitgedagt-Frons JE, Iglesias E, Deyà-Martinez A, Camacho-Lovillo M, Menche J, Bock C, Huppa JB, Pickl WF, Distel M, Yoder JA, Traver D, Engelhardt KR, Linden T, Kager L, Hannich JT, Hoischen A, Hambleton S, Illsinger S, Da Costa L, Kutsche K, Chavoshzadeh Z, van Buul JD, Antón J, Calzada-Hernández J, Neth O, Viaud J, Nishikimi A, Dupré L, Boztug K. Systemic Inflammation and Normocytic Anemia in DOCK11 Deficiency. *N Engl J Med.* **2023** Jun 21. doi: 10.1056/NEJMoa2210054. Epub ahead of print. PMID: 37342957.

Kostel Bal S, Giuliani S, **Block J**, Repiscak P, Hafemeister C, Shahin T, Kasap N, Ransmayr B, Miao Y, van de Wetering C, Frohne A, Jimenez-Heredia R, Schuster MK, Zoghi S, Hertlein V, Thian M, Bykov A, Babayeva R, Bilgic Eltan S, Karakoc-Aydiner E, Shaw LE, Chowdhury I, Varjosalo M, Argüello RJ, Farlik M, Ozen A, Serfling EAE, Dupré L, Bock C, Halbritter F, Hannich JT, Castanon I, Kraakman MJ, Baris S, Boztug K. Biallelic NFATC1 mutations cause an inborn error of immunity with impaired CD8+ T-cell function and perturbed glycolysis. *Blood.* **2023** May 30: blood.2022018303. doi: 10.1182/blood.2022018303. Epub ahead of print. PMID: 37249233.

Salzer E, Zoghi S, Kiss MG, Kage F, Rashkova C, Stahnke S, Haimel M, Platzer R, Caldera M, Ardy RC, Hoeger B, **Block J**, Medgyesi D, Sin C, Shahkarami S, Kain R, Ziaee V, Hammerl P, Bock C, Menche J, Dupré L, Huppa JB, Sixt M, Lomakin A, Rottner K, Binder CJ, Stradal TEB, Rezaei N, Boztug K. The cytoskeletal regulator HEM1 governs B cell development and prevents autoimmunity. *Sci Immunol.* **2020** Jul 10;5(49):eabc3979. doi: 10.1126/sciimmunol.abc3979. PMID: 32646852; PMCID: PMC7116756.